IE MERRELL LOCALITY

(24BE1659)

& Centennial Valley, Southwest Montana

Pleistocene Geology, Paleontology & Prehistoric Archaeology

Edited by

Christopher L. Hill and Leslie B. Davis

BUREAU OF LAND MANAGEMENT CULTURAL RESOURCES SERIES No. 4, 2005 • MONTANA STATE OFFICE • BILLINGS, MONTANA

THE MERRELL LOCALITY

(24BE1659)

& Centennial Valley, Southwest Montana

Pleistocene Geology, Paleontology & Prehistoric Archaeology

by
Christopher L. Hill, John P. Albanese, Robert G. Dundas, Leslie B. Davis, David C. Batten,
Dale P. Herbott, James K. Huber, Susan C. Mulholland, James K. Feathers, and Matthew J. Root

Leslie B. Davis and Christopher L. Hill, Co-Principal Investigators
Leslie B. Davis, Project Director
Compiled and Edited by Christopher L. Hill and Leslie B. Davis

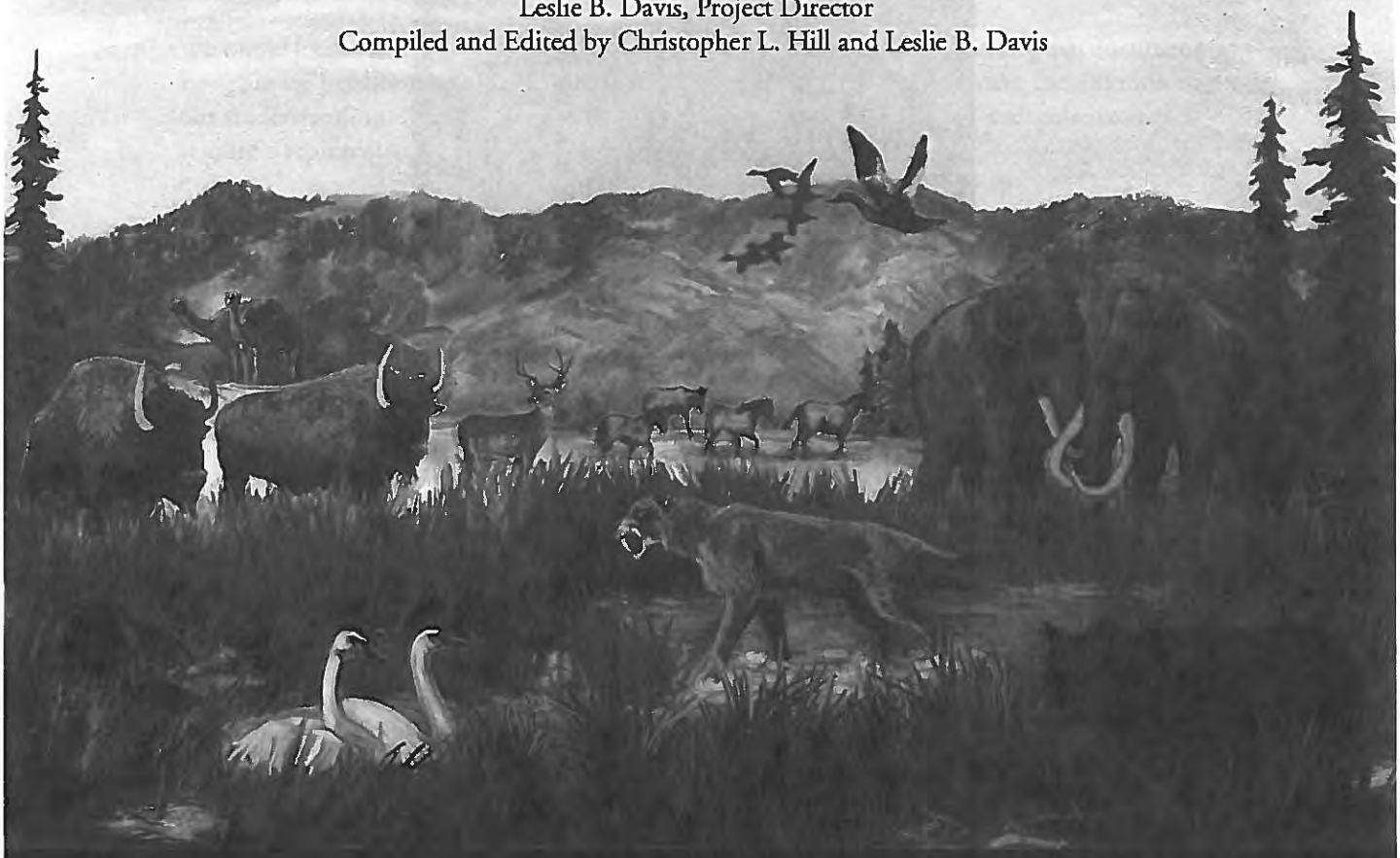

Technical Report to the Dillon Resource Office,
Butte District, U.S.D.I. Bureau of Land Management

Fieldwork Authorization #94-MT-070-076-004, Cultural Resource Permit #M82329
and Paleontological Resources Use Permit #M79222 by the Bureau of Land Management, 1995 through 1999

A project and product of the First Montanans Search Program (Ice-Age and Paleoindian Research Components) cosponsored by
the Kokopelli Archaeological Research Fund and the Bureau of Land Management under Cooperative Agreement # 1422E950-A4-008

MUSEUM OF THE ROCKIES • MONTANA STATE UNIVERSITY • BOZEMAN, MT 59717-2730 • 2005

The Bureau of Land Management is responsible for the stewardship of our public lands. It is committed to manage, protect, and improve these lands in a manner to serve the needs of the American people for all times. Management is based on the principles of multiple use and sustained yield of our nation's resources within a framework of environmental responsibility and scientific technology. These resources include recreation; rangelands; timber; minerals; watershed; fish and wildlife; wilderness; air; and scenic, scientific, and cultural values.

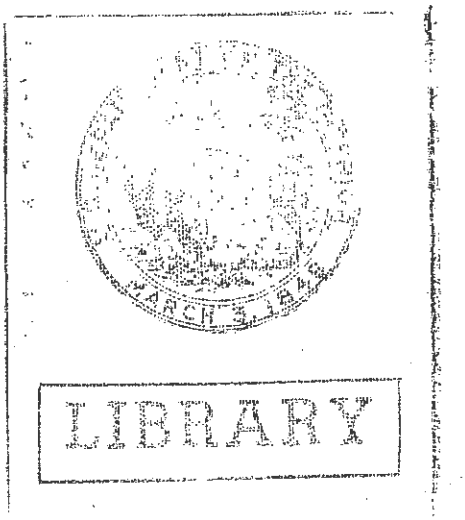

BLM/MT/ST-06/006+1050

ISBN 0-615-13043-7

Dedication

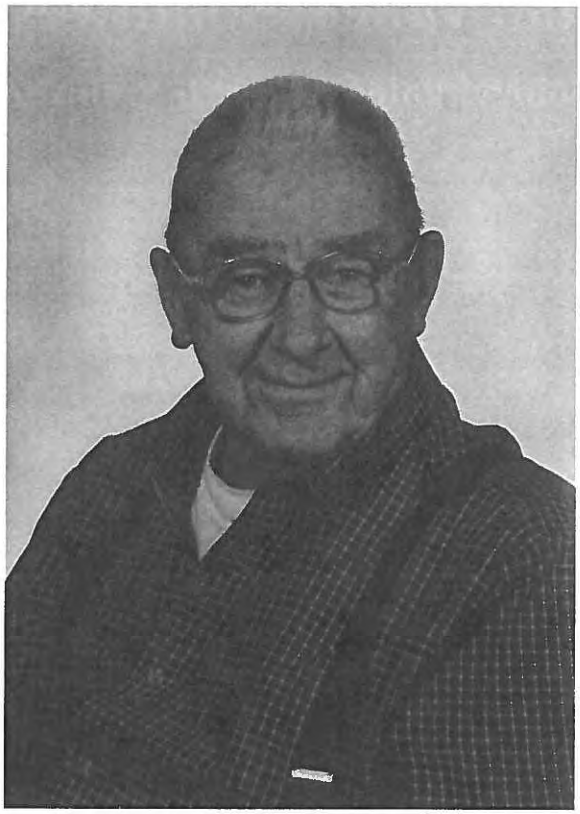

Donald G. Merrell

Donald Gene Merrell, a lifelong resident of Lima, Montana, married Lois Martinell in 1948 and raised a family in Lima. A 34-year employee of the Montana Department of Highways who retired in 1984, Don is a veteran goose, elk and deer hunter, fisherman, and collector of surface artifacts. Curious about the human past in the Centennials, he began collecting while a boy. Don much later came upon and recognized, while hunting geese along Lima Reservoir in 1988, bones of extinct mammals eroding onto the beach. He thereafter brought what came to be known as the Merrell paleontological site and locality to the attention of federal authorities in 1988. Don is recognized here as an uncommonly observant Montana citizen whose public-spiritedness and responsible actions led to the investigations and discoveries at this special place that takes his name. He was instrumental in stimulating Bureau of Land Management, Dillon Field Office, staff to take administrative and technical steps to preserve and protect this valuable heritage resource as a BLM responsibility. Findings derived from authorized research and mitigation studies at this important locality can now be shared with the public.

Foreword

This volume is the fourth contribution to a series of cultural resource monographs published by the Montana State Office of the Bureau of Land Management. The purpose of the series is, in part, to provide researchers and the intetested public with scholarly research that normally is not available or has limited distribution.

The BLM has statutory responsibilities to care for and manage cultural and paleontological resources under its jurisdiction. To that end, we have funded, through Cooperative Agreements and through contracts, research on archaeological and paleontological properties. This volume represents the best in this kind of research and should have great scholarly appeal to archaeologists, paleontologists, paleoecologists, and others who have an interest in this area and in good science.

We would like to thank Drs. Christopher L. Hill and Leslie B. Davis for making this document available for publication. We believe the research here has made a significant contribution to our understanding of the Pleistocene geology and to the archaeological and paleontological resources represented at the Merrell Locality and the Centennial Valley.

Gary P. Smith
Deputy Preservation Officer
Montana State Office
Bureau of Land Management
Billings, Montana

Cover: Artistic rendition of the Late Pleistocene Merrell Locality landscape and paleofauna, by K. L. Mather for the Museum of the Rockies.

Table of Contents

Lists of Figures, Plates, and Tables

List of Figures

List of Tables

Introduction

Leslie B. Davis

Merrell Locality and Site History

In 1983, at the initiative of Thomas A. Foor (Department of Anthropology, University of Montana), an opportunity was presented to Davis to continue and intensify archaeological and paleontological investigations of the Merrell Locality and site (24BE1659), in cooperation with the Bureau of Land Management (BLM). This site is located in southwestern Montana along one of the potential avenues/routes that could have been followed by early Native Americans making their way south of the Cordilleran ice sheets from northern entry points into North America or vice versa, heading northward (Figure 1). The Merrell Locality is situated along the northwest edge of Lima Reservoir in the Northern Rocky Mountain region of the Intermountain West (Figures 2 and 3).

Previous fieldwork directed by Foor under a cooperative agreement with the BLM had established and radiocarbon dated the presence of a late Ice-Age fauna exposed in weathering geological context, e.g., Dundas (1990, 1992) at Merrell.

Programmatic Ice-Age and Paleoindian Research

The Museum of the Rockies' First Montanans Search Program, formalized in 1990 and restructured in 1998 to include the Ice-Age and Paleoindian Research Programs, began in the 1980s as Paleoindian research initiated by Davis at the Indian Creek site (24BW626) for Montana State University. That programmatic approach involved location, evaluation, and investigation of productive Paleoindian campsites by examination of artifact collections, followup of leads provided by artifact collectors, reconnaissance surveys, and followup of site leads provided by U.S.D.A. Forest Service archaeologists.

While that multifaceted approach was beneficial, leading, in some instances, to fairly large-scale, multi-season, multidisciplinary field investigations, the location and study of Late Pleistocene vertebrate bonebeds and deposits had not been emphasized previously as a prospecting tactic by which to locate buried associated Early Prehistoric human contexts. Experience in recovering and researching the Lindsay mammoth in 1967 (24DW559) (Davis and Wilson 1995), continued acceleration mass spectroscopy (AMS) radiocarbon dating of the skeleton to ca. 11,400 B.P., and followup fieldwork at the site in 1997 (Hill and Davis 1998) provided important data from which carcass-scavenging by peoples possibly associated with a manifestation of the early Clovis complex is argued.

The tactical importance of locating and studying in situ Late Pleistocene-Early Holocene faunas, as a means of "tracking" Paleoindians in Montana, has been noted elsewhere (Davis 1997).

Considerable importance is placed on the discovery and investigation of paleontological/archaeological manifestations older than Clovis, that is, from 40,000 - 13,000 years B.P. Evidence from other locations in the Americas has suggested the occurrence of pre-Clovis human manifestations. Initial investigations at the Merrell Site by the University of Montana had dated Late Pleistocene faunas, in buried context, from that early interval. Whether equally early artifactual remains are associated with those bones and tusks was not known in 1994.

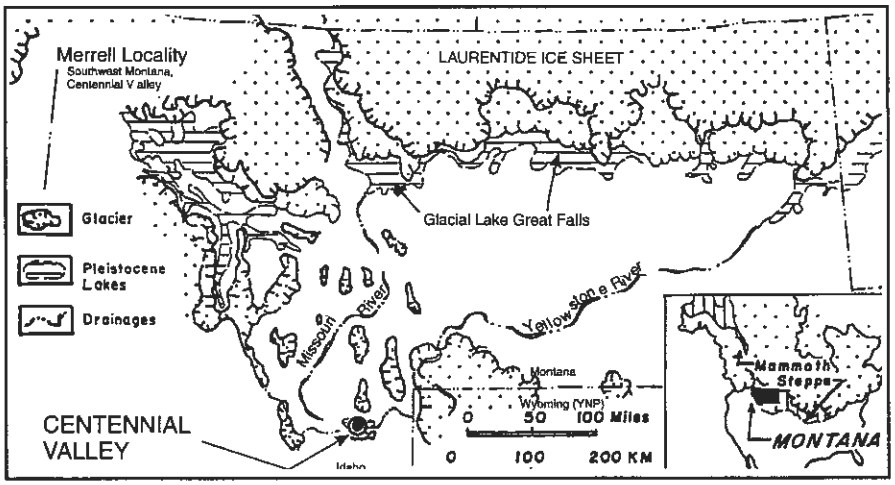

Figure 1. Map showing location of the Merrell Locality, Centennial Valley, in southwest Montana (compiled by C. L. Hill).

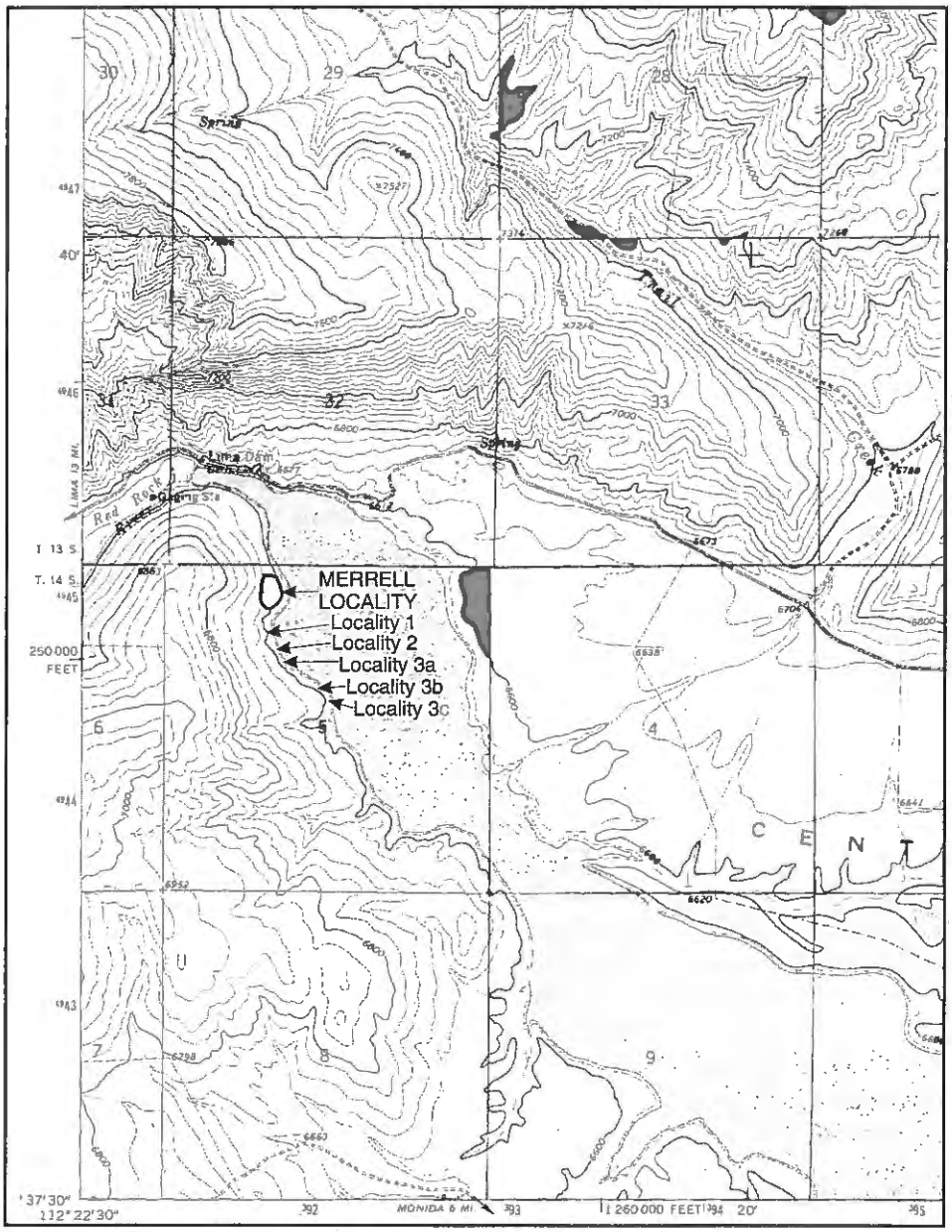

Figure 2. Map showing location of Merrell Locality (U.S.G.S. Lima Dam 7.5-minute quadrangle).

Figure 3. Photograph looking generally west toward Merrell Locality (C. L. Hill photo).

Field Methods

David C. Batten

Introduction

Field teams from the Museum of the Rockies (MOR) conducted excavations of the Merrell Site (part of the broader Merrell Locality) during the spring and summers in 1994, 1995, and 1996. The methodologies employed in these excavations are summarized here.

The 1994 Fieldwork

There were three stages to the fieldwork in 1994. During the first stage, the Merrell Site was gridded for magnetometry readings in the spring. The grid was oriented to 28° 40' west of True North in order to align the grid to the general direction of the embankment exposure over the lake (Lima Reservoir) (Figure 4). A north/south-aligned baseline was set up and given the designation 100 E. A parallel grid line was established at 120 E, and a grid of 20 x 20-m squares was established. The site datum was placed at 120 N/80E. The elevation of the site datum is 2,013.91 m above sea level (masl) (ca. 6,607.32 ft above sea level [fasl]).

During the second stage, a crew consisting of 10 archaeologists and a surveyor hand-excavated 24 m^2 of the site in eight spatially discrete Test Pits/Excavation Areas over a period of 11 days (June 8-18, 1994). The first task was the re-creation and extension of the grid imposed on the site during the magnetometer survey (Davis et al. 1995), and selection of Excavation Areas (designated as excavation units or XUs in the original field notes). Grid units were selected for excavation initially on the basis of magnetometer findings from the spring of 1994 which had indicated magnetic anomalies at specific locations. Four of these Test Pits/Excavation Areas were 2 x 2-m squares and the other four were 1 x 1-m squares. Two of the 2 x 2-m Test Pits were positioned near the eroding scarp edge (Figure 4) and were excavated to depths of 2.8 m (ca. 9.19 ft) below surface.

The Test Pits/Excavation Areas, which were nominally 2 m on a side, were oriented to the site grid. In fact, the 1994 Test Pits were excavated in halves; either the North half, South half, East half, or West half was excavated first, followed by the other half, alternating in such a way as to step the unit downward to its ultimate depth. Thus, material found in screens had a provenience of 1 x 2-m and 10 cm (ca. 4 in) depth. They were excavated in 10-cm levels, following the slope of the present-day ground surface. That is, at each level, each corner of the XU was a multiple of 10 cm below the surface at that corner (the bottom of level 3 would be 30 cm below the ground surface at each corner). Thus, in 1994, the excavation floor always maintained the approximate slope of the modern ground surface. Digging was mostly by shovel (shovel-shaving) and sediments were dry-screened through 1/4-in (0.63-cm) wire screens. When artifacts or identifiable bones were found in situ, their center points were located in three dimensions and mapped in planview on the level records. Trend (bearing) and plunge measurements were not recorded in 1994. The following Test Pits were excavated in 1994 (Table 1):

Table 1. Test Pits Excavated in 1994.

Test Pit	Half Excavated	Depth Excavation
A	N&S	100 cm? (ca. 39.4 in, 3.3 ft)
B	N&S	100 cm? (ca. 39.4 in, 3.3 ft)
C	N&S	280 cm (ca. 110 in, 9.2 ft)
D	N	100 cm (ca. 39.4 in, 3.3 ft)
E	N&S	270 cm (ca. 106.3 in, 8.9 ft)
F	?	30 cm (ca. 11.8 in, 1 ft)
G	?	30 cm (ca. 11.8 in, 1 ft)
H	?	30 cm (ca. 11.8 in, 1 ft)

Test Pit/Excavation Area A was thought to be a nonmetallic anomaly, while Test Pit/Excavation Area B was expected to yield a metal object. Test Pit/Excavation Area C was set up to investigate a stream channel tentatively identified in the cutbank exposure. This stream channel, which contained a mammoth tusk, is now considered to contain debris flow deposits with mammoth bones and teeth (see Albanese, this report). Test Pit C was expected to contribute information on the faunal materials exposed on the escarpment along the north end of the site. Test Pit/Excavation Area E was also located so as to expose Pleistocene mammal deposits identified in the cutbank over the reservoir. In Test Pit/Excavation Area E, these excavations exposed an intact bonebed indicated by the presence of mammoth teeth and bones. Test Pit/Excavation Area D was established to assess the upward and westward extent of archaeological deposits. Test Pits/Excavation Areas F, G, and H were selected arbitrarily to test the horizontal ex-

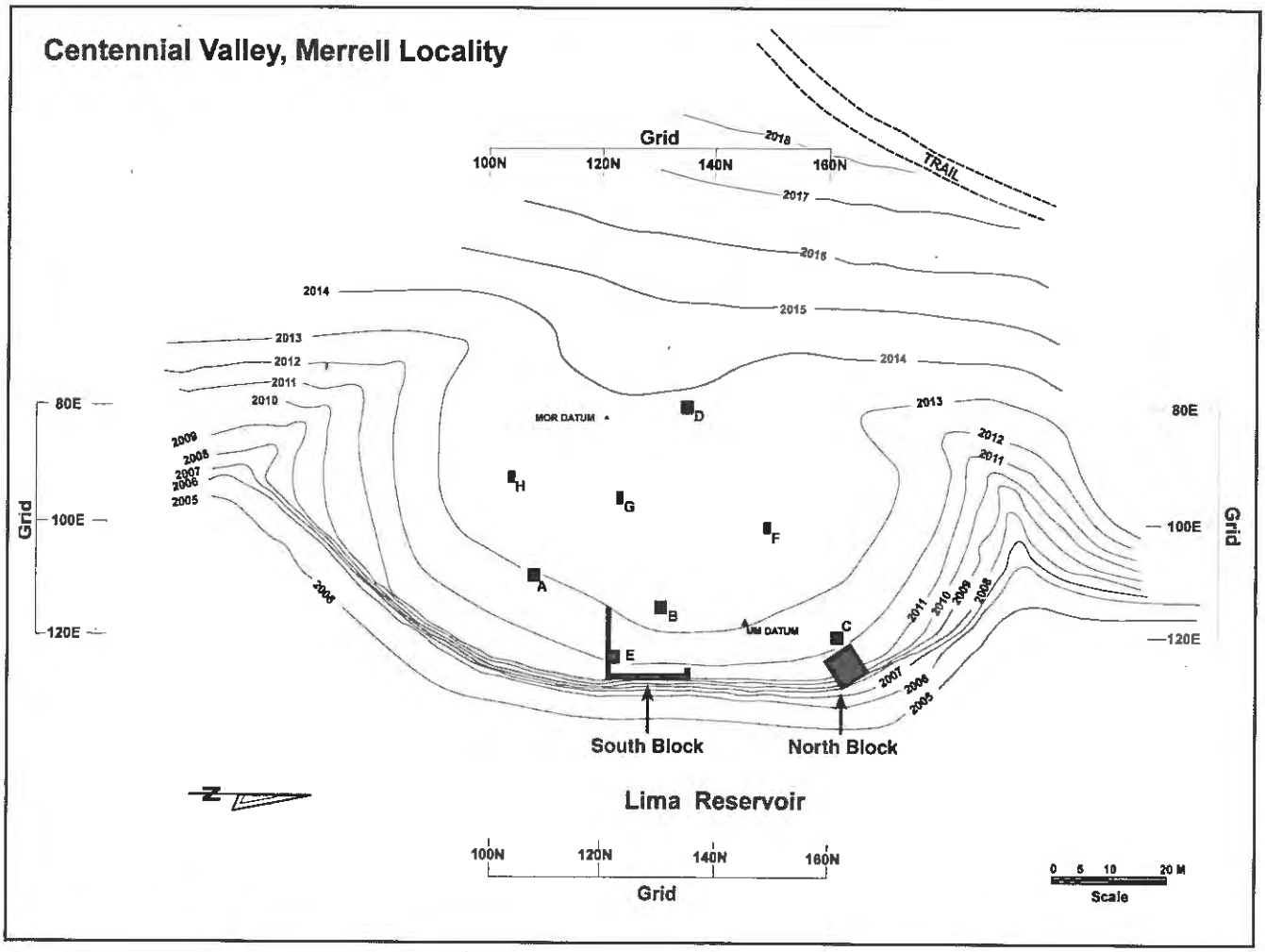

Figure 4. Topographic map of Merrell Locality, by Troy Helmick. Map shows locations of Test Pits/Excavation Areas, South and North Blocks, and grid system.

tent of subsurface archaeological deposits in the site area.

The third stage of the evaluation project consisted of fieldwork which focused on the stratigraphic and sedimentologic context of the Merrell Locality (August 15-17, 1994). Documentation and sample collection of the stratigraphic sequences in Test Pits/Excavation Areas C and E and along the face of the eroded scarp profile were conducted by C. Hill and J. Albanese (see papers by these authors in this report).

1994 Stratigraphic Descriptions of Test Pits/Excavation Areas

Profiles were drawn for each of the 1994 Test Pits/Excavation Areas. D. Batten profiled Test Pits A, B, D, F, G, and H (Figures 5-8) as excavations were completed, while Test Pits C and E were described at a later date by C. L. Hill and J. P. Albanese (see Hill, this report). For the descriptions made by Batten, two adjacent walls were profiled from each Test Pit/Excavation Area: often, the west and south walls or the west and north walls (Figures 5-8). Description involved observations of soil horizons, color, and texture. Sedimentological events were not considered. Relatively distinct boundaries between strata were indicated on the profiles with solid lines, while arbitrary divisions between deposits exhibiting gradual change are indicated with dashed lines. Particular notice was given to indicators of disturbance which could have caused upward or downward transport of bone or artifacts: tunneling by rodents appears to be common in the Merrell deposits.

It was possible to distinguish mostly between A and B soil horizons. Dark, organic-containing soils were generally classified as A-horizons. A-horizons at Merrell were light brown to dark brown sandy loams, sandy clay loams, and clay loams. The texture label was determined by application of the technique described in Foth et al. (1982). What were not A-horizons were generally considered to be B-horizons. In the West Wall profile of Test Pit/Excava-

tion Area A, a carbonate-rich silty clay was identified at the bottom of the profile (Figure 5). The higher clay content could be the result of size-sorting within the profile due to leaching or possibly sediments deposited by water or wind had undergone subsequent soil development. In this instance, it was not possible to interpret the deposits as loess. Features which appear to indicate rodent use were ubiquitous. Some runs and burrows were extremely fresh, while others looked as if they had been abandoned for a long time. No Test Pit/Excavation Area was free of evidence of rodent activity. Artifacts or bones were not infrequently found within such contexts.

Carbonates sometimes took the form of solid, rock-like (indurated) white deposits, but sometimes of horizontally extended patches of powdery white deposits. Oxidized areas were reddish orange deposits, occasionally extensive in planview, but appeared as discontinuous layers and rough geometric patterns in profile. Carbonates and oxides were restricted to Test Pits/Excavation Areas A and B (Figures 5 and 6). Test Pits/Excavation Areas D, F, G, and H did not exhibit much carbonate deposition or oxides.

The profiles of Test Pits/Excavation Areas A, B, D, F, G, and H show a topsoil development of varying thickness, but mostly of no more than 20 cm. Exceptions to this are small pockets of deeper soil (up to 50 cm [ca. 20 in]) in Test Pits A and B, likely attributable to rodent activity, and Test Pit D, which has a consistently deeper A-horizon of 20 to nearly 30 cm [ca. 8-12 in] (Figure 7). Test Pits F, G, and H present rather uninteresting profiles because of their shallow depth. However, among these units, Test Pit G is notable in that there is a fairly large lens of poorly sorted gravels (pea size to 10 cm [ca. 4 in]) in the northern and western parts of the profiles, at a depth of 16 cm (ca. 6 in) and below (Figure 8).

Test Pit/Excavation Area D is notable for the thickness of its A-horizon, as mentioned (Figure 7). The B-horizon continues to the bottom of the profile, gradually changing in color from light tan to tan with a greenish cast. This change takes place at a depth of 50 to 60 cm (ca. 20-24 in), and is accompanied by an increase in the clay content of the sediment. It is worth noting that Test Pit D was the most westerly excavation unit at the site and the unit most likely affected by deposition of colluvial sediments from the slope above.

Test Pits A and B had the most complex stratigraphy of the shallower excavation units. Much of this complexity is accounted for by the activity of rodents, which was extreme. Large portions of both units were disturbed, although Test Pit A was most affected by this activity (Figure 5). In parts of both Test Pit A and Test Pit B, there was no sharp boundary between the A-horizon, or topsoil, and the B-horizon. Instead, a transitional zone was noted. Below ca. 60 to 70 cm (ca. 24-28 in) in both excavation units was a marked increase in both calcium carbonate and oxidized deposits. While found together in some places, as in the eastern half of the North Wall of Test Pit A, in other areas, one type of chemical deposit clearly dominated. In the West Wall of Test Pit B, oxides dominated, but were underlain by a deposit dominated by carbonates.

The greatest significance of these profiles lies in the documentation of the extreme disturbance of the upper portion of the upper meter of sediment at the Merrell Site. Reference to the West Wall profile of Test Pit A demonstrates this point (Figure 5): there was virtually no stratigraphic integrity to the upper sediments. Thus, one can have very little confidence that artifactual materials within this sediment are in original context, and it seems that the spatial associations of these materials would be more likely to mislead than inform.

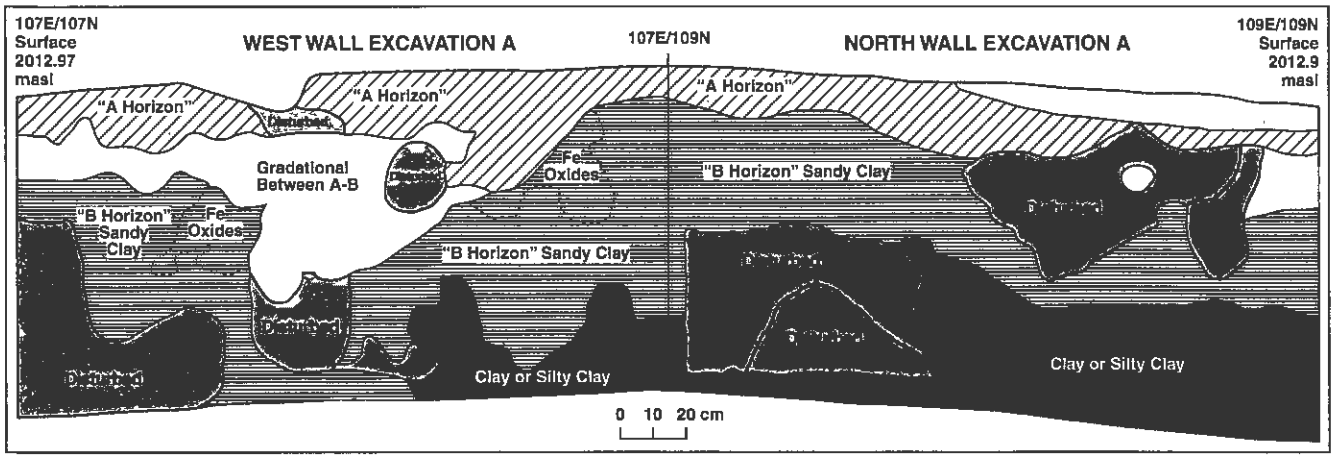

Figure 5. Stratigraphic section showing West and North Walls of Test Pit/Excavation Area A (D. Batten profile).

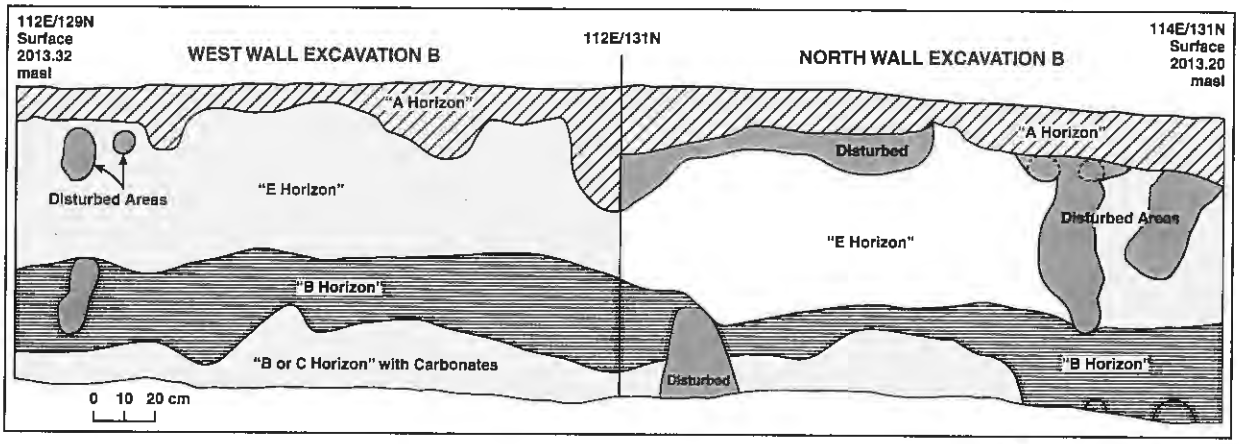

Figure 6. Stratigraphic section showing West and North Walls of Test Pit/Excavation Area B (D. Batten profile).

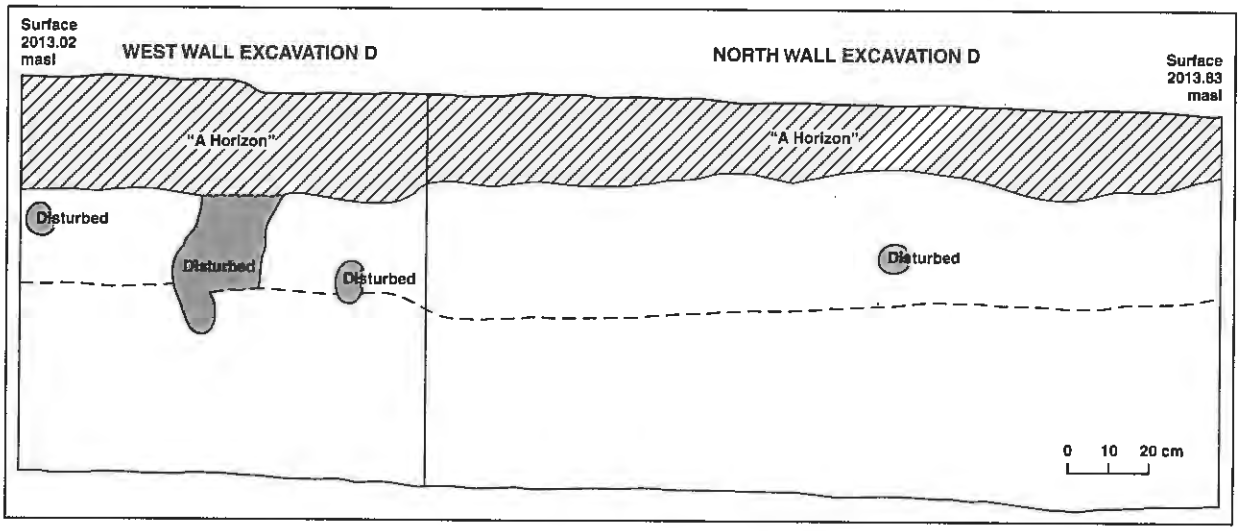

Figure 7. Stratigraphic section showing West and North Walls of Test Pit/Excavation Area D (D. Batten profile).

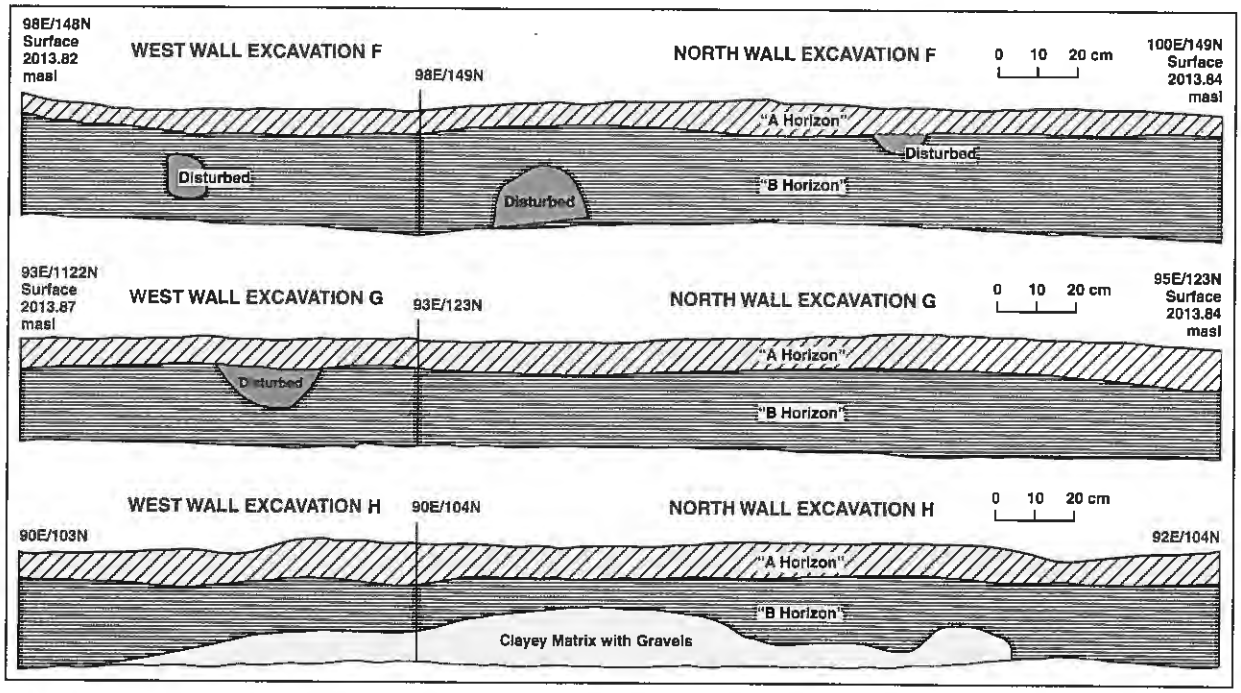

Figure 8. Stratigraphic section showing West and North Walls of Test Pits/Excavation Areas F-H (D. Batten profiles).

The 1995 Fieldwork

Because high water levels caused an overflow at the Lima Reservoir Dam, it was not possible to walk to the site in 1995. Daily trips to the site were made by boat.

Location of the Excavation Areas

Field studies during 1995 took place in two major locations at the site, designated the North Block and the South Block (Figures 4 and 9). Excavation Area I (the North Block) was oriented parallel to the embankment over the location of a mammoth tusk that was eroding out of a deposit identified as a debris flow. The purpose of excavation in the North Block was to determine the extent of the debris flow and study the nature of the depositional environment (thought to be the result of transportation of materials, including bones, from elsewhere, see Hill this report, Albanese this report). In order to more efficiently match the stratigraphy and (at least the present-day) topography, excavation squares in Excavation Area I were oriented according to those landmarks rather than to the site grid.

Excavation Area I was approximately 4.5 m NW/SE by about 5 m NE/SW (Figure 10). It was divided into 2-m x 2-m subunits by small letter designations: Ia - If. These were further subdivided into quadrants: SW, NW, NE, and SE. Only Ia and Ib were excavated. The SW corners of Ic and If were shot in for location in order to tie the entire North Block into the site grid (see Table 2).

The second area of excavation was designated the South Block (designated "South 95" in the 1995 field notes) and was laid out on the site grid, so excavation units correspond with the site grid (see Table 2) (Figure 11). This was the more extensive area excavated in 1995. Much of the overburden (top 200-250 cm [ca. 6.6-8.2 ft]) was removed by backhoe to roughly 2,010 masl (6,594.49 ft) in order to gain access to the sedimentary layer known as stratum B. The lower part of stratum B is a layer of dark sediment that apparently represents a marshy area, in which the position of fossil remains could fairly closely reflect where individual animals died, i.e., they would not have been transported any great distance. The South Block studies took place by Excavation Areas (2 m x 2 m in dimension) or portions of Excavation Areas.

Vertical Controls

For studies of the North and South Blocks, vertical control was maintained by use of a number of temporary datum points, labeled with a letter corresponding to the Excavation Area being worked or the general location of the datum point. The locations of these datum points were not recorded precisely because they were temporary, and because only their elevations were needed. Excavation progress and elevation of piece-plotted specimens was recorded in terms of centimeters of depth below one of these datum points. Whenever possible, a single datum was used for the entire excavation of any given unit. Sometimes, however, datum points were moved or destroyed by other earth-moving activities (overburden removal), and it became necessary to create new datum points. Whenever a datum was changed while excavation was in progress in a given Excavation Area, a new level form was started, and depth references were then made exclusively to the new datum point. For the elevations of the datum points, refer to Appendix A.

An elevation point was established for Excavation Area I (North Block) at the ground surface south of the unit and near the SE corner of the excavation. This was designated E3, and its location and elevation can be obtained

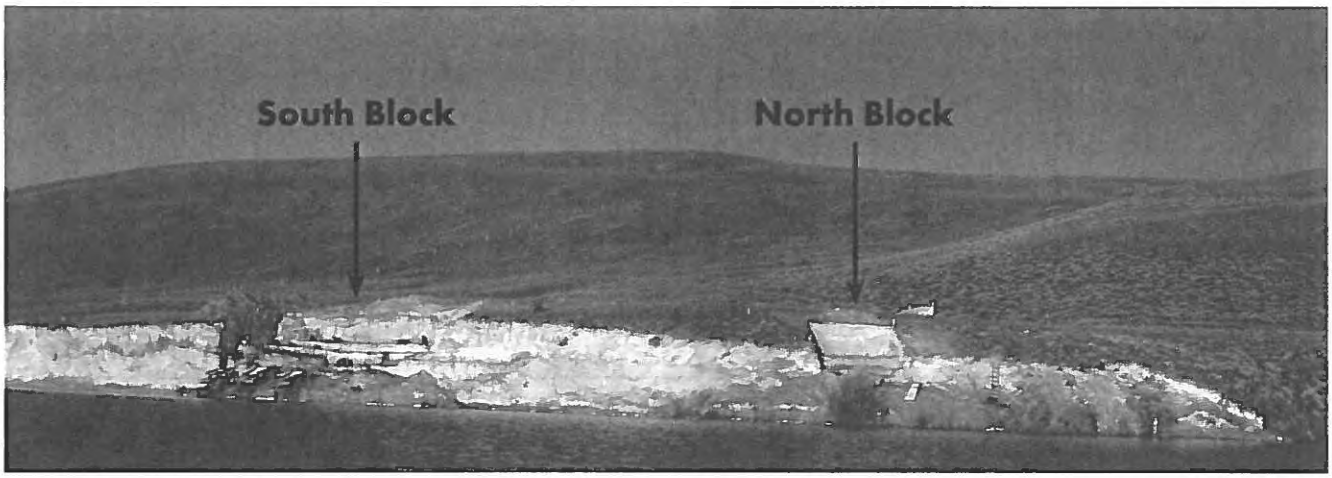

Figure 9. View showing South Block and North Block excavations (C. L. Hill photo).

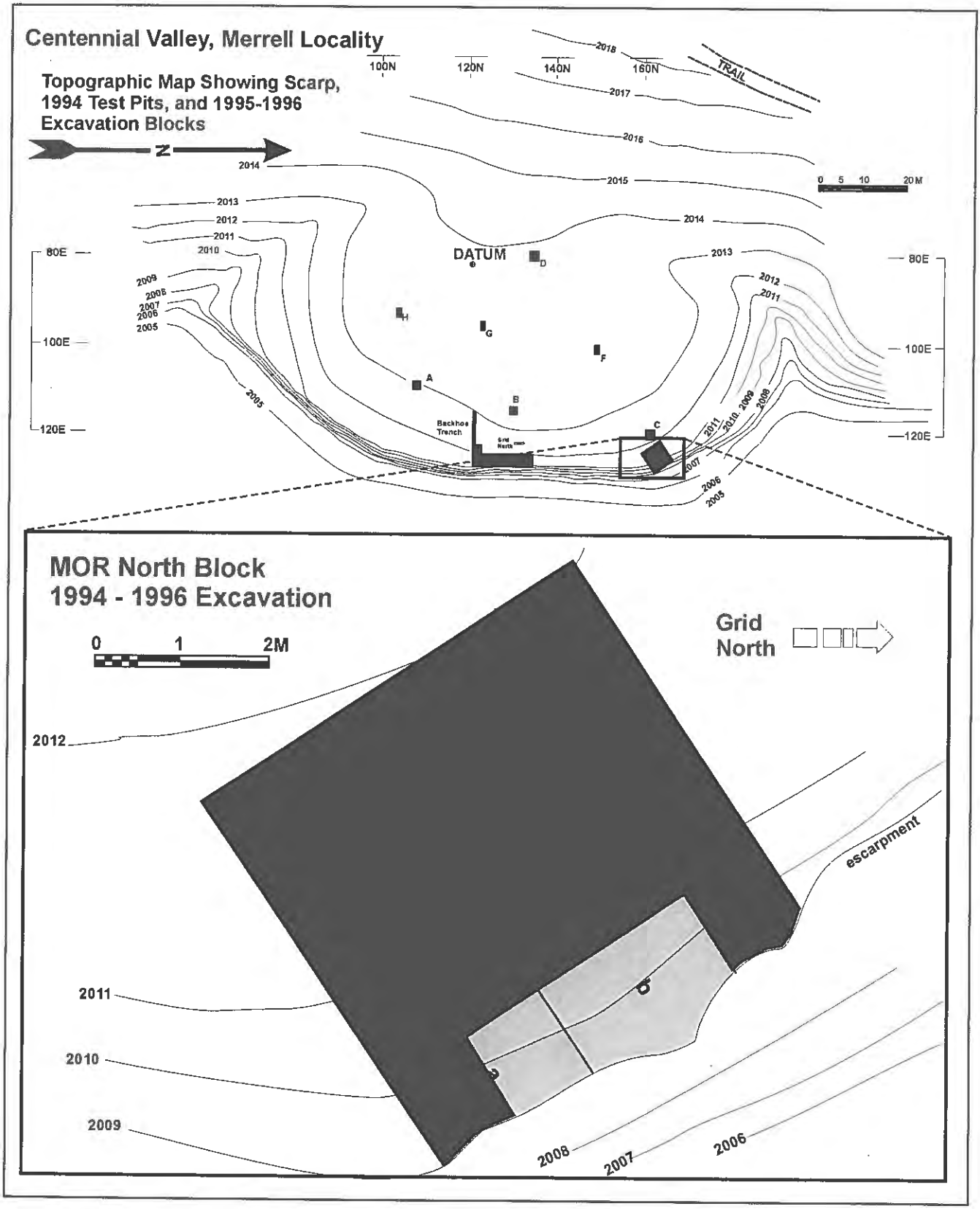

Figure 10. Map showing location and Excavation Area I (North Block) (compiled by C. L. Hill).

Table 2 . Excavation and Quadrant Labels (Note that only the west halves of Excavations J-P were present since the escarpment fell away between grid line 125E and grid line 126E).

Excavation	Quadrant	Northing	Easting	Excavation	Quadrant	Northing	Easting
E		121	121	S		123	123
E	n	South Half		S	se	123	124
E	s	South Half		S	ne	124	124
J		121	125	T		125	123
J	sw	121	125	T	sw	125	123
J	nw	122	125	T	nw	126	123
K		123	125	T	se	125	124
K	sw	123	125	T	ne	126	124
K	nw	124	125	U		127	123
L		125	125	U	sw	127	123
L	sw	125	125	U	nw	128	123
L	nw	126	125	U	se	127	124
M		127	125	U	ne	128	124
M	sw	127	125	V		129	123
M	nw	128	125	V	sw	129	123
N		129	125	V	nw	130	123
N	sw	129	125	V	se	129	124
N	nw	130	125	V	ne	130	124
O		131	125	W		131	123
O	sw	131	125	W	se	131	124
O	nw	132	125	W	ne	132	124
P		133	125	X		133	123
P	sw	133	125	X	se	133	124
P	nw	134	125	X	ne	134	124

from Table 2. Elevation point E2 was marked by a 1 x 2-in wooden stake driven all the way into the ground (a so-called "hub"), and another 1 x 2-in stake marking its location. The noted elevation is that of the top of the hub, i.e., very nearly ground surface elevation. One datum was established from which to refer excavation elevations for all of Excavation Area I. This was designated Datum I, with a ground surface elevation of 2,010.23 masl (ca. 6,595.24 fasl). Elevation at the string was 2,013.37 masl (6,605.55 fasl).

In the South Block, an elevation point was established halfway down the excavated face along the west wall of the excavation. This was designated E1, and its location and elevation can be obtained from Appendix A. This elevation point was marked by a 1 x 2-in wooden stake driven most of the way into a horizontal surface left by the backhoe part way up the west face of the excavation. The noted elevation is that of the top of the 1 x 2-in stake.

Excavation Procedures (General)

Excavation proceeded by 10-cm levels, water-screening through 1/4 in (0.635-cm) screen (Figures 12-14).

The Excavation Areas were 2 x 2-m squares, but the largest provenience (for bone recovered from the water screens) was a 1 x 1 m square, a quadrant of the Excavation Area. These were labeled simply SW, NW, NE, or SE quadrant (1/4). Most levels were arbitrary 10-cm (4-in) levels, but the levels changed whenever a stratigraphic break occurred in the middle of a 10-cm level, and a new level sheet was begun. Because important ecofacts were individually recorded in terms of their own unique proveniences, and because the strata were generally fairly thick, it seemed unnecessary to change level forms every time a new arbitrary level was begun. This procedure remained flexible. If an excavator was more comfortable changing forms with each level, that was done. If a datum point changed, or

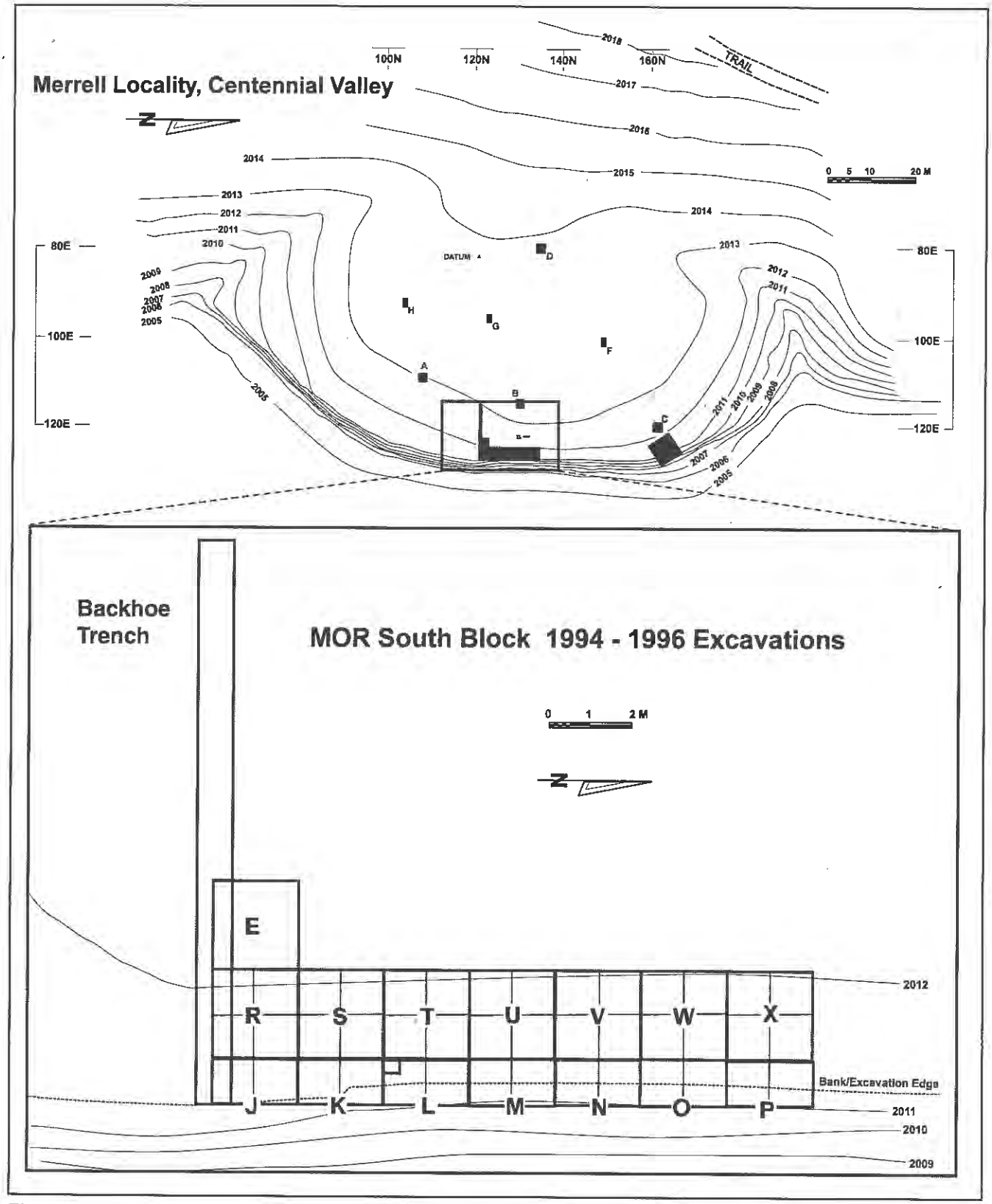

Figure 11. Map showing location and Excavation Area in South Block (compiled by C. L. Hill).

was accidentally moved, a new level form was begun to avoid confusing the reference point to which depths were compared. As stated above, a new level form was begun when a new stratum was encountered.

Whereas most of the digging was by arbitrary levels, the target fossil-bearing deposit (lower stratum B) was sometimes dug as a single unit. It was little more than 10 cm thick (ca. 4 in thick), and often deviated substantially from the horizontal. Thus, it would have been difficult to dig in 10-cm sublevels. The actual location of a substantial bonebed (if one existed) was expected to be at the interface between stratum B and the underlying deposit, stratum A (see Hill, this report, Albanese, this report). Thus, all areas excavated to that interface were continued another 10 cm into stratum A to ensure that the desired level had been reached.

Figure 12. Water-screening at South Block (1995 field season) (C. L. Hill photo).

North Block Studies (Excavation Area I)

This area (Excavation Area I) was marked off at the surface as a 4 x 5-m excavation block, and was excavated by hand (shovel, no screening) to a level some 20-30 cm (ca. 8-12 in) above the top of the fossil-bearing debris flow deposit. A margin of error was left in case the debris flow sloped up from the cutbank exposure, as was expected. The area encompassing the western portions of Excavation Areas Ia, Ib, and Ic was further excavated by shovel without screening until large cobbles from the debris flow were encountered. The area was then cleaned up and prepared for controlled excavation by 10-cm (4-in) levels and natural strata. Bones were quickly encountered in Excavation Area Ia, and excavation proceeded slowly as successive planview overlays were drawn of the complex cluster of fossil bones and their relationships to the cobbles and surrounding matrix (see Hill, this report).

South Block Studies

The backhoe removed approximately 200 cm (ca. 79 in, or 6.6 ft) of overburden. This was cleaned off and grid line 121E was set in with nails at 1-m intervals (Tier 1 in the Table of Excavation Areas). Another 40 cm (ca. 16 in) or so of sediment was removed east of a line about 20 cm (ca. 8 in) west of line 123E (including line 123E). Thus, in 1995, Excavation Areas J through Y were taken down to a level at about 2,009.47-2,010.29 masl (Tier 2). At that point, studies were initiated in Excavation Areas N and O.

The 1996 Fieldwork

Foot access to the site was prevented by the flow of water over the spillway of the Lima Reservoir Dam in 1996. The crew was ferried to the site across the reservoir daily by motor-powered boat. Equipment was delivered and removed from the site overland by truck.

The 1996 field season at Metrell took place over 10 days, from June 17 to June 26. Excavation was carried out by a crew of nine. The entire excavation took place in the South Block, from which considerable overburden had been removed by backhoe in 1995. An area of 22 m^2 (Figure 14) was excavated into nonfossiliferous sediments below the fossil-bearing deposits. Appendix A lists the starting and ending elevations for the 11 1 x 1-m units excavated in 1996.

The entire site had been laid out in 1994 according to a numeric grid system. Excavations in 1996 continued in the area established within the South Block in 1994. All locations within the site are related to an imaginary point of origin located in the southwest corner of the site (at 120 m north), according to distances north and east of the ori-

Figure 13. Excavations at South Block (1995 field season) (C. L. Hill photo).

Figure 14. Excavation at South Block. Dark-colored deposits are lower part of stratum B (1995 field season) (C. L. Hill photo).

gin and 80 m east, or at 120N/80E (Figure 4). A 1 x 1-m grid square would be identified by the coordinates of its southwest corner, e.g., 125N/124E. A bone fragment, for example, might then be located at 125.65N/124.32E, or 65 cm north and 32 cm east of the origin of that 1 x 1-m grid square.

The South Block designates a group of excavation grids exposed by backhoe and manual excavation in 1995, which runs roughly parallel to the edge of the cutbank. This cut was approximately 4-5 m wide (E/W) and 12+m long (N/S). In 1995, using exacting excavation and recording procedures in order to extract detailed taphonomic information, it was possible to fully or nearly fully excavate roughly 11 1 x 1-m grid squares within this block. These grid squares (most of which lay right on the edge of the cutbank on line 125 East) had been excavated to depths below the dark organic sediment stratum identified as stratum B (Albanese, this report, Hill, this report). The bulk of the fossil faunal assemblage from the 1994 test excavation was found in this stratum.

Stratum B was the target of investigation in 1996 as in 1995. To facilitate the excavation of this geological stratum, approximately 2 m of overlying sediments were removed by backhoe in 1995. Additional sediment was removed by shovel to get down near to the organic-enriched stratum of interest (lower stratum B). Stratum B had been subjected to considerable stress over about the last 40,000 years or since deposition, as evidenced by occasional dramatic changes in elevation and thickness, even within the small area chosen for excavation. The removal of overburden required some care to prevent the possibility of accidentally digging into stratum B itself with inappropriate tools.

In 1996, the South Block was effectively divided into three tiers. Excavation Squares Areas along line 125 East were either completely excavated to sterile sediment, or had been excavated to near the top of stratum B. In one case, Excavation Area 124N/125E had been excavated into stratum B, but not all the way through it to the underlying non-fossil-bearing deposit (stratum A). Excavation Areas 125-128N/125E were at the same level as the next tier to the west. On that tier, Excavation Areas along the line 124 East had been stripped of overburden to within about 15-40 cm (6-16 in) above stratum B. The exception, Excavation Area X, had been fully excavated to sterile sediment. The third tier represented the bottom of the backhoe excavation of 1995. This surface was generally 50-80 cm (20-32 in) or more above stratum B. This tier was more than 2 m (ca. 6.56 ft) wide in the north part of the block, but less than 2 m wide in the south end. Excavation Areas along line 123 East were excavated from this level.

Many of the grid points marked by nails in 1995 remained in 1996. However, many were covered by loose sediment that had sloughed or been washed down onto this surface during the intervening fall, winter, and spring. The loose sediment left by the backhoe had been removed by hand tools (shovels) in 1995, but had been replaced by new deposits in the interim. Excavation Areas along 125E were not greatly affected by this new deposition. Excavation Areas on line 124E required some cleaning along the uphill side (near line 124E), and Excavation Areas on line 123E required considerable removal of loose sediment before excavation could be initiated.

1996 excavations began with preparation of the South Block. Loose sediment that had accumulated since the 1995 field season was removed, and grid corner nails were relocated and marked with flagging tape indicating their grid locations. In preparation for the recovery of identifiable bone, a grid corner, the exact three-dimensional location

of which is known, was set up on the original ground surface overlooking the South Block. Determination of the precise three-dimensional location of finds was facilitated in 1996 by the use of a Topcon GTS-303 Electronic Total Station. This instrument can measure slope distance and vertical and horizontal (azimuth) angles, and calculates horizontal coordinate location and vertical distances, thus providing three-dimensional location on a digital readout. Only the true elevation must then be calculated by the operator, based on the determined height of the instrument and the height of the target prism.

This instrument was used to directly measure the locations of all bone removed from the fossil-bearing deposits at Merrell in 1996. Grid squares were thus of secondary importance in recording provenience: they provided provenience for small fragments of bone that were not diagnostic and those for which the original location could not be exactly determined (due to disturbance by trowel or shovel). Typically, the largest scale provenience in the 1996 excavation was the 1 x 1-m square and level. Ideally, the depth of each level was 10 cm (4 in), but, in many cases that year, the depth of some levels was considerably more than 10 cm. Elevation of levels was determined by using string, line levels, and flexible rules to measure the distance below local datums. Local datums were established for that purpose using the Total Station.

Fossil recovery was structured by the excavation of 1 x 1-m grid squares (see Appendix 9 for the recordation protocol). The upper sediments of the grid squares, well above the dark organic deposit of primary interest, were excavated by careful shovel-shaving. As excavation reached a level about 10 cm (4 in) above stratum B or, if dark sediment appeared on the floor of the grid square, further excavation was undertaken by trowel. Since the goal of the excavation was the recovery of recognizable faunal elements, and as a concession to the volume of sediment remaining to be excavated in a 10-day period, sediment from most of the grid squares was not screened. A sample of excavation squares was water-screened through 1/4 (0.63-cm) and 1/8-in (0.32-cm) screen, however, to ensure that we were not losing information in the form of small mammal bones that might be overlooked in the process of excavating by trowel. Excavation Areas 125N/125E (starting with Level 3), 126N/125E, and the remnant 124N/125E in the first tier, and 125N/124E in the second tier were water-screened; these were situated in the most productive area of the site in terms of bone density.

The final excavation walls retained fossil bones and stones for inclusion in the drafted profiles as absolute evidence of their geological provenience (see documentation by Hill, this report).

All bone pieces greater than about 8 cm, or which have features on them that might be useful for identification by the project faunal analyst, and which were found in situ, were located in three-dimensional space using the Total Station. Small fragments lacking recognizable markers were placed in a general bone bag for the grid square and level. Bones were bagged in curation-quality plastic bags, and tagged with acid-free paper. Records were kept on forms printed on acid-free paper, for permanent curation purposes.

Summary

Controlled excavations were conducted at the Merrell Site in, 1994, 1995, and 1996. In 1994, Test Pits (Excavation Areas A-H) were placed at various locations around the site (Figure 4). The stratigraphic profiles for Test Pits A, B, D, and F-H are documented in this paper, while Test Pits C and D are available in Hill (this report). In 1995, studies were expanded in the vicinity of the escarpment directly east of Test Pits/Excavation Areas C and D. The area near Test Pit C was designated Excavation Area I, or the North Block. Tusk and mammoth bone were exposed along the escarpment associated with debris flow deposits. The area near Test Pit C was designated as the South Block. Besides Test Pit/Excavation Area E, the South Block includes a backhoe trench and Excavation Areas J-X (Figure 11). The 1996 field studies focused on continued excavations of the South Block. In particular, the field studies were designed to recover more fossils from the lower part of stratum B.

A Field Reconnaissance Geologic Study

John P. Albanese

Introduction

This study was of a reconnaissance nature, the main objectives being the delineation of the stratigraphic sequence and past sedimentary regimes at the Merrell Locality. Seven days were spent in the field (August 15-18, 1994 and July 10-12, 1995) examining and mapping exposures of Quaternary sediment. No attempt was made to conduct laboratory analysis.

General Setting

The Merrell Locality is a Pleistocene vertebrate fossil occurrence located on the floor of the Centennial Valley in southwestern Montana (Figure 1). The site also contains an archaeological surface artifact scatter that mainly consists of debitage and a few tools. This latter occurrence is not considered to be significant. The Centennial Valley floor is approximately 9.7 km (ca. 6 mi) wide at a point located 8 km (ca. 5 mi) east of the Merrell Locality. However, in the vicinity of the Merrell Locality, it narrows and is only ±1 km (0.6 mi) wide. The wide valley floor east of the Merrell Locality displays inclinations of 1° or less. Here, the valley floor is underlain by undifferentiated Tertiary rocks (Ross, Andrews, and Witkind 1955).

The Centennial Valley floor is drained by the west-flowing Red Rock River, the source of which lies 64 km (ca. 40 mi) to the west of the Merrell Locality. The river has been dammed, resulting in the creation of Lima Reservoir. This elongate lake is approximately 17.6 km (ca. 11 mi) long and has a maximum width of 1.6 km (ca. 1 mi). The Merrell Locality lies on the southwest shore, near the northwest end of the reservoir. The dam and spillway lie only 730 m (2,395 ft) northwest of the site area (see Figure 2).

The Merrell Locality and Site is approximately 130 m (426 ft) long and lies adjacent to the reservoir shoreline. The vertebrate fossils lie beneath a Pleistocene terrace tread that is ±60 m (197 ft) wide and inclined 8°-2.5° to the east. A northwest (355°) trending, steep (45°-69°), 3-4-m (9.8-13.1 ft) high scarp parallels and adjoins the terrace tread on the east. A ±20-m (65.6-ft) wide beach borders the scarp on the east (Figures 15 and 16). The scarp has formed as a result of wave action directed toward the southwest shore of the reservoir. The scarp is retreating to the southwest, as a result of undercutting and scarp collapse. The beach shore surface is inclined 10°-15° to the northeast. Late Pleistocene vertebrate fossils, contained within sediment exposed in the aforementioned scarp, have accumulated on the reservoir beach.

A ±120-m (394-ft)-high, north-trending ridge borders the aforementioned Pleistocene terrace surface on the west. The ridge slopes average 14° in inclination and are covered by a veneer of colluvium that contains abundant well-rounded pebbles and cobbles. Most of the cobbles are composed of limestone, but some also consist of quartzite. The colluvium extends onto the Pleistocene terrace surface.

Figure 15. Escarpment at Merrell Locality (1994 field season) (C. L. Hill photo).

Site Stratigraphy

All sediments exposed or penetrated at the Merrell Locality are Quaternary in age. When viewed along the steep scarp that lies adjacent to the Lima Reservoir shoreline, five main sedimentary units are discernible. From oldest to youngest, they are labeled strata A through E. A brief description and discussion of each unit follows:

Stratum A (Pleistocene) - This is the basal and oldest unit exposed in the scarp face. It is present throughout the Merrell Locality. Exposures vary in thickness from 1.9 to 4.9 m (6.2-16 ft); actual thickness is unknown. When examined along the scarp, stratum A most commonly consists of massive, very-fine to fine-grained, silty, clayey sand that grades to a sandy, clayey silt. Locally within the basal portion of the unit are occurrences of thin (.5-4 cm [0.2-1.6 in]) horizontal lenses (±1 m [3.3 ft] long) that contain well-rounded, 1-4-cm (ca. 2.5-1.6-in)-long pebbles (usu-

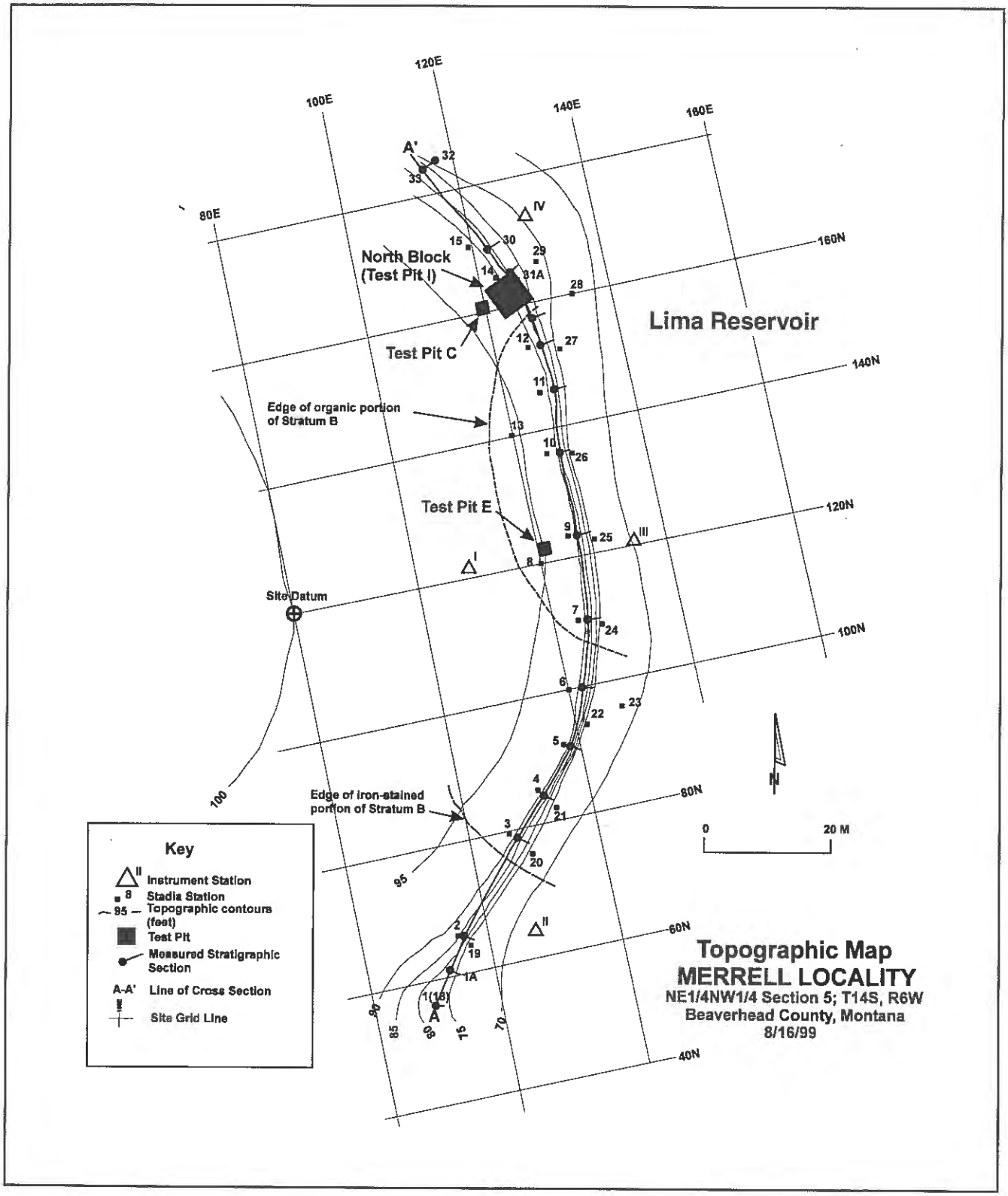

Figure 16. Topographic map and site grid of Merrell Locality (by J. Albanese). Test Pit E is slightly west of main South Block excavations conducted in 1995 and 1996.

ally limestone). Some pebble lenses also contain a coarse sand fraction. This unit commonly displays a closely spaced (2-5 cm [ca. 0.8-2.0 in]) rectangular "joint" system that contains "limonitic" staining along planar surfaces. A basal 110+ cm (3.6 ft) thick bed composed of light green, massive, clayey silt is present at Station 2. This facies was not observed north of Station 2. It may have accumulated in a lacustrine environment. At Station 14, located at the northern end of the site (see Figures 16 and 17), two types of sediment, different from those previously described, are exposed in the scarp face. These are labeled sub-stratum A(1) and A(2), with A(1) being the lower. Sub-stratum A(2) is 30-41 cm (ca. 12-16 in) thick and consists of sand with intermixed pebbles and cobbles (up to 20 cm [ca. 8 in] long) composed of limestone and quartzite. Underlying sub-stratum A(1) is 20+ cm (ca. 8 in) thick and is composed of thin-bedded (2-4 cm [ca. 0.8-1.6 in]), clean, well-sorted sand. See Appendix B for details regarding A(1) and A(2).

Stratum A is obviously a complex sequence composed of different, interfingering sedimentary facies. Most of it was probably deposited as alluvium under a low flow regime, but portions may be lacustrine (Station 2) in origin; some appear to have formed as colluvium or possibly as a debris flow.

to a sandy, very-fine, silty clay. In Test Pit/Excavation Area E (see Figure 16 for location), where it has been highly affected by soft sediment deformation, Hill (1995, this report) has described this unit in detail. LD1 (equivalent to stratum A) and LD2 (equivalent to stratum B) interfinger and splay as a result of deformation. Their combined thickness in Test Pit/Excavation Area E varies from 58 to 117 cm (ca. 2-3.8 ft). A mammoth tooth was present at the boundary between LD1 (lower) and LD2. Another isolated mammoth tooth was excavated in the center of LD2 (stratum 2), which is the darker of the two sub-strata and also contains the higher organic content (6-8%) (Hill 1995). A radiocarbon date of 36,520 ± 710 ^{14}C yr B.P. (Beta-74032) was secured from non-collagen organics extracted from a mammoth bone obtained from LD2 within stratum B.

Organic-rich stratum B (LD2) is displayed along 53 m (174 ft) of scarp face. It disappears, by truncation, at a point 38 m (125 ft) north of Test Pit/Excavation Area E. It "fades out" and merges into a "limonitic" stained, 125-cm-thick horizon at a point 15 m (49 ft) south of Test Pit/Excavation Area E. This "limonitic" horizon can be traced farther to the south for a distance of 36 m (118 ft), where it "rises" topographically and is truncated several meters south of Station 3 (see Figures 16 and 17). This "limo-

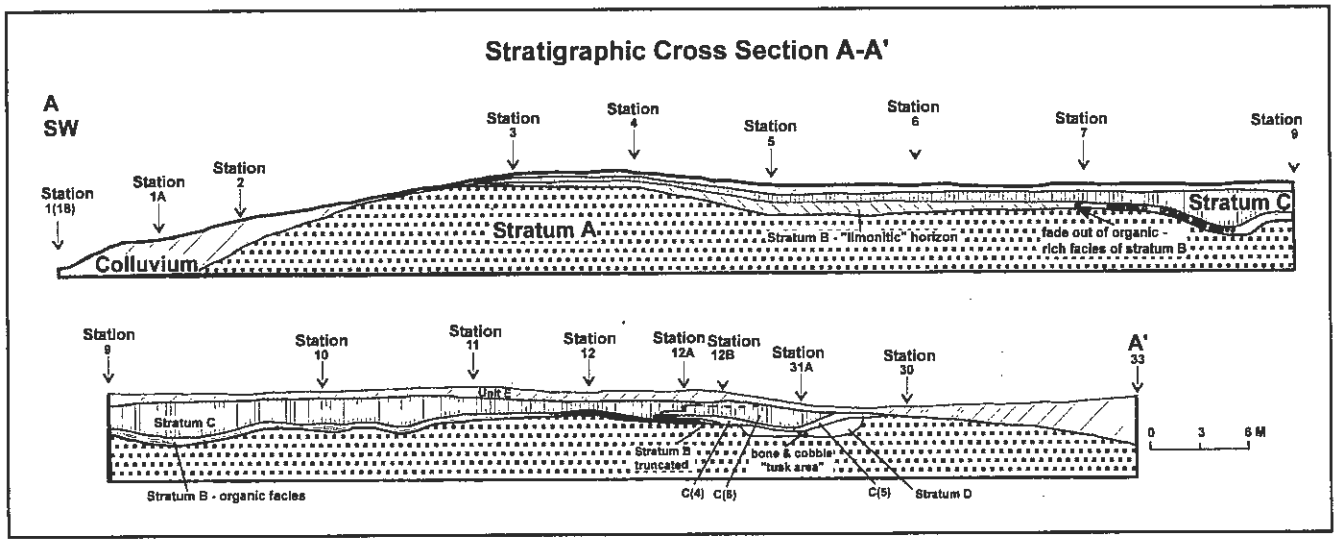

Figure 17. Stratigraphic section A-A' (by J. Albanese).

Stratum B (Pleistocene) - This is one of the two units that commonly contains vertebrate fossils. It unconformably overlies stratum A and varies in thickness from 30 to 120 cm (ca. 1-4 ft). Much of the variation in thickness is due to soft sediment deformation. Stratum B is a dark grayish brown, organic-rich, "coarsely" laminated bed that laterally varies in composition from a very-fine-grained silty, clayey sand, to a sandy, very-fine clayey silt,

nitic" horizon is interpreted to be an oxidized, gley soil that is the lateral equivalent of the organic-rich portion (LD2) of stratum B. Stratum B is interpreted as having formed in a "water-logged" marsh contained within a dish-shaped, topographic depression that was 88 m (289 ft) long and 2-3 m (6.6-9.8 ft) deep. This was one of many similar, marsh-like features situated on or adjacent to an ancient floodplain of Red Rock Creek. The absence of stratum B

in Test Pit/Excavation Area C, located 5 m (16 ft) due west of the truncated edge of stratum B, indicates that the northwest portion of the depression within which stratum B accumulated had been removed by erosion and that this truncated edge of stratum B is oriented to the northeast (see Figure 16).

Stratum C (Pleistocene) - This stratum can be traced for a horizontal distance of 87 m (285 ft) along the scarp face. It is absent several meters south of Station 3, due to truncation (see Figure 17). Along most of its exposure, stratum C is a fluvial sequence that consists of thin beds (0.5-4 cm [ca. 2-1.6 in]) and laminae of very-fine to fine-grained, silty clayey sand plus thin, 2-3 m (6.6-9.8 ft)-long interbeds containing ±1-cm (0.4 in)-long, rounded limestone pebbles and coarse sand. Sands grade laterally to sandy silts and clays. In Test Pit/Excavation Area E, Hill (1995) has subdivided stratum C into sub-strata LD3 (mostly silts) and LD4 (coarser clastic: sands and gravels), which have a combined thickness of 108-124 cm (3.5-4 ft). Both sub-strata consist of sands and pebbles and both contain shell fragments. LD4 is the coarser of the two and also contains ostracod shells. In the northern portion of the Merrell Locality, in the vicinity of Station 12A (see Figures 16 and 17), the thin-bedded alluvial facies of stratum C "merge" into a colluvial sequence that fills a broad, channel-like, topographic depression with a preserved maximum depth of 130 cm (4.4 ft) in the vicinity of Station 31A. The colluvial facies can locally be divided into two sub-strata, based on lithology and degree of $CaCO_3$ cementation.

The nature of the sedimentary succession exposed in Test Pit/Excavation Area C complicates the matter of stratum C stratigraphy. Easily identified stratum B is absent in this Test Pit, due to truncation; however, three other lithologic units are discernible (see Appendix B for detailed descriptions). One is stratum E (56 cm [22 in] thick) which unconformably overlies a 43-cm (17-in)-thick succession of thin-bedded sands and pebble lenses that is similar in appearance to stratum C in Test Pit/Excavation Area E. This thin-bedded sequence unconformably overlies a 183+ cm (6 ft)-thick deposit of massive, clayey, silty sand that grades to sandy silt. This interval contains ±1 percent disseminated pebbles and bone fragments (1-2 cm [0.4-0.8 in] long). On the basis of lithology, this interval would be placed within stratum A; however, the presence of bone fragments suggests that at least part of the sediment may have been derived from eroded portions of stratum B. If all of the sediment of stratum C beneath stratum E is lumped into stratum C, the thickness of stratum C in Test Pit/Excavation Area C would be 226+ cm (7.4 ft), in contrast to the ±120 cm (ca. 4 ft) of stratum C present in Test Pit/Excavation Area E. Soft sediment deformation in stratum C is not sufficiently pronounced to explain the difference in thicknesses between the two locales. Resolution of the correlation problem will require additional exposures.

Stratum D (Pleistocene) - This is the other major vertebrate bone-bearing unit present at the Merrell Locality. It is also the most restricted of the strata in occurrence, and, in 1994, was noted only at the northern end of the site in the vicinity of Station 31A. Here, it lies 139 cm (4.5 ft) beneath the surface and is only 21-60 cm (ca. 8-24 in) thick and ±7 m (23 ft) wide (see Figures 16 and 17). It unconformably overlies stratum A. The contact between the two units slopes ±25° to the east. Stratum D is composed of silty, clayey sand, cobbles, pebbles, bones, and bone fragments (principally of mammoth). Field observations in 1994 indicated that it had probably formed as a debris flow since the axes of long bones are generally parallel to the contact between stratum D and stratum A. Stratum D was inferred to have accumulated on the floor of an arroyo-type channel that was incised into strata C and A.

In 1995, a 5 x 5-m (ca. 16 x 16 ft) area designated as the North Block (or Excavation Area I) was excavated in the vicinity of Station 31A (see Figures 18-21). The depth of this excavation varied from 1.4 to 1.8 m (4.6-5.9 ft) below ground surface (bgs). Excavation penetrated stratum D to a depth of 20-80 cm (ca. 8-77 in) below its upper contact. Stratum D is mainly composed of silty, clayey sand, and randomly distributed, isolated cobbles and pebbles. These latter coarse clasts vary from 3 to 25 cm (1.2-9.8 in) in length. The average clast length and standard deviation is 9.6 ± 4.6 cm (3.8 ± 1.8 in) (n = 40). Approximately 95 percent of the cobbles and pebbles are composed of limestone, chiefly micritic. The remainder of the coarse clasts are composed of quartzite. Two quartzite cobbles measured 20 x 12 x 14 cm (7.8 x 4.7 x 5.5 in) and 25 x 23 x 4 cm (9.8 x 9 x 1.6 in).

In addition to the above-described sediment, stratum D also consists of aggregations composed chiefly of cobbles and intermixed mammoth bone. The largest observed aggregation was the one observed in 1994 at the surface exposure located at Station 31A. After excavation in 1995, this individual deposit of bones and cobbles was found to measure 150 x 100 x 50 cm (4.9 x 3.3 x 1.6 ft). Excavation also revealed that this aggregation, along with others, rests on an irregular erosional surface with an overall inclination of ± 25° to the east (see Figures 19-21). This surface forms the head of a paleo-arroyo within which the debris flow sediments of stratum D had accumulated. The preserved portion of the paleo-arroyo is approximately 7 m (23 ft) wide and ± 1 m (3.3 ft) thick. The upper portion of the paleo-arroyo was removed by erosion at some time after debris-flow sedimentation ceased. Subsequently, a broad

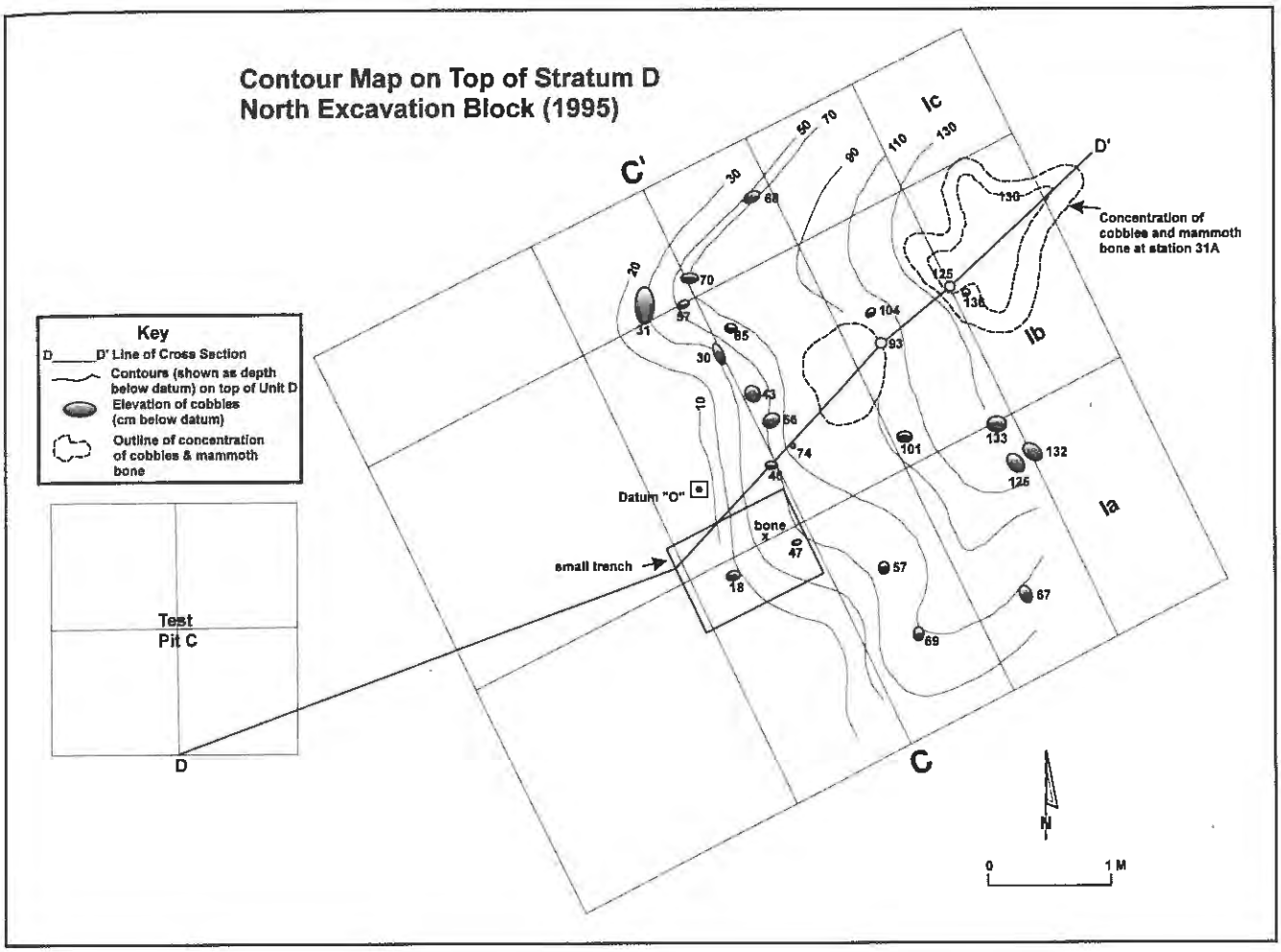

Figure 18. Map of 1995 North Block (Excavation Area I) (by J. Albanese).

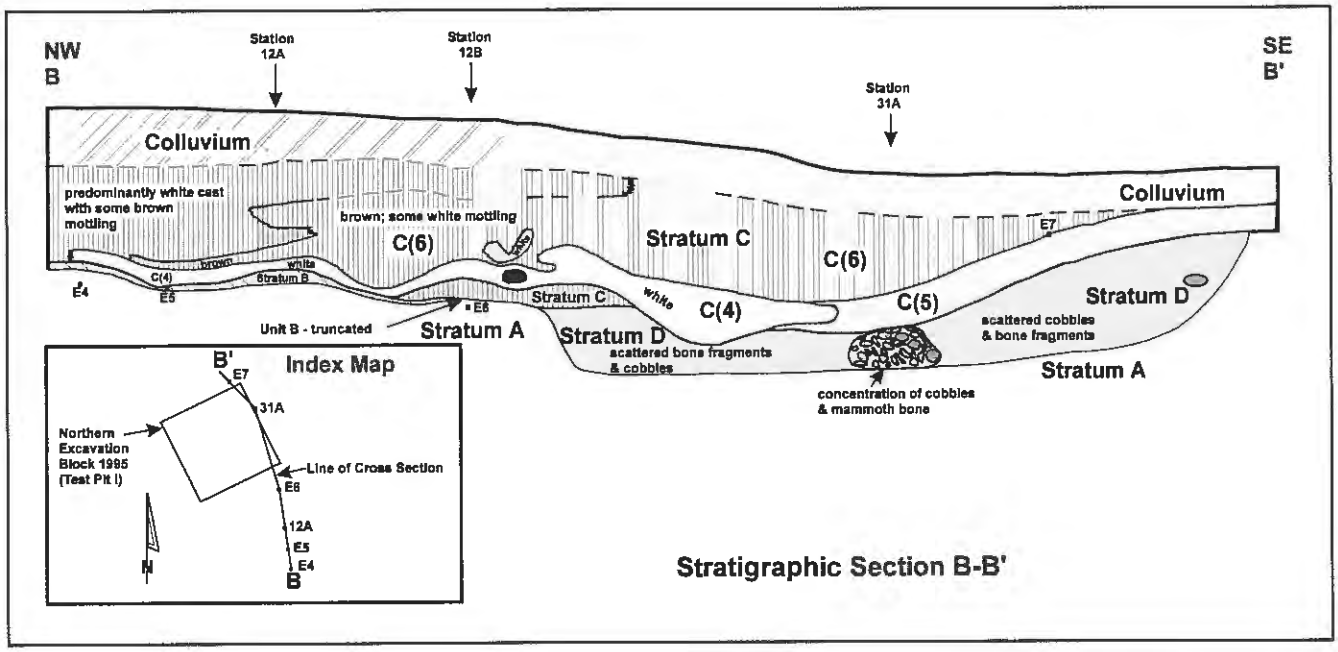

Figure 19. Stratigraphic section B-B' (by J. Albanese).

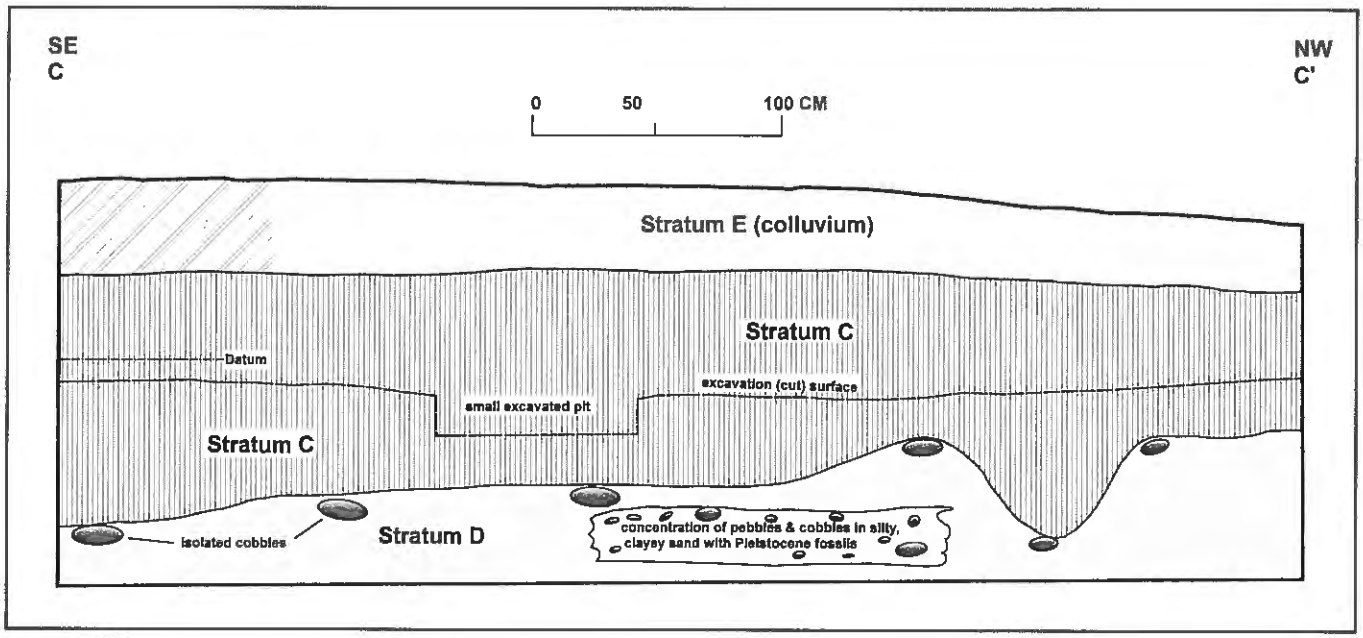

Figure 20. Stratigraphic section C-C' (by J. Albanese).

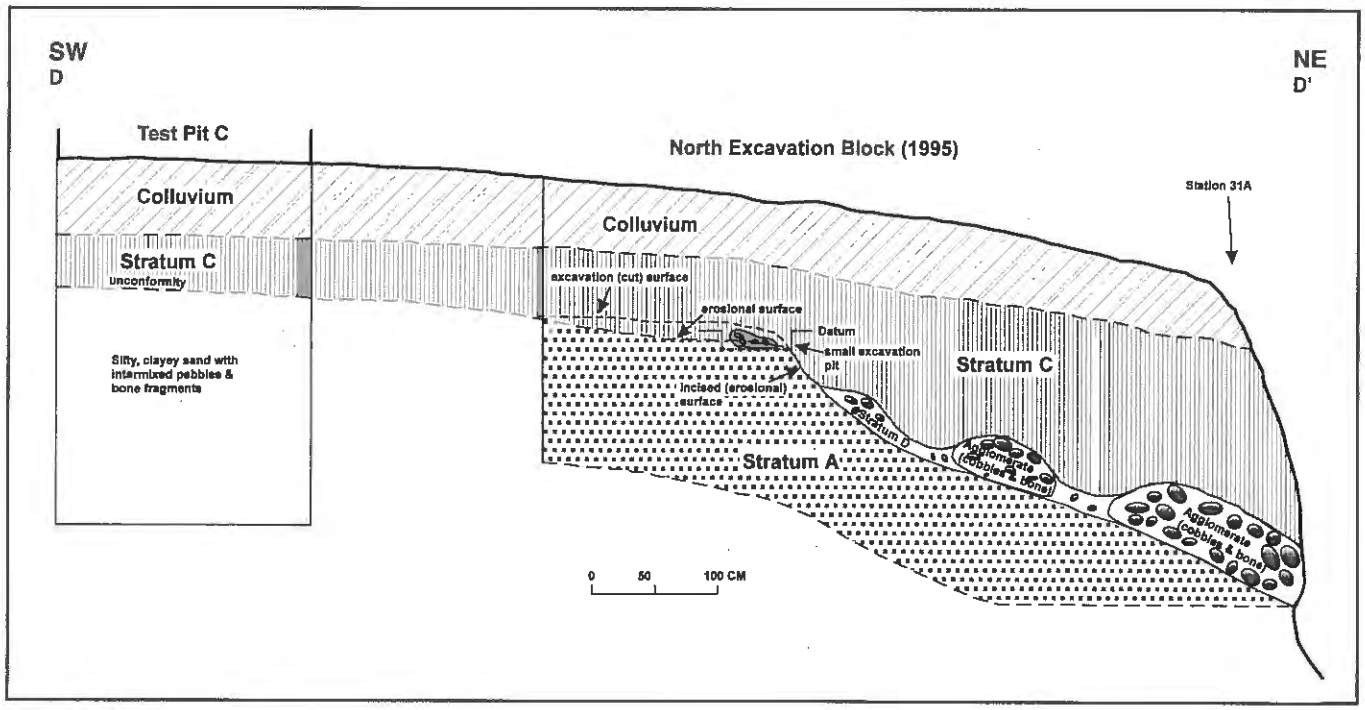

Figure 21. Stratigraphic section D-D' (by J. Albanese).

swale had formed in the vicinity of Station 31A. This feature, which was ± 24 m (78 ft) wide and ± 2.5 m (8.2 ft) deep, was later filled with the colluvial sediment facies of stratum C.

One (at least) unresolved problem remains in regard to the stratigraphic relationship between stratum D and underlying sediment. At the 1994 surface exposure in the vicinity of Station 31A, it was obvious that stratum D rested on stratum A. However, in the North Block, the 1995 penetration into stratum D was not deep enough to absolutely identify the sediment that underlies the stratum. In stratum C, which lies <1.5 m (4.9 ft) west of the North Block, stratum D cannot be definitely identified. As previously discussed in this paper, stratum C is only ±43 cm (17 in) thick and unconformably overlies 183+ cm (6 ft) of sediment that contains pebbles and bone scraps. If this latter

sedimentary unit underlies that portion of stratum D exposed in the North Block, one has to resort to stratigraphic and spatial "manipulation" to fit everything together. To resolve this problem, one would have to go back into the field. However, the 1995 excavations did prove that mammoth bone within stratum D was disarticulated, was contained within debris flow deposits, and was not abundant.

A radiocarbon age of 19,310 ± 90 ^{14}C yr B.P. (Beta-77826) was obtained from a mammoth bone excavated from stratum D. This date is considerably younger than the radiocarbon date of 36,520 ± 710 ^{14}C yr B.P. obtained from bone within stratum B in Test Pit/Excavation Area E. However, since stratum D had accumulated in an arroyo-type of depression, there is no problem in reconciling the two dates. Dundas (1992) reports the presence of bones, including the Pleistocene scimitar cat, *Homotherium serum*, from the Merrell Locality. He also reports the presence of bones within a channel fill deposit located at the western end of the Merrell Site: "A pure quartz sand lens and a gravel-boulder channel lag deposit occur on the west end of the terrace." A date of 25,030 ± 510 ^{14}C yr B.P. (Beta-26205) was secured from a "mammoth metatarsal" collected from the channel-fill deposit. This occurrence is almost certainly located in the vicinity of Station 31A. The "pure quartz sand lens" corresponds with sub-stratum A(1) and the "gravel-boulder channel deposit" would correspond to stratum D. The "west end" of the site referred to by Dundas would be more correctly termed the northwest end. The date of ca. 25,000 ^{14}C yr B.P. cited by Dundas (1992) does not differ greatly from the ca. 19,300 ^{14}C yr B.P. date obtained by the Museum of the Rockies. Additional details concerning the chronologic context of these deposits are presented in Feathers (this report) and Hill (this report).

Stratum E (Holocene) - This is the youngest sedimentary stratum and it is present throughout the Merrell Locality. It is a massive, colluvial deposit that unconformably overlies all older strata. It varies from 10 to 280+ cm (4 in to 9.2 ft) in thickness and consists of sand that varies from very-fine to medium in grain size and contains clay and silt fractions. The stratum also contains well-rounded, randomly distributed pebbles (chiefly limestone) that range up to 10 cm (4 in) in length. The percentage of pebbles within the sand varies from zero to 15 percent, depending on locale.

Other Studies

At the end of the 1994 field season, one afternoon was spent viewing sediments exposed along the lake shore in the area located south of and within 600 m (1,968 ft) of the Merrell Site. This very brief and limited reconnaissance revealed that the mode of deposition of the various strata is quite varied. Sediment types consist of alluvium, lacustrine, and colluvium/debris flows. At Locality 3 (see Figure 2 and Appendix B), an upward sucession from coarse-grained to fine-grained alluvium to fine-grained lacustrine sediment is present. At Locality 2, a thick deposit of coarse colluvium/debris flow sediment is "sandwiched" between beds of fine-grained alluvium. The bulk of the sediment exposed in the area located to the south of the Merrell Site appears ro be correlatable with stratum A at the site.

Soft Sediment Deformation

All stratigraphic units, except for stratum E, exhibit examples of soft sediment deformation, both on outcrop exposures and in excavation pits. The most evident example, present in the shoreline scarp, is the thickening, thinning undulations and folding involving stratum B. This conspicuous, dark outcrop "band" varies in thickness from 30 to 60 cm (1-2 ft) and displays inclinations from 5° to 20° (see Plate 3). "Flame structure" folds with amplitudes of 46 cm (1.5 ft) were observed within stratum A at Station 12. The best displays of soft sediment deformation were observed in Test Pits/Excavation Area C and E. They are most conspicuous in Test Pit/Excavation Area E, where Hill (1995) describes examples of interdigitation and splaying between sub-strata LD1 through LD4 (strata A, B, and C) and microfaults (normal) within sub-strata LD1 and LD2 (strata A and B). These intrusive features had apparently formed when the whole sedimentary section was water-saturated and plastic. If one could examine all portions of the sedimentary column at the Merrell Locality, one would probably find that the deformation structures are the most striking of any of the physical features present in the preserved sediments.

Soils

No attempt was made to examine the soils at the Merrell Site in detail. Bump (1989) conducted fieldwork at the site and described the fossils, soils, vegetation, and general setting. He described a 277-cm (9-ft)-thick soil profile that covers strata E, C, and B, and the upper portion of stratum A. The horizons within the profile are Ak (0-15 cm), Bk1 (15-33 cm [6-13 in]), Btk1 (33-50 cm [13-20 in]), Btk2 (50-79 cm [20-31 in]), Bk4 (79-178 cm [31-70 in]), 2 Cr (178-228 cm [70-90 in]), 3Ab (228-277 cm [90-109 in]), and 4 Crk (277+cm [109 in]). Horizons Ak, Bk1, and Btk1 are superimposed on stratum E, while Horizons Btk2, Bk4, and 2Cr lie within the interval occupied

by stratum C. Horizon 3Ab coincides with stratum B, while 4Crk is superimposed on the upper portion of stratum A. Bump (1989) classified the 3AB-horizon as a Cryaquoll soil that had "formed around shallow, intermittent ponds in closed depressions." At the Merrell Locality, they "were formed on low terraces on or near the Red Rock River floodplain."

As Bump (1989) points out, pedogenic $CaCO_3$ is a dominant constituent in soils at the Merrell Locality. Ak, Bk, and Ck soil horizons are prevalent in strata E and C at all locales (see Appendix B) and had probably formed under a modern-type of climatic regime.

A ubiquitous pedogenic feature in all units is a light brown ("limonitic") iron oxide stain. Its presence has already been referred to in the discussion concerning stratum B. The iron oxide stain was referred to as "limonitic" in previous portions of this paper; however, it is realized that the mineral stain may not be pure limonite, but could also be, wholly or in part, another iron oxide compound. However, the word "limonite" is used for ease of description. Iron oxide stain in soils and bedrock in soils and bedrock can form by oxidization of minerals or soils with a high iron content, e.g., oxidized gley soil formed by a vertically fluctuating water table. "Limonitic" staining can also result from the transport of soluble iron compounds in ground water and subsequent precipitation. In most cases, "limonitic" staining forms in a water-saturated environment and its presence indicates relatively high water tables, a situation that obviously existed in the past at the Merrell Locality.

Summary

The sediments exposed at the Merrell Locality, except for stratum E, are Pleistocene in age and were deposited in an environment cooler and more moist than the present. Hill (1995, this report) presents a detailed resume concerning past variations in climatic regimes, glaciation, and types of sedimentation. Glacial deposits are not conspicuous on the Centennial Valley floor, but lacustrine deposits have been documented. Extensive lakes covered the valley floor during the Late Pliocene and Early Pleistocene (Mannick 1980). Sonderegger et al. (1982) report the presence of a lake (or lakes) that covered most of the Centennial Valley ca. 12,000-10,000 B.P.

The presence of lacustrine beds in the area located ±600 m (1,968 ft) south of the Merrell Site also suggests the presence of lakes in the area during the same general time period that the sediments of stratum A at the Merrell Locality were being deposited.

Glacial deposits per se are not present at the Merrell Locality. The bulk of the sediment at the site appears to have formed on or near the floodplain of Red Rock Creek, as alluvium deposited under a low flow regime. The bulk of stratum C sediment was probably deposited under shallow, braided-stream conditions. Stratum B had formed in a minor, marsh-filled, topographic depression located on or near an ancient floodplain of Red Rock Creek. The isolated marsh was probably one of many that dotted the nearly flat terrain along the valley margins. Stratum A is a complex aggregation of alluvium, colluvium, and possibly lacustrine sediment. The largest portion of the stratum was deposited under a low flow regime by shallow braided streams (thin gravels), as overbank sediments, or possibly under a slack water, flooding environment. No river channel sands per se are present at the site. The alluvial sediment was deposited under shallow conditions away from the main river channel or center of stream transport. The question of whether there are lacustrine sediments within stratum A at the Merrell Locality is open to further investigation. The light green massive silts present in stratum A at Station 2 may be lacustrine, but a more detailed examination is warranted.

Sediment of colluvial and debris-flow origin is locally present in strata A and C. This indicates that the Merrell Locality has been at or close to the edge of the Centennial Valley alluvial plain throughout that portion of the Pleistocene represented by the exposed strata. The presence of an arroyo or deep-sided draw, within which stratum D was deposited, also testifies to the proximity of a valley margin. The presence of thick colluvium/debris flow deposits that are stratigraphically equivalent to stratum A in the area south of the Merrell Locality (see Appendix B) is additional evidence that the outer slopes of the Red Rock Creek Valley were unstable at times during the Late Pleistocene.

However, one could also surmise that this was the case during portions of the Pleistocene by merely looking at the U. S. Geological Survey Topographic Quad Sheet, "Lima Dam-1968," which shows that the Merrell Site lies at the edge of the narrowest (±1 km [0.62 mi]) portion of the Centennial Valley. In fact, this close proximity to the center of the valley and to an ancient river channel (or channels) makes one wonder why more evidence of a major channel or channels is not present at the site. Has the river system been a very shallow, braided, low-energy system for the past 40,000+ years?

Spatial Distribution of Pleistocene and Holocene Faunal Remains, South Block Excavations

Christopher L. Hill and David C. Batten

Introduction

The fossil remains of mammoth and other Pleistocene fauna found along and near the escarpment of the west shore of Lima Reservoir in Centennial Valley have been the subject of field investigations since the 1980s. Summaries of earlier studies conducted at the locality are presented in various published and unpublished sources, including Albanese, Davis, and Hill (1995), Bump (1990), Davis and Batten (1996), Dundas (1989, 1990, 1996), Hill and Albanese (1996), and Hill, Davis, and Albanese (1995).

The spatial distribution of Pleistocene-age and Holocene-age fossils recovered during the Museum of the Rockies' (MOR) 1994-1996 excavations provides information pertinent to the stratigraphic and taphonomic interpretation of the Merrell Locality. The South Block designates excavations conducted within the site grid 120-140N. It includes Test Pit/Excavation Area E (excavated in 1994) and Excavation Areas J-X (excavated in 1995-1996) (Figures 4, 11, and 22). In this paper, each 2 x 2-m excavation square or portion of a 2 x 2-m test pit or excavation square aligned with the site grid in the South Block is referred to by the term "Excavation" or "Excavation Area" and a letter designation. These correspond to a grid location in the southwest corner of the 2 x 2. For example, Excavation Area K is the 2 x 2-m square with its southwest corner located at 123N/125E. Each 2 x 2-m square was divided into four 1 x 1-m quadrants, which were referred to by the letter and a lower case directional quadrant label, i.e., quadrant Knw is the northwestern quadrant of Excavation Area K, and its southwest corner is located at 124N/125E (see Table 2). Unless otherwise indicated, directions refer to an orientation based on grid north (Figure 4). Only the west halves of Excavation Areas J-P were studied since the east halves of these Excavated Areas had been destroyed by erosion. The escarpment adjacent to the reservoir exists between grid line 125E and grid line 126E and marks the location of active erosion.

Data pertaining to the spatial location of fossils in this area were derived from standardized field records compiled during each of the three field seasons under supervision by Batten (see Batten 1994, 1995, 1996). The locations of fossils recovered from 1994 and 1995 were initially compiled and placed on a master grid by Hill. This compilation was then reviewed and corrected by Batten. Throughout this report, the designation of fossils collected by MOR follows primarily the identifications available in Dundas (this report), although subsequent studies of the mammal collection have been undertaken by Hill. The locations of fossils recovered in 1996 were superimposed on this grid using the standardized field records and information documented in Batten and Davis (1996). There is the possibility of a fairly secure assessment of the associations of fossils and lithostratigraphic contexts from the 1996 excavations because of the practice of collecting paired fossil and sediment field specimens (see inventory in Batten and Davis 1996) and the placement of excavation level markers on the stratigraphic exposures.

Additional observations on the stratigraphic context of the South Block were made by Hill during geologic studies between 1994 and 2001; besides interpretations in this paper, those observations are partially summarized in Hill (this report).

Figure 22. Excavations during the 1995 field season of the South Block, Merrell Locality (C. L. Hill photo).

Spatial Distribution of Faunal Remains

Information regarding the spatial distribution of bones recovered from the Merrell Site is available from a variety of sources. Prior to the MOR excavations, spatially controlled excavations were made under the auspices of the Bureau of Land Management (BLM) by Robert Bump, and the University of Montana (UM) under the direction of Tom Foor. A draft report of the fieldwork completed in 1988 and 1989 by Bump is on file at the Dillon, Montana office of the BLM (Bump 1990). Details concerning the UM studies are derived from notations made by Foor on a topographic map of the locality drafted by Troy Helmick for the MOR. Additional information was provided by Robert Dundas in the form of an inventory connecting the notations made by Foor with fossils recovered during these excavations. Based on discussions with Dundas in September of 1997, additional information may be available that would allow the investigations made by the UM to be correlated with the MOR project's stratigraphic descriptions and interpretations.

The 1994-1996 MOR investigations included testing in areas designated Excavation Areas E, J-X, a backhoe trench, and along the escarpment (Figure 11). These sources provide data regarding the vertical and horizontal arrangement as well as the general stratigraphic context of the fossils. Bones were recovered throughout the sequence of sedimentary deposits studied.

Faunal Remains Recovered from the South Block Area Prior to 1994

Based on Map 2 in the 1989 Bump report, long bones of mammoth were recovered during excavations in the vicinity of what is now designated the South Block (Figure 11). The general location of the profile described by Bump was verified during his visit to the locality in 1996. The approximate horizontal location of these bones would be along the escarpment intersection with MOR grid coordinate 121N (Figure 16). Besides in situ fossil material, bones were also recovered along the beach in front of the escarpment. These fossils can be assigned a tentative horizontal provenience by correlating Bump's soil study with the stratigraphic sequence described by the MOR (Hill 1995, this report; Albanese, this report). Bump observed Pleistocene vertebrate fossils in level 3 and underlying level 4. Level 3 is thought to be equivalent to the lowermost organic facies of stratum B (=local lithology 2a at Test Pit/Excavation Area E), and level 4 is interpreted as probably equivalent to the top of stratum A. Bump observed the presence of impressions made by bone within the stratum A equivalent sediments when the long bones of mammoth were removed. Similar bone impressions in the sediments were observed during the MOR excavations. The bones observed in stratum A were interpreted by Bump as having original context in stratum B; he proposed that the bones had been displaced downward into stratum A through cracks or faults.

Remains of mammoth were recovered by the UM along the escarpment in the vicinity of the MOR South Block (F18 and A103, UM Paleontology Collections, Department of Anthropology field record, data from T. Foor and R. Dundas). It might be possible to connect the horizontal and vertical locations of those materials with the MOR studies using records not available at the time this paper was written.

Spatial Distribution of Faunal Remains from Museum of the Rockies Excavations

Both horizontal and vertical information are available for fossils collected during the MOR excavation in the South Block (Figure 23). Details are provided in a series of summaries developed after each field season (Batten 1994, 1996; Batten and Davis 1996) as well as the field records and forms archived at the MOR. In general terms, both vertical and horizontal control over the location of fossils is predicated either on (1) the direct measurement of specimens in relation to a three-dimensional site grid or (2) recovery as part of a collection of materials found within an excavation interval of known thickness within a known coordinate location in the site grid. In many instances, there is also the possibility that the fossil specimens can be placed within the context of the sedimentary matrix. However, especially in regard to materials not recovered in situ, assemblages of specimens collected from some excavation intervals may represent fossils derived from several different sedimentary deposits.

Description and Interpretation of Spatial Distribution of Faunal Remains

The approximate horizontal distribution of fossils mapped in situ within the South Block is presented in Figures 23-25. The maps are based on data available in the field records of the 1994-1996 MOR excavations. The taxonomic designation of fossils follows essentially the identifications made by Dundas (1996, 1997, this report).

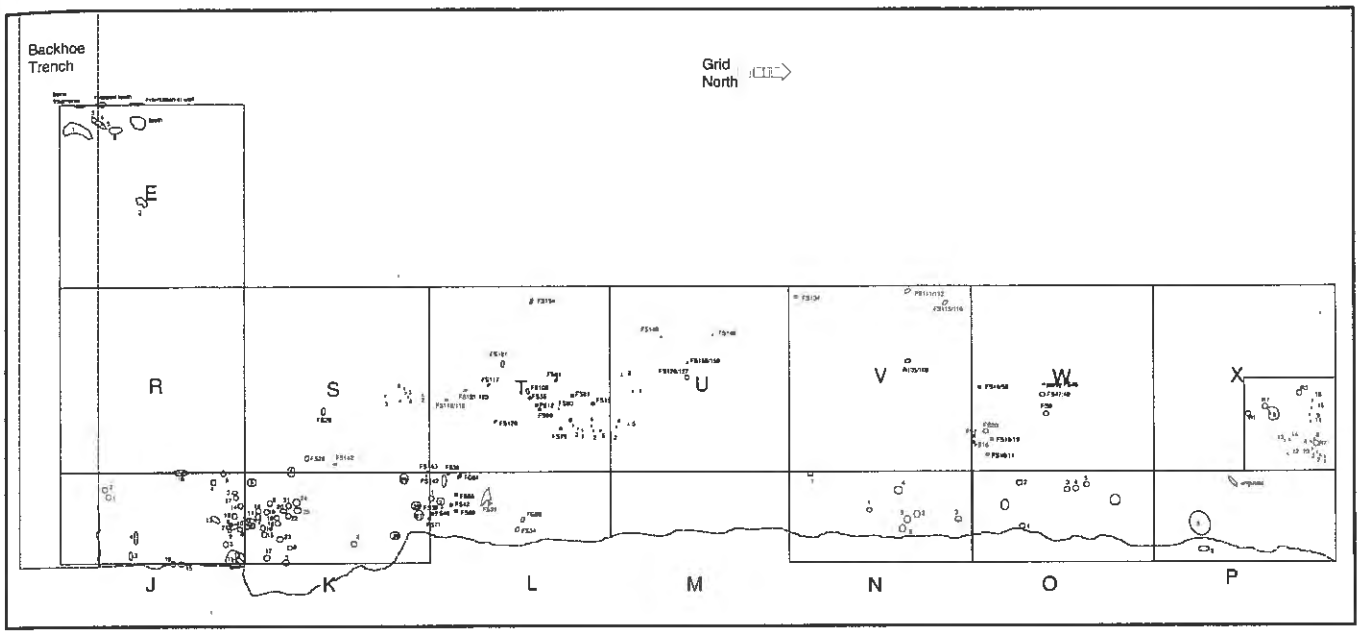

Figure 23. Spatial distribution of fossils at South Block, Merrell Locality (compiled by C. L. Hill).

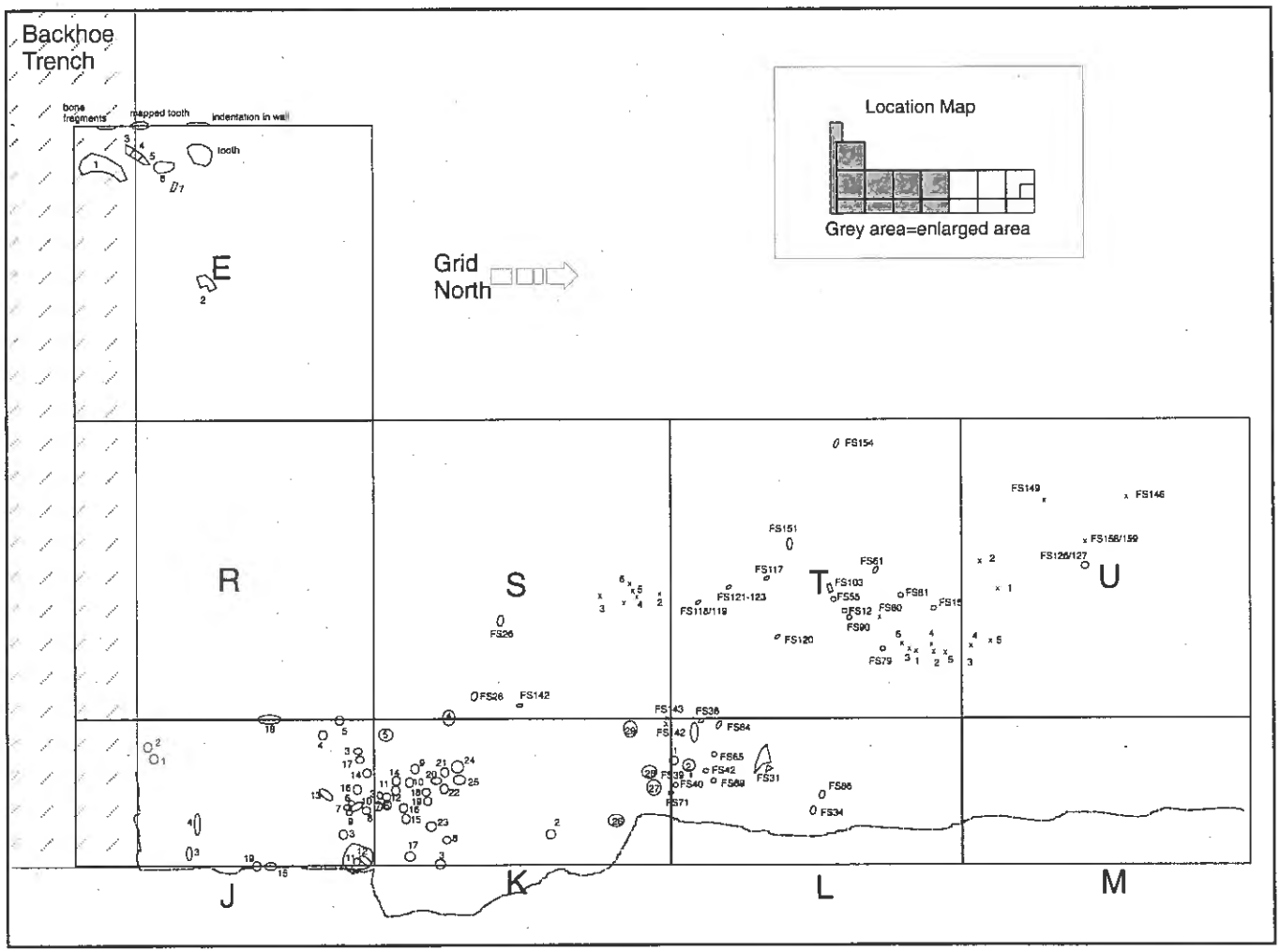

Figure 24. Spatial distribution of fossils in Excavation Areas E, J-M, and R-U, South Block (compiled by C. L. Hill).

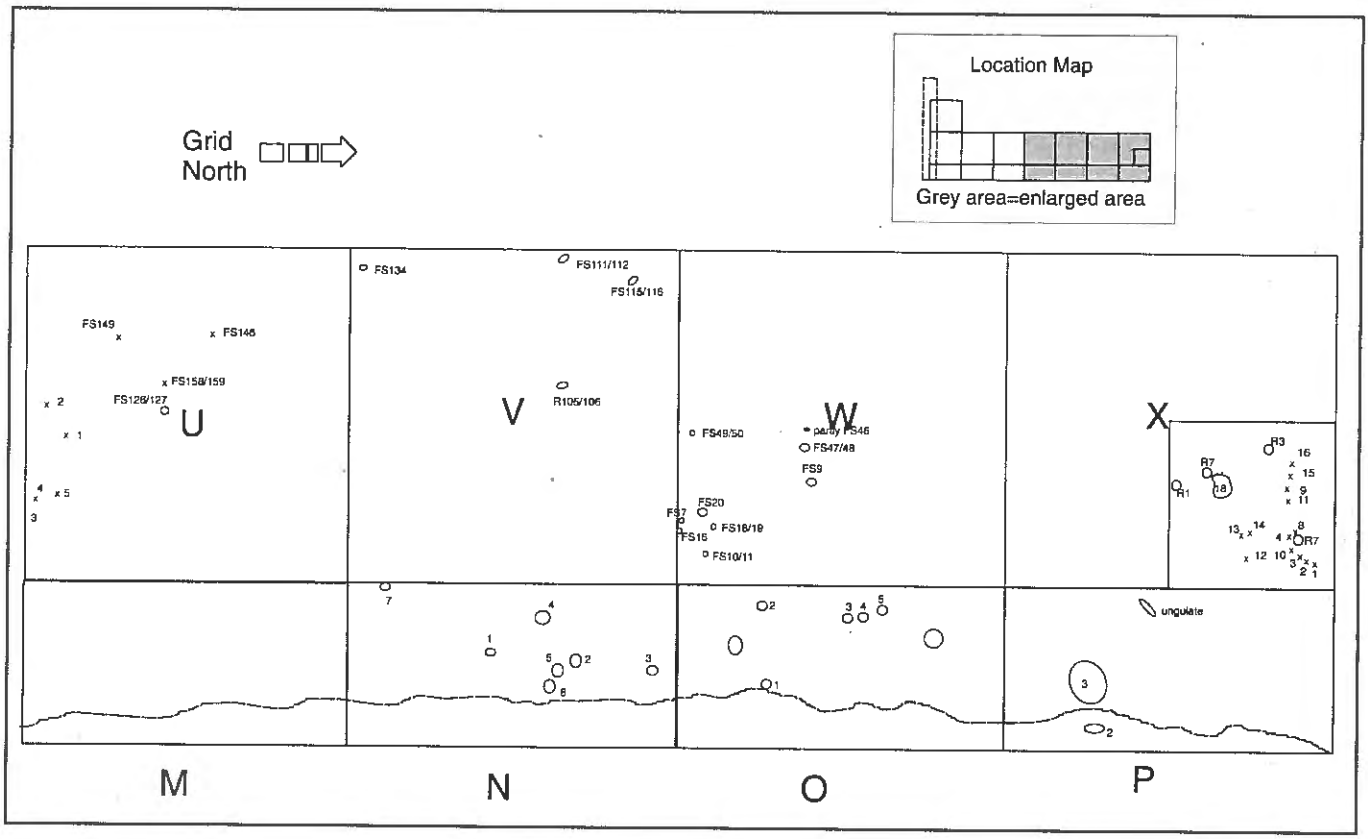

Figure 25. Spatial distribution of fossils in Excavation Areas M-P and U-X, South Block (compiled by C. L. Hill).

Excavation Area E

Excavation Area E (referred to as 1994 Test Pit E in Davis et al. 1995) was situated at approximately 121-123N/121-123E on the site grid (Figures 4 and 11). The landform surface in this vicinity slopes toward the south and east. Thus, the surface elevation of the SW corner of Excavation Area E at about 2,012.15 masl (6,601 fasl) is about 5 cm (2 in) lower than the NW corner, about 9 cm (3.5 in) higher than the NE corner, and 23 cm (9 in) higher than the SE corner at ground surface. Depth elevations for the 1994 MOR excavations were measured with reference to these known surface elevations. (Whenever depths are referred to, they should be understood to be depths below ground surface [b.s.].) In terms of the spatial distribution of fossils, the excavations in Excavation Area E are important because they provide an indication of the kinds of fossils recovered throughout the entire South Block sedimentary sequence (including a screened sample of the entire thickness of stratum C).

Two forms of mixing are potentially indicated within Test Pit/Excavation Area E. From level 20 and above, the presence of Holocene-age ground squirrel remains, as well as sedimentary structures thought to be the result of rodent burrowing, hint at the possibility of fossil movement due to bioturbation. Faulting and liquefaction features also indicated potential for the redistribution of fossils within the sequence.

In the northern half of the excavation (En), stratum C (primarily silty sediments with lenses of sands and gravels) Hill (1995, this report) characterized the sequence to about 150-160 cm (59-63 in) b.s. At about this depth, pockets of a darker, generally reddish brown dark silt (referred to as "dark red clay" in some of the excavation field records) began to be observed, indicating the presence of the upper facies of stratum B. In the south half of the excavation (Es), gravels or sands of stratum C were still present at 150-170 cm (59-67 in) b.s., with the upper facies of stratum B dominating below about 160 cm b.s. Above this, the faunal remains generally can be attributed to either (1) the uppermost colluvium, (2) stratum C (either of the local lithofacies of coarser clastics or silts), and/or (3) areas of bioturbation (Figure 26).

Within levels 1-20, in both the north half and the south half of the excavation (En and Es), ground squirrel (*Spermophilus* sp., Dundas, this report) bones were found. These appear to be Holocene-age bones and are one indication of the degree of bioturbation that has affected the Excavation E sequence. Remains of muskrat (*Ondatra*

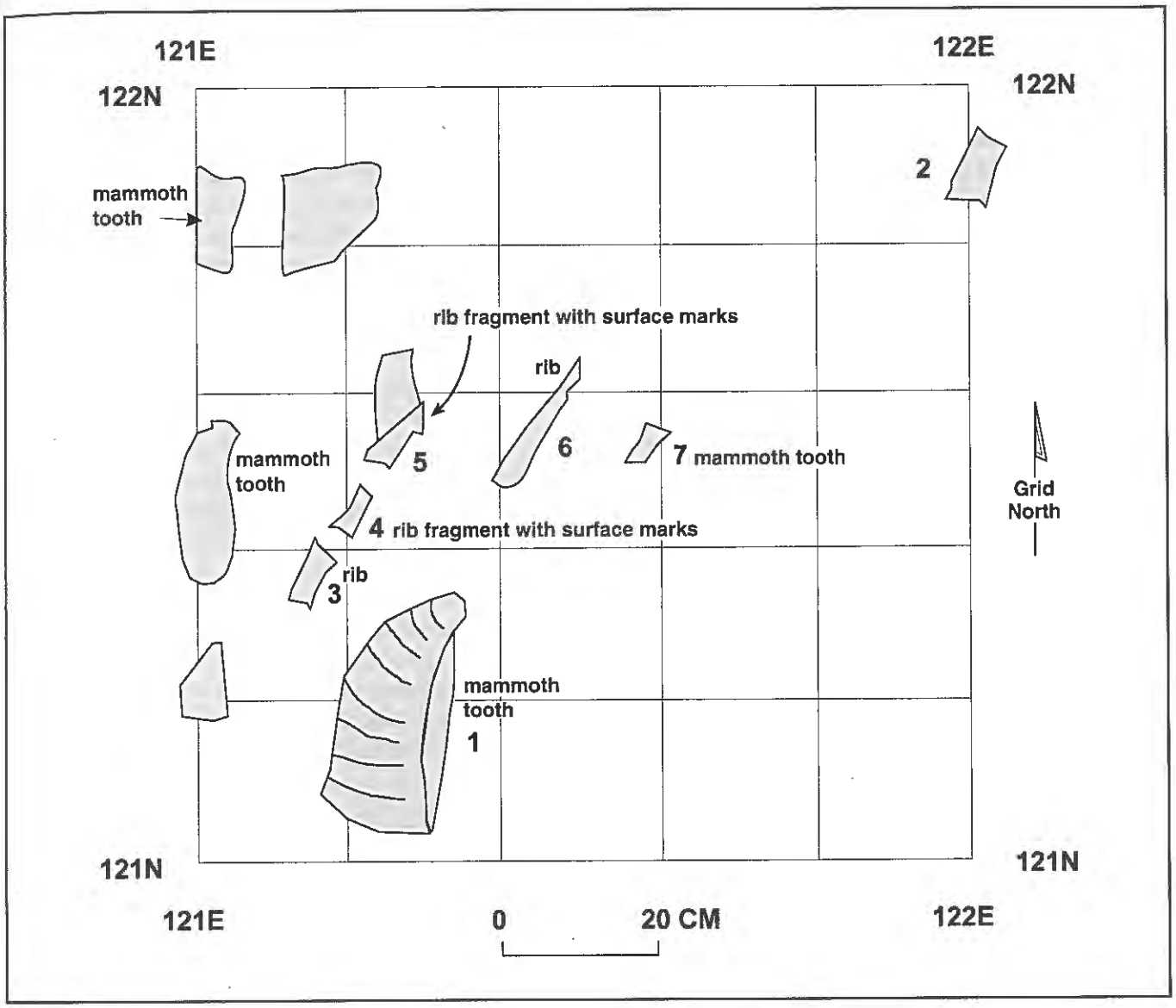

Figure 26. Remains of mammoth mapped in Test Pit/Excavation Area E, South Block (compiled by C. L. Hill).

zibethicus) were recovered in Es level 7 and near the bottom of Es level 25; bones perhaps of a pocket gopher (cf. *Thomomys*) were found in Es level 11.

Remains of mammoth were recovered in two "sets." The upper set consists of four excavation intervals found only in En between levels 8 and 17. Level 8 (70-80 cm [27-31 in] b.s.) contained a limb bone fragment possibly referable to mammoth (*Mammuthus* sp., Dundas, this report). Level 12 contained fragments of a mammoth molar (Dundas, this report). Level 14 (in En) also contained fragments of enamel referable to mammoth (Dundas, this report). Finally, mammoth remains were also recovered from level 17. Except for the lowermost specimen, these mammoth remains are probably either derived from stratum C or had been moved into this part of the sedimentary sequence, perhaps principally by burrowing ground squirrels. The level 17 (about 160-170 cm [63-67 in] b.s.) remains could be attributable to stratum B.

The lower set of mammoth remains was found in levels 25-27 in both halves of the 2 x 2. Within Es level 25 (depth 240-250 cm [94-98 in] b.s.), a mammoth tooth fragment (specimen Es-25-1) and a rib (specimen Es-25-3) were found in the dark-colored sediments of stratum B (Figures 24 and 26). Excavation Area En level 26 contained fragments of rib (En-26-3), tusk (specimen En-26-1), teeth, and phalange probably attributable to mammoth (Dundas, this report), while Es level 26 contained mammoth tooth fragments (e.g., Es-26-7). This level contained sediments characteristic of both strata A and B. Thus, the remains of mammoth from level Es-26 are probably derived from stratum A, but could also be from stratum B. Level 27 also contained part of a mammoth tooth as well as tusk frag-

ments. The fossils were mostly in the lowermost portion of stratum B, but perhaps at least partially directly on sands of stratum A in the southwest corner of the excavation. Bones (including fragments of mammoth teeth, cf. Dundas, this report) recovered from Es level 27 (260-270 cm [102-106 in] b.s.) could be derived from either stratum B or stratum A, since dark-colored sediments were present on the east side of the excavation and sands were observed on the west side at that level.

Bone fragments of large ungulates (Dundas, this report) were found in En levels 6, 9, 15, 18, 20, and 21. A fragment of camel bone (*Camelops* sp.) was recovered from the north half of Excavation E at level 15 (specimen EN-15-2) (Dundas, this report). Below about 160 cm (En level 17, ca. 160-170 cm [63-67] b.s.), most faunal remains can likely be attributed to either stratum B or the top of stratum A, although bioturbation in the form of rodent burrows signals the possibility of intrusion and mixing. Below about 160 cm [63 in] b.s., the upper facies of stratum B were encountered and most of the fossils recovered can likely be attributed to these deposits (including a tooth fragment of a large ungulate recovered from level 18, ca. 170-180 cm [67-71 in] b.s.).

The presence of gravels within Excavation Area En levels 19 and 20 (180-210 cm [71-83 in] b.s.) indicates the possibility of fossils from stratum C in those levels. However, isolated gravels were also observed in stratum A. Several tooth fragments and bone were recovered from these levels, including the extreme distal end of a left humerus referable to duck (Anatidae) in level 20 (Dundas, this report).

The darker, more organic-rich facies of stratum B was observed during excavation of the En unit at ca. 220 cm [87 in] b.s. Small patches of gray sediments observed in level 24 (230-240 cm [90-95 in] b.s.) indicate the potential intrusion of stratum A deposits, although the lower facies of stratum B persists in the eastern half of the unit until level 27 (260-270 cm [102-106 in] b.s.). Excavation E level 25 contained a bivalve; bivalves are more commonly found in stratum C elsewhere at the Merrell Locality.

In Excavation Area Es, the lowest gravels (indicating the potential presence of fossils derived from stratum C) occur in level 19 (180-190 cm [71-75] b.s.). Above this, in level 7, a right calcaneum referable to muskrat (*Ondatra zibethicus*) was recovered (Dundas, this report). From about level 14 and below (at depth > 140 cm [55 in] b.s.), most faunal remains can probably be attributed to various sedimentary facies of stratum B or the uppermost part of stratum A, although some rodent burrows are also present. The lower, more organic-rich facies of stratum B was encountered within Es level 23 (220-230 cm [87-90 in] b.s.). Pockets of what was apparently the uppermost part of stratum A were also encountered at this level. Es level 25 (240-250 cm [94-98 in] b.s.) also contained a muskrat tooth (*Ondatra zibethicus*, Dundas, this report). In Es levels 26 (250-260 cm [98-102 in] b.s.) and 27 (260-270 cm [102-106 in]b.s.), sediments characteristic of stratum A (sandy facies) and stratum B (fine-grained clastics noticeably darker due to higher amounts of organics) were encountered. Thus, fossil remains from these levels could be from the older stratum A or younger stratum B.

Excavation Area J

During the 1995 season, the southern portion of Excavation Area Jsw (sw121N/125E) was excavated as part of a backhoe trench for stratigraphic studies (Figures 11 and 23). The stratigraphy at this location is presented in Figure 27 (after Hill, this report). The north half of Jsw and all of Jnw (sw122N/125E) were excavated by levels in controlled intervals. The 1995 studies of Excavation Area J began approximately at the top of the upper facies of stratum B, although portions of stratum C were also present. Bones were recovered from levels 1 and 2 (bones J1-12 are at depths of 2,009.26 to 2,009.11 masl [ca. 6,592.06-6591.57 fasl]). These include unidentifiable bone fragments as well as limb and rib bones comparable to mammoth recovered at elevations ranging from 2,009.16 and 2,009.21 masl (ca. 6,591.73-6591.90 fasl) (J4, J8, and J12, Dundas, this report). These mammoth remains were likely recovered from the lowest part of stratum C or the upper part of stratum B.

The darkest sediments of stratum B were primarily encountered in levels 2 and 3. Bones appeared to occur in clusters within the darker sediment. Level 3 bones (J13-17) are at elevations between ca. 2,009.11 and 2,009.16 masl (ca. 6,591.57 and 6,591.73 fasl) and include a possible limb bone of a mammoth at an elevation of 2,009.11 masl (ca. 6,591.57 fasl) (J13), as well as unidentifiable fragments of a large mammal limb bone (J16, Dundas, this report). The mammoth limb bone can be fairly confidently attributed to the lowermost, organic-rich lithofacies of stratum B.

Level 4 in excavation Jnw was mostly within the sandy top of stratum A and contained some bones at elevations of 2,009.12 and ca. 2,009 masl (ca. 6591.60 and 6591.20 fasl). Two pieces of a possible mammoth rib (J19, Dundas, this report) were recovered from the top part of stratum A (elevation 2,008.995 masl [ca. 6,591.2 fasl]). Bones J1-J4, J5, J9, J10, J11, J15, J17, and J18 recovered from Jnw were unidentifiable (Dundas, this report).

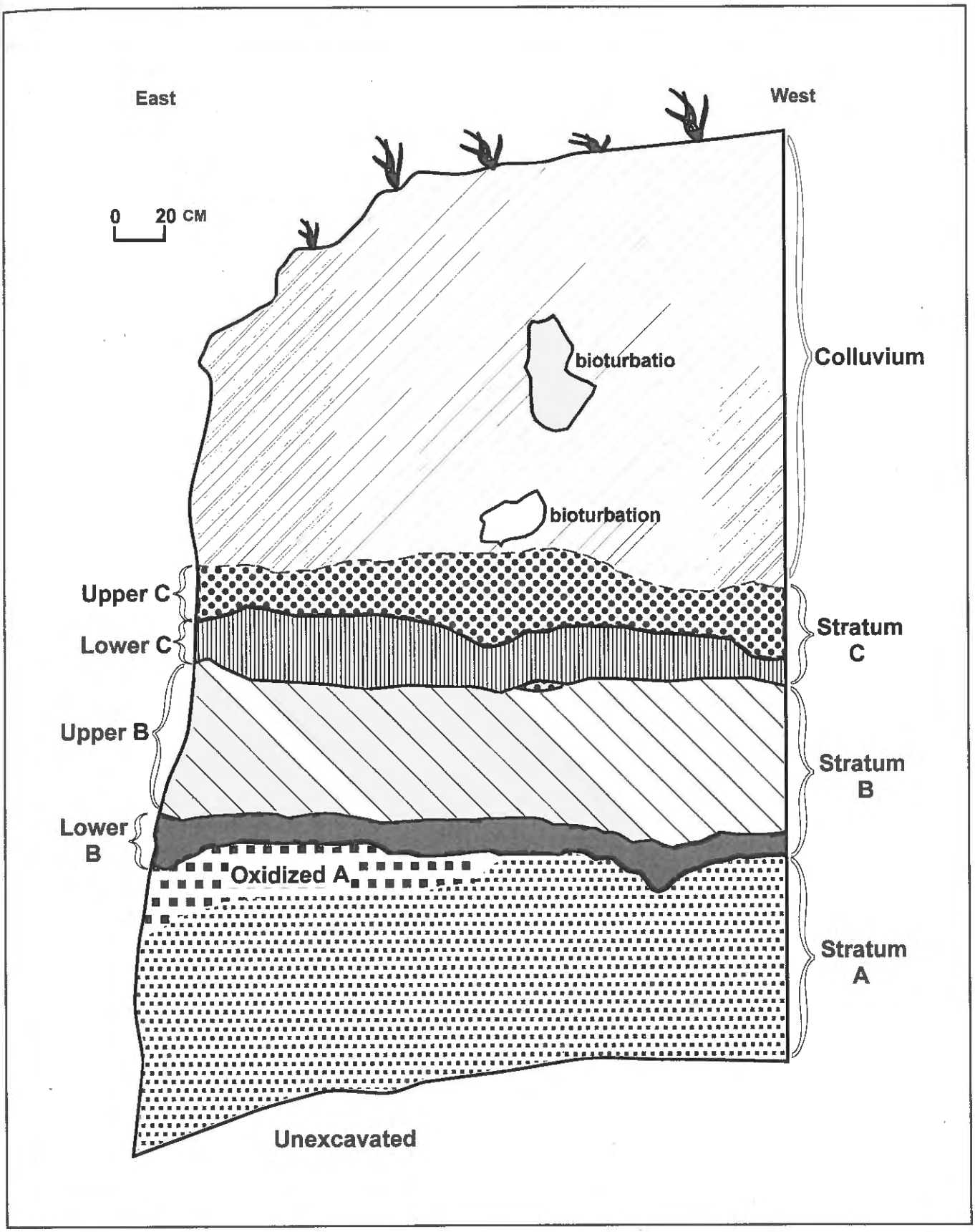

Figure 27. General stratigraphy at east end of backhoe trench, South Block (C. L. Hill profile).

Excavation Area K

Excavation Area K was studied in 1995 and 1996. In 1995, both Ksw (sw123N/125E) and Knw (sw124N/125E) were excavated. Bones were recovered at depths ranging from 2,009.26 to 2,008.99 masl (6,592.06-6,591.17 fasl). Sediments above the darkest facies of stratum B contained fossils in Excavation Area K. Bones were found along the interface of strata B and A (Figure 24) at elevations of 2,009.01 masl (6,591.24 fasl) and ca. 2,009.13-2,009.15 masl (ca. 6,591.60-6,591.70 fasl) (K1 and K2 [a rib fragment referable to mammoth, Dundas, this report]). Mammoth rib fragment specimen K2 was found along the interface between lowest stratum B and the top of stratum A at an elevation of 2,009.13 masl (6,591.63 fasl).

Other bones possibly referable to mammoth (Dundas, this report) were found at the base of stratum B (including K3, a mammoth rib fragment, at an elevation of 2,009.16 masl [6,591.73 fasl]). Limb bone, rib, and tusk fragments probably of mammoth were recovered from the 1995 excavation of K. Specimens K9, K19, K22, K23, and K29 were identified as mammoth, while specimens K4, K6, K13, K17, K21, and K27 are possible or probable mammoth remains (Dundas, this report, Appendix D; MS-767). Knw levels 1 and 2 contained an accumulation of tusk fragments, and level 5 contained a possible fragment of a mammoth phalange (Dundas, this report). Other bones could be identified only as belonging to a large mammal (specimens K12, K15, K20, and K24). Bones recovered in levels 1-4 are probably mostly from the dark, lowermost facies of stratum B, although the top of stratum A began to be uncovered during excavations in level 4. Presumably, bones recovered from the 1995 K level 5 can be attributed to the uppermost part of stratum A.

A single 17-cm-thick level of Knw (sw124N/125E) was excavated in 1996 (Batten and Davis 1996). Tusk fragments (FS142, Dundas, this report) were recovered within this excavation level of Knw (level 1) at an elevation of 2,008.79 masl (ca. 6,590.51 fasl). This is part of the same bone concentration found in level 5 (124N/124N) of Excavation Area Sne (FS143). These and other tusk fragments (FS143) recovered through screening (not found in situ) are attributed to mammoth. They were likely recovered from the darkest-colored facies of stratum B (lowest stratum B).

Excavation Area L

A small portion of Lsw (sw125N/125E) excavated in 1995 contained tusk fragments derived from the lower, organic-rich facies of stratum B (specimen L2) (Figures 23 and 24).

The west half of Excavation Area L was studied in 1996 (Batten and Davis 1996). Two types of sediments were found within levels 1-5 of Excavation Area Lsw (sw125N/125E). Within the 48 cm of exposed sediments, coarser sediments (silty sands, a facies variant of stratum C), generally tan in appearance, dominate the higher levels. Dark red (generally reddish brown) finer sediments, typically associated with an upper facies of stratum B, occur along the west side of the excavations in levels 1 and 2 and dominate levels 3 and 4. Sediment samples collected from level 3 are primarily representative of stratum B (FS38, FS41, and FS66). Unidentifiable bones mapped in place within the brown sediments include FS31 (level 1); FS34 (level 2); and FS39, FS40, FS42, FS65, FS67, FS69, FS71, FS73, and FS75, all from sediment matrix sample FS86 (level 4). Tusk fragments recovered from levels 3 (ca. 2,009.15 masl) (FS36, FS37, FS63) and 4 (ca. 2,009 masl) are likely derived from part of stratum B (as indicated by matrix sample FS38). Bones found in the "dark red clay" may be in the lower facies of stratum B. They were mapped in place in level 3 (FS36, FS64). This dark clay contrasts with a "light brown silty sand" containing many unidentifiable bone fragments which seemed to have been recovered from the top part of stratum A.

In Excavation Area Lnw (sw126N/125E), five levels forming a 49-cm-thick (ca. 19-in-thick) sequence were excavated in 1996 (Batten and Davis 1996). The first four levels show a heterogeneous mixture of brown sandy silts (fine clastics) and clayey sands (coarse clastics) higher in carbonates. The coarser calcareous sediments dominate levels 2 and 3, but brown sandy silts (fine clastics) dominate levels 4 and 5. The coarser sediments may be part of a facies of lower stratum C, while the brown silts may be a facies of stratum B. The only identifiable faunal remains consist of tusk fragments recovered in levels 3 and 4 (ca. 2,009.95 masl [6,594.32 fasl]). These levels appear to have contained deposits from lower stratum B and uppermost stratum A. Matrix sample FS87 from Excavation Area level 4 consists of sediments associated primarily with stratum B, with some sediment from stratum A.

Excavation Area M

Sediments were exposed in the west half of Excavation Area M during the 1996 season (Batten and Davis 1996) (Figures 24 and 25). Studies of Excavation Msw (sw127N/125E) exposed a 44-cm-thick (17-in-thick) sedimentary sequence (Batten and Davis 1996). Three sediment types were observed at the top of the sequence. Levels 1 and 2 contain light gray mixed sands, more organic-rich sediments, and "transitional" sediments. The organic-rich sediments are perhaps variants of the lower facies of stratum B, while lighter-colored "transitional" sediments observed are perhaps an upper facies variant of stratum B. The light

gray sands seem to be lower stratum C deposits. Thus, the bone collections from these levels probably contain a mixture of fossils from various strata. Two stratigraphic profiles are available for Excavation Area M. A profile depicting the stratigraphy along the South Wall (127N/125.80E to 127N/125E) indicates that stratum C or upper, lighter colored stratum B dominated all but the lower part of level 1. The darker, organic-rich facies of stratum B was observed at the base of level 1 and in the upper part of level 2. Stratum A was present in about the lower third of level 2 and continued in levels 3 and 4. The only identifiable fossil recovered was a fragment of rugose coral from level 3, which could indicate a correlation with stratum A. The coral fragment is interpreted as a redeposited "bedrock" inclusion in the locality's sedimentary matrix.

Excavation Area Mnw (128N/125E) consisted of a 44-cm-thick (17-in-thick) sequence (Batten and Davis 1996). The boundaries of the deposits appear to dip toward the north as indicated by a profile depicting the stratigraphy of the West Wall of Excavation Area M from 128N/125E to 129N/125E. In this part of Excavation M, level 1 and the north part of level 2 and parts of level 3 were composed of either stratum C or lighter-colored sediments from the upper part of stratum B. The dark facies of stratum B was first observed on the south side of level 2 and the top surface of this deposit dips northward near the base of level 3. Thus, level 3 probably contains a mixture of strata A-C. Level 4 contains stratum A and, in the north, stratum B. Level 5 appears to consist of only stratum A. Levels 1, 2, and parts of 3 contain what appear to be lithofacies variants of stratum C. Long bone fragments recovered from level 1 were unidentifiable (FS3, Dundas, this report). Level 3 contains both gravels and oxidized sands and silts (without bones) and, based on the profile, must be the equivalent of stratum A. The top of stratum A typically is composed of sand, but, on occasion, the sandy matrix contains isolated gravel-sized particles. Level 3 also contained darker-colored sediments with bones (possibly a facies of stratum B). The dark-colored sediments are found only in level 3. Tusk fragments recovered from the silty sands in level 4 (FS23, Dundas, this report) can be presumed to be from the top of stratum A. No fossils were recovered from level 5, which would also appear to represent excavations within stratum A.

Excavation Area N

Excavation Area N was studied in 1995. Materials recovered from levels 1-7 are probably attributable to stratum C (Figures 23 and 25). Tusk fragments (N1, Dundas, this report) recovered at an elevation of 2,009.5 masl (6,592.85 fasl) from level 1 seem to be from this deposit. Excavations in level 2 recovered small shell fragments. In Nsw (sw129N/125E) level 2, a fish vertebra (Pisces) and the right dentary of a sagebrush vole (*Lemmiscus curtatus*) were recovered, along with fragments of enamel referable to mammoth (*Mammuthus*). A skull fragment of fish (Pisces) was recovered from Nnw (sw130N/125E) level 1 (Dundas, this report). Level 4 yielded the distal end of a proximal phalanx referable to horse (*Equus* sp., Dundas, this report), but no shell. Small bone fragments were found throughout, with a few shells recovered in level 6. All of these specimens seem to have been recovered from stratum C.

The most organic-rich facies of stratum B was observed at the top of level 8 (at elevations ca. 2,008.90 masl [6.590.88 fasl]). Bones or teeth of large mammals (FS3-8, Dundas, this report) were recovered from organic-rich sediments at elevations from 2,008.86 to 2,008.75 masl (ca. 6,590.75-6,590.38 fasl) (Figure 25).

The top of stratum A was excavated within level 9 and was devoid of bones.

Excavation Area O

The 1995 work in Excavation Area O indicated that shell fragments of bivalves and gastropods were common in levels 1-4 which were, primarily, lower deposits of stratum C (Figures 23 and 25). Figure 25 shows the location of bones recovered at elevations ranging from 2,009.84 to 2,009.14 masl (ca. 6593.96-6,591.67 fasl). These include gastropods found in situ as well as fragments of bones. A left distal humerus referable to frog (cf. *Rana*) was recovered from Osw level 3 (Dundas, this report). A fragment of Paleozoic coral was also recovered from stratum C.

The generally reddish-brown silts of the upper facies of stratum B were observed first in level 4. Levels 4-7 consist primarily of sediments associated with the upper, lighter- colored ("redder") facies of stratum B. None of the in situ mapped vertebrate remains from Excavation Area O were identifiable (Dundas, this report).

The darkest facies of stratum B was 10 to 20 cm (4-8-in-thick) in Excavation Area O; it was excavated as level 8. Bone appeared to have been concentrated in the lower part of this facies. Fragments of shells were recovered from this level. The interface between lowest B and highest A was used to separate levels 8 and 9.

Level 9 consisted mostly of the sands of the top part of stratum A and contained no identifiable fossils.

Excavation Area P

During 1995, sediments of stratum C from Excavation P were mostly removed by backhoe (Figures 23 and 25). Measured level excavations in Excavation P (sw133N/

125E) were begun starting near the top of the darker-colored sediments of stratum B, although the level 1 collection might contain fossil specimens recovered from the lower deposits of stratum C. Bone was recovered in situ at elevations of ca. 2,009.48 and 2,009.5 masl (ca. 6,592.78-6,592.85 fasl): (P1, an ungulate limb bone fragment, Dundas, this report) and 2,008.87-2,008.83 masl (ca. 6,590.78-6,590.65) (P2, unidentifiable). Tusk fragments recovered from Excavation Area Pnw levels 2 and 3 as well as Psw level 4 can all be attributed with some certainty to the lowermost dark facies of stratum B, as can a skull fragment of a large mammal recovered from level 3 (P3, Dundas, this report). Level 5 is mostly the top of stratum A, although some sediments from stratum B were also observed.

Excavation Area S

Excavations during 1995 recovered fragments of bone, all probably from the lower part of stratum C (Figures 23 and 24). The bones clustered at two elevations: 2,009.72-2,009.77 masl (6,593.57-6,593.3 fasl) (P1-3, including a possible metapodial fragment of a large artiodactyl, cf. Dundas, this report) and ca. 2,009.52-2,009.53 masl (ca. 6,592.91 fasl) (including rib fragments, bones P4-6, all unidentifiable to a particular animal taxon, Dundas, this report). The horizontal location of these specimens from stratum C is shown in Figure 24.

The 1996 studies of Excavation Areas Sse and Sne started at an elevation of ca. 2,009.59 masl (ca. 6,593.14 fasl) and continued to a depth of 2,009.04-2,009.04 masl (6,591.34-6,591.34 fasl) (Batten and Davis 1996). Two types of sediments were observed within the interval containing levels 1 and 2. The apparent base of stratum C was observed, as were lower stratum B darker-colored sediments high in organics and fragments of fossils.

In Excavation Area Sse (sw123N/124E), bones recovered from level 2 (FS25) and level 3 (FS26-29, FS54) are primarily from stratum B. Matrix samples FS27 and FS28 from level 2 are composed of stratum B. This includes tusk fragments (FS28). Fossils collected from levels 4 and 5 (FS92, FS98) could be from either organic-rich stratum B or the underlying sands of stratum A.

In Excavation Area Sne (sw124N/124E), specimens FS107 and FS113 (tusk fragments from level 2) are apparently from stratum C sediments (or perhaps an upper, lighter-colored facies of stratum B), while level 3 tusk fragments (FS124) appear to be most likely connected with the lowermost organic facies of stratum B. Most of the tusk fragments from level 4 are also presumably from the base of stratum B (FS139) as are specimens recovered in the northeast part of quadrant Sne (sw124N/124E) (FS141, see also FS142 from level 1 sw124N/125E). Tusk fragments recovered in levels 5 and 6 (FS140, FS141) are most likely derived from the top of stratum A.

Excavation Area T

In 1995, bone was recovered in Excavation Area T from what appear to be stratum C deposits overlying stratum B at depths of 2,009.39 and 2,009.43 masl (6,592.49 and 6,592.62 fasl) (Figures 23 and 24). All bones mapped in situ (T1-6) were medial sections of rib fragments from a large mammal (Dundas, this report). The bones formed a small cluster slightly southwest of coordinate 127N/125E (Figure 24).

In the 1996 excavation of Tsw (sw125N/123E), two levels exposed a 71-cm-thick sequence (Batten and Davis 1996). The upper sediments in the sequence were excavated as level 1 and an unidentifiable bone fragment was recovered (FS145, Dundas, this report). At the base of level 2 (ca. 2,009.25 masl [6,592.03 fasl]), Batten and Davis 1996), the higher organic content lower facies of stratum B was collected (FS152), and an unidentifiable bone was found in situ (FS151, see Figure 24).

In Excavation Area Tse (sw125N/124E), three levels were studied in a 54-cm-thick (21-in-thick) sedimentary sequence (Batten and Davis 1996). Each level contained a mixture of sediment types and fairly high concentrations of bone fragments. Fragments recovered in the level 1 tan silty sands and finer dark reddish brown sediments (probably the base of stratum C and upper facies of stratum B) include bivalves, molluscs, and tusk (Dundas, this report, FS91). On the basis of other observations, it may be reasonable to place the molluscs and bivalves within stratum C and the tusk fragments within stratum B, although mammoth remains were recovered from stratum C in Test Pit/Excavation Area E. Darker-colored, fine-grained sediments in level 2 are probably mostly from the lower facies of stratum B (FS117-123, FS129). These include fragments of tusk, some (FS120 and 122) recovered in situ (Figure 24) in what seems to be the lower facies of stratum B (FS122) matrix. More tusk fragments were collected from Tse (sw125N/124E) in level 3 (FS138), apparently from near the base of stratum B.

A 81-cm-thick sequence (three levels from 2,009.91 to 2,009.10 masl [6,594.19 to 6,591.53 fasl]) (Batten and Davis 1996) was exposed in Excavation Area Tnw (sw126N/123E). The presence of silty clay is documented in the nw corner of level 1, with some organic-rich sediments (stratum B) in level 2. By level 3, most of the deposits encountered were high in organics, with some sands present. Level 3 contained relatively large amounts of unidentifiable bone (FS154) along with tusk fragments

(FS156) presumably accumulated within stratum B, perhaps near the base of stratum B along the interface with the upper surface of stratum A (see matrix sample FS153).

In Excavation Area Tne (sw126N/124E), a 57-cm-thick sequence was separated into four levels ranging in elevation from 2,009.42 to 2,008.85 masl (6,592.58 to 6,590.71 fasl) (Batten and Davis 1996). Level 1 contained calcareous sediments with Fe stains (likely a facies of stratum C) as well as organic-rich sediments (stratum B). Unidentifiable bone fragments were recovered from stratum C. Figure 28 depicts level 2, showing the presence of stratum A and stratum B sediments. Organic-rich sediments of stratum B with unidentifiable fossils (FS55, FS79, FS90) are underlain by gray sandy sediments of stratum A. Stratum A contains tusk fragments (FS61, FS80, FS81) that were mapped in situ at elevations of 2,009.07-2,009.06 masl. Other tusk fragments were recovered as part of the general collection from level 2 (FS62). Decomposed fossil fragments, including some possible mammoth tusk pieces, were also found in level 3 (FS136, Dundas, this report) which would likely be the top of stratum A. Unidentifiable bone recovered in situ from level 4 is also presumably from the top part of stratum A (FS103), since matrix sample FS104 appears to consist of sediments found along the strata A-B boundary.

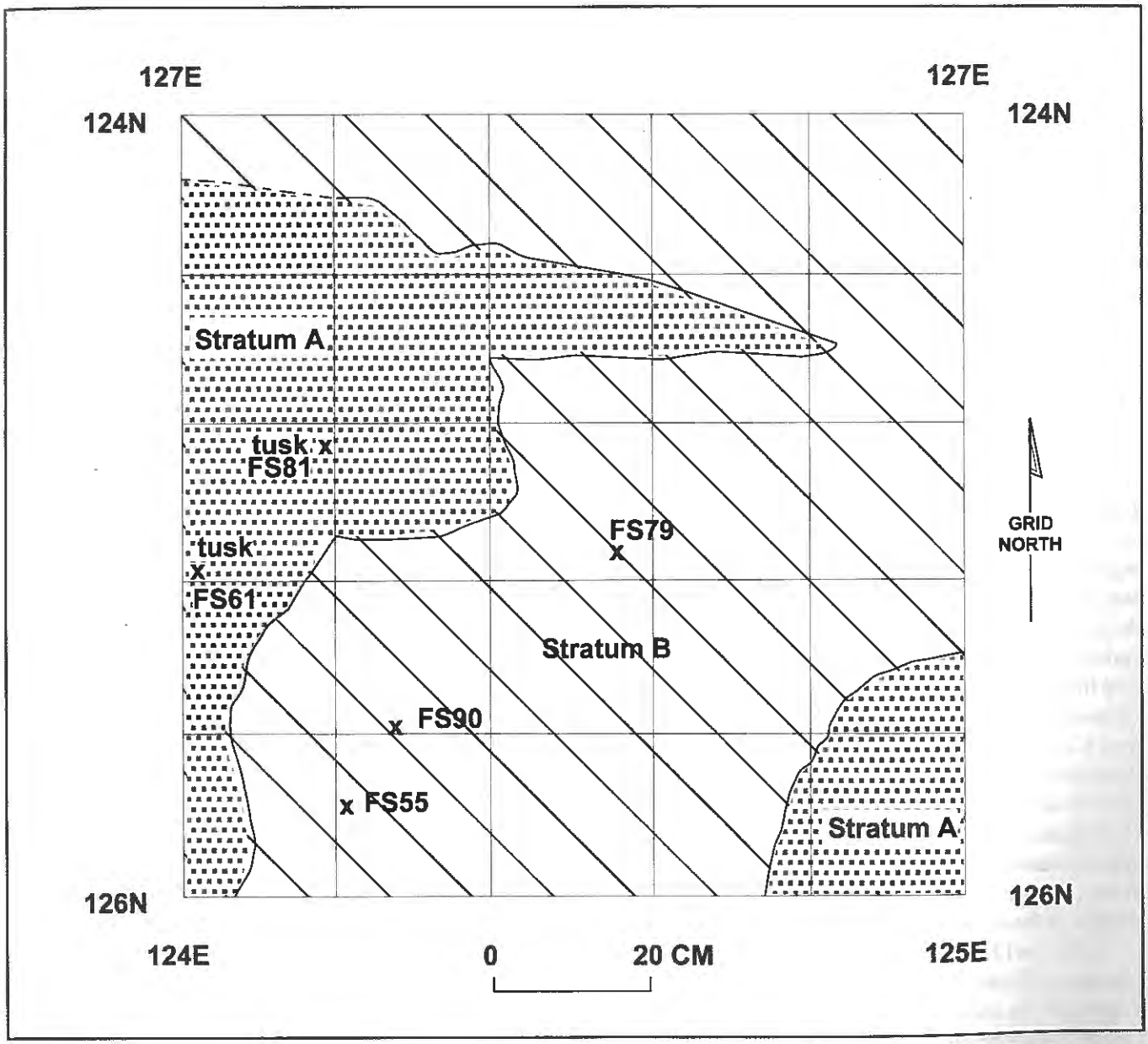

Figure 28. Plan view of Excavation Area T, showing relationship of strata A and B and fossils, South Block (compiled by C. L. Hill).

Excavation Area U

During the 1995 field season, in situ bones were recovered along the south side of Excavation Area U (sw127N/123E). They are plotted on Figure 25 (U1-5). The assemblage consists of two groups of bones at slightly different elevations. Specimens U1 and U2 at 2,009.25-2,009.28 masl (6,592.03-6,592.12 fasl) were unidentifiable bone fragments, and specimens U3-5 at elevations ca. 2,009.36-2,009.37 masl (6,592.39-6,592.42 fasl) were either unidentifiable or rib fragments of a large mammal (Dundas, this report).

All four quadrants of Excavation Area U were studied in 1996. A 37-cm-thick (15-in-thick) sequence was exposed in Excavation Area Usw (sw127N/123E) (Batten and Davis 1996). Unidentifiable bones of level 1 (starting elevation 2,009.96 masl [6,594.36 fasl]) were mapped as FS126 (Figure 25) within gray-colored, fine-grained sediments. These lie above the organic-rich facies of stratum B observed in level 2. Unidentifiable bones were present in this organic-rich deposit (FS148), which was underlain by gray sands of stratum A. In level 3, bones were recovered from both the organic-rich sediments of stratum B and the uppermost light gray sandy deposits of stratum A. The highest concentration of bone fragments was at the very base of stratum B and within the top part of stratum A in Usw (sw127N/123E). These include tusk fragments, some mapped in situ (cf. FS159, elevation 2,008.94 masl [6,591.01 fasl]). Sedimentary matrix from FS159 appears to consist mostly of stratum A with some stratum B.

The 1996 studies of Excavation Area Use (sw127N/124E) consisted of five levels ranging from 2,009.33 to 2,008.76 masl [6,592.29-6,590.42 fasl], for a total thickness of 57 cm (22 in) (Batten and Davis 1996). The darker, organic-rich facies of stratum B was visible in the south and west portion of levels 1-3. Most of the sediments in these levels consisted of Fe-stained, calcareous sediments perhaps related to stratum C. Tusk fragments were recovered from level 3 (FS57). Sands observed in levels 3 and 4 are probably the top part of stratum A which characterizes level 5. Level 4 contained tusk fragments (FS5). Stratum B (lower dark facies) was present in the north half of the excavation in level 4, but disappeared near the top of level 5. Overall, the intervals of excavation appear to contain a heterogeneous mixture of sediment types. This implies that bone specimens collected from any excavation level could be derived from more than one stratum.

Unw (sw128N/123E) was excavated in three levels, exposing a 67-cm-thick sequence. Level 1 and part of level 2 appear to be sediments from above the dark-colored facies of stratum B. Most of level 2 is the stratum B organic-rich deposit. Level 2 contained tusk fragments, some of which were mapped in situ (FS146, elevation 2,009 masl [6,591.21 fasl], and FS132). Level 3 apparently corresponds to stratum A sandy clays and also contained fragments of tusk (FS133).

Four levels were excavated in Une (sw128N/124E), exposing a 54-cm-thick (21.26-in-thick) sedimentary sequence (Batten and Davis 1996). Levels 1-3 contain sediments and unidentifiable fossils (FS96) above the dark organic zone of stratum B. Level 3 contains both this darker part of stratum B and sandy clay sediments (most likely uppermost stratum A). Bones recovered in level 3 were unidentifiable (FS97). Bones found in only the dark organic zone of stratum B in level 4 were also unidentifiable (FS99, Dundas, this report).

Excavation Area V

The 1996 field studies of Excavation Area V exposed 90 to 102 cm (35 to 40 in) of sediments in three levels (Batten and Davis 1996) (Figure 25). In Excavation Area Vsw (sw129N123E) level 1, grey clayey sediments, apparently of stratum C, overlie the organic-rich facies of stratum B. The top of this organic-rich stratum is in level 1 and it dominates level 2. The underlying sediments of stratum A were also exposed in the southwest corner of the excavations. Thus, level 2 contains sediments above the organic-rich facies of stratum B, the high-organic zone of stratum B, and sands of stratum A directly below stratum B. Unidentifiable bone fragments (FS134) were recovered in situ from within or at the base of the organic-rich deposit in level 3. Level 4 consists of sandy silts, presumably from the top of stratum A, and contained some fossils (FS131).

In Excavation Area Vse (sw129N/124E), level 1 was more than 70-cm (28-in) thick and was composed of sediments above the distinct organic-rich deposit of the lowermost facies of stratum B observed in level 2. Level 2 contained some tusk fragments (FS83). Level 3 was composed mostly of sandy clay (likely a facies of stratum A) underlying stratum B.

Excavation Area Vnw (sw130N/123E) contained light-colored sediments in level 1. These upper sediments were followed by dark-colored sediments (stratum B) in levels 2 and 3 with mapped in situ unidentifiable bones (FS105, FS111, FS115/116). Unidentifiable bones FS110 and FS114 seem most likely to also be derived from the dark organic facies of stratum B.

Within Excavation Area Vne (sw130N/124E), the lower portions of gray (stratum C?) and reddish (stratum B, upper facies?) sediments were found above the more organic-rich facies of stratum B in level 1. Level 2 contained mostly the lowermost organic-rich facies of stratum

B, but also the uppermost part of stratum A (FS16, FS58). All fossils in level 2 were unidentifiable. However, FS16, recovered in situ from the lowermost facies of stratum B (as indicated by matrix sample FS17) at an elevation of 2,008.74 masl (6,590.35 fasl), may be a fragment from a mammoth, based on size (see Dundas, this report). Level 3 consisted of only stratum A and apparently contained no fossils.

Excavation Area W

The 1996 excavation within the east portion of W exposed a 96-97-cm (ca. 38-in)-thick sediment sequence (elevations range from 2,009.62 to 2,008.6 masl [6,593.24 to 6,589.89 fasl], Batten and Davis 1996: Table 1) (Figure 25). Excavation of Wse (sw131N/124E) level 1 exposed tan and gray sediments directly above the dark facies of stratum B. The organic-rich portion of stratum B was also well-defined and two bones were recovered at the base of the level (the bones were mapped in place, but were unidentifiable) (FS7, FS9, Dundas, this report). Level 2 consisted primarily of the darker-colored facies of stratum B (bones for the entire level are FS46, all unidentifiable). Two in situ unidentifiable mapped bones (FS10, FS18) were recovered in the grid southeast part of the excavation of level 2. Sediments from the top of strarum A, underlying the darker sediments of stratum B, were found in level 3. On the west side of this level, bones were found and mapped in situ (FS47/48, FS49/50), although none were identifiable (Dundas, this report).

Excavation Area Wne (sw132/N124E) level 1 contained grey and Fe-stained sediments (apparently lower stratum C deposits) and some dark organic deposits (a facies of stratum B, as indicated by matrix sample FS8). The darkest part of stratum B (represented by matrix samples FS10, 19, and 57) was excavated as level 2 (it contained unidentifiable bone fragments, FS45). The boundary between stratum B and the underlying sediments of stratum A was encountered in level 3. Tusk fragments (FS51, FS52, FS59) from level 3 are likely from stratum A, although matrix samples collected from this level also contain stratum B sediments (FS48, FS50, FS52).

Excavation Area X

Excavation Area X was first studied in 1995. A small basin was clearly delineated by an erosional surface along the interface separating sands of stratum C and lower deposits which include stratum B (Figure 25). Bones were discovered in situ during the excavation of stratum C. Most of the 17 bones mapped in situ were unidentifiable, except for X7 (*Canis latrans*). Bone X2 might be a rib fragment from a large mammal, X6 a possible metapodial from a large artiodactyl, X8 a limb bone fragment from a large mammal, X16 a partial podial of a large mammal, and X17 fragments from a large herbivore limb bone (Dundas, this report). The horizontal relationships of these bones is shown in Figure 29, based on data collected by D. Batten. Tusk fragments were recovered from water-screened sedimentary matrix from Excavation Area X.

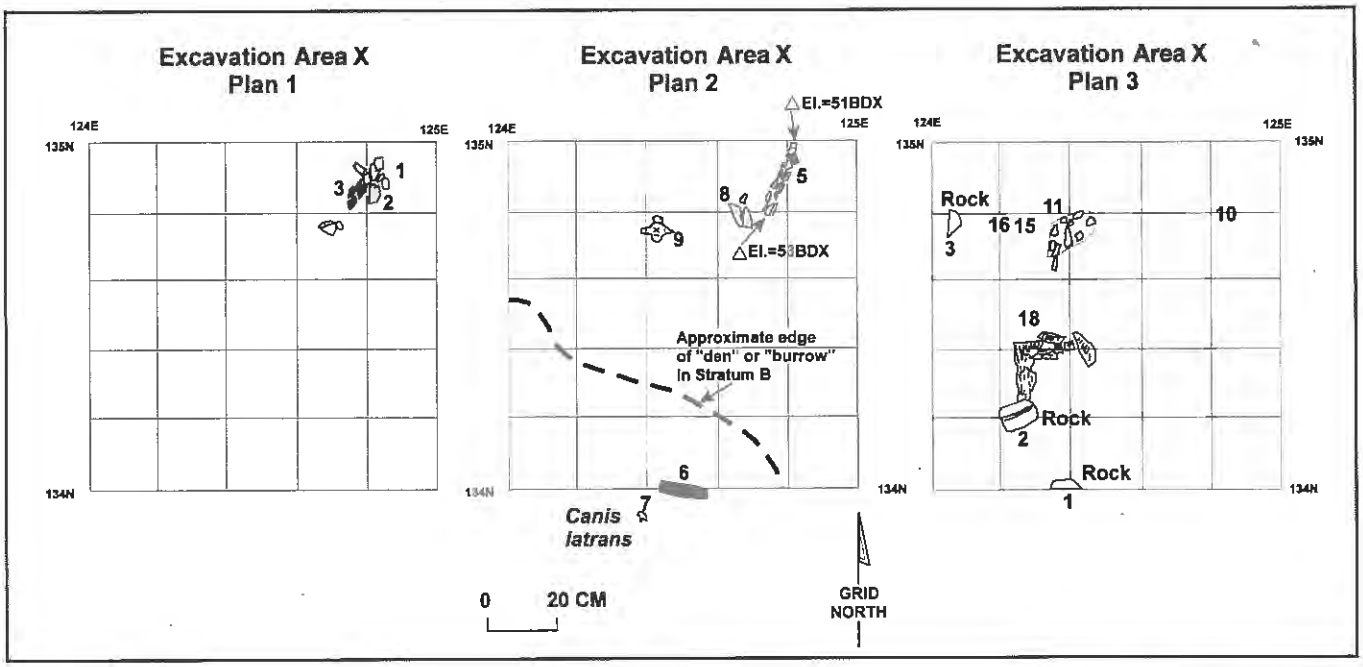

Figure 29. Plan view of Excavation Area X, South Block (data from D. Batten, compiled by C. L. Hill).

In 1996, two additional levels were studied at Excavation Area Xse (sw133N/124E), exposing a 53-cm-thick (21-in-thick) sequence (elevations ca. 2,009.15-2,008.62 masl [6,591.70-6,589.96 fasl]; Batten and Davis 1996). Level 1 consisted of sediments above the darkest part of stratum B, while unidentifiable bone material (FS84, Dundas, this report) recovered from level 2 can be attributed to the organic-rich facies of stratum B.

Summary

Fossils of Pleistocene fauna, chiefly bones and tusk fragments that can be attributed to mammoth, were recovered from several different geologic contexts in the Merrell Site South Block. The horizontal and vertical distribution of fossils recovered in the South Block area were recorded by one of two procedures. Typically, collections were made of all fossil material found within a specified excavation interval, commonly a measured excavation interval of a 1 x 1-m square ("Excavation Area") aligned along the coordinates of the site grid. Fossils found in situ were mapped. Different specific methodologies were applied in each of the field seasons, and details of the procedures used in each field season are available in the MOR field records and end-of-season reviews (as summarized in Batten, this report).

The horizontal distribution of fossils mapped in place is shown as Figure 23. This map is a compilation of all in situ fossils (identifiable and unidentifiable based on comparative morphology) in planview. The distribution pattern no doubt partially reflects different collection strategies. Nevertheless, some patterns are apparent. There appears to have been a fairly high concentration of mammoth bone fragments on the south side of the South Block, close to the escarpment edge (approximately between 122-126N and 125-126E on the site grid, mostly in Excavation Areas Jsw, Jnw, Ksw, Knw, and Lsw, Figure 24). Identified bones in this area are nearly all mammoth remains, which include fragments of limb bones, ribs, vertebrae, and tusk.

Another fairly high concentration of mammoth remains was present in the grid southwest part of Test Pit/Excavation Area E (ca. 121-122N/123E on the site grid). This was the general location of three mammoth molars as well as tusk and rib fragments.

A more diffuse scatter of in situ fossils was found spread between ca. grid 126-128N, mostly within 124-125 E (mostly in the western portions of Excavation Areas Sse, Sne, Tse, and Tne). The 1995 in situ remains from this area were largely unidentifiable.

Another moderately dense scatter of fossils was mapped in situ in the vicinity of Excavation Area Xne. A fragment of a coyote (*Canis latrans*, MOR-LI95.2.309) tooth and an ungulate bone were recovered in place in this area.

The vertical locations of fossils found in situ are known with some precision, and the elevations of the fossils recovered in general context are known within the vertical thickness of the excavation levels. Here, again, the thickness of the excavation interval and the means of collection varied during the three seasons of field studies and any potential patterns should be interpreted within the constraints of this variation. In some instances, the excavation intervals conform closely to geologic strata or are intervals mostly within a well-defined geologic deposit. For example, excavators were commonly able to discern the organic-rich facies of the lower part of stratum B and the underlying sands or sandy clays of the top of stratum A. However, even in the instance of the organic-rich dark deposit of stratum B, it is apparent that some excavation intervals that contained it also included portions of stratigraphically higher or lower deposits. This was due at least in part to the fluctuating thickness and changing elevations of the deposits. Some of the excavation levels contained fossils found within at least two distinct geologic deposits, and sometimes perhaps more. Elevational control in-and-of-itself appears to be of only limited value because of extreme postdepositional alteration (faulting, liquefaction, bioturbation) that has deformed the deposits.

Despite these constraints, it is possible to attribute specific fossil specimens recovered from the South Block excavations to particular strata. In terms of taphonomic considerations, it would seem prudent to remember that the presence of fossils within a particular geologic deposit does not necessarily lead to the inference that the fauna associated with these remains were living contemporaries of the environment of deposition. What can be inferred is that the fossils are the remains of animals that lived either at about the same time as the sedimentational event that incorporated them into the deposit (where they were recovered) or that they lived at an earlier time.

During the MOR excavations of the South Block, fossils were recovered from the top of stratum A, along the interface between the top of stratum A and the base of stratum B, within stratum B (apparently often near the base of the darkest, most organic-rich facies of the lower part of stratum B), and also in stratum C. Postdepositional horizontal and vertical movement of the sediments and disturbance of the fossils within these deposits appears to have influenced the final spatial patterns. Remains of mammoth found in the Merrell South Block were recovered

along the interface of stratum A and stratum B, often within the base of stratum B, but also in contexts where they could have originally been within the top of stratum A. This is the pattern along the southeast side of the South Block near the escarpment as well as in Test Pit/Excavation Area E. Other bone concentrations can, for the most part, be attributed to have been from within or near the base of stratum B and within stratum C with some confidence. For instance, the remains of *Canis latrans* can be attributed to stratum C. Some other fossils were also recovered from stratum C, including *Lemmiscus curtatus*, *Mammuthus* sp., and Osteichthyes. These bones, especially when found in the silty (low-energy) facies of stratum C, may be an indication of paleoenvironmental conditions directly associated with the time of deposition. There is a greater chance that fossils recovered within the coarser (higher energy) facies of stratum C have a more complicated taphonomic trajectory. If stratum C reflects predominantly episodic fluvial deposition, then the isolated faunal elements incorporated into these sediments may be older Pleistocene faunal remains redeposited into younger sediments.

Geology of Centennial Valley and Stratigraphy of Pleistocene Fossil-Bearing Sediments

Christopher L. Hill

Introduction and Previous Research

This paper is based on stratigraphic studies conducted at the Merrell Locality and other locations in Centennial Valley. The Merrell Locality is situated in southwest Montana, on the western end of Centennial Valley (Figure 30). It is notable for containing the fossil vertebrate remains of mammoth (*Mammuthus* cf. *M. columbi*), scimitar cat (a member of the sabertooths, *Homotherium serum*), horse (Equidae) and Yesterday's camel (*Camelops* cf. *hesternus*), as well as other plant and animal fossils of Pleistocene age (Dundas 1990; Dundas, Hill, and Batten 1996). Summaries and reports of research conducted at the locality include Albanese (1995); Albanese, Davis, and Hill (1995); Batten and Davis (1996); Bump (1989); Davis et al. (1995); Dundas (1990); Dundas (1992); Hill, Davis, and Albanese (1995); Hill and Albanese (1996); Hill (1999, 2001a, 2001b).

Excavations at the Merrell Locality were undertaken by the Museum of the Rockies at Montana State University-Bozeman in 1994, 1995, and 1996. D. C. Batten served as field director. J. P. Albanese conducted on-site geologic studies in 1994 and 1995. J. Feathers collected sediment samples for luminescence dating in 1997. R. I. Kuntzelman and C. L. Wofford Hill served as field assistants during 1998-2001. This paper provides a summary of stratigraphic studies conducted in conjunction with these efforts and is based on field observations at the Merrell Locality made between 1994 and 2001.

Summary of the Cenozoic Geology of Centennial Valley

Background

The Merrell Locality is situated on the extreme western end (NW1/4,NE1/4,NW1/4, Sec. 5, T14S, R6W, United States Geological Survey Lima Dam 7.5-Minute Quadrangle) of the Centennial Valley (Figure 31). Centennial Valley is a generally east-west-trending structural basin surrounded by the Centennial Mountains to the south and the Snowcrest and Gravelly Ranges to the north (Figures 30 and 31). The valley averages about 6 mi (3.7 km) in width. The present-day drainage of the Red Rock River flows from the Red Rock Pass divide area in the east to the western end where the valley is constricted west of Lima Reservoir where a dam regulates flow.

Bedrock Stratigraphic Sequence

Rocks of all the major geologic time intervals (Precambrian, Paleozoic, Mesozoic, and Cenozoic) occur within the region. Precambrian rocks are exposed along the eastern end of Centennial Valley (Witkind 1972, 1975a, 1975b, 1976; Witkind and Prostka 1980). They consist of metamorphosed older sedimentary rocks and younger igneous rocks associated with granodiritic, gabbroic, and diabase intrusions. Paleozoic rocks consist of Middle Cambrian-Mississippian carbonate, shales, and sandstones. Most of the Mesozoic rocks are sandstone, siltstone, and shale with some coal. Triassic rocks include the Dinwoody, Wooldside, and Thaynes Formations. The Jurassic is represented by the Morrison Formation which is overlain by the Kootenai and Aspen Formations.

During the late part of the Mesozoic, structural compression of the Earth's crust associated with the Laramide Orogeny affected the older rocks. Compressional forces associated with the Laramide Orogeny created the Metzal Creek Anticline and probably the Odell Creek Fault (Honkala 1949). Upper Cretaceous and younger strata are exposed along the down-dropped (western) block associated with the Odell Creek Fault. The uplifted (eastern) block has exposed a Precambrian to Lower Cretaceous sequence. The sequence is covered by Quaternary volcanics.

The area around the western end of the Lima Reservoir is underlain by a conglomerate. The conglomerate is exposed along the south side escarpment of the Lima Reservoir Dam as well as between the Lima Reservoir Dam and the Merrell Locality. This conglomerate is also exposed north of the dam where it has been assigned to the Lima Conglomerate. The Beaverhead Group contains the Lima Conglomerate (Nichols, Perry, and Haley 1985; Schmitt et al. 1995).

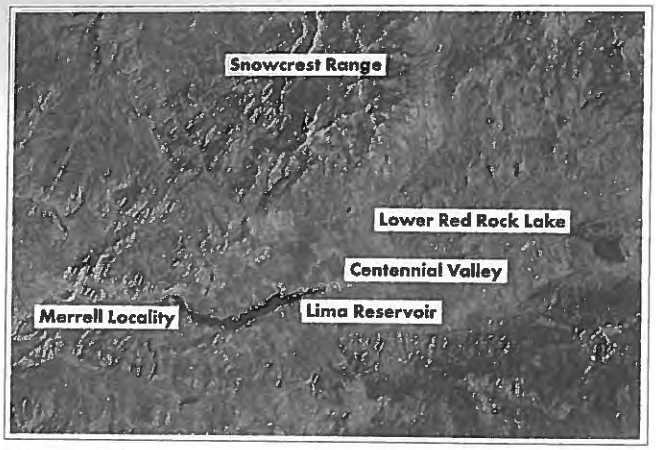

Figure 30. Air photograph showing Merrell Locality within Centennial Valley.

Tectonics and Volcanism

The general chronology of Cenozoic geologic events in southwestern Montana includes continued compressional deformation associated with the Laramide Orogeny, followed by extensional tectonic events and associated volcanism. The younger tectonic activity and volcanism have been connected with the Yellowstone Hotspot and the Snake River Plain (Pierce and Morgan 1992). Centennial Valley and its structural counterpart, Jackson Hole, along with the Centennial Range, and its structural counterpart, the Teton Range, have undergone dynamic tectonic activity during the Quaternary (Myers and Hamilton 1964).

Structural and Depositional Context

The Laramide Orogeny began in the Cretaceous (late Mesozoic) and continued through the Eocene (early Cenozoic). Erosion from early Tertiary uplift resulted in the deposition of clastics, principally the Beaverhead Formation (Eardley 1960; Honkala 1960). During the Eocene, compressional forces formed a thrust fault through the Beaverhead in the west (Honkala 1960). Block-faulting along the Cliff Lake Fault appears to have begun during the Oligocene. Fluvial deposition during the Miocene filled the valley with sediments as the Centennial Range began to be uplifted.

Several generally north-south-trending faults cut across the Centennial Valley. The Odell Creek Fault (Secs. 1 and 12, T15S, R2W; Sec. 36, T14S, R2W; Sec. 31, T14S, R1W) is a high-angle normal fault hidden under the later Tertiary-Quaternary sediments and Pleistocene volcanics in the Centennial Valley. The stratigraphic throw of the Odell Creek Fault has been estimated at about 4,500 ft (1,372 m), with a displacement of 3,000 ft (915 m) (Honkala 1949, 1960).

Regionally, the features associated with the Snake River Plain were initiated during the Oligocene. There appears to be a direct connection between the greater Yellowstone tectonic and volcanic system and the Snake River Plain. The Centennial Range is, in fact, part of the north rim of the Snake River Basin (Alden 1953:39). The range stretches about 45 mi (72.6 km) from the edge of Henrys Lake in the east, to a gap at Monida in the west (Figures 31 and 32). By Late Pliocene and Early Pleistocene times, the volcanism and tectonics of the Snake River Plain Hotspot began to affect the Centennial (as well as the Teton) system (Hamilton 1965). The system migrated eastward, tilting the Centennials southward (Pardee 1950).

Pleistocene Volcanism

Several large volcanic explosions affected the region during the Pleistocene. The area contains the most extensive exposure of Pleistocene igneous rock in Montana. The three units that form the Yellowstone Group volcanics (Christiansen and Blank 1972; Christiansen and Embree 1987) are found in the vicinity. About 2 million years ago, an eruption from the Island Park caldera emplaced the Huckleberry Ridge Tuff (HRT) along the southern margin of the Gravelly Range. The caldera extends from the west side of Island Park to the Central Plateau of Yellowstone National Park (Figure 32). The tuff has been traced into the Centennial Valley area and northward into the Madison Valley. Dated exposures include tuff about a mile north-northwest of Hidden Lake (91 m or 299 ft thick), Elk Lake (123 m or 403 ft thick), a cliff face near Wall Canyon along the Madison River (48 m or 157 ft thick), and the slope of Flatiron Mountain (Sonderegger et al. 1982; Mannick 1980). At Targhee Pass, the HRT is about 200 m (656 ft) thick.

The HRT is exposed on the north side of the Centennial Valley about 17.7 km (11 mi) west of the Upper Red Rocks Lakes Quadrangle (Sonderegger et al. 1982). The tuff is thicker in the east and thins toward the west, indicating the general direction of movement of the ash-tuff. The spatial character of the tuff has been used to argue that, during the early Pleistocene, the Centennial Range was lower than at present, which allowed the tuff to sweep northwestward into the Valley.

Within the Centennial Valley, the HRT has been displaced along the Centennial Fault, providing an indication of uplift over the last 2 million years. There has been a displacement of up to 1,830 m (ca. 6,004 ft). At about the

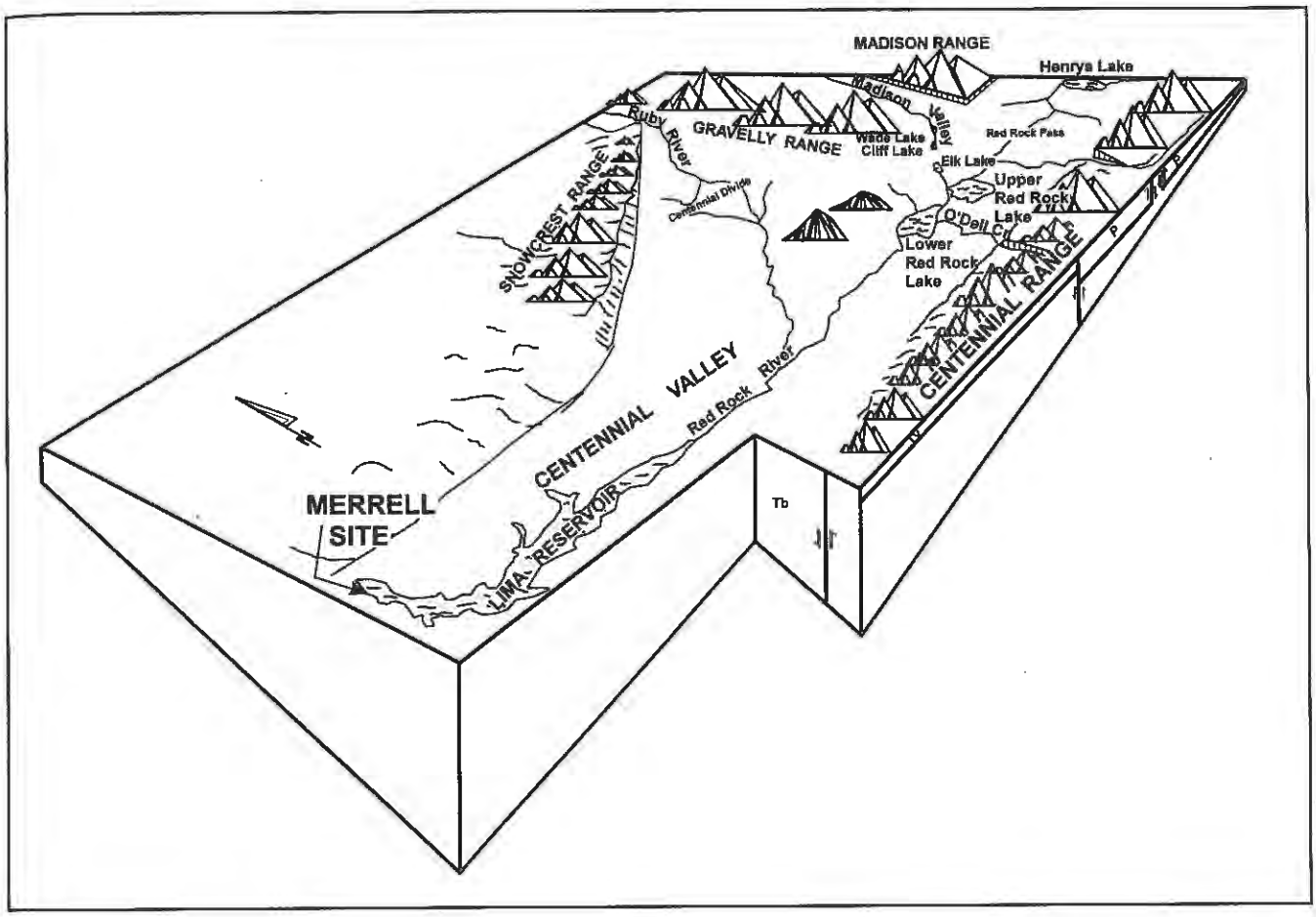

Figure 31. Schematic drawing showing general setting for the Merrell Site (by C. L. Hill).

same time that the Huckleberry Ridge eruption occurred, volcanic lava was extruded along the northeast side of the Centennial Valley. Basalt at Elk Lake has a K-Ar date of ca. 1.95 million years (Sonderegger et al. 1982).

The Mesa Falls Ash (MFA) exploded from a smaller caldera nested against the northwest wall of the older Island Park caldera about 1.2 million years ago. By that time, uplift along the Centennial Fault system appears to have been great enough so that the Centennial Mountains blocked the northward flow of the ash. The MFA is found locally only in the Centennial Valley, near the divide at Hell Roaring Canyon in the Centennial Valley (Witkind 1976) as well as southeast of Cliff Lake and in the Madison Valley. The Lava Creek eruption ca. 600,000 years ago was emplaced only along the southeastern margin of the Centennial Range, indicating that its northward flow was blocked by the increasing height of the mountains.

The Pleistocene volcanics appear to overlie and conceal a buried valley that once connected the Centennial Mountains and the southern Madison Valley (Sonderegger et al. 1982). Before the Yellowstone explosions, this valley had probably served as a drainage for the Centennial Valley.

Structure and Late Quaternary Tectonics

The Centennial Valley is part of a zone of Holocene faulting and seismicity defined as the Centennial Tectonic Belt (CTB). It is part of the northeastern portion of the Basin and Range Province connected with the Snake River Plain and the migrating Yellowstone Hot Spot (Stickney and Bartholomew 1987; Good and Pierce 1996). The CTB is an east-west-trending belt of earthquake activity and Late Quaternary faulting that extends from northwestern Yellowstone National Park to Idaho along the northern flank of the Snake River Plain, including Red Rock Valley, the southern Gravelly Range, the Centennial Valley, and the Hebgen Lake area (Figure 32).

The Centennial Mountains consist of a fault block that tilts southward under the Pleistocene lava and tuffs of the Snake River Plain (Pardee 1950). The Centennial Fault system consists of several segments (Pardee 1950; Witkind 1975; Shofield 1981; Sonderegger et al. 1982). There are two high-angle normal faults. One branch is buried under sediments and one branch is exposed along the surface. The north slope of the Centennial Range consists of a front

that rises 3,000 ft (914 m) in 1 mi (1.6 km) (Myers and Hamilton 1964; Schofield 1981). There appears to have been more than 10,000 ft (3,027 m) of vertical displacement, mostly in the last 10 million years (indicating that there is about 7,000 ft [2,135 m] of valley fill). The fault scarp along the north face of the Centennials reaches heights of 50 ft (18 m). In the eastern part of the valley, the fault scarp appears to be buried beneath glacial, alluvial, and landslide deposits, but, in the west, there is a very obvious scarp. Glacial, alluvial, and Late Pleistocene lake sediments are offset along the fault scarps (Myers and Hamilton 1964). The Red Rock Lakes segment of the Centennial Fault passes into a glacial moraine. It cuts across pre-Bull Lake to Bull Lake and post-Bull Lake to Pinedale deposits, but is covered by Pinedale moraines (Pardee 1950; Stickney and Bartholomew 1987).

The western segment of the Centennial Fault appears to have been active more recently. The scarp cuts across Early Holocene and Pleistocene deposits, but is covered by later Holocene alluvial fans (Stickney and Bartholomew 1987). In the alluvial plain of Jones Creek, the Centennial Fault diverges into two segments and then is buried under a landslide that extends along the range front for about 7 mi (11.3 km) (Pardee 1950). A short scarp crosses till, but appears not to cut older deposits along Sawtell Peak (Witkind 1975). Closer to the Merrell Locality, the scarp associated with the Lima Reservoir Graben offsets a post-Bull Lake to Pinedale/post-Pinedale to pre-Holocene surface as well as the youngest stream terraces. It is cut by a Late Holocene stream (Stickney and Bartholomew 1987).

Glacial lake features within the valley have been used to estimate the rate of movement along the Centennial Fault since the Late Pleistocene. The altitude of glacial lake shorelines appears to indicate that movement along the fault has been about 2.54 cm per year since the latest Pinedale glaciation (Sonderegger et al. 1982). The lakeshore is broken by faults and has been warped by at least 60 ft (18.2 m), rising from 6,630 ft (2,021 m) near Upper Red Rock Lake to 6,690 ft (2,039 m) 3 mi (4.8 km) eastward (Myers and Hamilton 1964). Around Lakeview, landslide deposits cut by the road are another indicator of Holocene tectonic activity in the valley.

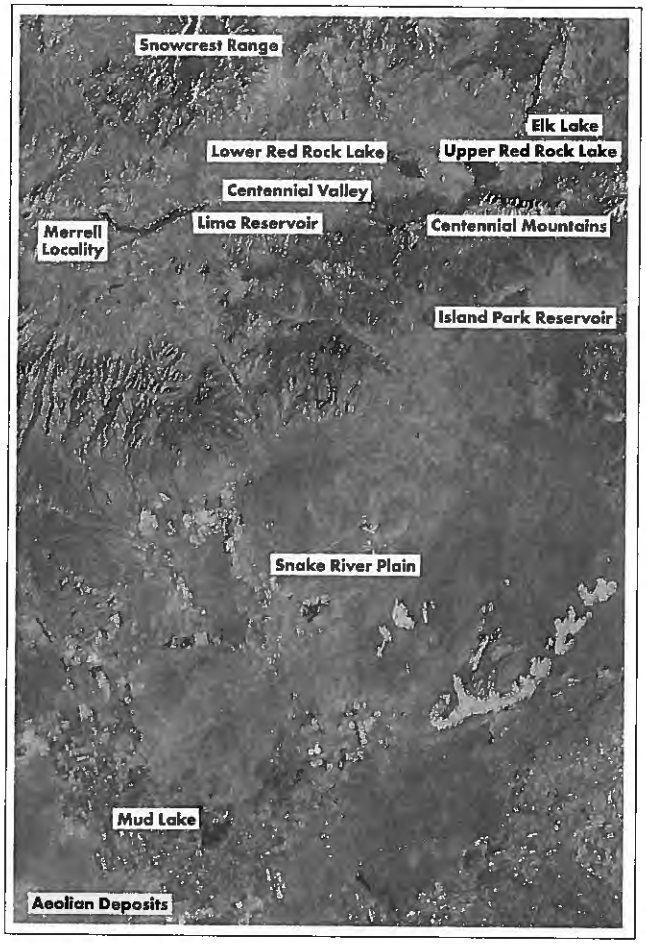

Figure 32. Air photograph showing Merrell Locality in relation to Snake River Plain.

Geomorphology and Paleohydrology

Glacial Context

The Pleistocene and postglacial physical paleoenvironmental context of the Centennial region can be inferred from stratigraphic and geomorphic evidence. Pleistocene volcanics are present, along with sediments interpreted as indicating the presence of glacial-related (moraines, outwash), mass movement (debris flow, landslides), alluvial, lacustrine, and eolian paleoenvironmental contexts.

Along with faulting and volcanism associated with the Late Cenozoic regional extensional tectonics, Centennial Valley was affected by climate change during the Pleistocene. A series of nested moraines (Figure 33) is present along the slope of the Centennial Mountains in the eastern Centennial Valley (Alden 1953; Myers and Hamilton 1964). Landforms interpreted as Bull Lake-age moraines have been mapped in the vicinity of Upper and Lower Red Rock Lakes (Alden 1953; Myers and Hamilton 1964; Witkind 1975). Alden (1953:175) observed moraines representing two distinct stages of glaciation south and southeast of Upper Red Rock Lake. In Sections 27 and 28, T14S, R1W (4-5 mi [6.5-8.1 km] east of Lakeview), the abrupt 300-ft (91.4-m) margin of a terminal moraine (ca. 6,750 fasl [2,057 masl]) is situated directly in front of a glaciated trough and cirque. The cirque hangs high above the valley flat. A glacial advance attributed to the Wisconsinan moved through a narrow trough, creating a new set of ridges with

top surfaces about 100 ft (30.5 m) lower and to the side of the older moraine (Alden 1954:175). Several terminal moraines occur east of the old moraine. Wooded moraines 5-9 mi (8.1-14.5 km) east of Lakeview are visible from the road along the southeastern part of the Centennial Valley (Witkind 1975, 1976).

Ice-Age Lakes and Drainage Patterns

The Centennial Valley has apparently contained lakes intermittently throughout the Tertiary and Quaternary (Figure 34). The size of the lakes may have enlarged during the Pleistocene due to increased runoff (Honkala 1949:130). Shorelines and beach features mark the edges of the paleolakes (Figure 35). Well-developed and fairly prominent beaches are situated on the north side of the Red Rock Lakes, but beaches are also observable on the south side (Witkind 1976; Sonderegger et al. 1982). Some of these lake margins are correlated with Pleistocene glaciation (Kennedy 1948).

There are indications that some of the lake features within the valley are older than some glacial events. Air photos have been interpreted as indicating that a few of the moraines derived from glaciers in the Centennial Mountains over-ride beach features of a Pleistocene Red Rock Lake (McMannis and Honkala 1960). Some of the beach lines are marked by lines of bushes on the air photos. Features interpreted as lake terraces have also cut into alluvial fans, equivalent to the "Old Alluvial Fans" (Witkind 1976) (Figure 35). The present lakes within the valley are considered to be remnants of larger Pleistocene lakes (McMannis and Honkala 1960).

Glacial meltwater has been proposed as a mechanism for the formation of a large lake in the Centennial Valley during the Pleistocene (Sonderegger 1981; Sonderegger et al. 1982). During part of this time at least, and perhaps even during the Holocene, the Centennial Valley drained northeastward through an outlet that followed along the Cliff Lake Fault (McMannis and Honkala 1960; Myers and Hamilton 1964). This outlet was partially blocked by mass-wasting events (Mansfield 1911). The West Fork of the Madison River appears to have begun to incise during Late Pleistocene-Early Holocene times (Sonderegger et al. 1982). Before the Late Pleistocene, the Madison River apparently flowed southwest of its present course to Cliff Lake. Tilting eastward diverted the river (Meyers and Hamilton 1964:91). To the south, the divide at Reynolds Pass separates the drainage of the Snake River and Henrys Lake from the Madison River drainage to the north. The eastern end of the Centennial Valley and the southern end of the Madison Valley appear to have been changed by the eruption resulting in the HRT, causing a change of the drainage pattern in the region (Schneider 1990).

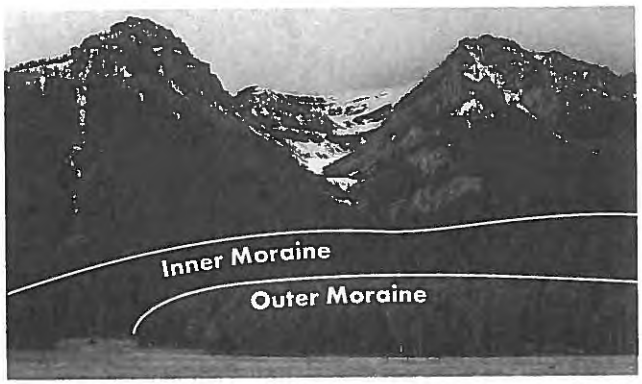

Figure 33. Moraines on east side of Centennial Valley (C. L. Hill photo).

The drainage to the east and north may have been blocked by debris flows that eventually led to drainage to the west through the Lima Reservoir Dam pass (cf. Myers and Hamilton 1964:95) (Figure 31). The Red Rock River presently flows westward out of the Centennial Valley at a constriction regulated by the Lima Reservoir Dam. Alden (1953) indicated the presence of limestones, but perhaps conglomerates are a more characteristic lithology. To the west (about 2 mi [3.2 km] from the dam), bench surfaces at heights of 1,000 ft (305 m), 800 ft (245 m), and "several hundred" feet above the valley have been interpreted as probably reflecting the Pliocene and early Pleistocene downcutting of Red Rock Lake west of an outlet from the Centennial Valley (Alden 1953:15,38,40). Two river terraces southeast of Lima and along the Red Rock River are thought to be probably Pleistocene in age and related to mountain glaciation (Scholten, Keenmon, and Kupsch 1965). The valley is very wide and broad until it narrows at the dam, 15 mi (24.2 km) east of Lima.

Deposits in the Western Centennial Valley

The areas bounded on the east by Lower Red Rock Lake and on the west by the eastern margin of the Lima Reservoir were studied by Honkala (1949). G. C. Kennedy mapped part of the U.S.G.S. Lyon Quadrangle in 1947-1948. Honkala described a Pleistocene alluvium exposure (Sec. 2, T145, R4W, U.S.G.S Antelope Peak Quadrangle, between Lima Reservoir and Lower Red Rock Lake) of a 10-m-thick sedimentary sequence composed of mainly silt and marl. The first unit is about 30 ft thick (9.1 m). It consists of gray silts, white marl, and gravel lenses. There are several marls up to about 5 in (12.8 cm) thick. Some of the gravel lenses are 6 in (15.4 cm) thick. The bedding is very irregular. Gastropods (*Lymnae caperata*) were found at a depth of 15 ft (4.6 m) from the surface, as were gopher (*Thomomys talpoides*) and ground squirrel (*Citellus*) bones

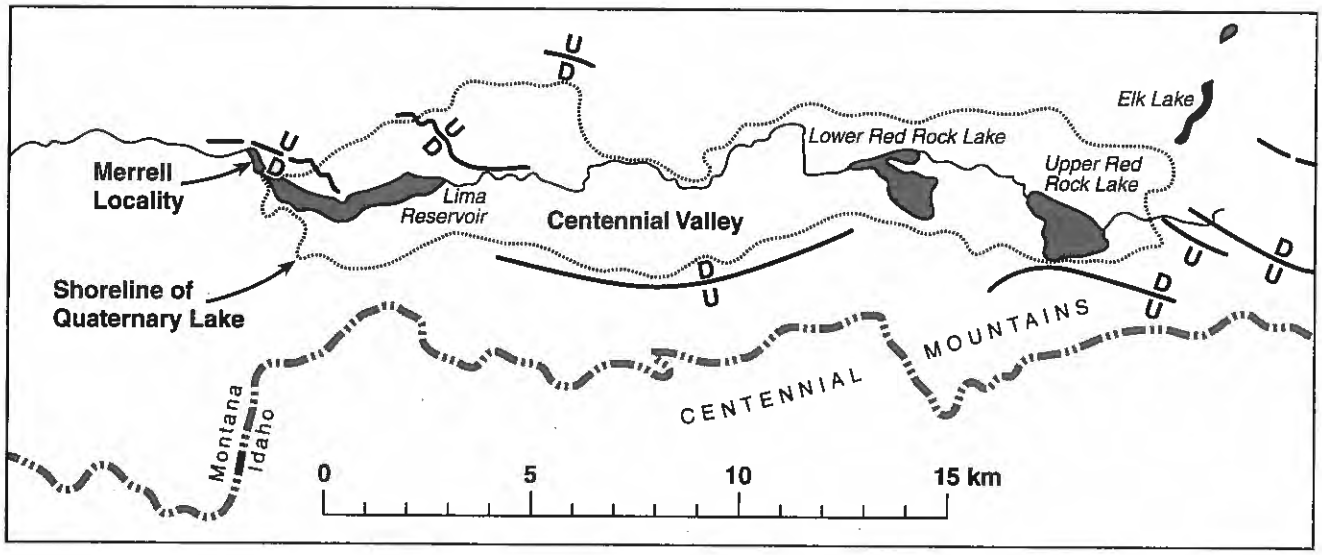

Figure 34. Shorelines and faults in Centennial Valley (after Myers and Hamilton 1964).

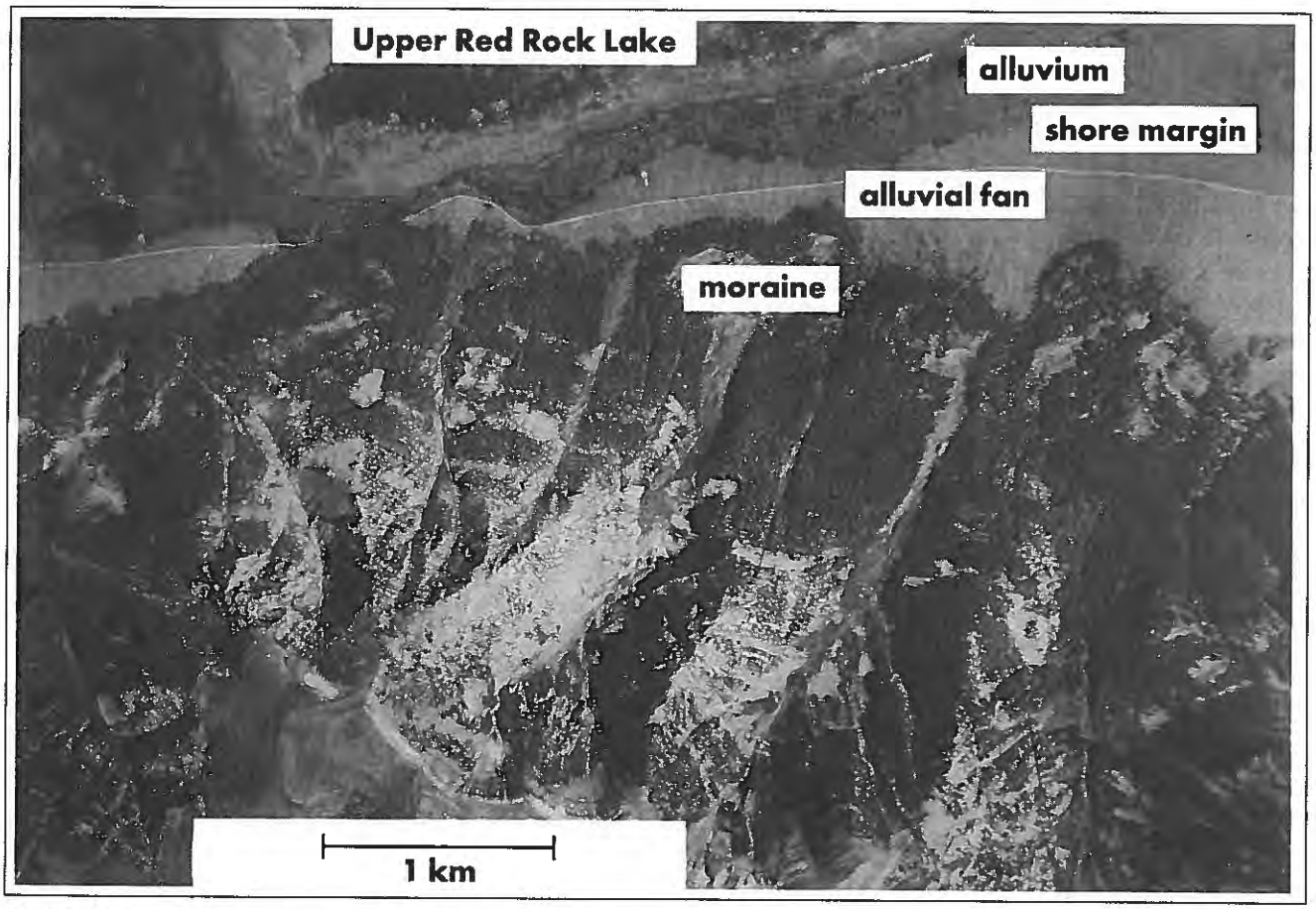

Figure 35. Air photograph of Quaternary shorelines and other geomorphic features near south side of Upper Red Rock Lake.

(identified by Claude Hibbard). The gastropods are considered to be freshwater forms that inhabit pools in lake-like settings. The second major stratigraphic unit is a silty, white, unconsolidated marl. It is about 5 ft (1.5 m) thick and contains bone fragments of rodents. Honkala (1949:100) interpreted this to indicate that small lakes or larger temporary lakes intermittently occupied all or parts of the Centennial Valley. He observed old beach lines on

the valley slopes and wave truncation spurs extending into the valley.

The general scenario envisioned by Honkala is a model where sediments eroded from the uplifted mountains during the Pleistocene were deposited within the Centennial Valley as broad, sloping alluvial fans and as lake sediments (Honkala 1949:123). Honkala postulated that, during the Late Pleistocene and Holocene, waters supplied by melting glaciers covered the Centennial Valley. When the glacial lakes receded, the areas of unconsolidated sediments (mostly sands and silts) were exposed to wind action. Sand dunes and beaches in Centennial Valley (T13S, R2W), mapped by Witkind (1975) and Sonderegger et al. (1982), provide support for the basic model. Sand deposits overlying lacustrine sediments have been interpreted as evidence of Holocene aeolian activity within the valley.

The shorelines of prehistoric lakes were recognized on aerial photographs and in the field by Meyers and Hamilton (1964). A prominent shoreline cuts into alluvial fans thought to have been deposited as a result of sedimentation associated with the youngest Pinedale moraines. This implies that a lake existed in postglacial times, which Meyers and Hamilton tentatively propose at ca. 4,000 years ago.

The shoreline north of Upper Red Rock Lake has been eroded away by the lateral migration of the floodplain of present-day Red Rock Creek. South of the floodplain, the shoreline is deformed, ranging in elevations of 6,630-6,690 ft (2,020-2,040 m), while, to the north, it seems to have an elevation of about 6,650 ft (2,030 m) (Myers and Hamilton 1964). The present Red Rock River is entrenched up to 50 ft (15.2 m). Downcutting of tributaries has caused incision into the landforms that is visible on aerial photographs as well as on U.S.G.S. topographic maps. The most reasonable explanation for this incision would be the relative lowering of the divide near the present-day site of the Lima Reservoir Dam. Recurrent lowering and uplift connected with faulting in the Centennial Valley may be a partial explanation for aggradational and erosional episodes recorded in the sedimentary sequence at the Merrell Locality.

On the west side of the Centennial Valley, there are two faults north of Lima Reservoir (Myers and Hamilton 1964) (Figure 34). Both faults trend generally northwest-southeast, have a down-dropped southwest side and an uplifted northeast side, and cut across the shoreline of a Late Quaternary lake thought to have filled the entire valley. The fault north and east of the Lima Reservoir extends from about the paleolake shoreline to the present-day floodplain of the Red Rock River. The fault along the west extends from near the north shore of the reservoir, across the paleolake shoreline westward past the Lima Reservoir Dam (Figure 34). North of Lima Reservoir, the surface of the paleolake floor has been offset about 20 ft (6.1 m) along irregular fault scarps. The faulting associated with a major earthquake has been proposed as a tectonic event that emptied the paleolake (Myers and Hamilton 1964).

Within the Lima Reservoir Graben, there is a Late Pleistocene surface (ascribed as post-Bull Lake to Pinedale/post-Pinedale to pre-Holocene) as well as stream terraces (Stickney and Bartholomew 1987). These are all offset by the Lima Reservoir Fault scarp (Stickney, Bartholomew, and Wilde 1987). The stratigraphic sequence indicates at least 5 m (=16 ft) of pre-Pinedale (?) deposits offset along the scarp, accompanied by sandblows. After this Pleistocene faulting, along the downthrown side, gravels were deposited at the base of the scarp. The fluvial gravels are overlain by silts interpreted as loess. A buried soil formed at the top of these silts is overlain by a younger silt deposit, also interpreted as a loess. This upper silt is overlain by the present-day soil (Stickney, Bartholomew, and Wilde 1987).

In summary, a combination of tectonic and climatic processes should be considered when developing models to interpret the Pleistocene geomorphic and sedimentologic record of the Centennial Valley. Volcanism, faulting, and landform features connected with seismic activity within the valley are interconnected, with fluctuating climatic conditions that have prevailed over about the last 2 million years.

Merrell Locality Stratigraphy

The geomorphic, stratigraphic, and sedimentologic context of the Merrell Locality and environs was studied between 1994 and 2001. Field research in 1994 was focused on the stratigraphic exposures in MOR Test Pits/Excavation Areas E and C and along the escarpment (Figures 16-38). The geologic research was undertaken in collaboration with Albanese (Albanese 1995; Albanese, Davis, and Hill 1995; Hill, Davis, and Albanese 1995; Hill and Albanese 1996). In 1995, more detailed stratigraphic studies were conducted along the exposed escarpment and the sequences exposed by MOR excavations in the South and North Blocks (Figure 39). Albanese also conducted field studies in 1995 that were principally focused on North Block stratigraphy, but also collaborated on more detailed studies along the escarpment and within the South Block excavations.

The 1996 stratigraphic studies were conducted by Hill independently after the MOR excavations for that year. Studies included documentation of the sequences exposed by the 1996 MOR excavations as well as more detailed documentation of the sequence along the escarpment, pri-

marily south of the South Block. Visits to the Merrell Locality in summer 1997 were connected with obtaining chronometric samples for luminescence measurements as part of a collaborative Pleistocene dating program with Jim Feathers, University of Washington (Feathers, this report). This included reexamination of the escarpment sequence and sampling of both the South and North Block areas. Brief visits to assess site erosion were undertaken in 1998-2001. Drought conditions in 2001 provided an opportunity to observe the vicinity of the Merrell Locality as it may have appeared prior to the installation of the dam. The low water levels made it possible to see the generally "pre-dam" topography and the location of the Red Rock River channel.

Stratigraphic Descriptions

The stratigraphy at the Merrell Locality has been studied within the three-dimensional grid-coordinate system used during the MOR excavations (Figure 4). Besides the U.S.G.S. 7.5-minute topographic map, two other more-detailed maps have been used, each with the MOR grid-coordinate system superimposed on the topographic map. A topographic map produced by Troy Helmick shows the locations of the 1994 MOR excavations in relation to site physiography (Figure 4). A second topographic map was made by Albanese in 1994 with special reference to the MOR excavations and the escarpment (Figure 16). Albanese placed a series of mapping stations on this map which were connected to the MOR grid-coordinate system. In 1995, a new series of survey stations was placed primarily along the escarpment. These were connected to the grid system in 1995 by Batten, and some of the stations were resurveyed by Batten in 1996. Both Hill and Albanese used the same set of survey stations in 1995 which were marked with rebar and flagging tape. Studies along the escarpment from 1996 to 2001 used the 1995 reference stations as temporary datum points, especially along the escarpment away from the South and North Block excavations.

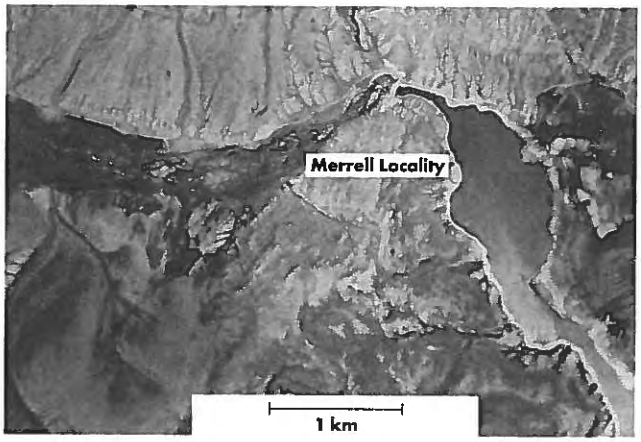

Figure 36. Air photograph of Merrell Locality and the west side of Centennial Valley.

Grid 80-120 N Escarpment Stratigraphy (South of South Block)

This area includes the south part of the escarpment, which is the area south of the MOR South Block excavations (Figure 39). Fossil specimens from this area include University of Montana collections FS55-57 (beach collections?), F7-12, F16, and F17 (escarpment collections?) based on a map provided by Tom Foor which connects the University of Montana study area with the MOR topographic map produced by Helmick. Faunal remains recovered by the 1989 University of Montana excavations from this general part of the Locality included *Mammuthus* sp., *Camelops*, *Ondatra zibethicus*, *Castor canadensis*, and *Equus* (based on data in the Dundas inventory). The area farther

Figure 37. View looking generally east toward the Merrell Locality (C. L. Hill photo).

Figure 38. View looking generally southeast toward the Merrell Locality (C. L. Hill photo).

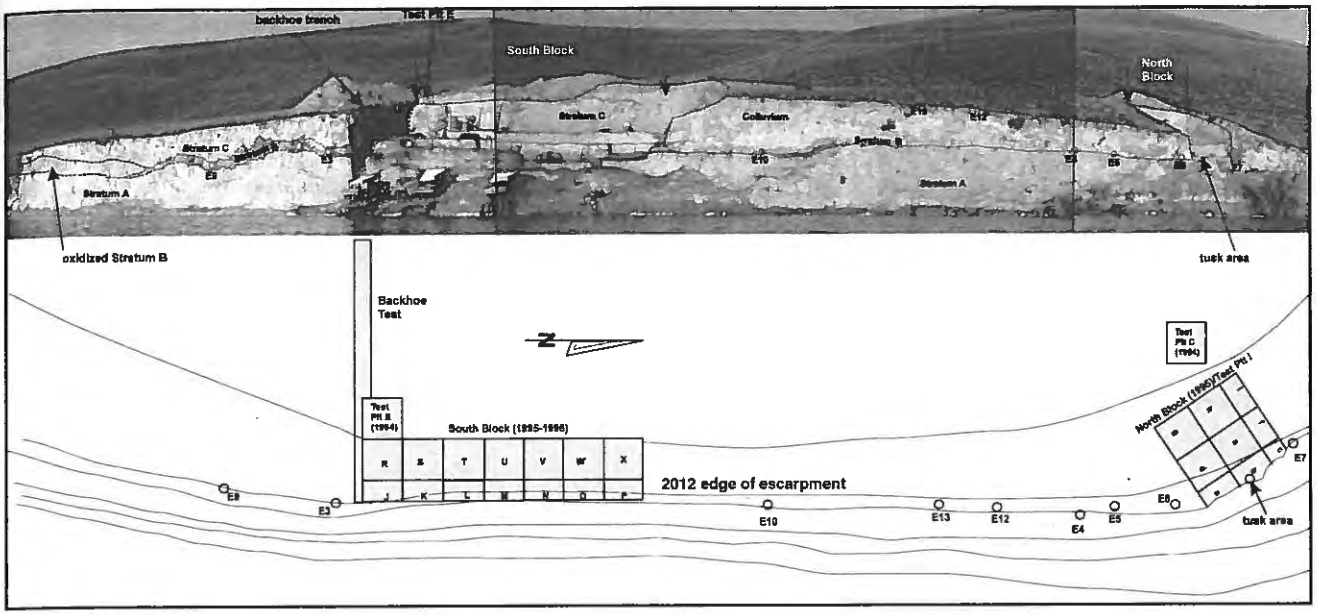

Figure 39. Map and photograph showing North and South Blocks, major strata, Merrell Locality (C. L. Hill photo and map).

to the south was studied by Albanese and Hill in 1994 and by Hill in 2001, including the area where University of Montana collections F2-F6 were made.

Albanese mapped this part of the escarpment in 1994 (Albanese 1995, this report). In 1995, Hill produced a 1:20 field sketch of this area using the approximate locations of the 1994 Albanese mapping stations A4-7, A22, and A24 and 1995 survey stations E9 and E3. Some of this area was remapped again in 1996 when inspection revealed fossils apparently in situ within stratum A (Figure 40).

The land surface along this part of the Merrell Locality escarpment slopes toward the south. Facies variants of the principal strata at the site were clearly observable. The lowermost geologic unit, stratum A, can be separated into several substrata. Lower deposits tend to contain a higher amount of clay and silt-sized particles, while sands appear more prominent near the top of the stratum. The upper part is generally more massive and can contain varying degrees of clay, silt, and occasional pebbles within a generally fine sand matrix. Although the lower part of stratum A appears to consistently contain beds of well-sorted silts and clays, it also contains lenses of sand and gravel.

The distinct, dark (organic-rich) facies of stratum B lies above stratum A along the north side of this part of the escarpment. It has been strongly affected by micro-faulting. Toward the south, at around grid intersection 105N with the escarpment, there is a lateral facies change in stratum B. From about 105N to 75N, stratum B is present as a zone of higher oxidation (Figure 17).

Stratum C overlies stratum B and consists primarily of silt-dominated sediments with lenses of sands and gravel. Along this part of the escarpment, its upper surface is severely disturbed by rodent burrows and is overlain by colluvium. A soil had developed in the overlying colluvium.

Grid 120-140 N Stratigraphy (South Block Excavations)

Detailed stratigraphic studies were conducted between Grid 120 and 140 in the central part of the escarpment (Figures 11 and 39). This area includes the MOR South Block excavations (Hill and Batten 1997, this report). In 1994, the Test Pit/Excavation Area E stratigraphy was studied along with mapping along the escarpment exposure (Albanese 1995, mapping stations 9, 10, 25, and 26). The general area includes the 1995 survey stations E3 (just south of 120N along the escarpment edge) and E10 (just north of 140N along the escarpment, Figure 39). In 1995, a detailed description was made of the profile exposed just north of 120N as well as sequences exposed in Excavation Areas J-X. The stratigraphy exposed during the 1996 MOR excavations was also in this general vicinity. The sequence consists of strata A, B, C, and the overlying colluvium (Figure 41).

This part of the Locality includes the area examined by Robert Bump and the FS58 and F18 collections by the University of Montana (based on map provided by T. Foor). F18 contained the remains of *Mammuthus* sp. (according to the inventory prepared by R. Dundas from the 1989 University of Montana collections, see Dundas, this report).

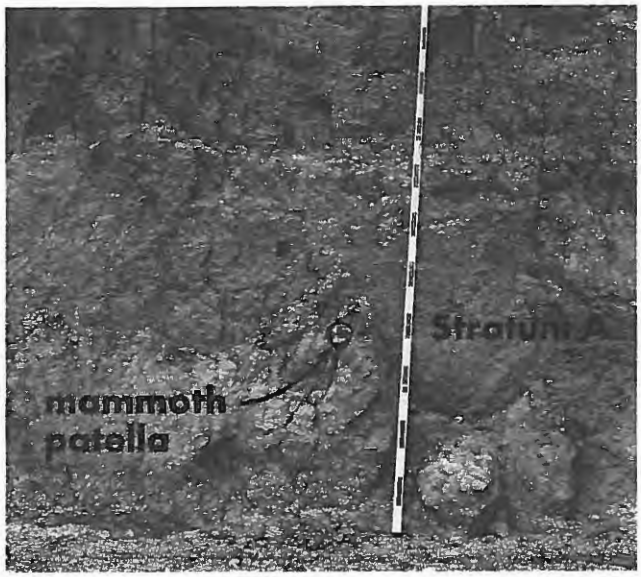

Figure 40. Fossil in stratum A (C. L. Hill photo).

Excavation Area E Stratigraphy (1994 Test Pit E)

The stratigraphic sequence exposed in Test Pit/Excavation Area E is described in some detail since it served as the initial basis for the designation of strata A, B, and C and the overlying colluvium (Figures 41-47). In its major lithologies and relationships, it was essentially duplicated in the 1995 backhoe trench stratigraphy, in Excavation Areas J-X, and along the escarpment exposed from about 105N-160 N. At Excavation Area E, the sequence was originally separated into six major lithologies (Merrell 1994 Test Pit local lithologies, in Hill, Davis, and Albanese 1995). The 1995 backhoe trench made a direct connection between these Excavation Area E deposits and those observed on the natural escarpment exposure directly to the east (Figure 39). The sequence has been extensively subjected to postdepositional alteration, including liquefaction deformation, microfaulting, and bioturbation. The description here follows the stratigraphic designations published in Albanese, Davis, and Hill (1995).

Stratum A (sandy facies, LL1 of Hill, Davis, and Albanese 1995, lowest observed sediments in Test Pit/Excavation Area E). This is primarily a light brownish gray (2.5Y 6/2) muddy sand (Figure 46 and 47). It appears massive (structureless), with some Fe-oxide streak stains (7.5YR 6/6). Nodules and concretions of $CaCO_3$ within the matrix are less than 2 cm and white (10YR 8/2). Fragments of bone occur within the upper part of the deposit as well as along the boundary with stratum B. In Excavation E, deposits of stratum A interfinger and splay into stratum B (Figures 41 and 44). Splays are directly connected to stratum A, and there also appear to be isolated lenses of stratum A within stratum B (one with a mammoth molar). These splays are interpreted as indicators of postdepositional liquefaction deformation. Similar deformation seems to be indicated by intrusions of stratum B sediments downward into stratum A. A mammoth molar was lying on the upper boundary between these two strata.

Compositional information derived from loss-on-ignition is presented in Huber (1997, this report). Organic content is less than 3 percent, with less than 4 percent carbonate; this stratum has the highest amount of siliciclastics and the least amount of carbonate in the Excavation Area E (1994 Test Pit E) sequence.

Stratum B (high organic facies, LL2 in Hill, Davis, and Albanese 1995). This is a dark-colored series of deposits (Figures 41 and 43), higher in organics and clearly visible on the escarpment exposure east of Excavation Area E. It is composed of sandy mud and silts (Figures 46 and 47). The base contains vertebrate remains, including mammoth bone, which include organics radiocarbon dated to ca. 37,000 yr B.P. (Table 7; Hill 1999). These organics may be younger than the age of the bone. Some of the sub-

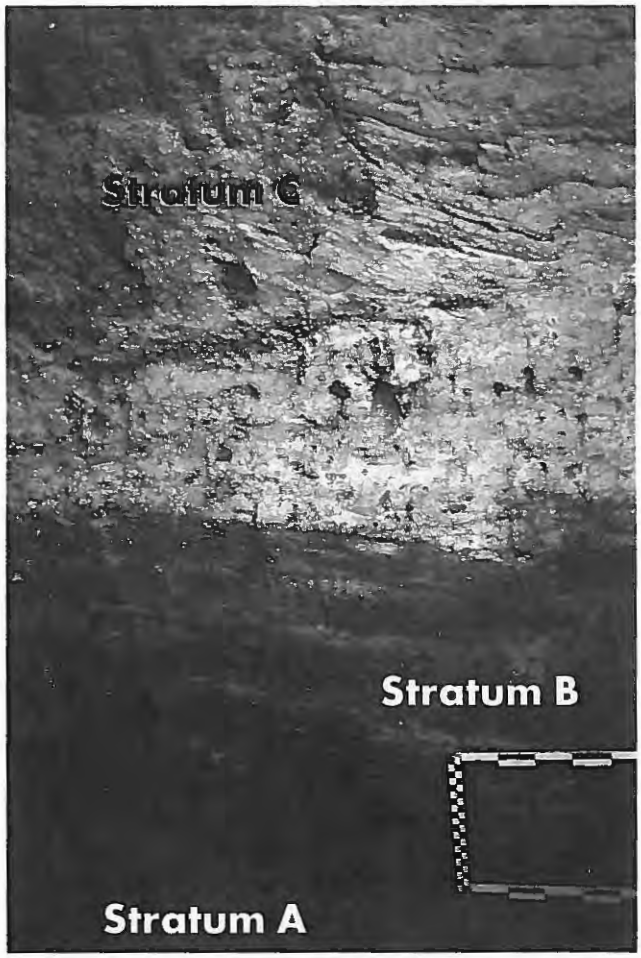

Figure 41. Strata A-C, Test Pit/Excavation Area E, South Block, Merrell Locality (C. L. Hill photo).

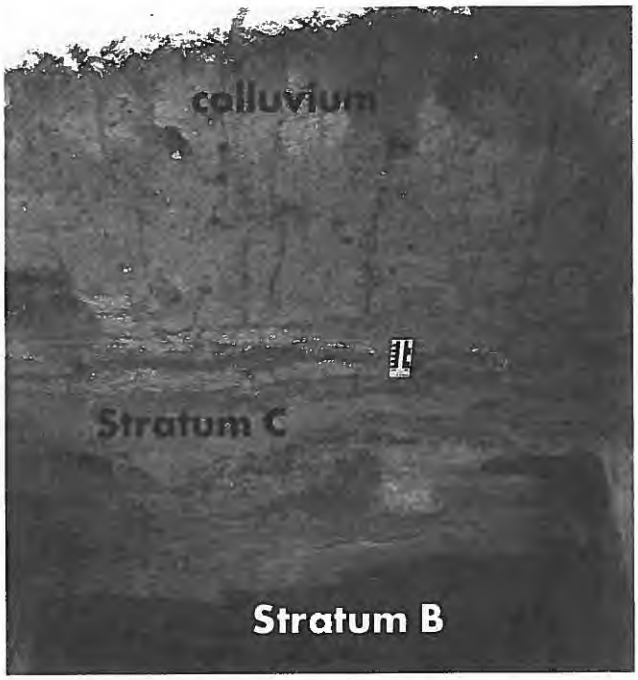

Figure 42. Strata B and C and overlying colluvium, Test Pit/Excavation Area E, South Block, Merrell Locality (C. L. Hill photo).

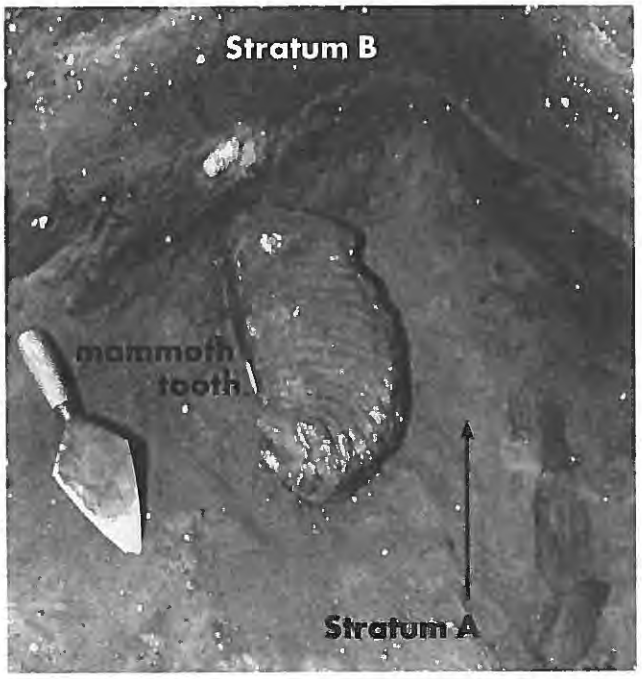

Figure 43. Mammoth tooth and rib fragments along interface of upper stratum A and lower stratum B, Test Pit/Excavation Area E, South Block, Merrell Locality (photo by D. Batten).

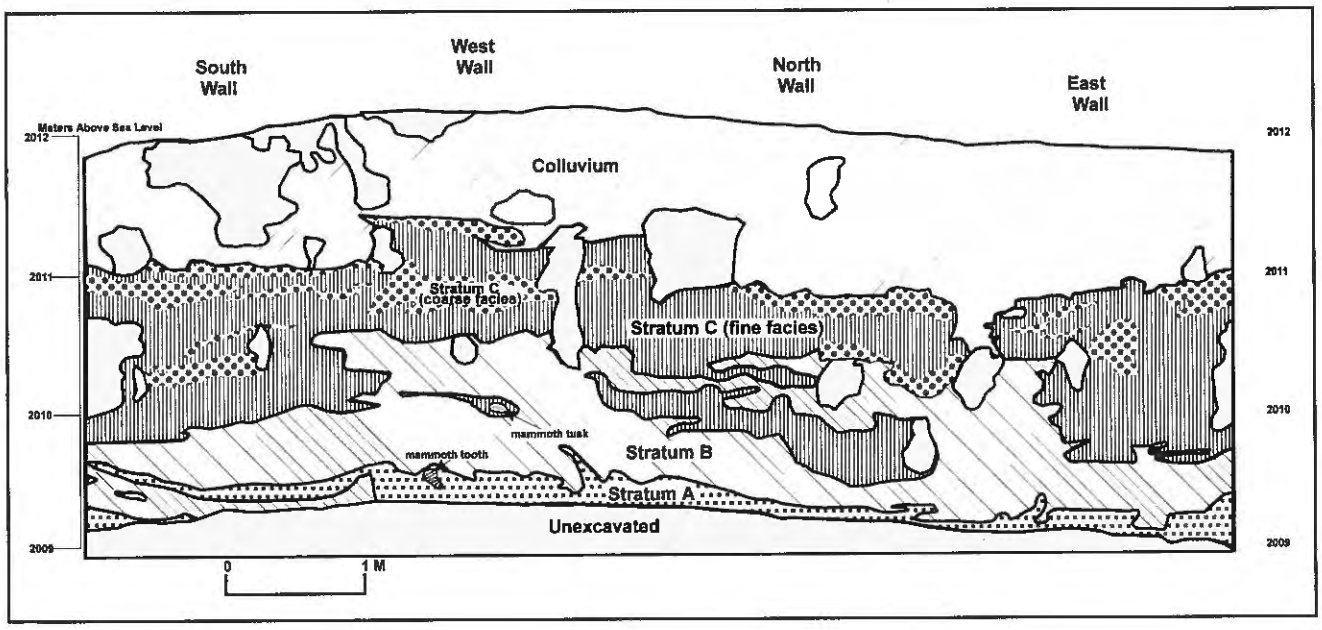

Figure 44. Stratigraphic sketch of Test Pit/Excavation Area E, South Block, Merrell Locality (profile by C. L. Hill).

facies in this stratum are interdigitated with stratum A, apparently as a result of postdepositional deformation. Stratum B can be generally separated into a series of differently colored darker beds (facies) that interfinger with lenses of light-colored muddy sands of stratum A. Postdepositional deformation has caused intrusive splays of stratum B into both stratum A and the lower layers of stratum C.

Some differences in the lithologic characteristics of deposits in stratum B appear to reflect various depositional facies. The lowermost facies is a very dark grayish brown (10YR 3/2) massive organic silt layer. Another facies overlies this splay of stratum A (LL1) and contains a mam-

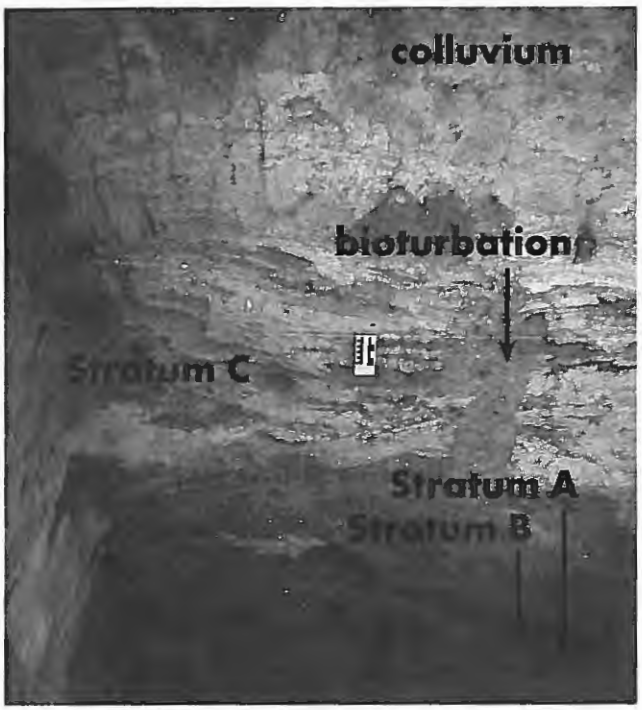

Figure 45. Test Pit/Excavation Area E, showing strata A-C, colluvium, and bioturbated areas (C. L. Hill photo).

moth molar along its lower boundary. Another facies consists of a pale brown (10YR 6/3) massive silt that forms the upper part of stratum B. It is apparently more oxidized and contains less organics. Lenses of high oxidation and reddish yellow (7.5YR 6/6) streaks occur within the substratum. Possible splays of stratum C (perhaps even stratum A) are mixed within the darker beds of stratum B; they are unoxidized light brownish gray (2.5Y 6/2) lenses. Another lithologically distinctive facies is a light brownish gray (2.5Y 6/2) layer. Coarse-texture areas within this stratum are more oxidized.

Loss-on-ignition measurements (Huber 1997, this report) indicate that stratum B has an organic carbon composition of 6 to 8 percent, with carbonate about 5 percent; these contain the highest amount of organic carbon and the second highest amount of residual clastics within the Excavation Area E sequence.

Stratum C (silt facies, LL3 of Hill, Davis, and Albanese 1995). Two major lithofacies occur within stratum C (Figures 46 and 47). Beds are composed predominantly of light-colored, fine-grained clastics (mostly silts) and interbedded coarse clastic lenses (mostly sands, granules, and pebbles). Both facies contain deformation structures and microfaulting. Mollusc fragments occur within both of these lithologies. The molluscs within the coarser facies are more likely to be in secondary, lag position.

Stratum C always overlies stratum B. The fine-grained

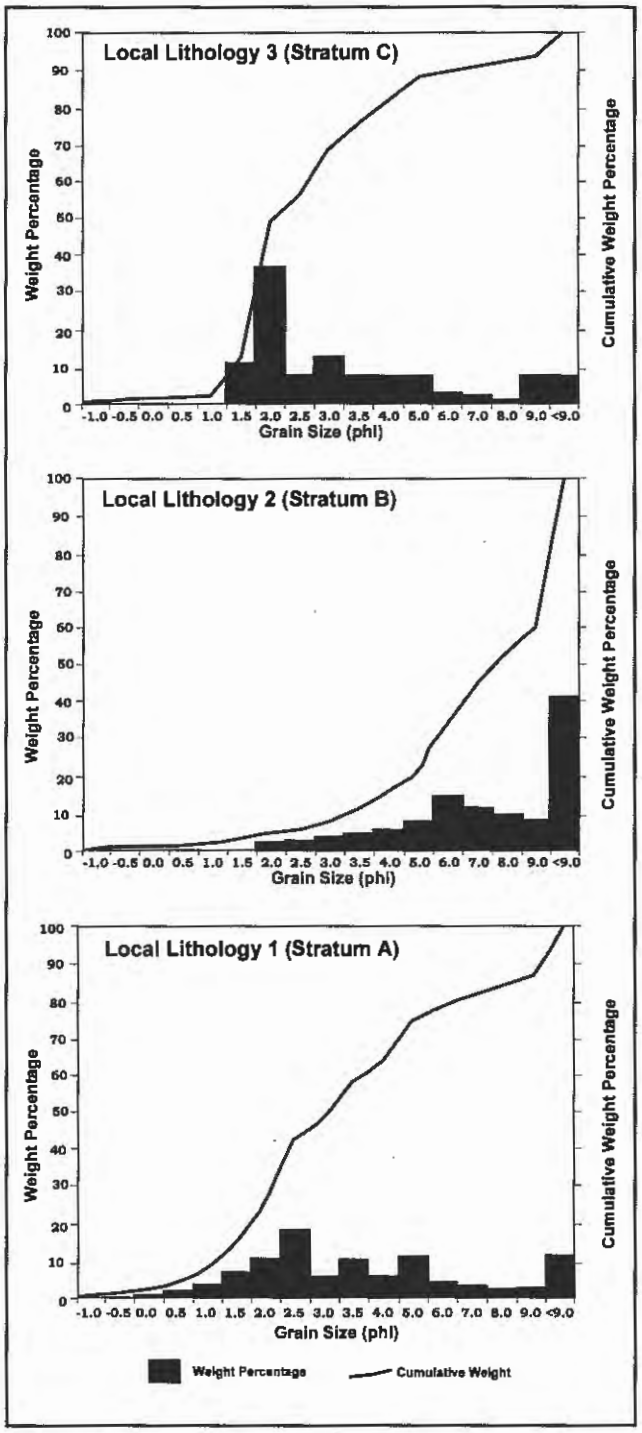

Figure 46. Grain size histograms for strata A-C.

facies consists of massive light gray (2.5Y 7/2) sandy silt or mud with shell fragments. It contains $CaCO_3$ concretions that are > 2 cm in diameter. Probably because of postdepositional deformation, it contains lenses of what appear to be stratum B. The lowermost facies is a massive light gray (2.5Y 7/2) silt. It is separated from the overlying deposits by a very distinct erosional unconformity and a

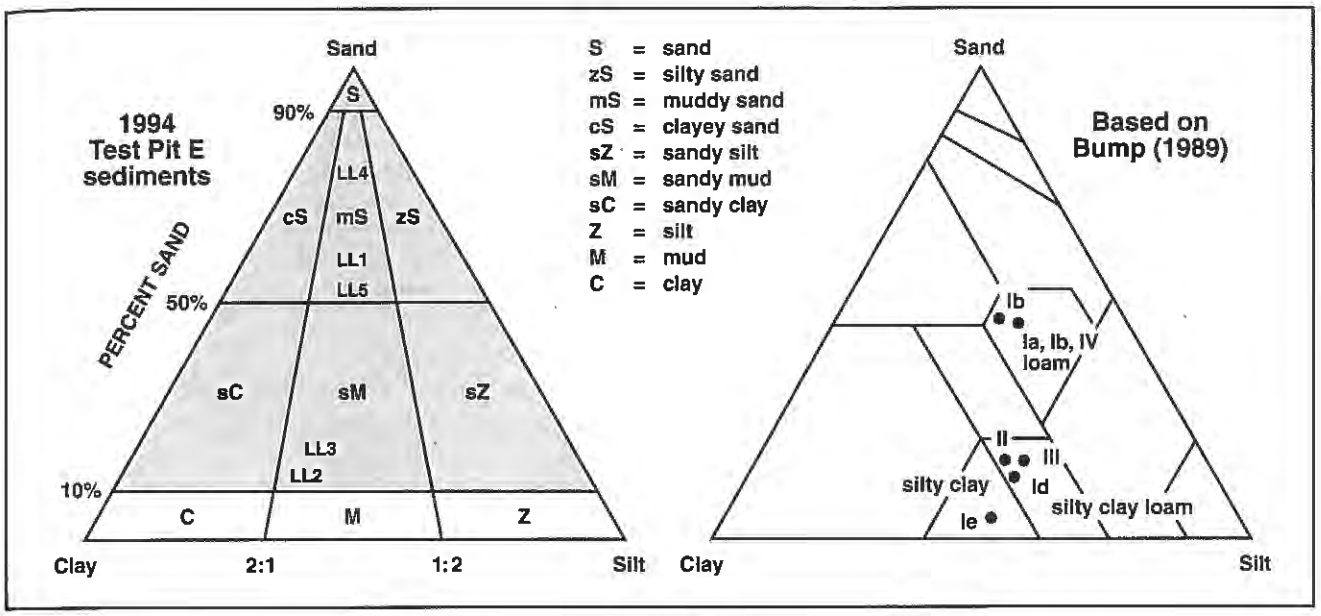

Figure 47. Texture of sediments of stratum A (LL1), stratum B (LL2), stratum C (LL3, LL4), and colluvium (LL5, equivalent to stratum E in Albanese, this report).

thin lens of coarser clastics. The overlying bed of stratum C is slightly lighter in color, but the difference is not detectable with the Munsell color chart. Another fairly massive silt overlies this bed. The uppermost subfacies of the fine clastic series overlies coarse clastic lenses and seems to grade upward into a less well-sorted sedimentary matrix interpreted as colluvium (Figures 42 and 44).

Compositional estimates, based on loss-on-ignition measurements (Huber 1997, this report) for the stratum C silts, are organics 3-4 percent and carbonates 26-33 percent. These constitute the highest amounts of carbonate, the second highest organics, and the lowest proportion of clastics in the stratigraphic sequence from Excavation Area E. Mollusc fragments and ostracods are present in these beds. The presence of ostracods is one of the primary criteria for including the lower facies of stratum C within this geologic unit, even though a major erosional unconformity separates it from the rest of the stratum.

Stratum C (coarser clastic facies, LL4 of Hill, Davis, and Albanese 1995). Interbedded within the silts of stratum C are lenses that consist of clearly visible coarser clastics (sometimes muddy sands, Figures 46 and 47). The laminations and beds of the coarser clastic lenses are highly convoluted and distorted, and they commonly exhibit oxidation stains. Besides these convolutions, some of the lenses exhibit distinct normal micro-faulting (Figure 48). The sediment-size fractions range from fine sand to pebbles and are typically very well-sorted. The lenses contain areas of higher secondary carbonate or gypsum. The sands and gravels are commonly subrounded to subangular and light gray (2.5Y 7/2). The convoluted stains and oxidation boundaries for these coarser clastics are reddish yellow (7.5YR 7/8). These are laminated to thinly bedded and contain (redeposited?) shell fragments.

The loss-on-ignition data presented by Huber (1997, this report) indicate that, compositionally, organic content is low (1-3%) and carbonate content can range from ca. 15 to 25 percent. The carbonate is presumably secondary. These coarse clastic facies of stratum C contain the least amount of organic carbon, relatively high amounts of carbonate (but lower than the silts of stratum C), and higher amounts of clastics compared to the stratum C silts.

Unsorted Matrix (colluvial facies, LL5 of Hill, Davis, and Albanese 1995). In the higher part of the Excavation Area E sequence are occasional areas of light gray (10YR 7/2) muddy sand, sometimes highly disturbed, which at times show a gradational transition with the silt facies of stratum B along with the introduction of some colluviation (Figures 45 and 47). They seem to exhibit less-convoluted bedding, no discernible laminae of coarser clastics, and incipient pedogenic structures (including turbation features) which had been superimposed on and which sometimes had obliterated the original structure and textures. Within this less well-sorted matrix, bedding planes are less apparent, less oxidized, and less convoluted. The bedding planes which are apparent are observable because of light oxidation along the boundaries.

Compositional values based on loss-on-ignition (Huber 1997, this report) indicate that organics are less than 3 percent and carbonate content is greater than 23 percent.

Table 3. Radiocarbon Ages and Stable Isotope Measurements from the Merrell Site.

Laboratory Number	Conventional ^{14}C Age B.P.	Material	Isotope Ratio	Location	Approximate Date Based on U-Series Correlation	Rocky Mountain Climatic-Chronologic Context
Beta-26205	25,030 ± 510	mammoth metatarsal, collagen extraction	not provided	"channel fill" (stratum D debris flow deposits)	about 28,000 years ago	Main Pinedale Deckard Flat advance in Yellowstone; Middle Pinedale in Tobbacco Root Mountains
Beta-77826	19,310 ± 90	bone collagen, extracted with alkali	-23.7 (C3 pathway)	stratum D, debris flow deposits	22,000 years ago	end of Main Pinedale or following interstadial (glacial recession)
Beta-118755	21,530 ± 100	bone collagen, extracted with alkali	-20.9	Stratum D	25,000 years ago	Main Pinedale Deckard Flat advance in Yellowstone; Middle Pinedale in Tobacco Root Mountains
Beta-110647	43,970 ± 370	bone collagen, extracted with alkali, *Cygnus*	-11.1	beach surface	about 45,000 years ago	Early Pinedale
Beta-74032	36,500 ± 710	organic retrieved from within bone	-26.0 (C3 pathway)	stratum B (Test Pit 1994 E, LL2)	about 39,000 years ago	Early Pinedale
Beta-36206	>33,990	mammoth fibula, collagen extraction	not provided	2.1-m zone within main section (likely stratum B)	older than 36,000 years ago	Early Pinedale or older
Beta-111325	32,470 ± 270	tusk collagen, extracted with alkali	-25.2	stratum B	about 35,000 years ago	Early Pinedale, possibly late transition
Beta-83614	>41,900	humates	-28.2	stratum B	> 43,000 years ago	Early Pinedale or older
Beta-116519	49,350 ± 1,500	mammoth bone collagen extracted with alkali	-19.2	stratum A	about 49,000 years ago	Early Pinedale

These contents are similar to some sediments within stratum C. Mollusc fragments and ostracods are present within the matrix.

Disturbed Areas ("rodent burrows," LL6 of Hill 1995). Throughout the sequence are highly disturbed areas that contain poorly sorted (unsorted) and bioturbated sediments (Figure 45). They generally occur higher in the sequence, although they do interrupt deposits of stratum B and stratum C.

A description of the potential locations of fossils recovered from Test Pit/Excavation Area E is available in Hill and Batten (1997), this report.

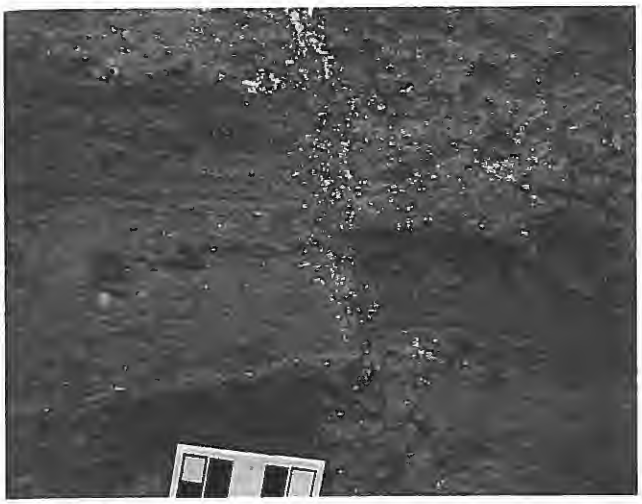

Figure 48. Normal faulting of stratum C (C. L. Hill photo).

The 1995 Backhoe Sequence

In 1995, a backhoe trench was placed along the east-west axis of the site grid, slightly grid north of 120N (Figure 34). This trench was cut from the edge of the escarpment through the southern portion of Excavation Area J and the south wall of Excavation Area E. Thus, the stratigraphic sequence provides an exposure of the sedimentary sequence essentially 90° from the escarpment exposure as well as directly linking the sequence at Test Pit/Excavation Area E with the escarpment stratigraphy and the J-X Excavation Areas within the South Block.

Figure 49 is a generalized depiction of the stratigraphic sequence exposed in the backhoe trench. The trench exposed a 13-m-long (43 ft) stratigraphic sequence (running from 113-126E, the edge of the escarpment is around 126E). All of the major strata described from Excavation Area E are present (Figure 50).

Stratum A. There is a general eastward dip to the top surface of stratum A. An oxidation zone was also easily observable at the top of the stratum. Fossils occur within the top of stratum A in this part of the site.

Stratum B. Two major subfacies are present (Figure 49). The lowest part of the stratum is darker and higher in organics. Fossil bones were mapped in situ within these deposits. A lighter-colored series of beds overlies this lowermost facies. They are in places highly contorted and splay into stratum C. Humates obtained from a sediment sample collected from the wall of the backhoe trench yielded a conventional radiocarbon age of >41,940 ^{14}C yr B.P. (Table 3; Hill 1999).

Stratum C. The silts and coarse clastics of this stratum are highly contorted. The same normal fault mapped in Test Pit/Excavation E was mapped in this section. Some areas within this stratum are interpreted as rodent burrows.

Colluvium. About 1 m (3.3 ft) of unsorted sediment is interpreted as colluvium with disturbance areas.

Deposits Observed Along the Exposure and in J-X Excavation Areas

The stratigraphic profiles measured along 121-135N were recorded in conjunction with detailed excavations of the lower part of stratum C, stratum B, and the top of stratum A in Excavation Areas J-X during 1995 and 1996 (Figure 51). These can be connected to the 1995 backhoe trench and to the Test Pit/Excavation Area E sequence

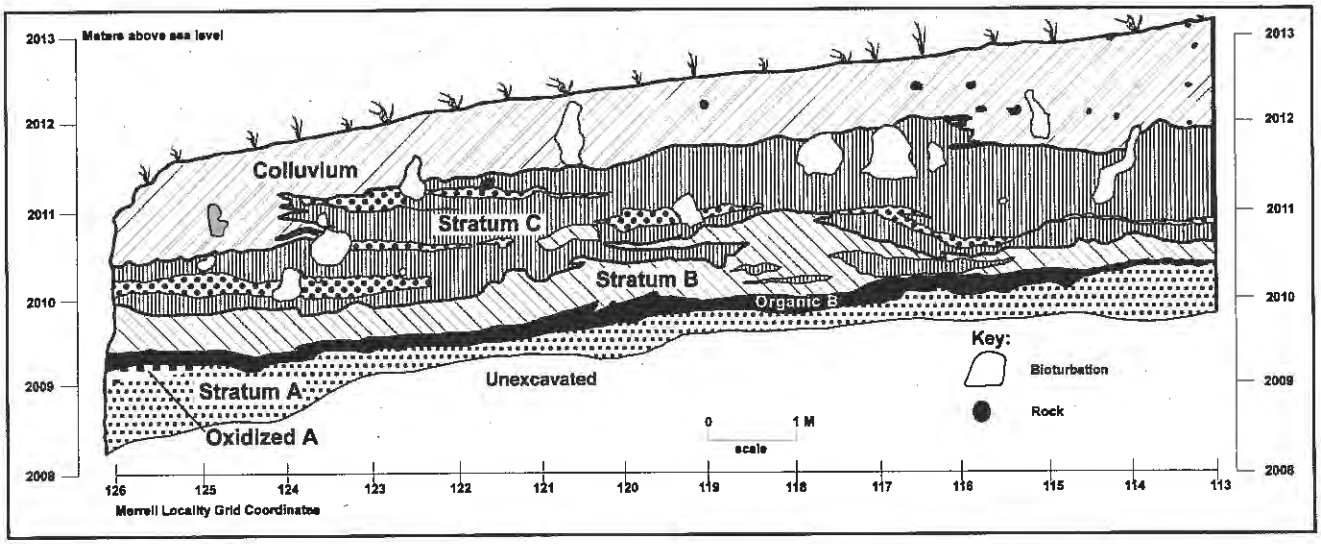

Figure 49. Stratigraphic section of backhoe trench, south side of South Block (profile by C.L. Hill).

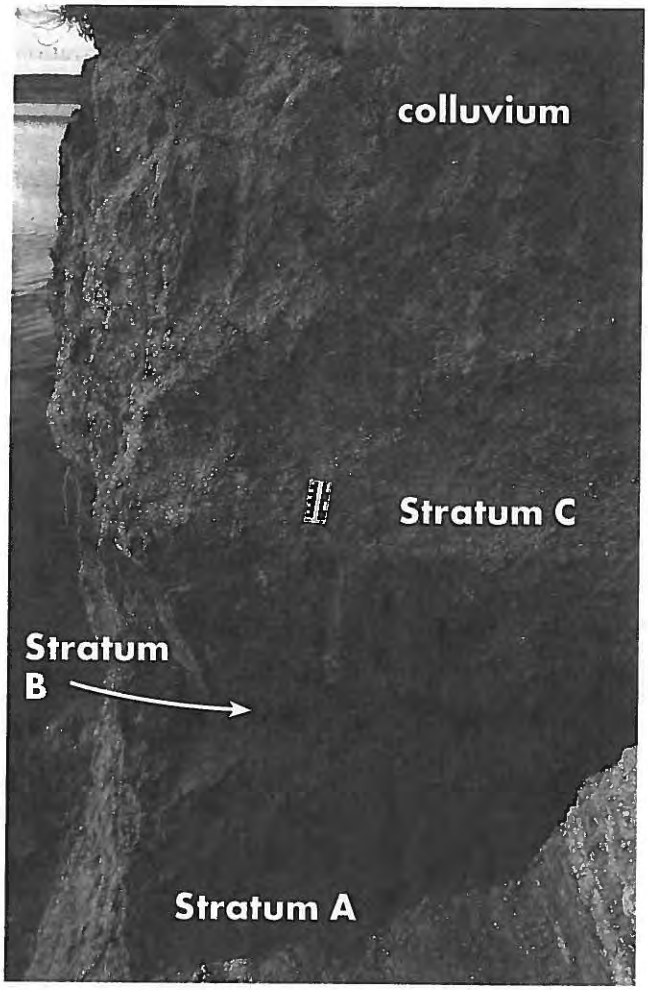

Figure 50. East side of backhoe trench (compare with Figure 27) (C. L. Hill photo).

within the South Block and also to the grid south and escarpment exposures. The measured stratigraphic sequences are presented as Figures 52-55. An analysis of the spatial distribution of fossils recovered in these deposits is available in Hill and Batten (1997, this report). Fragments of tusk recovered from stratum B in Excavation Area L provided a conventional radiocarbon age of ca. 32,470 ^{14}C yr B.P (Table 7; Hill 1999).

Correlation of Descriptions

The soil profile documented by Bump (1989) from the east-facing exposure of the escarpment appears to have been situated at around 120N (Figure 4), approximately at the south end of the South Block (based on Map 2 and Figure 3 in Bump 1989). Four levels (numbered from top to bottom) were described. The lowest (level 4CrK or IVCrK) resembles stratum A. It is described as a light yellowish brown (10YR 6/4), very fine sandstone with massive structure. Mammal bones found within this level were considered by Bump to have come from the overlying level through cracks. Bone was observed within the top of stratum A during the MOR excavations and along its upper boundary with stratum B (Hill and Batten 1997, this report). Hill also observed large fragments of mammoth bone seemingly within stratum A in 1996.

Level 3Ab (or IIIAb) overlies level 4. It is marked by a clear, wavy boundary (Bump 1989) and is a dark gray (10YR4/1) silt with strong medium subangular soil structure. It is probably equivalent to stratum B. Non-effervescence to HCl, indicating an absence of carbonate (attributed to postdepositional leaching), is reported by Bump, although thermal analysis (loss-on-ignition) implies the possible presence of about 5 percent carbonate for stratum B (Huber 1997, this report). Besides the presence of Pleistocene vertebrate remains, this level was reported to contain molluscs. Compared to all other levels, 3Ab is more acidic (pH 5.6-5.8, compared to >7.2 for all others). The level has characteristics interpreted as a buried soil equivalent to paleo-Cryaquolls and a Mollic epipedon. It was described as having a gradual boundary with the overlying level 2.

Level 2Cr (or IICr) is a light yellow brown (10YR 6/4) massive deposit that contains molluscs and oxidation stains. It is probably equivalent to stratum C, although the boundary between stratum B and stratum C was observed to be

Figure 51. 1995 excavations, South Block, Merrell Locality (C. L. Hill photo).

distinct and not gradational. This could be an indication that the level 3/level 2 boundary described by Bump refers to the clear erosional unconformity that separates the lower and upper stratum C deposits, using the nomenclature that Albanese, Davis, and Hill (1995) adopted for this report. The upper boundary between levels 2 and 1 was described

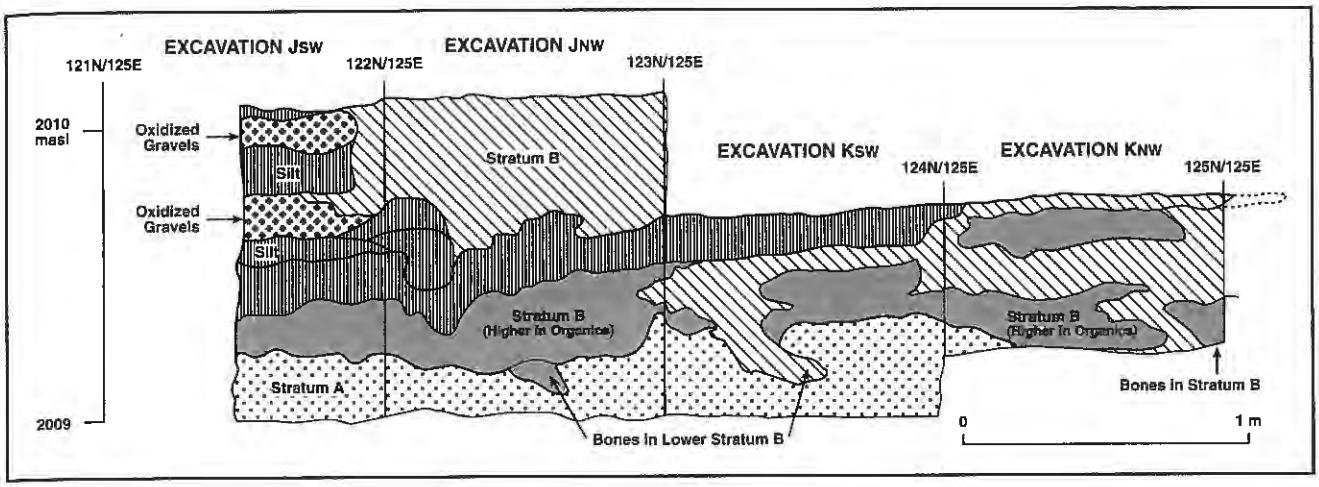

Figure 52. Generalized stratigraphy in Excavation Areas J and K, South Block, Merrell Locality (profile by C. L. Hill).

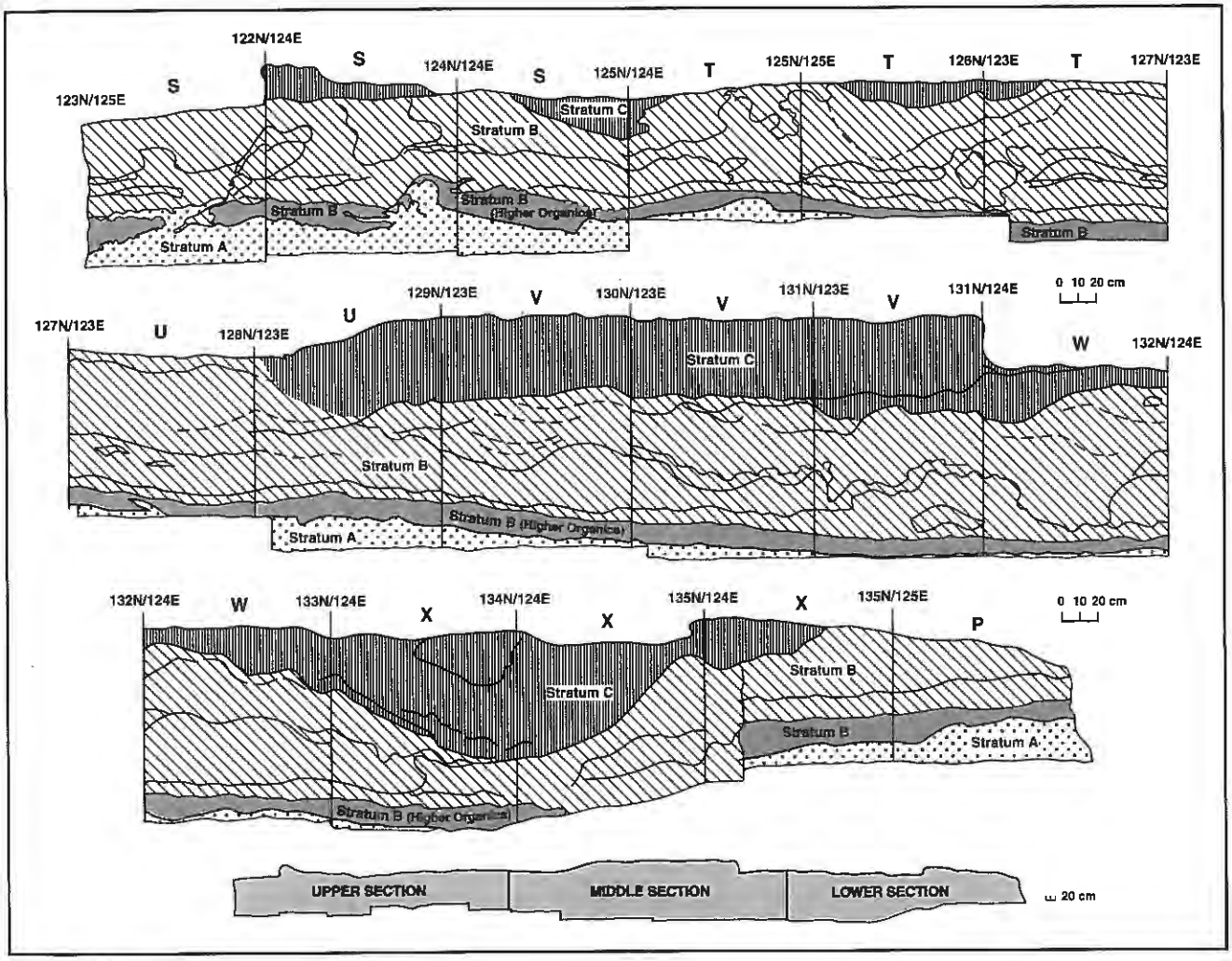

Figure 53. Generalized stratigraphy in Excavation Areas P and S-X in South Block, Merrell Locality (profile by C. L. Hill).

Figure 54. View looking toward grid south, showing strata A-B at Excavation Area K, South Block, Merrell Locality. Figure is standing on stratum A and is pointing toward lower section of stratum B (C. L. Hill photo).

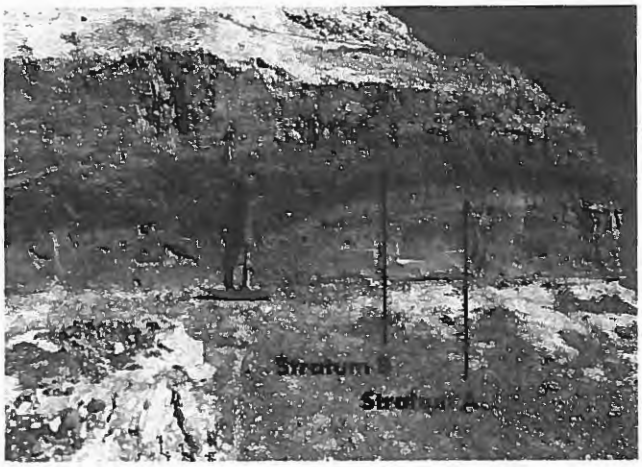

Figure 55. View looking toward grid north, showing strata A-B at Excavation Areas X and P, South Block, Merrell Locality (C. L. Hill photo).

as abrupt, and that may mark the gravel deposit at the top of this stratum C facies (gravels were observed by Bump).

Level 1 (or I) was separated into four horizons (Bump 1994) which seem to correspond to the colluvial matrix at the top of the sequence. It also seems to include some sublithologies of stratum C. The lowest horizon seems to correspond mostly to the top of stratum C and lenses of the uppermost colluvial matrix. This horizon overlies 2Cr and was designated as either Btk2 or BK4. It is very pale brown (10YR 7/6), subangular, and alkaline (pH=7.8-8). A gradual boundary separates this horizon from a 29-cm-thick, light gray (10YR 7/6) horizon with subangular blocky soil structure designated as either Btk2 or Btk1 (Bump 1989). This would seem to correspond to the upper parts of stratum C which generally exhibit more $CaCO_3$ concretions and Fe_2O_3 staining. This and the overlying two horizons have alkaline pH values >8. The boundary separating this from the overlying horizon is also gradational (Bump 1989). The overlying horizon, designated as either Btk1 or BK2, is about 17 cm thick and contains gastropods and a higher fraction of gravel (ca. 15-20%). It seems to correspond mostly to the various higher lenses of the overlying colluvium and upper parts of stratum C, unless some of the coarse fractions refer to rodent burrow deposits.

The uppermost two horizons of Bump's sequence were described as an Ak-Bk1 sequence with a total thickness of ca. 33 cm. The horizons are slightly more acidic (less alkaline) than the other B-horizons. These horizons seem to correspond mostly to the higher colluvial sediments.

The upper part of stratum A and most of stratum B (syn. LL1 and 2 in Hill, Davis, and Albanese 1995) can be correlated with the "2.1 m zone within the main section of the terrace" described by Dundas (1992:12). The date of >33,990 yr B.P. (B-36206) (Table 7) from a mammoth fibula is most likely related to the date of ca. 37,000 yr B.P. (Table 7) on organics from mammoth bone obtained from Unit B (see below). The mammoth long bones and uncollected exposed ribs from the south side of the Locality mapped by Bump (1991) are likely derived from strata A and B. Hill had an opportunity to go over these correlations with Bump in the field during the 1995 excavations. It seems fair to say that Bump concurs with this general assessment.

Grid 140-170N Escarpment and North Block Stratigraphy

Escarpment Exposure

Besides the studies by Albanese in 1994, a stratigraphic profile was measured and sketched along the escarpment from Grid 140 N to Grid 170 N in 1995 (Figure 4). The area includes the 11, 12/27, 19/31/29, and 15/30 station points of Albanese (1995) and the 1995 E10, E13, E12, E4, E5, E6, E7, and E8 survey points (Figure 39). It also is the area that includes the A103 (FS58) mammoth bone collections made by the University of Montana. A fragment of a tooth attributable to *Camelops* was recovered from deposits of stratum C at station E4.

Excavation Area C (1994 Test Pit C)

Excavation Areas C (Test Pit C 1994) and I ("the tusk area") were situated in the vicinity of Grid 160 N (Figure 4). Radiocarbon dates were obtained from this area as a result of the 1989 University of Montana investigations (Table 7) and later by the MOR/MSU studies. This in-

cluded the area of the mapping stations used in 1995 (Albanese 1995). Along the escarpment, this includes the F13, F14, F15, and FS59 collections made by Montana State University (based on data provided by T. Foor).

Studies at Excavation Area C (Test Pit C) (Figure 39) were conducted under the supervision of D. Batten and T. Wolfgram during the 1994 field season. The sedimentary sequence was exposed to a depth of 280 cm (9.19 ft) below surface (b.s.) (Figures 56 and 58). The deposits are mostly silts with some coarse clastic lenses and is generally reminiscent of stratum C in Test Pit/Excavation Area E. No deposits similar in lithology to stratum B at Test Pit/Excavation Area E or along the edge of the escarpment were encountered. Thus, the bones recovered from Excavation Area C would appear to provide an indication of the kinds of remains present in a lateral facies of stratum C and possibly some overlying colluvium, along with intrusives associated with younger bioturbation (primarily rodent-burrowing). Although silts dominated the sequence, cobble-sized rocks were encountered in south half excavation levels 5-7 (40-70 cm [16-28 in]b.s.) and north half levels 8 (70-90 cm [27-35 in] b.s.). The biostratigraphic record is likely a mixture of chronologic ages, especially for the uppermost 2 m [6.56 ft] of the Excavation Area. The lower 60 cm [23.6 in] of the sequence exhibited less evidence of bioturbation or potential for disturbance and may be a slightly more informative indicator of the types of fossil fauna preserved within a lateral facies of stratum C.

Recent remains of ground squirrel (*Spermophilus* sp.) were identified in Cn levels 4, 6, 7, 10, 13, 16, 19-21, and 25 and in Cs levels 2, 3, 5, 7, 8, 11, 14, 16, 18, 21, and 22 (Dundas, this report). This is a hint that there is potential for the mixing of fossils throughout the Test Pit/Excavation Area C sedimentary sequence. Remains of *Lepus* sp. were recovered in Cn level 9 and 14 and Cs level 19. These are probably Late Holocene in age. Remains of *Thomomys* were found in Cn level 14.

A mammoth molar was recovered from the north half excavations within level 16 (150-160 cm b.s). This level also contained rodent burrows. The presence of a mammoth molar would indicate the occurrence of at least redeposited Pleistocene-age sediments within the Excavation Area C sequence. The mammoth molar fragment from level 16 was conjoined with a molar root section recovered from level 18, providing another indication of mixing. At level 23 (north half 220-230 cm b.s.), the sediments are more heterogeneous in color (greys, reds, and tan silty clays with gravels?) and fragments of teeth were present (perhaps a mammoth molar, specimen 9). Fragmentary remains of mammoth were found in almost every level below level 3. In the Cn, mammoth remains were recovered from levels 4, 5, 7-9, 11, 12, 14, 16, 20, 21, 24, and 25 while, in Cs, mammoth remains were recovered from levels 11-14, 17, 18, 20, 21, 24, 26, and 28 (see also Dundas, this report). Collagen extracted from a mammoth tooth fragment from Cs level 21 provided a conventional radiocarbon age of

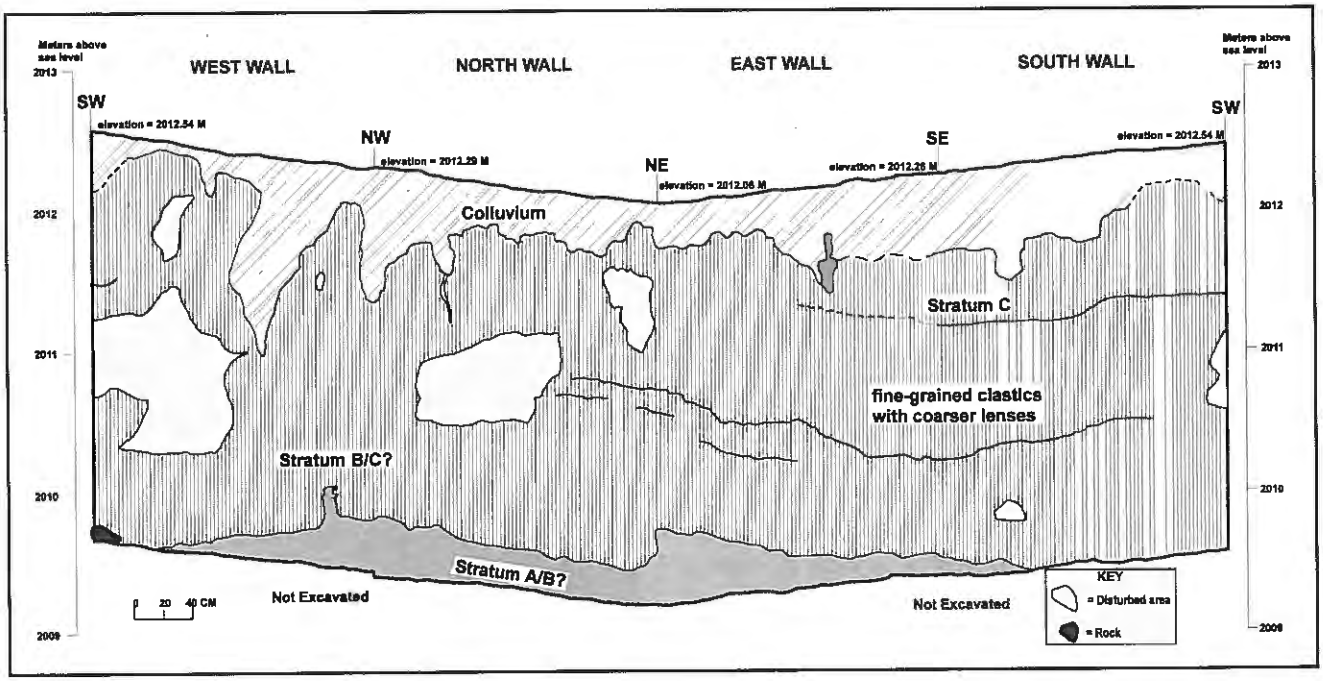

Figure 56. Generalized stratigraphy in Test Pit/Excavation Area C (near the North Block) (profile by C. L. Hill).

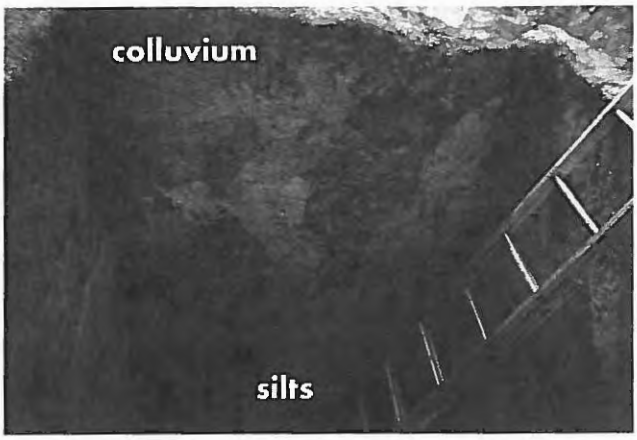

Figure 57. Test Pit/Excavation Area C West Wall, showing bioturbation (C. L. Hill photo).

about 49,350 B.P. (Table 7) (Hill 1999). Fish remains were found in Cn levels 17 and 18. Fragments of horse remains were found in Cn levels 6 and 11 and Cs levels 18 and 24. Camel was identified from Cs level 20 (Dundas, this report).

Although the Test Pit/Excavation Area C sequence shows evidence of considerable bioturbation, especially in the upper part (Figures 56 and 57), the sediments contain the remains of at least three Pleistocene species (mammoth, camel, and horse). The taphonomic interpretation of these remains needs to take into consideration at least two redepositional events, one possibly associated with fluctuating high and low-energy conditions associated with the formation of the facies variant of stratum C and another connected with younger bioturbation characterized by mixing by burrowing mammals.

Excavation Area I

Along the north part of the scarp, a vertebrate bonebed was present as part of a deposit composed of sand, cobbles, and pebbles (see Albanese, this report, Figures 18-21 and 60-61). Bone fragments, principally of mammoth, had been incorporated into the deposit (Figures 62 and 63). These date to 25,000-19,310 ^{14}C yr B.P. (Table 7) and provide a maximum age for the deposit. The deposit can be interpreted as a debris flow that may have accumulated on the floor of an arroyo-type channel that was incised into strata C and A (see Albanese, this report).

Both Dundas (1990) and Bump (1991) provide descriptions of the context of fossils recovered from this part of the Merrell Locality. In notes reviewing Hill's attempt at correlations, Dundas concurred that the "pure quartz sand lens and a gravel-boulder channel lag deposit" that he described (Dundas 1990) are the same deposits designated by Albanese (1995, this report) as substrata A1, A2, and stratum D. The well-sorted sand below the mammal bones was sampled for luminescence dating, providing an age of ca. 63,000 OSL years B.P. for this facies of stratum A (Feathers, this report) (Figure 61). The mammoth bone dated at ca. 25,030 ^{14}C yr B.P. (Table 7), along with the dates of ca. 21,530 and 19,000 ^{14}C yr B.P. (Table 7) from mammoth bone incorporated into stratum D (the debris flow), seem to indicate that the deposit contains faunal remains that may range over an interval of 5,000 years, and that it is younger than the faunal remains found mostly in stratum B or at the top part of stratum A. Because stratum D lies on the eroded surfaces of strata A-C, it is possible that some fossils originally in these older strata could be incorporated in the debris flow. These deposits are also likely the same as those that contained exposed mammoth tusk and long bones mapped by Bump (1991), based on Hill's discussions with Bump in the field in 1995. Detailed taphonomic studies of this bonebed were undertaken in 1994 (Figures 64-66). Most of the bones can be attributed to *Mammuthus*

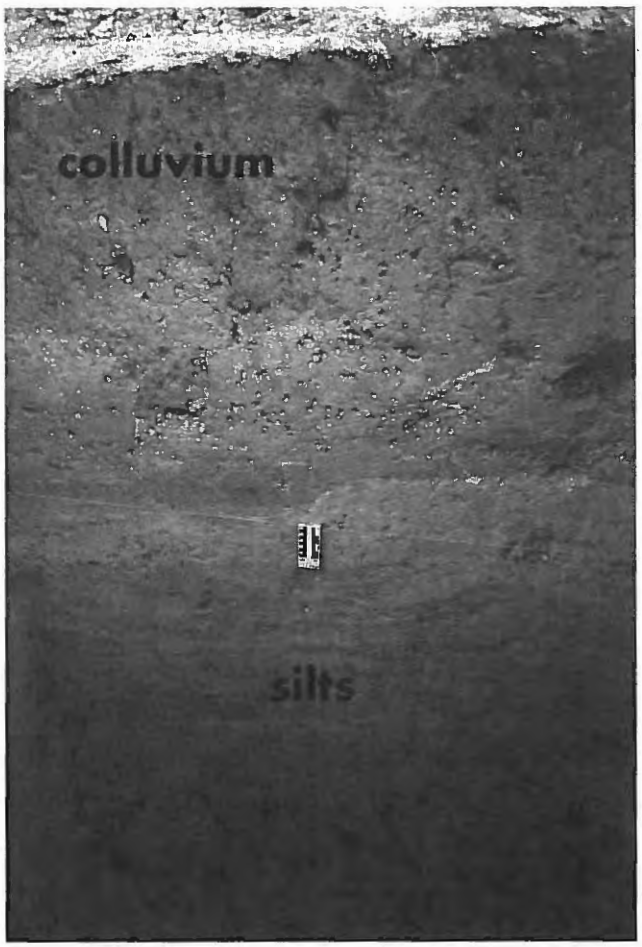

Figure 58. Test Pit/Excavation Area C South Wall (C. L. Hill photo).

(cf. *M. columbi*). Rare elements from *Bison* and *Equus* (Figure 64) are also associated with the deposits at Excavation Area I.

Site-Specific Stratigraphic Integration and Lithostratigraphic Interpretations

Stratum A contains a wide variety of lithologies (textures and structures). It seems to contain a variety of sedimentary facies indicating alluvial, colluvial, and possibly lacustrine depositional conditions. The lowermost facies of stratum B is thought to have formed in a marsh-like setting. The deposits high in organics represent the marsh-basin facies, while the oxidized zones represent the edge of the basin. Stratum B may represent the initial filling of an isolated depression. The size of the water body may have later expanded, increasing in depth and resulting in the deposition of some of the overlying deposits of strata B and C. Taphonomically, the vertebrate fossils found along the interface between strata A and B may be have eroded from stratum A. They may also have been incorporated into the shallow basin and deposited as part of stratum B. They appear to reflect the remains of animals that died in or near a shallow swamp.

Figure 59. View looking generally south at North Block excavations. Figure is at the "tusk area." (C. L. Hill photo).

Most of stratum C seems to indicate a shallow, braided-stream setting typified by fluctuating flow regimes (Albanese 1995, this report). A potential alternative interpretation is that the strata dominated by fine-grained sediments represent a transgressive phase deposition within a basin, and the coarse-grained sediments indicate higher energy regimes

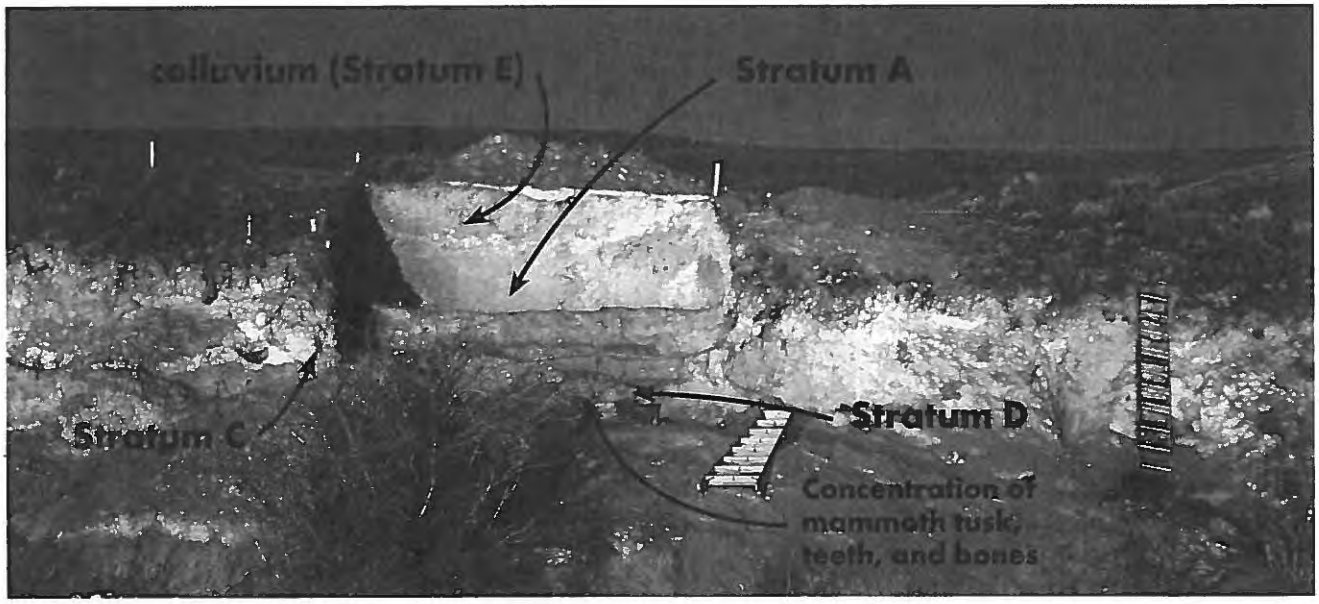

Figure 60. View of strata A-E at North Block (Excavation Area I), looking west (C. L. Hill photo).

Figure 61. View of tusk area and debris flow at North Block (Excavation Area I), looking west. Well-sorted sands are a sub-facies of stratum A (C. L. Hill photo).

associated with basin margins and regressive phase deposition. However, very similar sedimentary textures and structures can be observed today forming banks along the Red Rock River (Figures 67-68), implying that stratum C reflects primarily fluvial conditions. In restricted areas, strata A and C contain deposits that are probably of colluvial or debris-flow origin.

At Excavation Area E (1994 Test Pit E) and the backhoe area (Figures 39, 46-47), stratum C is a massive sandy mud. It may represent continued deposition in an expanding lake setting, initially represented by the marsh-like deposits of stratum B (LL2). A very distinct erosional unconformity marked by a thin layer of coarser clastics separates this lower lithology from the rest of the stratum C sedimentary package. The rest of the sequence consists of alternating lenses or beds of fine- and coarse-dominated clastics. Along the scarp face, stratum C consists of thin beds and laminae of muddy sand and interbeds composed of limestone pebbles and coarse sand. The sands grade laterally into sandy muds (sand, silts, and clays). These deposits would appear to indicate a sequence of alternating transport energies and depositional conditions potentially associated with alluvial and fluvial settings, perhaps mostly with shallow braided streams. The faunal remains from stratum C seem to have been deposited under fluvial conditions. Liquefaction features and normal microfaulting are pervasive throughout strata B and C.

Figures 62, 63. Fossils in debris flow, North Block (Excavation Area I) (C. L. Hill photos).

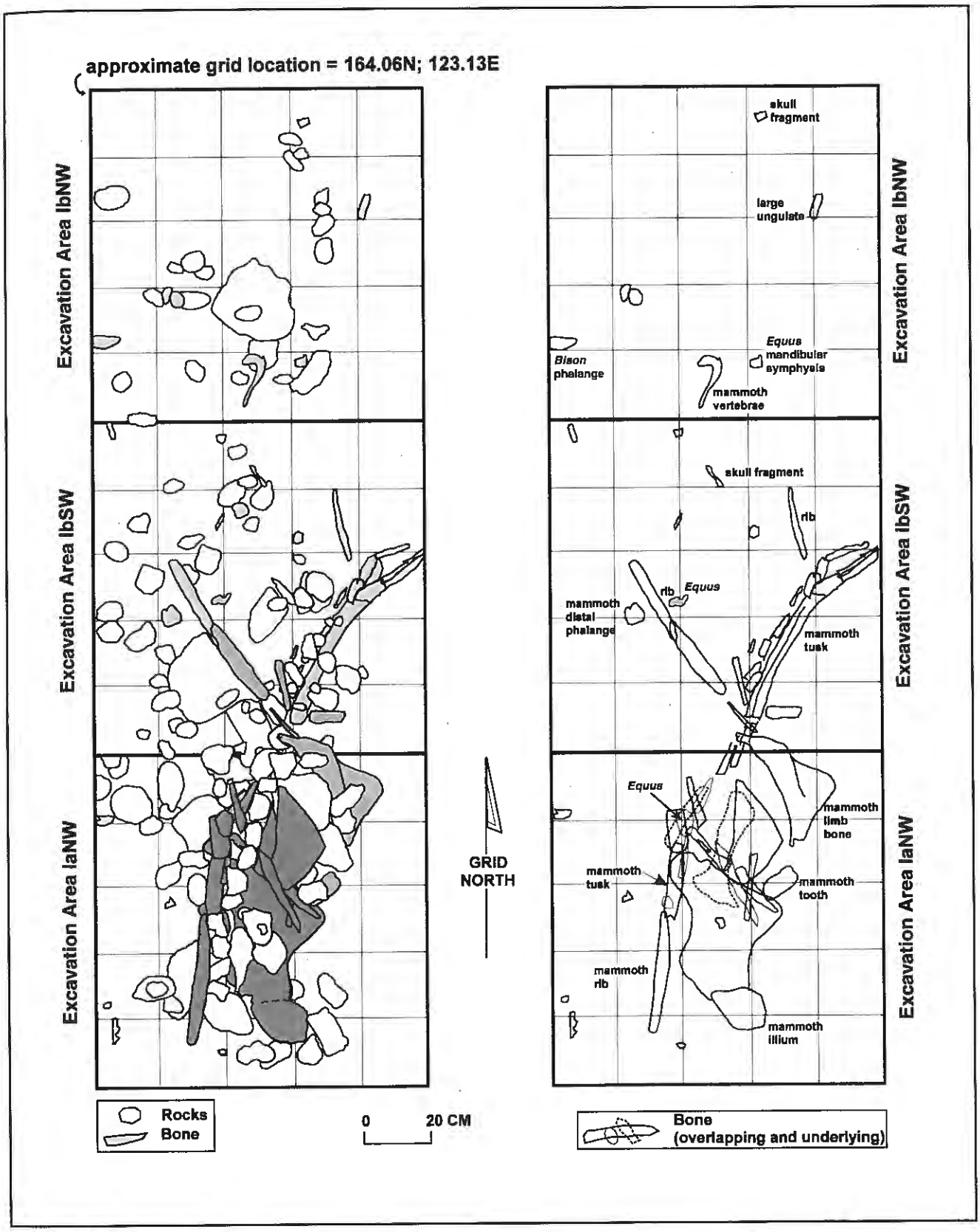

Figure 64. Spatial distribution of fossil remains in Excavation Areas Ia and Ib (map by C. L. Hill).

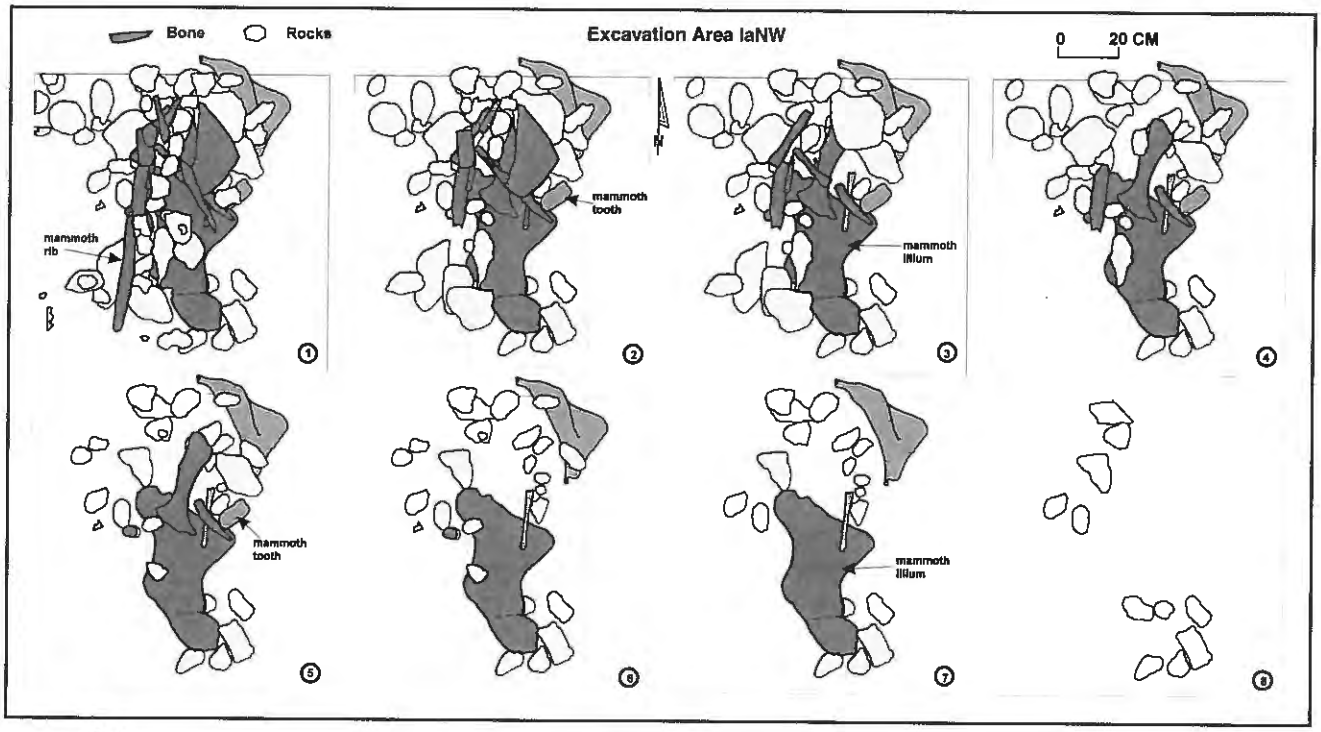

Figure 65. Spatial distribution of fossil remains in Excavation Area Ia. The top of the debris flow is depicted in Figure 65-1 with the lowest part of the deposit shown in Figure 65-8 (map by C. L. Hill).

Stratum D is an isolated deposit on the north side of the Merrell Locality (Figures 39 and 59-66). The debris-flow deposit is locally restricted (on the north end of the scarp) and seems to have been deposited around or after ca. 19,000 ^{14}C yr B.P. It also contains mammoth remains with ages of ca. 25,000-21,000 ^{14}C yr B.P. and may contain fossils redeposited from older sediments (strata A-C). Stratum D is localized to Excavation Area I (the North Block), which also contains sediments associated with various facies of stratum A and stratum C. Throughout the entire Merrell Locality, colluvium, probably mostly of Holocene age, overlies the strata A-C sequence (Figure 69). The colluvial deposits are heavily bioturbated.

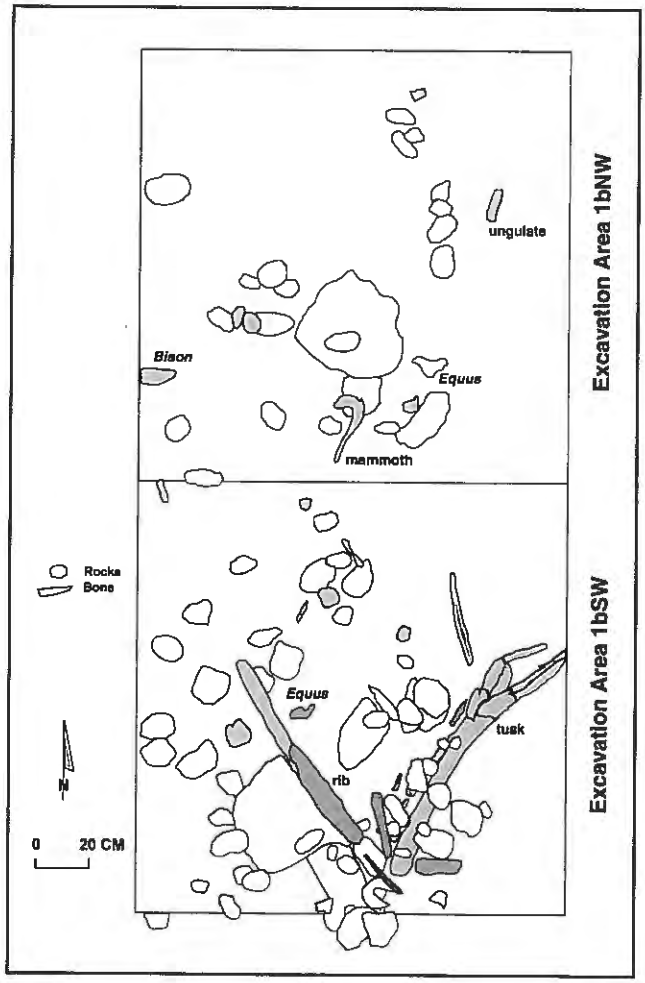

Figure 66.
Spatial distribution of fossils in Excavation Area I (map by C. L. Hill).

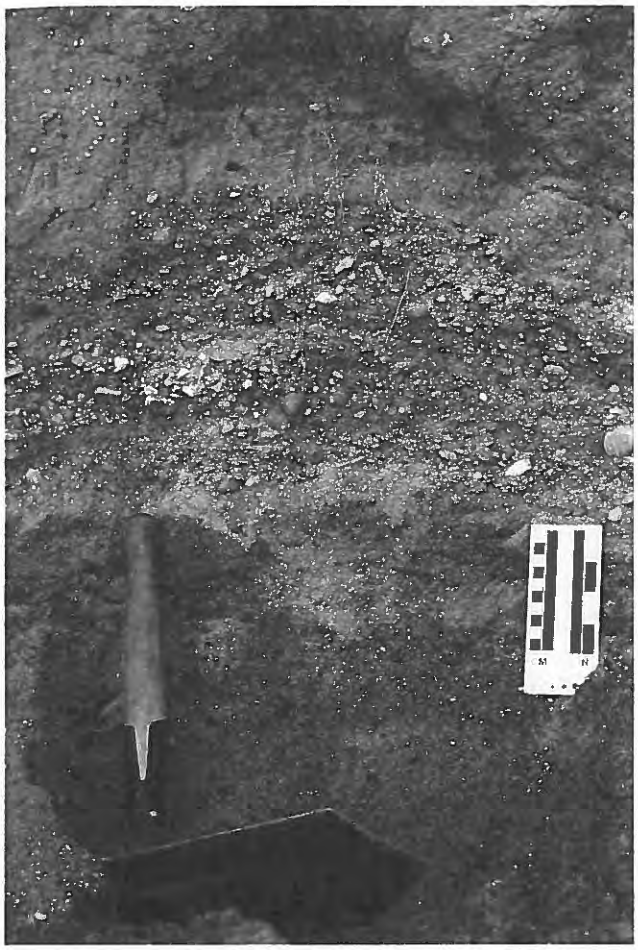

Figure 67. Alluvial deposits along Red Rock River, Centennial Valley (C. L. Hill photo).

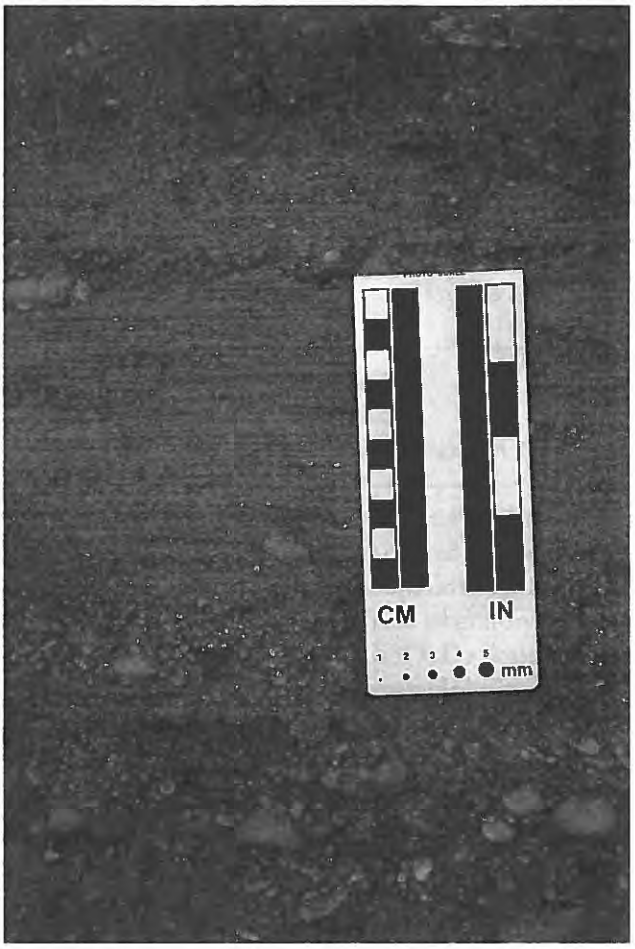

Figure 68. Alluvial deposits along Red Rock River, Centennial Valley (C. L. Hill photo).

Figure 69. Colluvium (stratum E) at North Block (Excavation Area I). J. Albanese for scale (C. L. Hill photo).

Luminescence Dating of the Merrell Site

James K. Feathers

Introduction

Three sediment samples for luminescence dating were obtained from the Merrell Locality on the southwest shore of the present Lima Reservoir in the Centennial Valley of southwestern Montana (Feathers and Hill 2001). The locality is notable for its fossil record, containing mammoths and other Pleistocene-age vertebrates. Four Pleistocene strata have been identified in excavations (Albanese, this report and Hill, this report). Stratum A consists of massive muddy sand or sandy mud, interpreted as probably lacustrine in origin. Stratum B consists of silts high in organics, interpreted as swamp sediments deposited in a smaller basin, once the lake of stratum A had silted up. Stratum C is a massive sandy mud consisting of interbedded silts and coarser clastics, indicating alternating transport energies, perhaps associated with shallow braided streams. Radiocarbon dates from stratum B include 36,500 (organics), >42,000 (humates), >33,900 (collagen), and 32,500 (collagen). In the North Block of the excavations, a well-sorted sand, which may correlate with stratum A, is unconformably overlain by stratum D. The latter consists of sand, cobbles, and pebbles and has been interpreted as a debris flow. Radiocarbon dates on collagen from stratum D are 25,000, 21,500, and 19,300. One further date from a nearby test pit (Excavation Area C) of 49,400 on mammoth enamel came from a stratum that probably correlates also with stratum A.

Two of the luminescence samples were obtained from Excavation Area E in the South Block. One was from the top of stratum A and one from stratum C, both collected from sandy lenses. Stratum B was judged too complicated by the high organic content to be useful for luminescence dating. The third sample was taken from the well-sorted sands below the debris flow in the north section. Laboratory numbers and proveniences are given in Table 4.

Table 4. Merrell Site Luminescence Samples and Proveniences.

Sample #	Provenience
UW352	stratum A, South Block
UW353	stratum C, South Block
UW354	Sorted sands; facies of stratum A: North Block

Samples were collected on a very rainy day by driving light-tight metal cylinders into the cleared profiles, removing them, and securing rubber clamps onto the ends. The two exposed ends were removed in the laboratory and used to measure moisture content. A $CaSO_4$:Dy dosimeter was placed 30 cm into the back of each sample hole and left for one year. Because the stratigraphy was complex, additional samples for radioactivity measurements were taken from above and below the sample from lenses of different grain size distributions. This was intended to measure the heterogeneity of the radioactivity in the sample vicinity.

Optically stimulated luminescence (OSL) on 90-125 μm quartz grains was chosen for dating. Quartz grains were isolated by sieving for grain size, treating with HCl and H_2O_2, resieving, etching for 40 minutes with 48 percent HF, sieving again, and density separation using a 2.68 specific gravity solution of sodium polytungstate. Grains were secured on Al discs with silicone spray and measured for luminescence on a Daybreak 1100 reader using 500-540 nm light for stimulation and 5 mm Hoya U340 (ultraviolet) filters in front of a 9235Q photomultiplier for emission. Calibrating irradiations were from a $^{90}Sr/^{90}Y$ beta source. Radioactivity of the samples used for dating was measured by high-resolution gamma spectrometry. Radioactivity of the additional samples to test sparial heterogeneity was measured by thick source alpha counting and by flame photometry. Cosmic radiation was calculated following Prescott and Hutton (1988).

Radioactivity

The samples measured by gamma spectrometry appeared to be in secular equilibrium. Radioactivity of those and the additional samples are given in Table 5.

Table 5. Radioactivity of Merrell Site Luminescence Samples.

Sample	^{238}U (ppm)	^{232}TH (ppm)	K_2O(%)
UW352	1.83±0.14	5.81±0.22	1.96+0.03
5-9 cm above	3.77±0.29	16.46±1.63	1.90+0.07
21-26cm above	3.32±0.18	12.83±1.10	2.39+0.01
4-9 cm below	1.82±0.19	10.78±1.55	2.07+0.01
UW353	1.18±0.12	4.16±0.23	1.57+0.04
6-15 cm above	1.60±0.15	8.15±1.15	1.57+0.01
8-15 cm below	2.07±0.18	9.80±1.20	1.60+0.02
UW354	1.11±0.12	4.17±0.20	1.83+0.03
50 cm above	2.77±0.21	9.48±1.26	1.77+0.04

The table suggests considerable variability in radioactivity across the site, probably reflecting in large part the differential distribution of clay minerals, which tend to be enriched in radionuclides. The dating samples were drawn from sandy lens with lower radioactivity. Since the various lenses had more or less horizontal distributions, the gamma radiation affecting the dating samples was calculated using a gradient, as suggested by Aitken (1985: Appendix H), for UW352 and UW353. Since UW354 was from a fairly homogeneous deposit, with different radioactivity probably at least 50 cm away, only the radioactivity of the dating sample was used. These calculated gradients can be compared with results from the dosimeters. Unfortunately, two of the dosimeters had been pulled out, probably by animals, when retrieved. The one for UW352 was still intact, however. It showed a dose rate of 1.473 ± 0.292 Gy/ka, compared to the gamma and cosmic rate calculated as above of 1.148 ± 0.065 Gy/ka. These are within error terms and suggest that the gradient method produced a reasonably accurate assessment.

Even though the samples were collected on a very rainy day, the as-collected measurements of moisture contents were low, ranging from 2 to 8 percent, due in part to the sandy nature of the sediments. Considering that some of the dose rate originated from silts and clays with much higher water retention and that moisture contents are and were probably higher in winter and during the Pleistocene, moisture contents were estimated at 0.15 ± 0.5 for UW352, 0.10 ± 0.05 for UW353, and 0.06 ± 0.02 for UW354. The differences reflect slightly different textures of the samples and their surroundings.

Equivalent Dose

OSL measurements require a proper preheat to remove unstable signal and equalize sensitivity between natural and irradiated aliquots. To determine a suitable preheat, the following procedure was used. Several aliquots of natural material were given different 5-minute preheats ranging from 180°C to 230°C and then exposed to 400s of 550 nm light, recording the first 60 seconds. The aliquots were then given 30 Gy, preheated again to the same level, and then exposed again. The ratio of the natural signal to the regenerated 30 Gy signal was plotted against preheat temperature (Figure 70). Little change after 190 to 200°C is apparent (the values for UW353 and UW354 have been multiplied by a constant to ease presentation), so higher preheats should be suitable.

Equivalent dose was first measured using a multi-aliquot technique called the "Australian slide" (Prescott, Huntley, and Hatton 1993). Thirty aliquots for each sample were prepared. All were initially normalized by a 0.1 s exposure to OSL. All subsequent OSL measurements were for 450s at 100°C and were preceded by a 220°C 5-minute preheat. The first 60 seconds was used in calculations, and the last 50s used to determine an average background. On 15 aliquots, the natural signal was first measured, followed by a 30-minute exposure to a solar simulator to zero the signal. Then, incremental doses were applied and the regenerated signals measured. On the other 15 aliquots, incremental doses were added to the natural material and the added dose signals then measured. The regeneration and additive dose curves were then plotted and the horizontal distance between them was taken as the equivalent dose. This distance was determined using a fitting program written by David Huntley of Simon Fraser University. Saturating exponential functions were used in the fitting. Figure

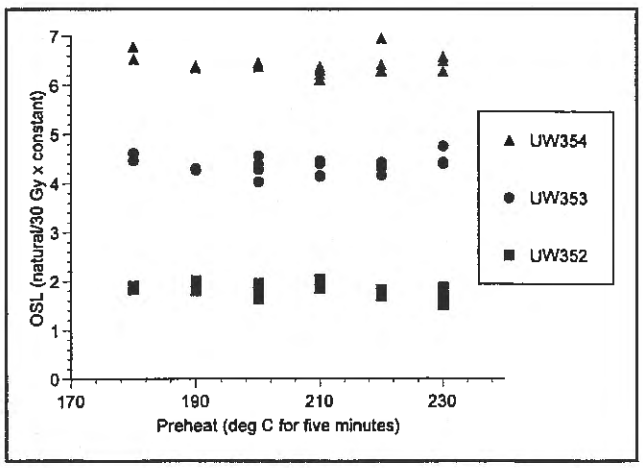

Figure 70. OSL vs. preheat temperatures.

71 shows the fits after the two curves have been shifted together by the derived equivalent dose. No significant sensitivity change was detected in the regeneration curves. For UW354, the natural signal was close to saturation. To get a proper fit, most of the natural signals had to be eliminated because they were higher than any of the added dose points. Such "radiation quenching" is known to affect some quartz samples close to saturation.

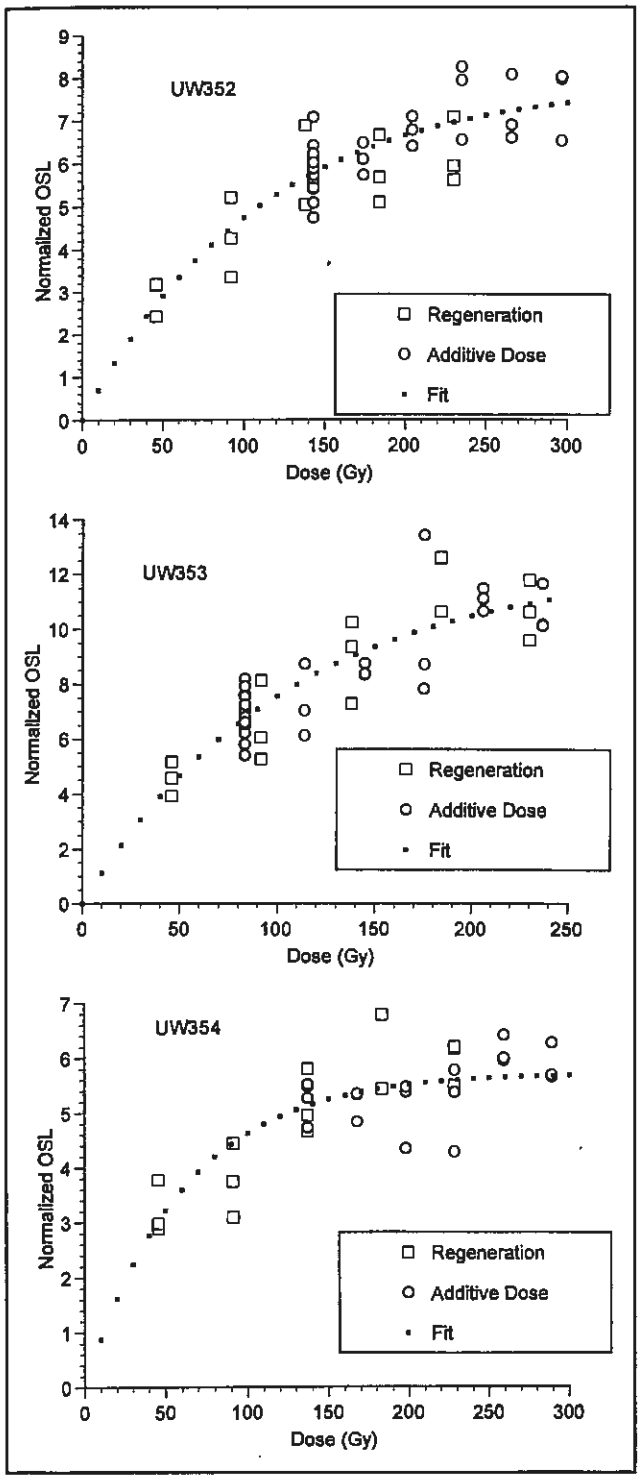

Figure 71. Normalized OSL vs. dose.

Because of the nature of the deposition, the question arises about how well the samples were zeroed at the time of deposition. Lakes are traps for deposits of different origin and some of them may have had only limited sunlight exposure. Multi-aliquot analyses utilize thousands of grains and the results reflect the averaging of the luminescence signal among them. Dating individual grains will reveal a distribution of ages that may reflect differential zeroing. If the distribution is multi-modal, only one mode may reflect the age of deposition. The drawback to dating individual grains is that grains vary greatly in their luminescence sensitivity so that there are marked differences in the precision at which dates can be derived. A great number of single grains must be dated to overcome these statistical problems, and this requires specialized equipment.

As an illustration, the luminescence signal over the first 5s of exposure was measured on 38 single grains from UW353. Figure 72 shows that only one grain had a relatively bright signal. From counting statistics, the precision in measuring this signal is quite good (3%). The precision is quite a bit lower (10-25% error) for the handful of grains with 100-400 counts and intolerable for those with less

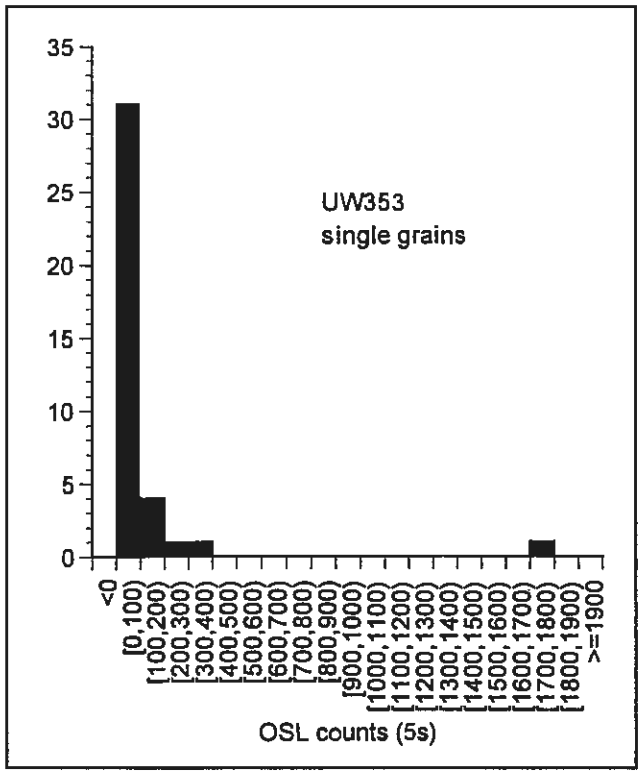

Figure 72. Histogram of OSL counts for sample UW353.

than 100 counts. To increase the number of single aliquots with a signal of reasonable precision, we created aliquots of 60-100 grains. These should have on average 2-3 bright grains, 10-15 relatively dull grains, and numerous grains not contributing to the signal. Any differential zeroing among grains, then, should be observable as differential ages among these single aliquots. We used the SAR method (Murray and Wintle 2000) to determine equivalent dose. This involves a series of regeneration doses on the same aliquot on which the natural signal was measured and thereby constructs a regeneration curve for each aliquot. All signals are corrected for sensitivity change using the signal from a test dose. Table 6 presents the laboratory protocol.

Table 6. The Protocol for Merrell Site Luminescence Dating.

1. Preheat (260°C for 10s)
2. Measure natural signal (99s at 100°C)
3. Test dose (12-15 Gy)
4. Heat to 160°C
5. Measure test dose signal (99s at 100°C)
6. Regeneration dose
7. Preheat (260°C for 10s)
8. Measure regeneration signal (99s at 100°C)
9. Test dose (12-15 Gy)
10. Heat to 160°C
11. Measure test dose signal (99s at 100°C)
12. Repeat steps 6-11 with different regeneration doses

The preheat was higher, but of much shorter duration (for time savings) and should be equivalent to preheats within the plateau region discussed above. The test doses were relatively high because of the low sensitivity of these samples to luminescence and the need for a large enough dose to produce a measurable signal. The first 5s of all signals, corrected for the average background of the last 10s, were used for calculations. The main signals (steps 2 and 8) are divided by their respective test dose signals to correct for sensitivity changes. Precision was determined by counting statistics (Banerjee, Bøtter-Jensen, and Murphy 2000). Regeneration doses were chosen so that their signals bracketed the natural signal. Saturating exponential functions were used to fit the resulting regeneration curves. The last regeneration dose matched the first one in the cycle to test the validity of the protocol. The ratio of signals from these two doses (the recycling test) should be close to one. Aliquots where these signals differed by more than 15 percent were eliminated from analysis. A regeneration dose of zero was also employed to test for thermal transfer. In all cases, this returned an equivalent dose not different from zero.

Results from the single aliquot analyses were less than satisfying. Two batches of 19 aliquots each were excluded from consideration because the derived equivalent doses were much lower than the multi-aliquot result. If the multi-aliquot result represents an average, the single aliquot results should group around that average, not be substantially below it. In both cases, discs that may not have been properly cleaned were used and this was thought to be the problem. Another batch of 19 did not produce reliable data because of an equipment malfunction. This left six batches of 19 each that produced credible data: three for UW352, two for UW353, and one for UW354. Of these, 30 percent failed the recycle test and several other discs were excluded because of poor precision. That left 34 discs for UW352, 16 for UW353, and 17 for UW354 which were considered to have good data.

Aside from the disc and equipment problems, this poor showing may partly reflect the scarcity of bright grains and the low sensitivity of these samples. A preponderance of dull grains, coupled with very few if any bright grains, could produce a signal that represents the accumulation of poor precision data. This poor precision would not be reflecting the counting statistics error, which does not include the propagation of errors from grain to grain. A third of the "good" aliquots had natural signals less than the accumulated signal of the 38 single grains measured. Only 10 of the good aliquots had test dose signals greater than this signal. Many of the recycling failures could simply be due to poor precision.

Figure 73 shows the distribution in equivalent dose of the "good" aliquots for each sample. All three show broad distributions, which again may reflect some poor precision. For UW352 and UW354, no significant correlation can be drawn between the equivalent dose and the test dose (which is a good measure of relative brightness), so either younger or older grains could reflect poor precision (Figure 74). Some correlation is apparent for UW353, with younger grains having lower test doses. UW352 has the broadest range, but is roughly bimodal, with one mode centered around 87 Gy and a smaller, less-defined mode around 188 Gy. UW353 is more tightly clustered, with a main mode at about 97 Gy. A lesser mode around 37 Gy may reflect poor precision since these aliquots tend to have the smallest test doses. UW354 also has a broad range with the main mode about 97 Gy.

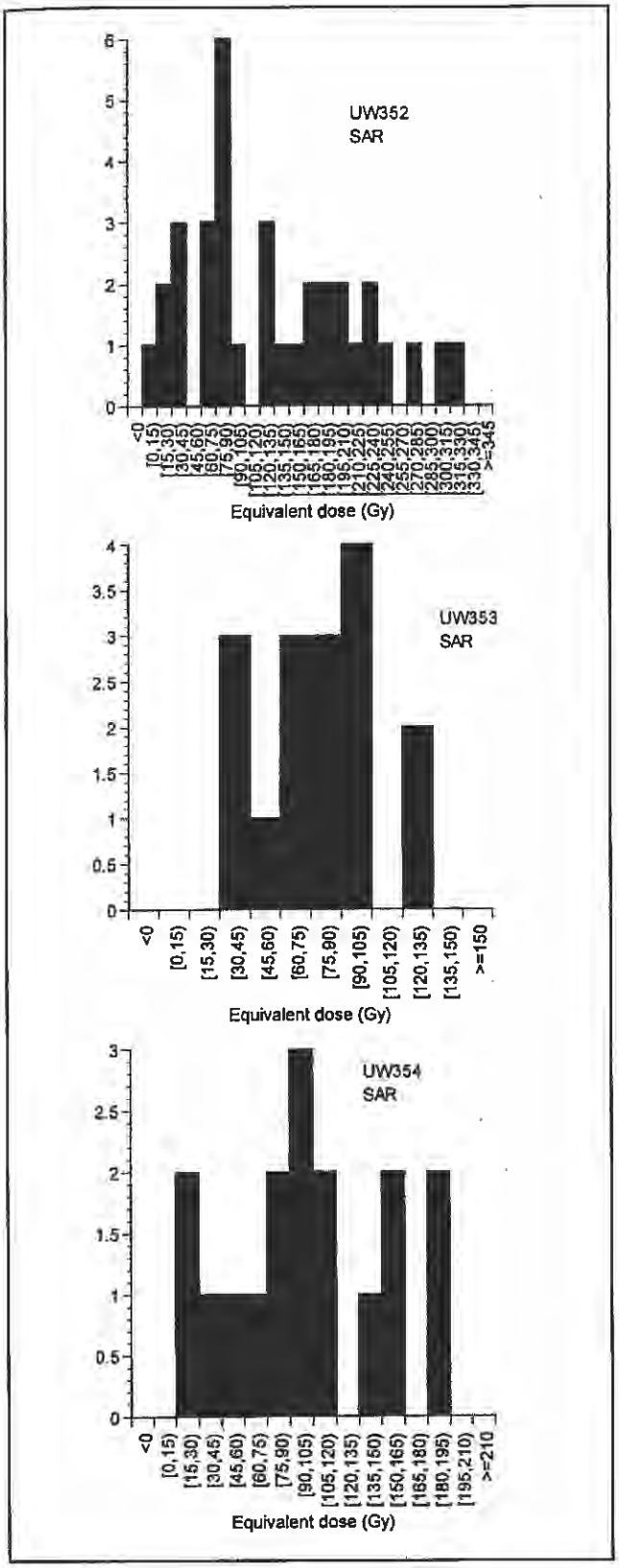

Figure 73. Histogram of equivalent doses for UW352, UW353, and UW354.

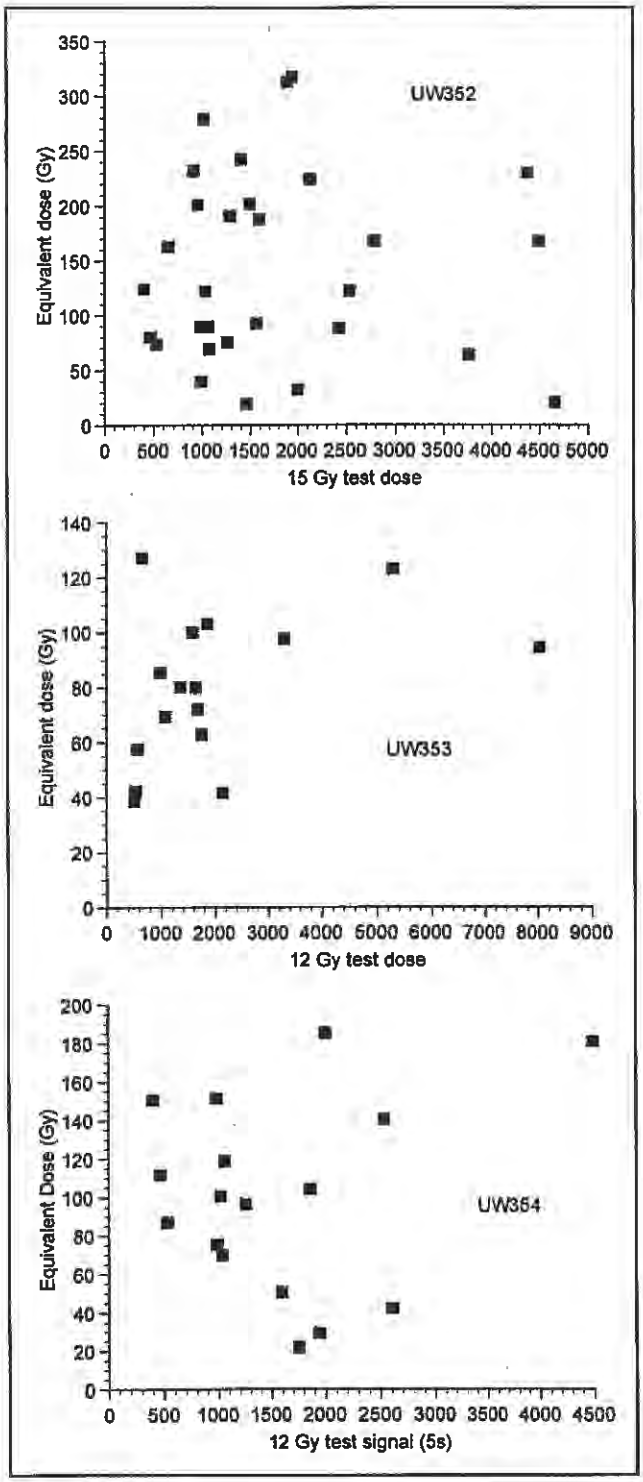

Figure 74. Equivalent dose vs. 12 Gy test dose for UW352, UW353, and UW354.

Age Determination

Table 7 presents the equivalent doses from the various techniques and the associated dates. Data sheets containing the information used to derive the dates are appended (Appendix E). Equivalent doses for modes are the unweighted mean values.

Table 7. Luminescence Samples, Technique, Equivalent Dose, and Ages of Merrell Site Samples.

Sample	Technique	Equivalent Dose (Gy)	Age (ka)
UW352	Multi-aliquot	143.4 ± 14.3	58.1 ± 6.2
	SAR-model 6-105 GY	79.9 ± 10.5	32.4 ± 4.4
	SAR – mode 165-210 Gy	186 ± 17.5	75.4 ± 7.7
UW353	Multi-aliquot	83.4 ± 8.3	42.0 ± 4.6
	SAR – mode 60-105 Gy	76.5 ± 30.2	38.5 ± 15.3
UW354	Multi-aliquot	136.9 ± 28.4	63.3 ± 13.3
	SAR – mode 75-120 Gy	99.2 ± 15.5	45.9 ± 7.3

The multi-aliquot dates compare relatively well with the radiocarbon chronology. Stratum B – between UW352 and UW353 – has been dated 32,000-42,000 by radiocarbon. These are uncalibrated dates, so the corresponding calendar dates are 2-3,000 years older. The OSL age for UW353, from stratum C, then, is nearly contemporaneous or slightly younger. The main mode from the SAR analysis agrees. As the SAR distribution is relatively tightly clustered, this sample was probably well-bleached at the time of deposition. The age corresponding to the high SAR mode for UW352 is only slightly higher than the multi-aliquot age, and these are consistent stratigraphically with the radiocarbon dates. The SAR distribution shows a substantial number of younger grains, so the possibility of mixing of different aged grains in this sample cannot be excluded. The multi-aliquot and SAR mode ages for UW354 are in statistical agreement. Although the error is high, these ages are nonetheless older than the overlying radiocarbon dates. It is likely that this sand unit is roughly contemporaneous with stratum A (UW352) and with the lower part of Test Pit C, where a 49,000-year-old radiocarbon date was obtained.

The broad range of the SAR distributions may suggest substantial mixing of different aged sediments in these samples, but, at this juncture, Feathers cannot be sure this is not just a precision problem. The agreement of the multi-aliquot dates with the radiocarbon chronology suggests precision problems are a strong possibility. This can likely be resolved by single-grain dating.

Geochronology of Merrell Locality Strata and Regional Paleoenvironmental Contexts

Christopher L. Hill

Chronologic Interpretations

An assessment of the age of the deposits and the fossils incorporated within them at the Merrell Locality is based on radiocarbon measurements from bone and tusk collagen and organic sediments (Table 3 and Figures 75-76), and luminescence measurements on sediments (Feathers, this report). Nine radiocarbon dates are available from the site; seven are finite and two are infinite. The finite dates range from ca. 49,000 to 19,000 ^{14}C yr B.P. (Figure 75).

The oldest finite date of ca. 49,350 ^{14}C yr B.P. is based on measurements of collagen derived from mammoth remains from a deposit which is possibly a facies of stratum A (Hill 1999). Feathers (this report) provides two luminescence ages from deposits that are facies of stratum A. At one standard deviation, these measurements range in age from about 50,000 to about 76,000 OSL years (= calendar yr B.P.) (Figure 75). Thus, there are some indications that the sediments and vertebrate remains within stratum A can be correlated with a long interval perhaps spanning the end of isotope stage 5, all of stage 4, and the beginning of isotope stage 3. The deposits could be associated with the late Sangamon Episode (sensu lato, e.g., Karrow, Dreimanis, and Barnett 2000) and the early and middle Wisconsin (Figure 77). Fragments of tusk and teeth of *Mammuthus* were recovered from the stratum A sediments.

The radiocarbon dates from stratum B range in age from >44,000 to 32,000 ^{14}C yr B.P., or ca. 35,000 years ago (calendar yr B.P., cf. Van Andel 1997) (Figure 75). The stratum B deposits are dominantly from swamp, plaudal, and small lake environments. Fossils were typically found at the boundary of strata A and B and within the lower, more organic-rich deposits of stratum B (Figures 76 and 78). These deposits may contain fossils which

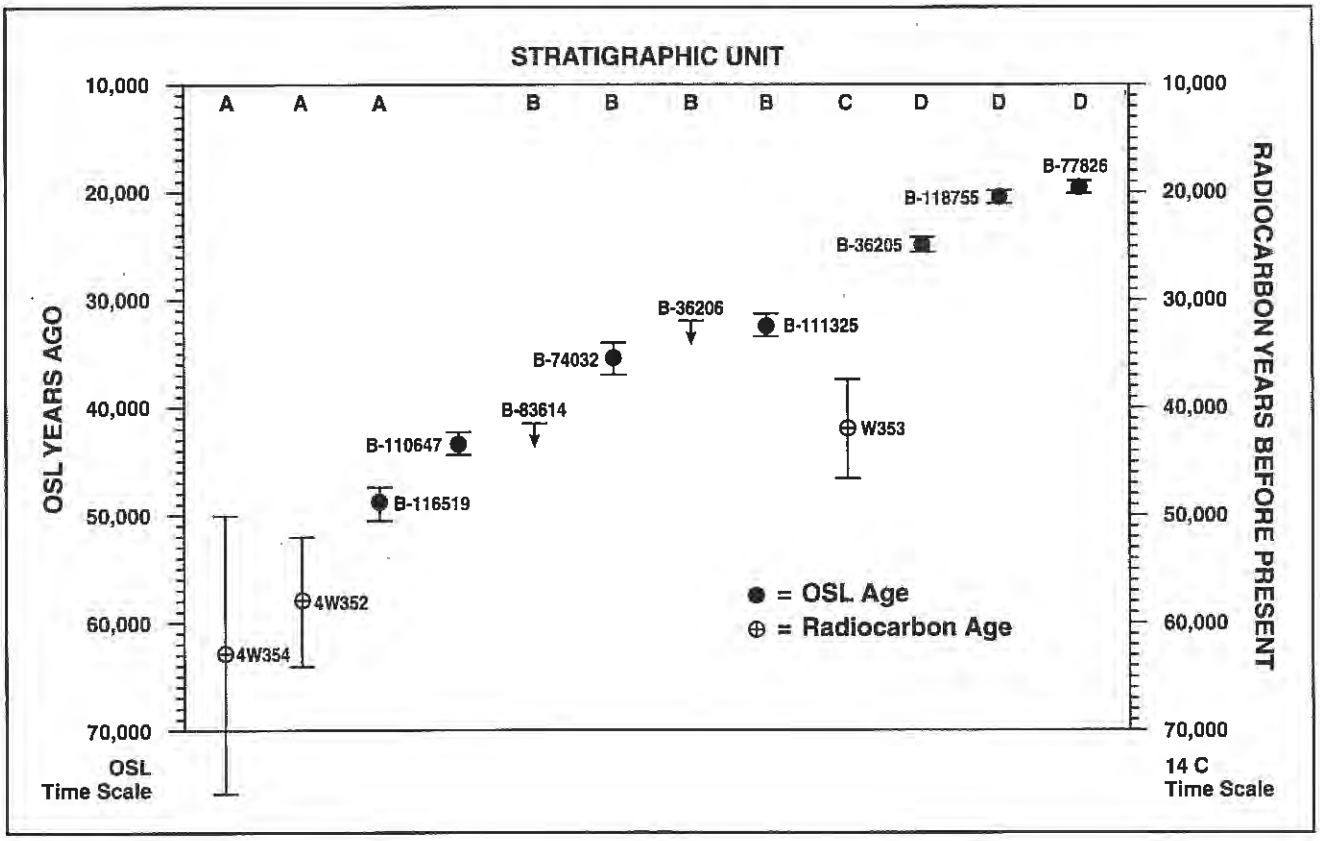

Figure 75. OSL and radiocarbon ages for samples from Merrell Locality, Centennial Valley.

were originally within stratum A that were later redeposited into stratum B, or fossils from animals that were contemporary with the stratum B depositional contexts. Based on the luminescence and radiocarbon measurements, stratum A and possibly some stratum B deposits are older than 40,000 ^{14}C yr B.P. (Figure 79). Organic material retrieved from a bone recovered from the lower, dark facies of stratum B has been dated ca. 36,500 ^{14}C yr B.P. (or ca. 39,000 calendar yr B.P.). This would imply that some of the stratum B deposits are associated with isotope stage 3 and possibly the Early Pinedale glaciation. Tusk collagen from a specimen obtained from the lower facies of stratum B provided a date of ca. 32,470 ^{14}C yr B.P. (ca. 35,000 calendar yr B.P). This measurement would indicate that some of the fossils incorporated into stratum B are associated with the younger part of isotope stage 3 (Figure 77). They could thus be roughly contemporary with the Farmdale phase in the midcontinent (cf. Karrow et al. 2000). However, a date of roughly 35,000 B.P. would also correspond to the end of the Early Pinedale glaciation on the nearby Yellowstone Plateau, dated between 47,000 and 34,000 calendar yr B.P., which was followed by an interstadial lasting from ca. 34,000 to 30,000 years ago (Sturchio et al. 1994).

Based on stratigraphic relationships and radiocarbon measurements available from stratum B and from stratum D, the fluvial sediments of stratum C would seem to be associated with the end of isotope stage 3 or the transition to isotope stage 2. The luminescence age is approximately 42,000 calendar yr B.P. (multi-aliquot method) or 38,500 calendar yr B.P. (SAR method, with a fairly large standard deviation) (Feathers, this report). This would indicate that the sediments in stratum C were deposited during the early or middle part of isotope stage 3 (Figure 77). The luminescence date implies that the stratum C sediments were deposited during some part of the Early Pinedale advance on the Yellowstone Plateau (Sturchio et al. 1994), while the stratigraphic relationship with stratum B would seem to indicate possible contemporaneity with either the interstadial documented on the Yellowstone Plateau (ca. 34,000 to 30,000 calendar yr B.P.) or the major Pinedale advance (ca. 30,000 to 22,500 calendar yr B.P.).

Stratum D consists of a debris-flow with bones of *Equus*, *Bison*, and *Mammuthus* (Figures 62-66 and 80). It is a localized set of deposits found along the north side of the Merrell Site, in the North Block or Excavation Area I. The deposits of stratum D seem to rest on eroded surfaces

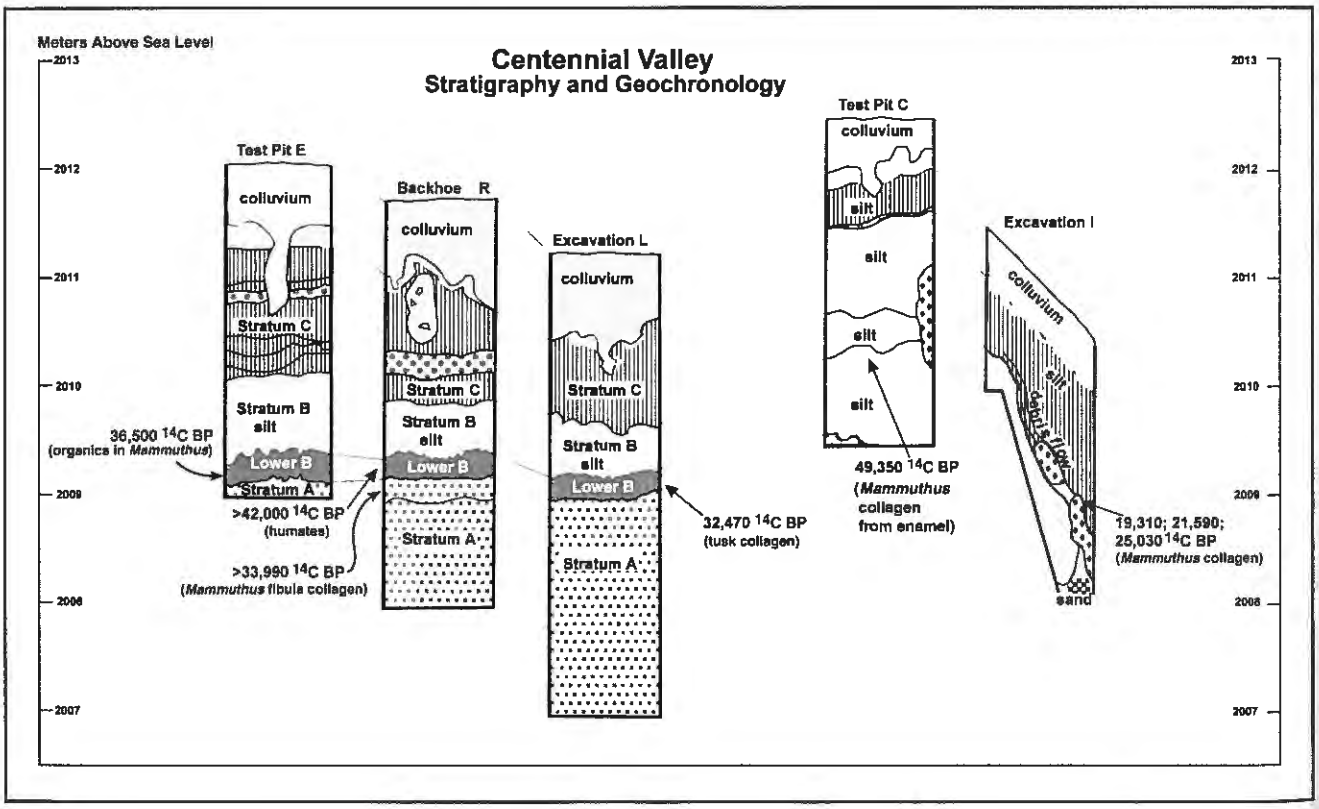

Figure 76. General stratigraphic relationships of OSL and radiocarbon samples collected from Merrell Locality, Centennial Valley (profiles by C. L. Hill).

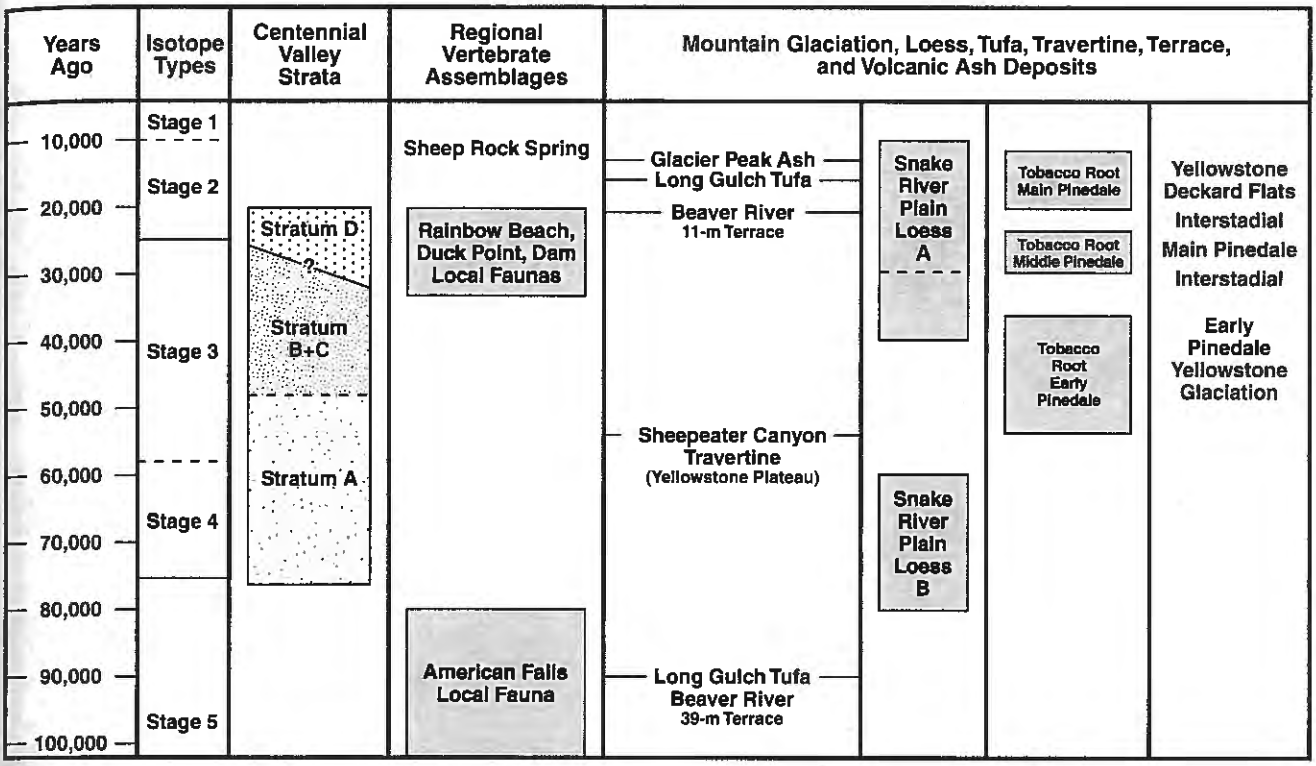

Figure 77. Late Pleistocene chronological relationships.

Figure 78. Strata A and B, South Block, Merrell Locality, looking generally toward grid north (C. L. Hill photo).

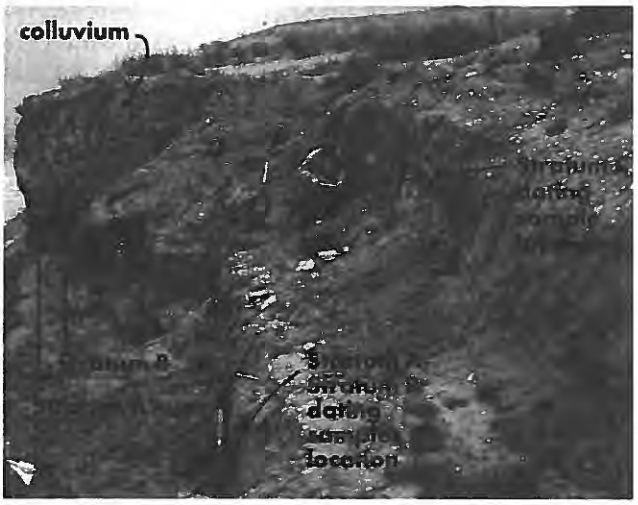

Figure 79. Collection of OSL samples from South Block, Merrell Locality (C. L. Hill photo).

of strata A-C. Thus, there is the potential that stratum D may contain fossil remains younger than stratum C as well as, potentially, fossils originally in strata A-C. The stratum D fossil assemblage definitely appears to be in secondary position and seems to have incorporated bones of several ages. The youngest date of ca. 19,000 ^{14}C yr B.P. or about 22,000 years ago (Table 3, Figure 77) was obtained from collagen in mammoth bone. This provides a maximum age for the deposit. It implies that some of the fossils in the debris flow are slightly older than the Last Glacial Maximum (isotope stage 2). Another date of ca. 25,000 ^{14}C yr B.P. or ca. 28,000 years ago (Table 7, Figure 75) is also from bone incorporated into this deposit (Dundas 1992). This date indicates that some of the assemblage may be associated with the transition connected with isotope stages 2 and 3. There is also the possibiliry that older fossils origi-

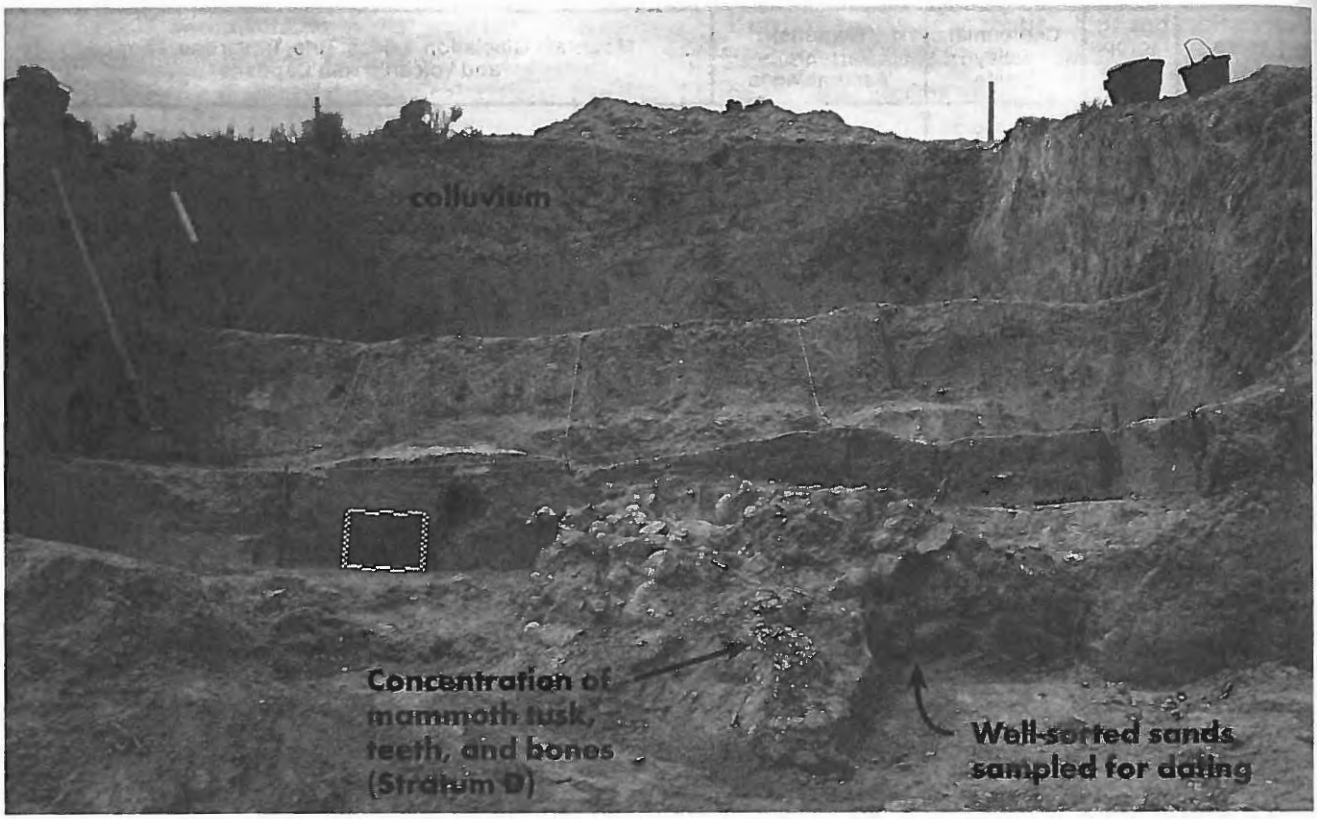

Figure 80. Location of OSL sample from stratum A below stratum D, North Block, Merrell Locality (C. L. Hill photo).

nally associated with strata A-C may be mixed within the debris flow. The date of 19,000 ^{14}C yr B.P. (ca. 22,000 years ago) appears to indicate that the youngest Pleistocene fossils from Merrell are slightly older than the Last Glacial Maximum, but are within the local "full glacial" advance on the Yellowstone Plateau (Sturchio et al. 1994). The debris flow itself could be younger.

General Discussion of Chronologic Framework

The luminescence measurements of two sedimentary facies of stratum A and the radiocarbon date of a mammoth remains from a possible facies of stratum A seem to demonstrate that stratum A is likely associated with isotope stage 4 and the early part of isotope stage 3 (Figure 75). Some of the bones incorporated into the deposits of stratum A may be too old to obtain finite radiocarbon ages. Others may be around 50,000 yr B.P.

Stratum B appears to be primarily associated with isotope stage 3 (Figure 75). There seems to be a strong possibility that the stratigraphic sequence associated with stratum B dates a local example of a changing environment associated with a marsh or pond-lake basin in the Centennial Valley. The possible presence of Pleistocene lakes within the valley is likely related to a combination of tectonic, geomorphic, and climatic processes. Organic deposits associated with bone from stratum B date ca. 36,500 ^{14}C yr B.P. or ca. 39,000 years ago, while bone collagen from mammoth dates to >34,000 ^{14}C yr B.P. Calibrated for comparison with the U-series chronology, the dates of ca. 37,000 ^{14}C yr B.P. may imply an age closer to 40,000 B.P. for the deposition of organics in stratum B. If not actually beyond the ability of radiocarbon measurement, the dates from stratum B would indicate a potential temporal association with two Pinedale alpine glacier advances and possibly the intervening inrerstadial. Using the glacial chronology developed for the region immediately to the east of Centennial Valley (Sturchio et al. 1994), the radiocarbon- dated organics can be correlated with the Early Pinedale glacial advance that centered ca. 40,000 calendar yr B.P. (Figure 77).

A date of 25,000 ^{14}C B.P. (Table 3) from collagen from the debris flow or channel (Dundas 1992) is estimated to be about 28,000 calendar years B.P. (Van Andel 1998). The debris flow also contains bone dated ca. 19,310 ^{14}C yr B.P., or about 22,000 calendar yr B.P., based on calibration with the U-series chronology (cf. Sturchio et al. 1994; Bartlein et al. 1995; Bard et al. 1990; Van Andel 1998).

The Greenland ice core record (cf. GISP II) shows apparent warm interstadial events between about 33,000 and 23,000 calendar years B.P., with "full glacial" values from around 18,000 to 15,000 calendar years B.P. (cf. Sowers and Bender 1995). However, the glaciers on the Yellowstone Plateau appear to have reached their maximum several thousands of years before the Last Glacial Maximum (cf. Pierce, Obradovich, and Friedman 1976; Sturchio et al. 1994), when the LGM is related to low global sea levels around 18,000 ^{14}C yr B.P. or about 20,000 calendar years B.P. The maximum extent of the glaciers to the south in the Wind River Range may have been contemporary with the LGM, with Pinedale assigned ages of 23,000-16,000 yr B.P. based on ^{36}Cl/^{10}Be measurements (cf. Chadwick et al. 1997; Phillips et al. 1997). On the Yellowstone Plateau, there seems to have been a major Pinedale advance resulting in full-glacial conditions between 30,000 and 22,500 calendar yr B.P., followed by a recession and a late Pinedale (Deckard Flats) advance between 19,500 and 15,500 calendar yr B.P. (Sturchio et al. 1994) (Figure 77). The youngest fossil materials incorporated into the debris flow, therefore, appear to be associated with the local major Pinedale advance ("full-glacial"), while the radiocarbon-dated materials are within the interstadial interval observed in the Greenland ice core.

The bone dated within the debris flow is redeposited; it may be older than the debris flow in which it was incorporated. Thus, while the date of ca. 19,000 ^{14}C yr B.P. (22,000 calendar yr B.P.) provides a maximum age for the deposit, it also provides some chronologic control on the age of the vertebrate remains. Taking into account the departure of radiocarbon dates from the U-series chronology, this indicates the presence of elements of a mammoth biome in Centennial Valley perhaps ca. 22,000 calendar years B.P., thus linking these faunal elements with the "full-glacial" ice advance in the region immediately to the east, ranging from 29,900 to 22,500 calendar yr B.P. (Sturchio et al. 1994). A period of ice recession was followed by the Late Pinedale (Deckard Flats) ice advance after 19,500 calendar yr B.P. (cf. Sturchio et al. 1994), but there is no chronometric evidence that any of the fossils at the Merrell Locality can be assigned to this interval. The youngest radiocarbon dated fossil dates to ca. 22,000 years ago and thus is associated with local "full-glacial" conditions.

Paleoclimatic Context

The Centennial Valley is located within a region where a variety of paleoclimatic proxy indicators can assist in the evaluation of climate model simulations. Certain models (cf. Benson and Thompson 1987; Kutzbach and Wright 1985; Spaulding 1991; Clark and Bartlein 1994) indicate that climate change in the region during the Pleistocene was a response to changes in atmospheric circulation patterns--specifically, oscillations in the jet stream--that result in increases in winter precipitation and annual cooling during glacial intervals. There is also a potential climate-tectonic connection (cf. Ruddiman 1994) since tectonic uplift of the Rocky Mountains has been implicated as a factor in precipitation changes and alteration of jet stream and storm tracks over North America (Kutzbach 1994). Tectonic activity may also have played a direct role in influencing changes in the drainage system with the valley.

A regional climate model (RCM), using general circulation model (GCM) simulations as boundary conditions, indicates that glacial maximum temperatures were cooler and that winter precipitation was substantially greater in western North America (Hostetler et al. 1994a,b). These conditions would have been conducive to both the growth of mountain glaciers and the appearance of pluvial lakes, as well as the presence of lakes fed by glacial meltwater at glacial-interglacial transitions. Dynamic fluctuations in climate, which can influence habitat variability and biotic diversity (cf. Guthrie 1990), would be expected to influence adaptive responses of plant and animal populations in the region.

Mountain glaciers respond to global climate change (cf. Sturchio et al. 1994) and, in the Centennial region, three major sets of alpine glaciation are indicated: pre-Bull Lake, Bull Lake, and Pinedale (Sonderegger et al. 1982:8). Studies of the Yellowstone Plateau east of Centennial Valley also provide a chronologic framework of glaciation and deglaciation for comparison (Pierce 1979; Pierce et al. 1976; Porter, Pierce, and Hamilton 1983; Richmond 1986a, 1986b; Sturchio et al. 1994). The framework is potentially representative of Pleistocene glacier activity in the Northern Rockies (cf. Forman et al. 1993). In Yellowstone, two diamictons indicate glacial advance during the Plio-Pleistocene, and deposits indicate glacial advances within isotope stages 40 or 36 (pre-Illinoian J or I), 34 (1,580,000-1,510,000 B.P., advance H), and 14 (562,000-512,000 B.P., advance C). Lake sediments containing volcanic ash have dated to ca. 483,000 B.P. Separate tills correlate with isotope stages 14 and 12 (Richmond 1986a,b) and there are indications of glaciation ca. 375,000 B.P. (Sturchio et al. 1994). Isolated deposits identified as pre-Bull Lake tills have been mapped on the southeast side of the Centennial Valley (Witkind 1976), although care must be taken to demonstrate that the diamictons represent till related to glacial advances and not to mass-wasting events associated with tectonic activity.

In the Wind River Range, the three youngest Bull Lake

glaciations could date between 130,000 and 95,000 yr B.P., while the Pinedale glaciations range from 23,000 to 16,000 yr B.P. (Chadwick et al. 1997; Phillips et al. 1997). On the Yellowstone Plateau, a Bull Lake glacial advance seems to have occurred prior to ca. 134,000 calendar yr B.P., perhaps about 150-140,000 calendar yr B.P. (cf. Pierce, Obradovich, and Friedman 1976; Porter, Pierce, and Hamilton 1983; Forman et al. 1993; Sturchio et al. 1994). This glaciation has been associated with stage 6 (ca. 150,000 B.P., Late Illinoian, Richmond 1986b; Richmond and Fullerton 1986). Glacial pulses are also associated with isotope substages 5d (ca. 117,000 B.P.) and 5b (ca. 90,000 B.P.), and possibly with stage 4 (79,000-65,000 B.P., Richmond and Fullerton 1986). Tufas dated to ca. 90,000 yr B.P. indicate that the 39-m (128-ft) terrace of the Beaverhead River northwest of Centennial Valley could be Sangamon or late Bull Lake (Bartholomew et al. 1999) (Figure 77). Isotope stage 5b has been correlated with a Late Bull Lake advance (Richmond 1986).

It has been proposed that there was no glacial advance during for the Middle Wisconsin, isotope stage 3 (ca. 65,000-35,000 yr B.P.), in the Rocky Mountains and Yellowstone (Richmond and Fullerton 1986). However, the Sheepeater Canyon travertine on the Yellowstone Plateau has a U-series age of ca. 55,000 calendar yr B.P. and is mantled by Pinedale till (Sturchio et al. 1994). The Early Pinedale advance on the Yellowestone Plateau may have begun by ca. 47,000 yr B.P. and continued until ca. 34,000 yr B.P. (Sturchio et al. 1994) (Figure 77). The nearby Lemhi Range contains evidence of three glacial advances estimated to date ca. 150,000, 60,000, and 25,000 yr B.P. (Butler et al. 1983). Within the Three Rivers Basin (Hill 2001a), two major Pinedale advances were recognized in the Tobacco Root Mountains (Roy and Hall 1981). The "early Pinedale" interval may have been initiated by 50,000-45,000 yr B.P. and continued beyond 35,000 yr B.P., while the "middle Pinedale" advance may date to ca. 22,400 yr B.P. (Roy and Hall 1981; Hall and Heiny 1983; Hall and Michaud 1988) (Figure 77).

Another indicator of glacial conditions in the region has been provided by the chronologic framework associated with loess deposition on the eastern Snake River Plain, south of the Centennial Valley (Foreman et al. 1993). There appear to be two intervals of loess deposition (Figure 77). The older loess sequence, deposited between 80,000 and 60,000 B.P., is considered to have probably been coincident with an "early Wisconsinan" glacial episode (Foreman et al. 1993). The younger loesss sequence is thought to have started forming between 40,000 and 30,000 yr B.P., with deposition continuing until ca. 10,000 yr B.P.; it also seems to have been associated with a regional glacial cycle (Foreman et al. 1993). The middle of the younger loess has luminescence age estimates of ca. 28,000 and 25,000 yr B.P., while a radiocarbon age of ca. 11,980 ^{14}C yr B.P. (ca. 14,000 years ago) provides an approximate date for the top of the sequence (Foreman et al. 1993; Bartlein et al. 1995).

Summary of Pleistocene Geologic Events

Tectonic activity and volcanism influenced the last 2.5 million years of prehistory in the Centennial Valley. The Centennial Mountains were lower in the Late Tertiary-Early Quaternary, which influenced glaciation and habitat settings. Just tectonic displacement at a specific locality would have effected a habitat change, regardless of fluctuations in the paleoclimate. For instance, some results of uplift--vegetation change, stream incision and erosion, and diamictons from mass-wasting--may also be indicators of climate change (cf. Ruddiman 1994).

Throughout the Quaternary, there has been tectonic displacement in the valley. The Huckleberry Tuff, derived from the Yellowstone Caldera and dated to 2 million years ago, appears to have diverted the ancestral Plio-Pleistocene Madison River which had flowed southward into the Centennial Valley (Mannick 1980). Displacement on the order of 5,000-6,000 ft (>1,500 m) has occurred in the upper (east side) Centennial Valley since deposition of the Huckleberry Tuff (Mannick 1980). On the east side of the valley, there has been greater than an inch of movement per year since the last glaciation; Post-Pinedale displacement has been estimated at 1.2 in (5.1 cm) per year (Mannick 1980). The Centennial Fault has a scarp on the west side of the valley, closer to the Merrell Locality, which shows a displacement of about one-fifth that in the eastern end (Sonderegger et al. 1982). Faults are also present north of the Lima Reservoir and close to the valley-dam constriction area (Stickney, Bartholomew, and Wilde 1987; Stickney and Bartholomew 1987; Myers and Hamilton 1964).

During the Late Pliocene-Early Pleistocene, the Centennial Valley was occupied by a large lake, indicated partially by the deposition of freshwater limestone (Mannick 1980). It has been proposed that glacial meltwater had accumulated in the Centennial Valley, forming a large lake (Sonderegger et al. 1982).

Alluvial fans had formed before and during the presence of a glacial lake, while younger fans were deposited after the lake had drained; a topographic break along the edges of some fans seems to indicate that parts of some alluvial fans were deposited underwater in delta-like con-

ditions. This break may be the result of currents in a former lake. Lacustrine deposits, including several beach deposits, mark former shorelines of a dwindling glacial lake (Witkind 1976). Younger streams have trenched and segmented the lacustrine deposits. Lake deposits reach elevations of 6,717 fasl (2,047 masl) north of Lower Red Rock Lake, and are above 6,800 fasl (2,073 masl) northeast of Upper Red Rock Lake. Some of the valley lakes may have been fed by warm spring activity, and are related to geothermal heat sources (Mannick 1980:67). The present lakes (and perhaps the Pleistocene lakes) are warmed by waters circulating along the Cligg Lake Fault and other faults. Travertine deposited along the eastern shore of Elk Lake reflects the past existence of thermal springs within the valley (Mannick 1980: 68).

A date of 36,500 ^{14}C yr B.P. (calibrated to ca. 40,000 B.P. in the U-series chronology, cf. Van Andel 1997) indicates that organics within sediment at the Merrell Locality in the Centennial Valley could have been deposited before or during an ice advance associated with isotope stage 3 (Early Pinedale). This dark organic deposit (stratum B, LL2, equivalent to level 3 [or III] of Bump 1989) seems to reflect a habitat setting related to the margins of a Pleistocene marsh.

Isotope stage 2 (ca. 35,000-13,000 yr B.P.) appears to have been associated with a major global glacial event. Pinedale till has been reported along the north face of the eastern Centennial Mountains (Witkind 1976). Pinedale moraines advanced beyond the valley mouths and coalesced on the east side of the valley. Within the interval from 34,000 to 29,000 B.P., the ice margin on the Yellowstone Plateau receded, indicating an interstadial event. Fossils dated ca. 25,000 ^{14}C yr B.P. (ca. 28,000 calendar yr B.P.) at Merrell would indicate the continued presence of a mammoth biome around the early part of this advance. Northwest of Centennial Valley, the 11-m terrace above the Beaverhead River is covered by a tufa dated to ca. 15,000 calendar yr B.P., implying an age of ca. 26,000 calendar yr B.P. and a possible association with the major Pinedale advance (Bartholomew et al. 1999) for the terrace deposits (Figure 77). It seems feasible that the youngest fossils recovered from stratum D in Centennial Valley are associated with the major Pinedale "full-glacial" advance or perhaps the transitional interval after ca. 22,500 yr B.P.

A major "full-glacial" advance, which appears to have occurred between ca. 30,000 and 22,500 yr B.P. (Sturchio et al. 1994), is associated with the youngest radiocarbon date from stratum D at the Merrell Site. The calibration curve indicates that the Last Glacial Maximum of ca. 18,000 ^{14}C yr B.P. probably occurred 22,000-21,000 B.P. (Tushingham and Peltier 1993). A major melting back of the ice margin between 22,500 and 19,500 yr B.P. was followed by a minor advance between 19,500 and 15,500 yr B.P. (centered on ca. 18,000 yr B.P., Sturchio et al. 1994) on the Yellowstone Plateau. A Late Pinedale readvance or standstill in the ice margin position seems to have occurred before 14,500 yr B.P. (ca. 13,000 ^{14}C yr B.P., cf. Porter, Pierce, and Hamilton 1983; Richmond 1986b).

Loess deposition in the region to the south of Centennial Valley between 40,000-30,000 yr B.P. and 10,000 yr B.P. has been correlated with the Pinedale glaciation (Foreman et al. 1993). Pluvial lake expansion from ca. 32,000 to 10,000 B.P. yr is also associated with regional Pinedale glaciation, with high stands contemporaneous with deglaciation events (cf. Currey and Oviatt 1985; Benson and Thompson 1987; Benson et al. 1990). A lake (or lakes) may have filled most of the Centennial Valley ca. 12,000-10,000 B.P. at the end of the last glacial period (Sonderegger et al. 1982:15).

Conclusions: Lithostratigraphic and Biostratigraphic Context

The stratigraphy of the Centennial Valley contains lithologic and biostratigraphic information that can be used to infer the paleoenvironmental and paleoclimatic context of the Upper Pleistocene of southwestern Montana. Several stratigraphic units contain Pleistocene vertebrate remains (strata A-D). Based on a calibration with the U-series chronology, the radiocarbon dates indicate the presence of a generalized mammoth biome within the Centennial Valley around or before 50,000 to perhaps ca. 22,000 years ago. The luminescence ages reported by Feathers (this report) seem to demonstrate that deposition of stratum A occurred prior to ca. 50,000 years ago. Vertebrate remains are found within and on the top of stratum A and the marsh deposits of stratum B, estimated to date to ca. 40,000 B.P., or earlier. The vertebrate remains found in the North Block (Excavation I) seem to have been incorporated into a debris flow (stratum D). The remains indicate the presence of mammoth biome-related fauna in the valley, perhaps associated with full-glacial conditions. The faunal assemblages from the Centennial Valley appear to be younger than the American Falls Local Fauna from Idaho (Figure 77). Younger Idaho fossil vertebrate assemblages (Rainbow Beach, Duck Point, and Dam Local Faunas) may be approximately contemporary with some fossils recovered from strata B-D (Figure 77).

The Late Pleistocene Vertebrate Fauna

Robert G. Dundas

Introduction

The Pleistocene fauna of southwestern Montana is not well understood. This is largely because little attention has been given to fossil sites in the region until recently. Since the late 1980s, fossil remains at the Merrell Locality have been the subject of a major research effort undertaken, in part, to enhance our knowledge of the region's fauna during the Late Pleistocene (Dundas 1992; Dundas, Hill, and Batten 1996).

This discussion provides a systematic account of the Pleistocene vertebrate fauna recovered from the Merrell Locality and Site, with comments on species paleoecology. Hill and Batten (this report) report the spatial distribution of the fossil remains. At present, the vertebrate fauna is composed of 19 species (Table 8), most of which occur at other Late Pleistocene sites in Montana and the surrounding region (Graham, Semken, and Graham 1987; Kurtén and Anderson 1980; FAUNMAP 1994; Harris 1985). Two species at Merrell are of particular interest; *Homotherium serum* (Scimitar cat) and *Olar buccinator* (Trumpeter swan), the second of which is reported for the first time in the fossil record of Montana. In addition to the vertebrate fauna, specimens of bivalves and gastropods were also recovered, but have not been studied.

Specimen Repository

Fossil material collected from the Merrell Locality in 1988 and 1989 by the BLM and the UM-Missoula is housed along with other specimens recovered from the site, at the Museum of the Rockies, Montana State University-Bozeman, Bozeman, Montana. A complete listing of all faunal remains in the Museum of the Rockies collections is provided in Appendices C and D.

Abbreviations and Institutional Acronyms

i - lower incisor
m - lower molar
p - lower premolar
M - upper molar
P - upper premolar
MOR - Museum of the Rockies
UMT - University of Montana Paleontology Museum
UMZM - University of Montana Zoology Museum
USNM - United States National Museum - Smithsonian Institution

Systematic Paleontology

Phylum Chordata (chordates)
Class Osteichthyes (bony fishes)

Referred specimens: MOR LI94.5.246, parietal fragment; MOR LI94.5.248, suborbital fragment; MOR LI94.5.249, skull bone fragment; MOR LI94.5.247, an opercular fragment and a parietal fragment; MOR LI95.2.21, skull bone fragment; MOR LI95.2.536, trunk vertebra.

Remarks: The fish remains were examined by paleoichthyologist Dr. Douglas Long. Dr. Long determined that the material is insufficient for further identification below the level of Osteichthyes (bony fishes). However, the specimens compare best with the Catostomidae (suckers) and Cyprinidae (carps and minnows). Both families

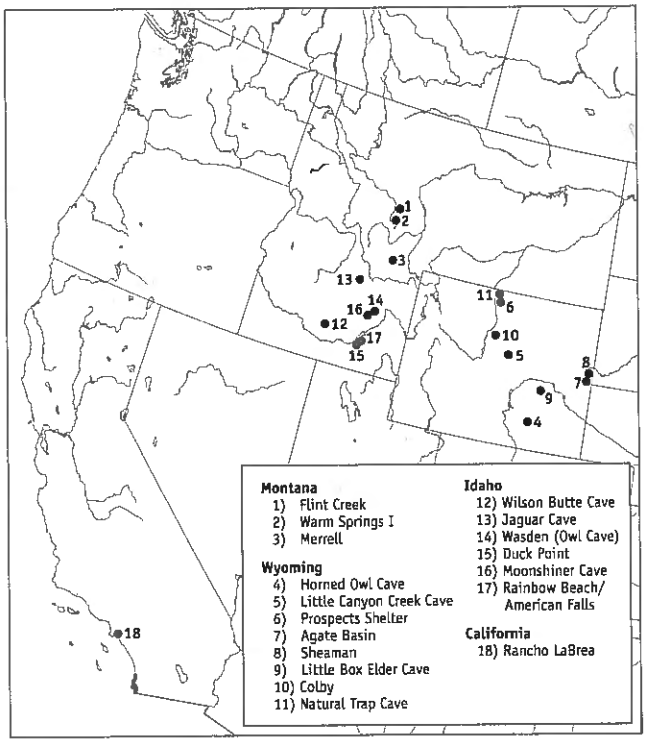

Figure 81. Late Wisconsinan localities and sites referenced in the text by R. G. Dundas.

Table 8. Late Pleistocene Merrell Locality Fauna.

Phylum Mollusca (mollusks)
- Class Bivalvia (clams and others)
- Class Gastropoda (snails)

Phylum Chordata (chordates)
- Class Osteichthyes (bony fishes)
- Class Aves (birds)
  - Order Anseriformes (waterfowl)
    - Family Anatidae (ducks, geese, swans)
      - Genus *Anas* cf. *A. platyrhynchos* (Mallard duck)
      - Genus and species *Olar buccinator* (Trumpeter swan)
- Class Amphibia (amphibians)
  - Order Anura (frogs and toads)
    - Family Ranidae (ranids)
      - Genus cf. *Rana* (true frogs)
- Class Mammalia (mammals)
  - Order Rodentia (rodents)
    - Family Muridae (voles, lemmings, muskrats, mice, and others)
      - Genus and Species *Lemmiscus curtatus* (sagebrush vole)
      - Genus and Species *Ondatra zibethicus* (muskrat)
    - Family Sciuridae (squirrels and others)
      - Genus *Spermophilus* sp. (ground squirrels)
    - Family Castoridae (beavers)
      - Genus and Species *Castor canadensis* (beaver)
  - Order Carnivora (carnivores)
    - Family Canidae (canids, i.e., dogs)
      - Genus and Species *Canis latrans* (coyote)
      - Genus and Species *Canis lupus* (gray or timber wolf)
    - Family Felidae (cats)
      - Genus and Species *Homotherium serum* (Scimitar cat)
    - Family Ursidae (bears)
      - Genus and Species *Ursus* sp. (bear)
  - Order Artiodactyla (artiodactyls)
    - Family Antilocapridae (pronghorns)
      - Genus and Species cf. *Antilocapra americana* (American pronghorn)
    - Family Cervidae (deer)
      - Genus indeterminate (large species)
      - Genus cf. *Odocoileus* sp. (white-tail or mule deer)
    - Family Bovidae (bovids)
      - Genus *Bison* sp. (bison)
    - Family Camelidae (camels)
      - Genus *Camelops* sp. (large camel)
  - Order Perissodactyla (perissodactyls)
    - Family Equidae (horses)
      - Genus *Equus* sp. (horse)
  - Order Proboscidea (proboscideans)
    - Family Elephantidae (elephants)
      - Genus and Species *Mammuthus columbi* (Columbian mammoth)

of fish are found in Montana today (Gould 1992). It is not unreasonable to suggest that the fossil specimens may represent one or both of these groups. A Holocene specimen of cf. *Catostomus*, right operculum, was recovered during the 1995 excavations at Merrell.

Class Aves (birds)
Order Anseriformes (waterfowl)
Family Anatidae (ducks, geese, swans)

Referred specimen: MOR LI94.5.245, thoracic vertebra.

Remarks: This specimen was examined by Dr. Steve Emslie, who referred it to the Anatidae. Further identification is not possible because of the lack of additional diagnostic features.

Anas cf. *A. platyrhynchos* (Mallard duck)

Referred specimen: MOR L194.5.455 (MS-685, EN-20-2), distal end of a left humerus.

Remarks: This specimen was examined by Dr. Steve Emslie and found to best compare with *Anas platyrhynchos*. The Mallard is a wide-ranging duck, found throughout most of North America, particularly around ponds and freshwater marshes (Robbins, Bruun, and Zim 1966).

Genus *Olar* (swan)
Olar buccinator (Trumpeter swan)
Figure 82

Referred specimen: MOR LI96.4.190, proximal end of a left humerus.

Remarks: MOR LI96.4.190 was compared with all of the North American swans: *Cygnus olor* (Mute swan), *Olar buccinator* (Trumpeter swan), and *Cygnus columbianus* (Whistling swan). The Mute swan is an introduced species in North America, having been brought from Europe in the 1800s (Stokes and Stokes 1996). The MOR specimen compares best in size and morphology to *Olar buccinator*. It compared especially well to a specimen of *Olar buccinator*, USNM 430266, from Alaska (Emslie, pers. comm., 1997).

The Trumpeter swan (*Olar buccinator*) is particularly interesting. Few fossil remains of this species are known. Fossil specimens have been recovered from Alaska, Oregon, Iowa, Illinois, Ohio, and Florida (Brodkorb 1964). Although widespread in North America in historic times, from Alaska to southern California and the Gulf Coast, it is rare today, and once nearly extinct (Pough 1953). Early this

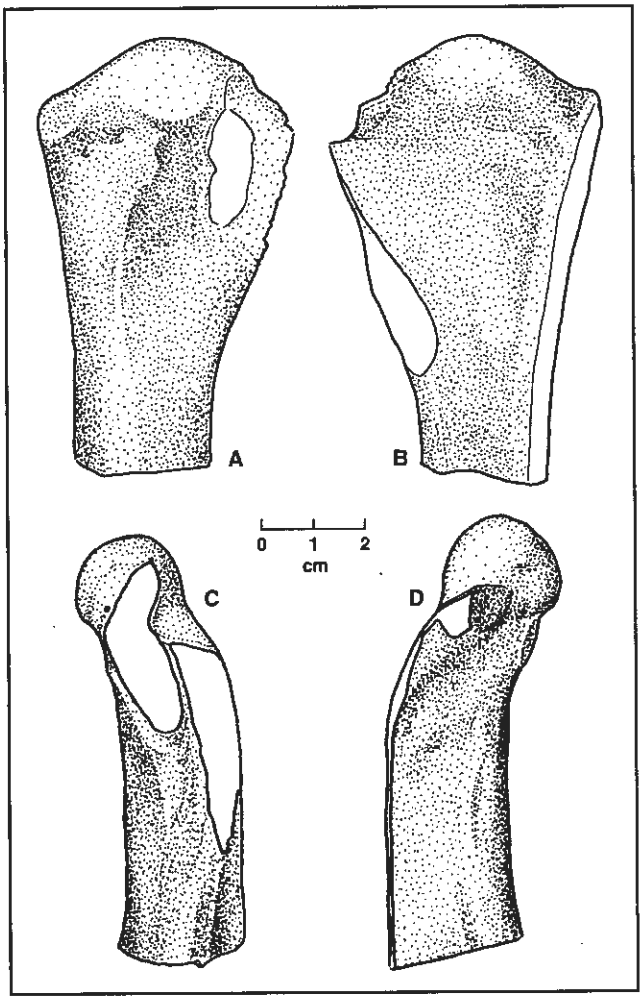

Figure 82. Trumpeter swan (*Olar buccinator*) (MOR LI96.4.190) proximal end of partial lft. humerus: a, anconal; b, palmar; c, ventral; and d, dorsal views.

century, the draining of marshes, hunting, lead poisoning, and other environmental disturbances nearly resulted in the extinction of the Trumpeter swan. Only a small number survived by the 1930s, but, with conservation efforts and reintroduction back into former habitat, the population increased to more than 3,000 by the 1970s (Udvardy 1977). It is one of North America's largest birds, and the largest member of the swan family in North America, with a length of up to 65 in (1.65 m), a wingspan of 100 in (2.54 m), and weighing about 30 lbs (13.6 kg). Their habitat is typically marshes, lakes, or rivers with dense vegetation. They are known to nest in old muskrat or beaver houses or small islets in shallow ponds or marshy areas. Food includes leaves, roots, and seeds of sedges and other aquatic plants, and mollusks (Pough 1953). They dip their head and neck in the water similar to a duck when feeding on bottom vegetation (Stokes and Stokes 1996). They also

forage along the shore. The Red Rock Lakes area to the east of Lima Reservoir is one of the few breeding grounds left for this species in the contiguous United States (Robbins, Bruun, and Zim 1966).

Class Amphibia (amphibians)
Order Anura (frogs and toads)
Family Ranidae (ranids)
cf. *Rana* (true frogs)
Figure 83

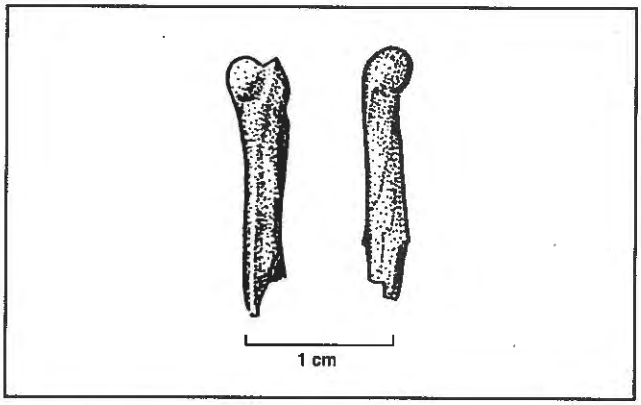

Figure 83. *Rana* distal lft. humerus.

Referred specimen: MOR LI95.2.535, distal end of a left humerus.

Remarks: The specimen is not *Scaphiopus* (Pelobatidae) because the condylar morphology is different for that group. The specimen is too robust for a hylid. Of Ranidae and Bufonidae, the specimen compares best with *Rana*. Twenty-five species of this genus occur in North America today, at least 10 of which are known from the Pleistocene. Most are aquatic frogs that prefer quiet water, although some species venture well into grassy and moist woodland areas (Holman 1995).

Class Mammalia (mammals)
Order Rodentia (rodents)
Family Muridae (voles, lemmings, muskrats, mice, etc.)
Genus *Lemmiscus*
Lemmiscus curtatus (sagebrush vole)
Figure 84

Referred specimen: MOR LI95.2.36, right dentary with i1, m1, and m2.

Remarks: The identification is based on the specimen being a microtine rodent with five triangles and no lingual wing development on the lingual side of the anterocap.

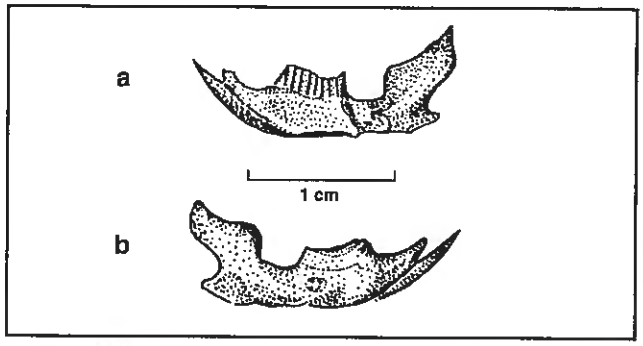

Figure 84. *Lemmiscus* rt. dentary: a, medial; and b, lateral views.

The sagebrush vole has been recovered from several Late Pleistocene localities in the region and occurs in the area today. Fossil occurrences in Idaho include Wilson Butte Cave, Jaguar Cave, Moonshiner Cave, and Wasden, while Bell Cave, Horned Owl Cave, Little Canyon Creek Cave, Prospects Shelter, Natural Trap Cave, Agate Basin, and Little Box Elder Cave record the species in Wyoming (Kurtén and Anderson 1980; FAUNMAP 1994). In Montana, *Lemmiscus* is known from the Late Wisconsinan-age Warm Springs site (Rasmussen 1974; Kurtén and Anderson 1980) and False Cougar Cave (FAUNMAP 1994). The species is typically found in semiarid, open environments. Usually, their habitat is dominated by sagebrush and bunchgrasses. They are often found living under sagebrush plants, constructing nests from its shredded bark, as well as leaves, stems, and grass seed-heads (Zeveloff 1988).

Genus *Ondatra* (muskrat)
Ondatra zibethicus (muskrat)
Figure 85

Referred specimens: UMT 10034, upper right incisor; MOR LI94.5.28, right calcaneum; MOR LI94.5.97, left m1; MOR LI94.5.454, partial left dentary with m2 and m3.

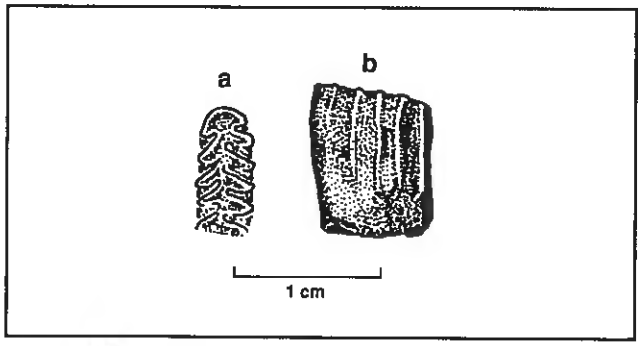

Figure 85. *Ondatra* lft. m1: a, occlusal; and b, side views.

Remarks: UMT 10034 was compared to rodent specimens in the University of Montana Zoology Museum. Of all rodents inhabiting North America during the Late Pleistocene, the size and morphology of the incisor compares best with *Ondatra zibethicus*. The remainder of the specimens are clearly identifiable as muskrat, based on comparisons with modern specimens.

Muskrat occur in the area today. Found in almost any aquatic environment, they are common around beaver ponds in the western United States. Aquatic plants compose much of the diet, with a preference for cattails. However, they also forage for animals such as freshwater clams, snails, frogs, crayfish, turtles, and fish. Muskrats build lodges from aquatic vegetation and also burrow into banks (Zeveloff 1988; Jones and Birney 1988). *Ondatra zibethicus* is also known from the Late Wisconsinan Warm Springs #1 site in Montana (Rasmussen 1974; FAUNMAP 1994). In the surrounding region, the species has been recovered from the Late Wisconsinan deposits at Rainbow Beach and the Dam Local Fauna in Idaho and Horned Owl Cave in Wyoming (FAUNMAP 1994).

Family Sciuridae (squirrels, etc.)
Spermophilus sp. (ground squirrels)

Referred specimen: MOR LI94.5.256, partial edentulous right dentary with alveoli for the m2 and m3 present.

Remarks: Species identification is not possible due to the lack of dentition. In general, all ground squirrels are burrowers, most hibernate, and many are colonial. Habitat of ground squirrels living in the area today is predominantly sagebrush and bunchgrass rangeland. However, species such as *Spermophilus lateralis* typically inhabit moist coniferous forests (Zeveloff 1988). Recent ground squirrel burrowing has resulted in considerable bioturbation at the Merrell Locality.

Spermophilus lateralis is a common ground squirrel found in the area today. *Spermophilus richardsonii* may also be a local resident at the present time. There is a possibility that a population of *Spermophilus townsendii* could reach as far north as the Centennial Valley as well. In Montana, *Spermophilus lateralis* is known from the Late Wisconsinan at False Cougar Cave, while *Spermophilus richardsonii* has been recovered from False Cougar Cave and Warm Springs #1. Other species of *Spermophilus* are also known from False Cougar Cave (FAUNMAP 1994).

Family Castoridae (beavers)
Genus *Castor* (beaver)
Castor canadensis (beaver)

Referred specimen: UMT 10035, a right p4.

Remarks: The size and morphology of the p4 from Merrell is indistinguishable from modern specimens of *Castor canadensis* in the collections of the University of Montana Zoology Museum.

Beaver live in the region today. In general, they are found wherever permanent water and enough woody vegetation is present. They have a great capacity for modifying their environment. Whenever moving into an area where water depth is not sufficient, they build dams across streams, where possible, using logs, sticks, and mud. The deep water serves a number of functions. Deep water protects lodges and bank dens, facilitates movement of food and building materials, and provides a greater area for swimming during winter when the water surface may become ice-covered. Also, flooding caused by damming saturates a large area of surrounding soil, a condition conducive to growth of favorite food items such as willow, aspen, alder, and cottonwood. Many other plant species are also eaten, such as grasses in summer. Beaver ponds attract a wide range of wildlife, including waterfowl, fish, muskrats, and others (Zeveloff 1988).

In the fossil record of the region, *Castor canadensis* is known from Late Wisconsinan sites at Rainbow Beach and the Dam Local Fauna in Idaho and the Little Box Elder Cave and Little Canyon Creek Cave in Wyoming (FAUNMAP 1994).

Order Carnivora (carnivores)
Family Canidae (canids, i.e., dogs)
Genus *Canis* (wolves, jackals, coyotes, domestic dog)
Canis latrans (coyote)
Figure 86

Referred specimen: MOR LI95.2.309, a right p4.

Remarks: MOR LI95.2.309 has a well-developed second cusplet, a third cusplet present, and a posteromedial cingulum. The specimen is 13.5 mm in length and 6.1 mm wide. It was compared with modern specimens of *Canis latrans* and *Canis lupus*. In general size, the specimen falls within the range of variation of nine specimens of *Canis latrans* in the UMZM; size range of the nine UMZM specimens, length 8.2-13.8 mm, width 4.7-6.7 mm. It is smaller than five specimens of *Canis lupus* in the UMZM; size range of the five UMZM specimens, length 15.8-17.6 mm, width 7.4-8.7 mm. In a comparison between *Canis latrans* and *Canis lupus*, the p4 of *Canis lupus* has more reduced cusplets, more ofren lacking a well-developed third cusplet and posteromedial cingulum. The p4 of *Canis latrans* has a second

cusplet, usually a pronounced third cusplet, and a posteromedial cingulum extending behind the third cusplet (Nowak 1979). Based on these characters, the Merrell p4 compares best with *Canis latrans.*

In general, Pleistocene coyotes are larger than modern specimens, although by Late Wisconsinan time they approach the size of the Recent forms (Kurtén and Anderson 1980). The species is one of the most common carnivores in the North American Late Pleistocene, recovered from around 100 localities, about a dozen of which are nearby in Idaho and Wyoming (Figure 86) (Nowak 1979). Late Wisconsinan occurrences are Jaguar Cave, Rainbow Beach, and the Dam Local Fauna in Idaho and Little Box Elder Cave in Wyoming (FAUNMAP 1994).

Today, the coyote continues to be a wide-ranging species, occupying most of North America and living in a variety of habitats (Jones and Birney 1988). They most often occupy open grasslands, brush country, and broken forest (Bekoff 1977; Nowak 1991). Coyotes are considered an opportunistic predator with a broad range of food items in the diet. Diet varies seasonally and according to geographic location, although 90 percent of food items are mammals, particularly rodents and rabbits. Large animals can be important in the winter diet and plant material may be an important dietary component. Scavenging is not uncommon (Bekoff 1977).

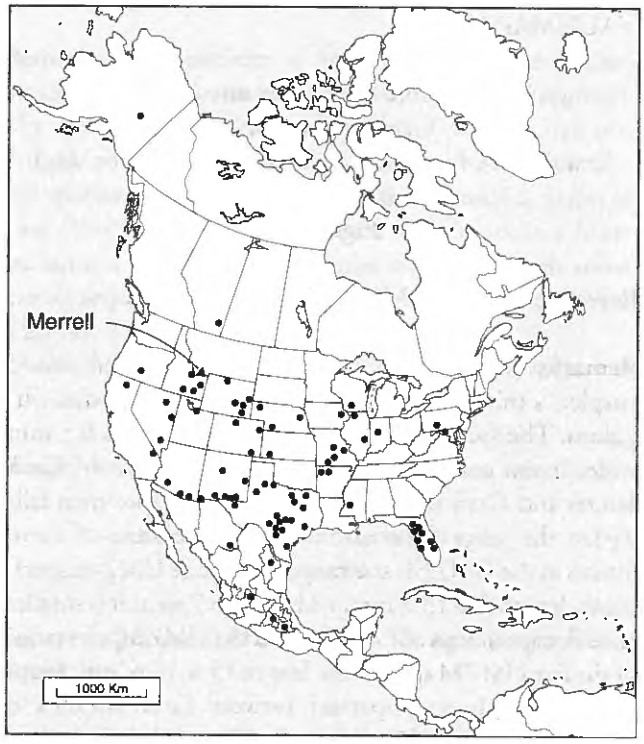

Figure 86. Late Pleistocene occurrences of coyote (after FAUNMAP).

Canis lupus (gray or timber wolf)
Figure 87

Referred specimen: MOR LI94.5.130, proximal half of a right metatarsal 3.

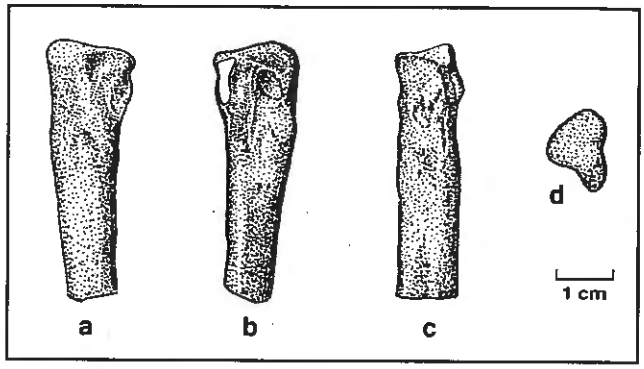

Figure 87. Gray or timber wolf (*Canis lupus*) (MOR LI 94.5.130) proximal half of a rt. metatarsal 3: a, medial; b, lateral; c, posterior; and d, proximal views.

Remarks: MOR LI94.5.130 compares very well in size to *Canis lupus* specimen UMZM 17652. The metapodials of *Canis lupus* are considerably larger than *Canis latrans.* The specimen does not generally compare well to *Canis dirus* in size. *Canis dirus* postcranial elements are more robust than *Canis lupus.* MOR LI94.5.130 is not out of the size range for known *Canis dirus,* but would be on the small end of the size range (e.g., Kisko 1967). The small end of the size range for dire wolf skeletal elements is represented mainly by specimens from southern dire wolf populations. Given that the MOR metatarsal compares extremely well in size to local gray wolf specimens, and in areas where *Canis dirus* and *Canis lupus* co-occur the dire wolf specimens are more robust, it seems highly unlikely that MOR LI94.5.130 could represent a specimen of *Canis dirus.* However, *Canis lupus* and *Canis dirus* likely co-occurred in the area, because a specimen of dire wolf is known from nearby Orr Cave in Beaverhead County, Montana (Kurtén 1984). *Canis lupus* is geographically widespread and occurs at over 50 localities of Late Pleistocene age in North America (Figure 88) (Nowak 1979). Late Wisconsinan occurrences in the region are Little Box Elder Cave and Prospects Shelter in Wyoming. Regional "Late-Glacial" records include Jaguar Cave, Idaho, and Agate Basin and Natural Trap Cave, Wyoming (FAUNMAP 1994). The species occupies a broad range of habitats, most commonly arctic tundra, steppe, savannah, and forests (Nowak 1991). Today, the gray wolf is one of North America's top predators, feeding primarily on deer, elk, caribou, moose, and bison (Zeveloff 1988).

Figure 88. Late Pleistocene occurrences of gray or timber wolf (after FAUNMAP).

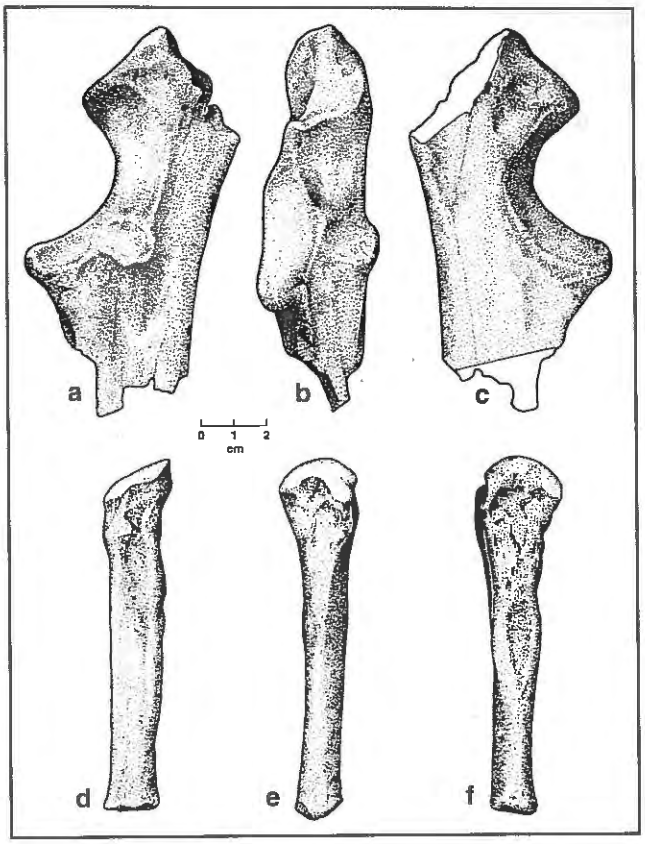

Figure 89. Scimitar cat (*Homotherium serum*) (UMT 100002): (a-c) proximal lft. ulna; and (d-f) lft. metacarpal 4.

Family Felidae (cats)
Genus *Homotherium* (Scimitar cats)
Homotherium serum (Scimitar cat)
Figures (89-90)

Referred specimens: UMT 10001, proximal left ulna; UMT 10002, left metacarpal 4.

Remarks: These two specimens of *Homotherium serum*, recovered from unprovenienced beach collections by the University of Montana field crew in 1989, were described by Dundas (1992). A sample of UMT 10001, a proximal left ulna, was submitted to Beta Analytic for radiocarbon dating; however, the specimen lacked datable protein (Les Davis, pers. comm., 1997).

One of the most significant discoveries among the faunal remains, this species is rare in the Pleistocene of North America, and this represents its first record in Montana. *Homotherium serum* is known from 18 Rancholabrean-age sites (Figure 90), the closest occurrences being at the Duck Point and American Falls localities in Idaho (Jefferson and Tejada-Flores 1993). Consistent with most records of *Homotherium* (Jefferson and Tejada-Flores 1993), the Merrell specimens represent one individual.

Figure 90. Late Pleistocene occurrences of Scimitar cat (after FAUNMAP).

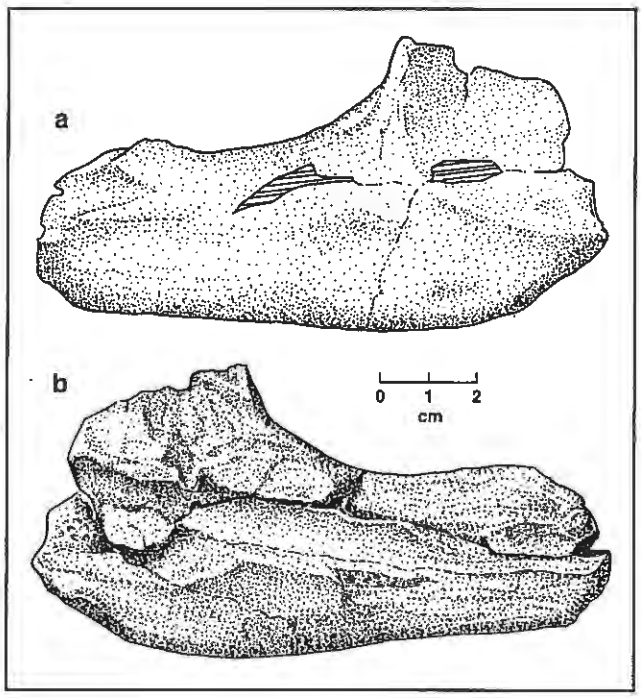

Figure 91. Bear (*Ursus* sp.) (UMT 10050) lft. dentary fragment: a, lateral and b, medial views.

Family Ursidae (bears)
Ursus sp.
Figure 91

Referred specimen: UMT 10050, left dentary fragment.

Remarks: An earlier referral of the dentary fragment to *Ursus americanus* (Dundas 1992; Dundas, Hill, and Batten 1996) was based on a comparison of only a couple of specimens. Examination of over two dozen mandibles of *Ursus arctos* (Grizzly bear) and *Ursus americanus* (American black bear) in the collections of the University of Montana Museum of Zoology indicates that diagnostic characters necessary to identify the specimen to species are lacking. The specimen is, therefore, referred to *Ursus* sp.

Order Artiodactyla (artiodactyls)
Family Antilocapridae (pronghorns)
cf. *Antilocapra americana* (American pronghorn)

Referred specimens: UMT 10049, pelvic fragment; MOR LI94.5.456, proximal end of a proximal phalange; MOR LI95.2.537, proximal phalange.

Remarks: MOR LI95.2.537, a proximal phalange, compares well with *Antilocapra americana* specimen UMZM 4027, although the Merrell specimen is slightly larger. Pronghorn occupy grassland habitat (Jones and Birney 1988). The species occurs in the area today (Zeveloff 1988). Not surprisingly, considering the species distribution, it is found at several late Wisconsinan sites in the region, including Rainbow Beach, Owl Cave, and the Dam Local Fauna in Idaho and Horned Owl Cave, Little Box Elder Cave, Prospects Shelter, and Natural Trap Cave in Wyoming. Other "Late-Glacial" sites in Wyoming include Agate Basin, Colby, and Sheaman (FAUNMAP 1994).

Family Cervidae (deer)
Genus and Species indeterminate (large cervid)

Referred specimens: MOR LI94.5.455, left i1 or i2; MOR LI94.5.457, deciduous lower left molariform tooth.

Remarks: MOR LI94.5.455, a lower incisor, compares well with *Cervus elaphus*, but is rather small for elk. The specimen also compares well with some specimens of *Odocoileus*, but is large for this genus of cervid. MOR LI94.5.457, a deciduous lower molariform tooth, was compared with the deciduous dentitions of specimens of *Cervus elaphus* (elk) and *Alces alces* (moose). The variation in the deciduous dentition of both of these large cervids is great enough to preclude assignment of the Merrell specimen to a genus. Both specimens are best identified as being referred to as Cervidae, albeit from large cervids.

cf. *Ococoileus* sp. (white-tail or mule deer)

Referred specimen: MOR uncat. (MS-685, EN-2), proximal phalange.

Remarks: The proximal phalange compares well with UMZM 4945, a proximal phalange of *Odocoileus hemionus* (mule deer). Deer occupy a variety of habitats from brushy, wooded areas to open plains. Both species of *Odocoileus* occur in the area today (Zeveloff 1988). *Odocoileus hemionus* is known from several Late Wisconsinan sites in Wyoming, including Horned Owl Cave, Little Box Elder Cave, and Little Canyon Creek Cave. The known Wisconsinan-age fossil record of the two species of *Odocoileus* is poor for the region (FAUNMAP 1994).

Family Bovidae (bovids)
Bison sp. (bison)
Figures 92-94

Referred specimens: UMT 10013, partial lower right m3; UMT 10032, proximal phalange; UMT 10064, partial left radius/ulna diaphysis; UMT 10071, distal end of a

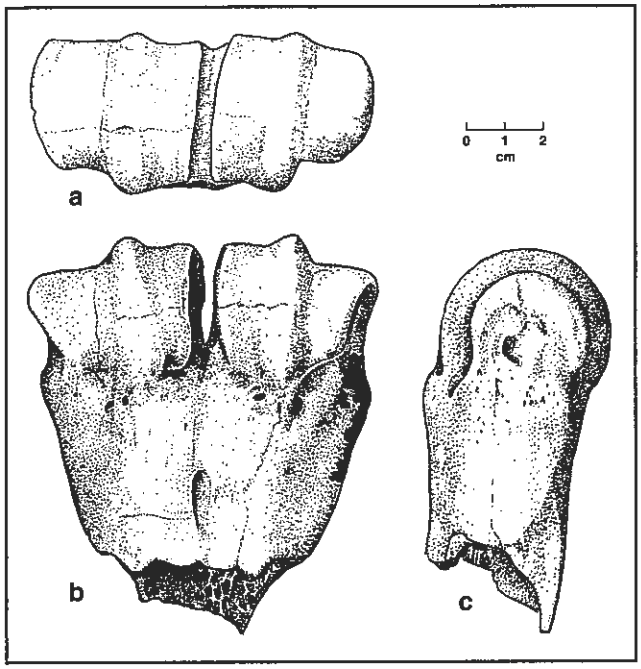

Figure 92. Bison (*Bison* sp.) (UMT 10071) distal end of metapodial: a, distal; b, anterior; and c, side views.

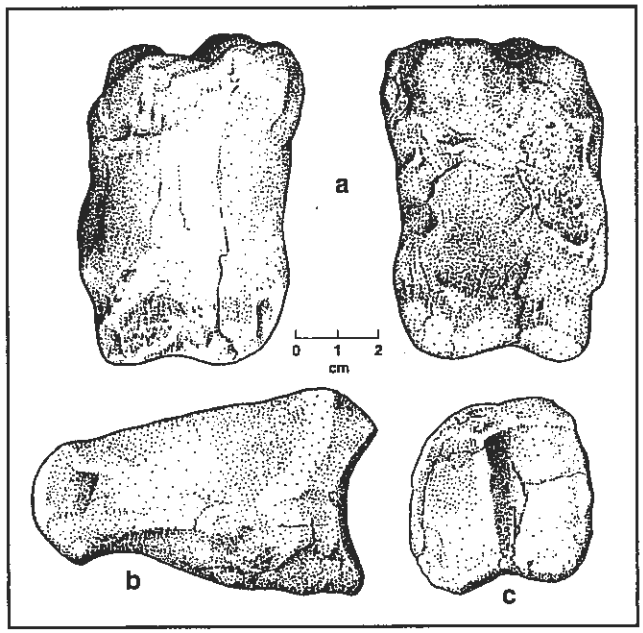

Figure 93. Bison (*Bison* sp.) (UMT 10032) proximal phalange: a, anterior and posterior views; b, side; and c, proximal views.

metapodial; MOR LI91.1.3, naviculocuboid; MOR LI91.1.5, partial proximal end of a metacarpal 3/4; MOR LI93.2.1, partial left innominate; MOR LI94.5.458, tooth fragment; MOR LI94.5.460, left medial phalange; MOR LI94.5.462, proximal end of a right ulna; MOR

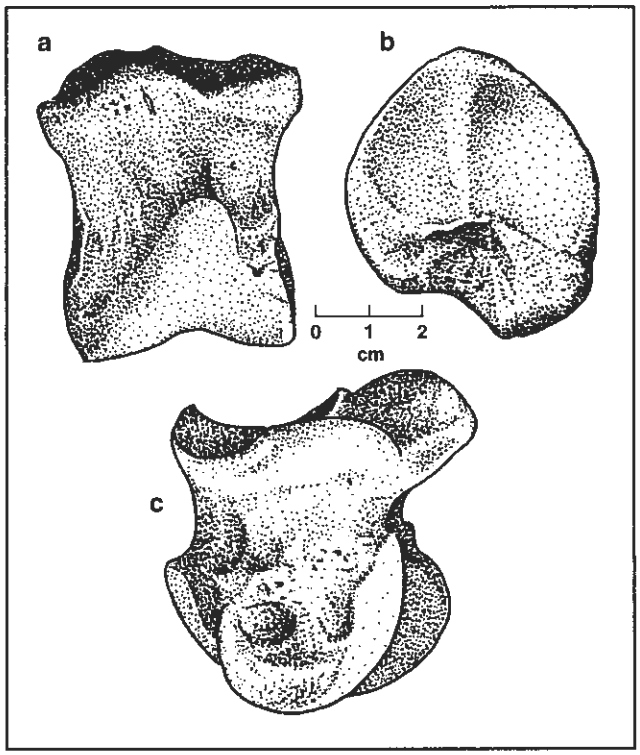

Figure 94. Bison (*Bison* sp.) (MOR LI 94.5.460) medial phalange: a, posterior; b, lft. proximal; and c, side views.

LI95.2.535, proximal phalange; MOR L191.1.3 (MS-562, BLM#27), right scaphoid.

Remarks: UMT 10032 is a proximal phalange missing the proximal epiphysis. The specimen is clearly from a juvenile. The remainder of the material is from adult animals.

Bison are grazers that occupy mainly open, grassland habitat in North America. They occasionally use forested areas, particularly for shade and feeding when the snow is too deep (Zeveloff 1988). Bison occurred in the area up into historic time before populations were reduced dramatically and the species nearly became extinct in the late 1800s (Zeveloff 1988). In the fossil record, bison are known from many Wisconsinan sites in the region (FAUNMAP 1994).

Family Camelidae (camels)
Camelops sp. (large camel)
Figure 95

Referred specimens: UMT 10020, left partial dentary with m3; MOR LI94.5.86, tooth fragment consisting of the buccal side of an M2 or M3; MOR LI94.5.459, distal end of a proximal phalange; MOR LI94.5.461, proximal epiphysis of a proximal phalange.

Remarks: Morphologically, UMT 10020, a left dentary fragment with m3, compares well with Rancho La Brea specimens of *Camelops hesternus* in the collections of the University of California Museum of Paleontology (Berkeley). *Camelops* was also reported from the Late Wisconsinan Flint Creek site, Montana (Dundas 1991). Nearby Late Wisconsinan occurrences in Idaho include Jaguar Cave, Dam Local Fauna, and Rainbow Beach (FAUNMAP 1994).

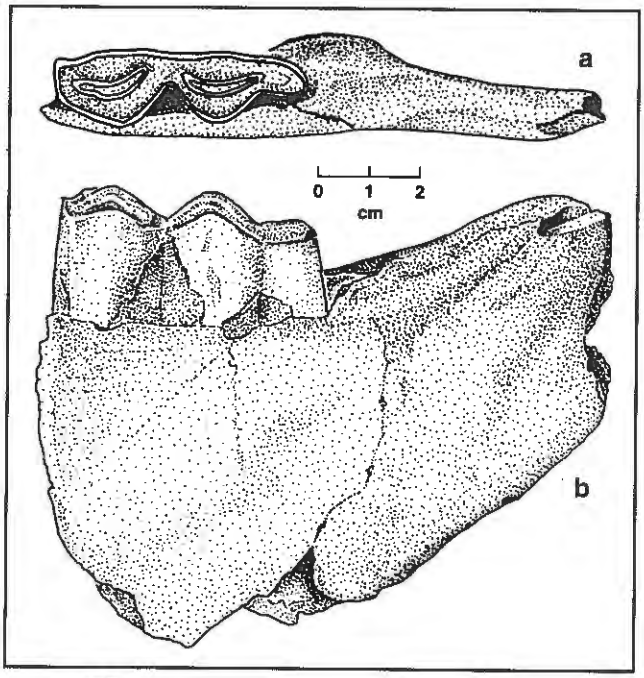

Figure 95. *Camelops hesternus* partial lft. dentary with m3: a, occlusal; and b, buccal views.

Order Perissodactyla (perissodactyls)
Family Equidae (horses)
Equus sp. (horse)

Referred specimens: UMT 10023, lower molariform tooth, not the p2 or m3; UMT 10039, lower right molariform tooth, not the p2 or m3; UMT 10043, partially erupted lower right molariform tooth; UMT 10048, left cuneiform; UMT 10051, partial distal phalanx; UMT 10062, lower right molariform tooth, not the p2 or m3; MOR LI91.1.4, partial right navicular; MOR LI91.1.6, partial medial phalange; MOR LI93.2.2, partial left innominate; MOR LI94.5.119, left trapezium; MOR LI94.5.185, proximal sesamoid of pes; MOR LI95.2.23, distal end of a proximal phalange; MOR LI95.2.106, left half of a medial phalange; MOR LI95.2.134, medial phalange; MOR LI95.2.155, unerupted partial upper left molariform tooth, not the P2 or M3; MOR LI95.2.162, mandibular symphysis with alveoli for right i1, i2, i3, and left i1; MOR LI96.4.96, right upper molariform tooth, not the P2 or M3; MOR LI96.4.191, distal half of a radius.

Remarks: Both adult and juvenile horse material is represented. No attempt is made here to assign this material to a species, for two reasons. First, the material is of limited value taxonomically, not possessing diagnostic characters necessary for species identification. Second, given the current state of confusion concerning the species level taxonomy of the genus *Equus*, little value exists in assigning the material to species.

Equus material is not uncommon in the Late Pleistocene of Montana, although most records are unpublished. In comparison to other Montana sites containing horse, which typically have few specimens, a considerable collection of *Equus* material was recovered from the Flint Creek site (Dundas 1991).

Order Proboscidea (proboscideans)
Family Elephantidae (elephants)
Genus *Mammuthus* (mammoths)
Mammuthus columbi (Columbian mammoth)
Figures 96-97

Referred specimens: UMT 10019, left metatarsal 3; UMT 10027, fibula; UMT 10028, patella; UMT 10029, right metatarsal 3; UMT 10038, partial lower right m3; UMT 10052, proximal end of a left scapula; UMT 10054, right tibia; UMT 10055, left metacarpal 5; UMT 10056, right magnum; UMT 10057, right metacarpal (4?); UMT 10059, right cuboid; UMT 10060, proximal phalange; UMT 10061, right metacarpal 1; UMT 10065, left cuneiform; UMT 10066, proximal phalange of digit 3; UMT 10067, proximal phalange; UMT 10068, proximal phalange of digit 5; UMT 10069, proximal phalange; UMT 10070, right lunar; UMT 10072, left metacarpal 2; UMT 10075, partial left magnum; UMT 10076, partial right magnum; UMT 10077, right ectocuneiform; UMT 10078, partial right navicular; UMT 10079, partial left unciform; UMT 10080, partial right calcaneum; UMT 10083, atlas; UMT 10085, medial phalange; MOR LI94.5.98, phalange; MOR LI94.5.100, tooth; MOR LI94.5.114, metapodial missing the proximal end; MOR LI94.5.115, ?left metacarpal 5; MOR LI94.5.120, proximal phalange; MOR LI94.5.134, basicranial fragment with one occipital condyle; MOR LI94.5.363, proximal phalange; MOR LI94.450, partial tooth; MOR LI94.5.451, partial tooth; MOR LI94.5.541, partial tooth; MOR LI95.2.118, proximal end of a left ulna; MOR LI95.2.140, partial innomi-

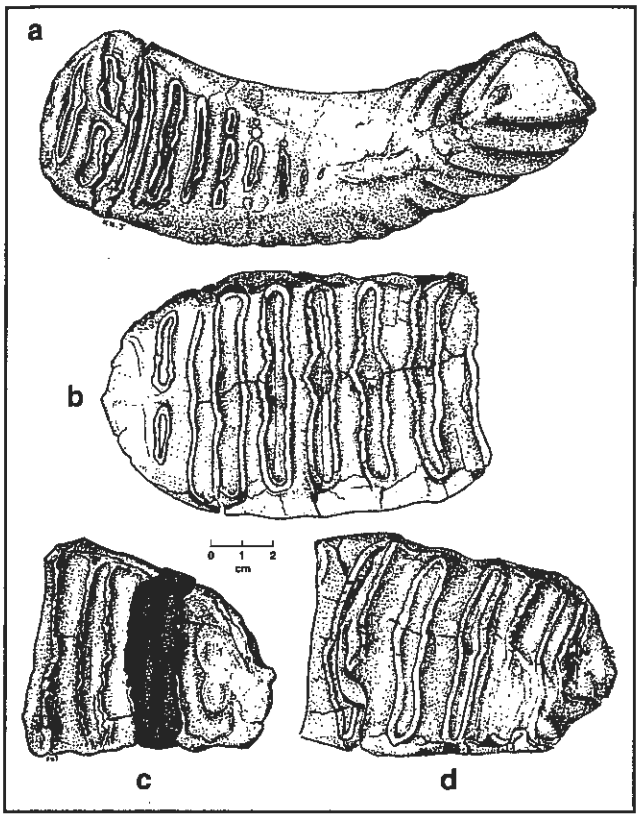

Figure 96. Occlusal surfaces of Columbian mammoth (*Mammuthus columbi*): a, MOR LI 94.5.100; (b-c), MOR LI94.5.450-452.

nate, mostly the ilium; MOR LI95.2.156, distal phalange; MOR LI96.4.63, right navicular; MOR LI96.4.90, proximal end of a left scapula; MOR LI96.4.91, metapodial; MOR LI96.4.95, phalange; MOR LI96.4.99, left astragalus; MOR LI96.4.182, right calcaneum; MOR LI96.4.183, right astragalus; MOR LI96.4.184, left metatarsal 5; MOR LI96.4.185, right metatarsal 3; MOR LI96.4.186, left metatarsal 4; MOR LI96.4.187, sesamoid; MOR LI96.4.188, right metatarsal 1; MOR LI96.4.189, distal phalange; MOR LI96.4.192, right metatarsal 4; MOR LI96.4.193, left calcaneum.

Remarks: UMT 10029 is a right metatarsal 3 with an unfused distal epiphysis, suggesting a subadult. Nearly all of the identifiable mammoth remains appears to be from adults. UMT 10027, a fibula, was radiocarbon dated.

There is some disagreement regarding North American mammoth taxonomy (Maglio 1973; Kurtén and Anderson 1980; Graham 1986; Agenbroad and Barton 1991) and, until a comprehensive revision is undertaken and a general consensus reached, it is particularly important to cite which taxonomy is being used. Here, the taxonomy follows Maglio (1973). Dental measurements were taken using procedures outlined by Maglio (1973).

Several partial teeth from Merrell allow some consideration to be given to species identification. Plate count, enamel thickness, and lamellar frequency are reported for the following specimens, where possible:

UMT 10038 - The anterior part of the lower right m3 is broken off. The remainder of UMT 10038 consists of 15 total plates, 11 of which are in wear. The enamel thickness is 2-2.8 mm, and the lamellar frequency is seven.

MOR LI94.5.100- 20 plates, 11 of which are in wear; enamel thickness of 2 mm; lamellar frequency of 6.

MOR LI94.5.450- a molar fragment with 5.5 plates. Enamel thickness is 2 mm.

MOR LI94.5.451- a molar fragment with 4 plates. Enamel thickness is 1.5 mm.

MOR LI94.5.452- a molar fragment with 7 plates. Enamel thickness is 2 mm.

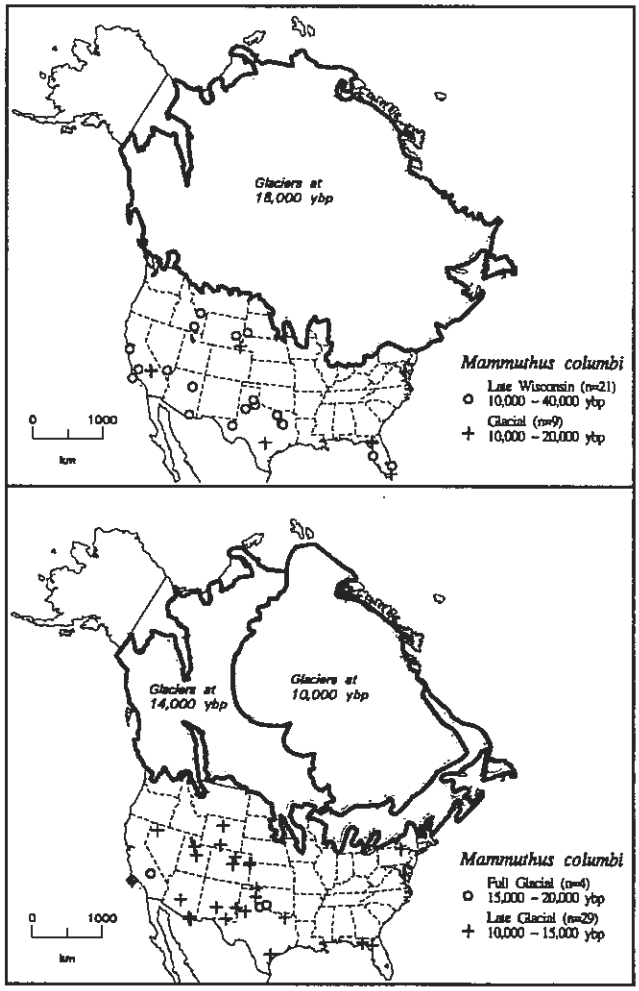

Figure 97. Columbian mammoth (*Mammuthus columbi*) distribution relative to Pleistocene glaciation.

Table 9. Comparison of Lamellar Frequency, Enamel Thickness, and Plates Per Tooth Between *M. columbi* Variants.

Characteristics	*M. columbi* (typical form)	*M. columbi* (derived form)	*M. primigenius*
lamellar frequency (lophs per 100 mm)	5-7	7-9	7-12
enamel thickness	2.0-3.0 mm	1.5-2.0 mm	1.0-2.0 mm
plates per tooth	20-24	24-30	20-27

Unfortunately, most of the Merrell mammoth teeth are incomplete. As a result, the characteristic of plates per tooth is of little value here. Maglio (1973) recognized two Late Pleistocene species of mammoth in North America: *Mammuthus columbi* (Columbian mammoth) and *Mammuthus primigenius* (Woolly mammoth). Maglio further recognized what he termed a "typical form" and a "derived form" of Columbian mammoth. The characteristics used to distinguish the species listed below are based on the 3rd molar.

Considering the Merrell material, the lamellar frequency of 6-7 and enamel thickness ranging from 1.5-2.8 mm support the assignment of these specimens to *Mammuthus columbi* (Table 9).

Discussion

The Merrell fauna is comprised of 21 taxa, of which 15 are mammals. Although many members of the fauna currently live in the area, several became extinct in North America near the end of the Pleistocene, including *Homotherium serum*, *Camelops*, *Equus*, and *Mammuthus columbi*. In regard to minimum number of individuals, all vertebrate species at the Merrell Site are represented by a minimum of one individual, except for *Bison* sp., *Equus* sp., and *Mammuthus columbi*. At least two *Bison* are represented; a juvenile is present while the remainder of the material is adult. Likewise, *Equus* is represented by a minimum of two individuals, based on partially erupted dentition indicating a young animal, while most of the material is adult. Probably more than two individuals are represented based on stratigraphic location of the juvenile dentitions. Mammoth is the most abundant material at Merrell. However, determining a minimum number of individuals based on the fragmentary nature of many of the specimens probably underestimates the actual number of individuals. Nevertheless, at least three individuals of mammoth are present, two adults and one subadult (or juvenile).

In general, discussion of faunules at the Merrell Site is not possible, in part, due to the considerable bioturbation present at the site. However, considering the five stratigraphic units at Merrell, the faunal remains were recovered from deposits of at least two ages. Specimens from the debris flow (stratum D), on the north end of the site, date to ca. 27,000 BP and 22,000 BP. Remains from stratum B (and upper stratum A) are dated to ca. 40,000 BP (Hill, this report: Table 9).

Several members of the fauna are indicative of a perennial, slow-moving water body in the area. The swan, duck, muskrat, and beaver all suggest a stream, marsh, or lake setting.

The sedimentary sequence contains a variety of fossil remains (cf. Dundas 1992). A list of the vertebrate fauna recovered from the Merrell Locality is presented as Table 8. The materials studied by Dundas were collected by a team directed by Foor in 1989 and were initially conserved in the University of Montana Museum of Paleontology vertebrate collections (Dundas 1992:9). Mammoth remains are present in both the stratum B (LL2) and stratum D deposits (Albanese, this report and Hill, this report). Bones were also observed in the uppermost part of and on the top of stratum A (along its boundary with stratum B). Other vertebrate remains that are biostratigraphic time markers include a Pleistocene variant of horse, Yesterday's camel, and Scimitar cat.

Invertebrates

Christopher L. Hill

Invertebrate fossils include molluscs and ostracods. Fragments of gastropods and bivalves were recovered from the uppermost part of stratum B (LL2e, Figure 6). Intact gastropods and ostracods were recovered from LL3a (Figure 6). Fragments of molluscs and ostracods occur throughout the upper sections of strata C and D. Bump (1989) reports the presence of four genera of gastropods and a bivalve genus from the sediments containing and overlying the vertebrate remains. All are associated with aquatic habitats, including stream settings or ponds.

Pollen and Algae

James K. Huber

Description

Three sediment samples from the Merrell Site were analyzed for pollen (Huber 1995; Huber and Hill 1997). The pollen spectra from the site indicate the presence of an open conifer parkland in the vicinity of the Merrell Site prior to the Last Glacial Maximum. Algae from the samples indicate an increase in nutrient influx to the basin and a change in the depositional environment through time.

Introduction

Palynology, the study of pollen and spores and their dispersal, is a primary tool for paleoecologists. Palynological data from bogs, marshes, and lakes are important in establishing past vegetational and climatic records (Kapp 1969; Faegri and Iverson 1975; Moore and Webb 1978). In recent years, however, paleontologists and archaeologists have realized the importance of palynological investigations as part of multidisciplinary paleontological and archaeological studies. The correlation of stratigraphically continuous pollen data with paleontological and archaeological sites in the same area may yield valuable paleoenvironmental reconstructions for sites (King 1973, 1985). Changes in both local and regional vegetation, as well as climate, may be very important in the interpretation of archaeological data (King 1985).

In the past, paleoecological investigations have relied heavily on pollen as a primary indicator of environmental change. Plant macrofossils have also been used in conjunction with pollen studies (Van Zant 1976, 1979; Watts and Bright 1968; Watts and Winter 1966). In subsequent years, more emphasis has been placed on the increased use of other organisms as paleoecological and paleoclimatic indicators (Williams 1981); among these organisms are algae (Van Geel 1986).

Previous subfossil algae studies have concentrated on *Pediastrum* associated with pollen. They were usually identified only to the genus level and presented as a percentage distribution of total *Pediastrum* (Cronberg 1986). However, *Pediastrum* are readily preserved in sediments and can be easily identified to the species level. They can also survive rigorous pollen extraction techniques (Cronberg 1986). In addition to *Pediastrum*; *Scenedesmus*, *Botryococcus*, and numerous other taxa of nonsiliceous algae can be recognized in subfossil records. Subfossil nonsiliceous algae found in conjunction with pollen can aid in paleoecological reconstructions (Cronberg 1986).

The objectives of this study were to assess palynomorph abundance and preservation at the Merrell Site and to provide information regarding the vegetational history of the area during deposition of the mammoth remains.

Palynomorph Analytical Methods

Three samples were analyzed for pollen and other palynomorphs. The pollen samples were treated with a modified Faegri and Iverson (1975) technique (addition of KOH, HCl, HF, and acetolysis), sieved through 7μ Nitex screens (Cwynar, Burden, and McAndrews 1979), stained with safranin, and stored in silicone oil for counting. In addition, one standard *Eucalyptus* tablet was added to each sample in order to determine pollen concentration values (Maher 1972).

Grains of trees, shrubs, herbs, and vascular cryptogams were identified and counted within the pollen sum. Indeterminable, unknown and aquatic pollen, nonsiliceous algae, and *Eucalyptus* spike grains were counted, but not included in the pollen sum. As a result of the extremely large abundance of Chrysophyte algae, their total number was estimated after counting three transects based on the proportion of *Eucalyptus* grains counted in three transects versus the whole slide. Pollen abundance is very low in the samples. Therefore, all palynomorphs encountered on each slide were identified and counted. The pollen sums for samples E94-3 (85 grains) and E94-4 (90 grains) are low and are not as statistically valid as the pollen sum for sample E94-6 (315 grains). Although the pollen sums are low, the pollen data do provide an indication of the vegetation in the area during the time of deposition. After completing each count, the microscope slide was then sealed and placed on permanent file at the Archaeometry Laboratory, where original copies of the pollen count sheets are also on file.

Pollen and spores were identified using keys in Maloney (1961), Kapp (1969), and McAndrews, Berti, and Norris (1973), and by comparison to the pollen reference collection at the Archaeometry Laboratory, University of Minnesota, Duluth. Algae were identified using keys in Prescott (1982) and Van Geel (1986).

Identifications were made to the lowest taxonomic level possible. The degree of certainty of identification for some taxa is indicated by the use of "type." The use of "type"

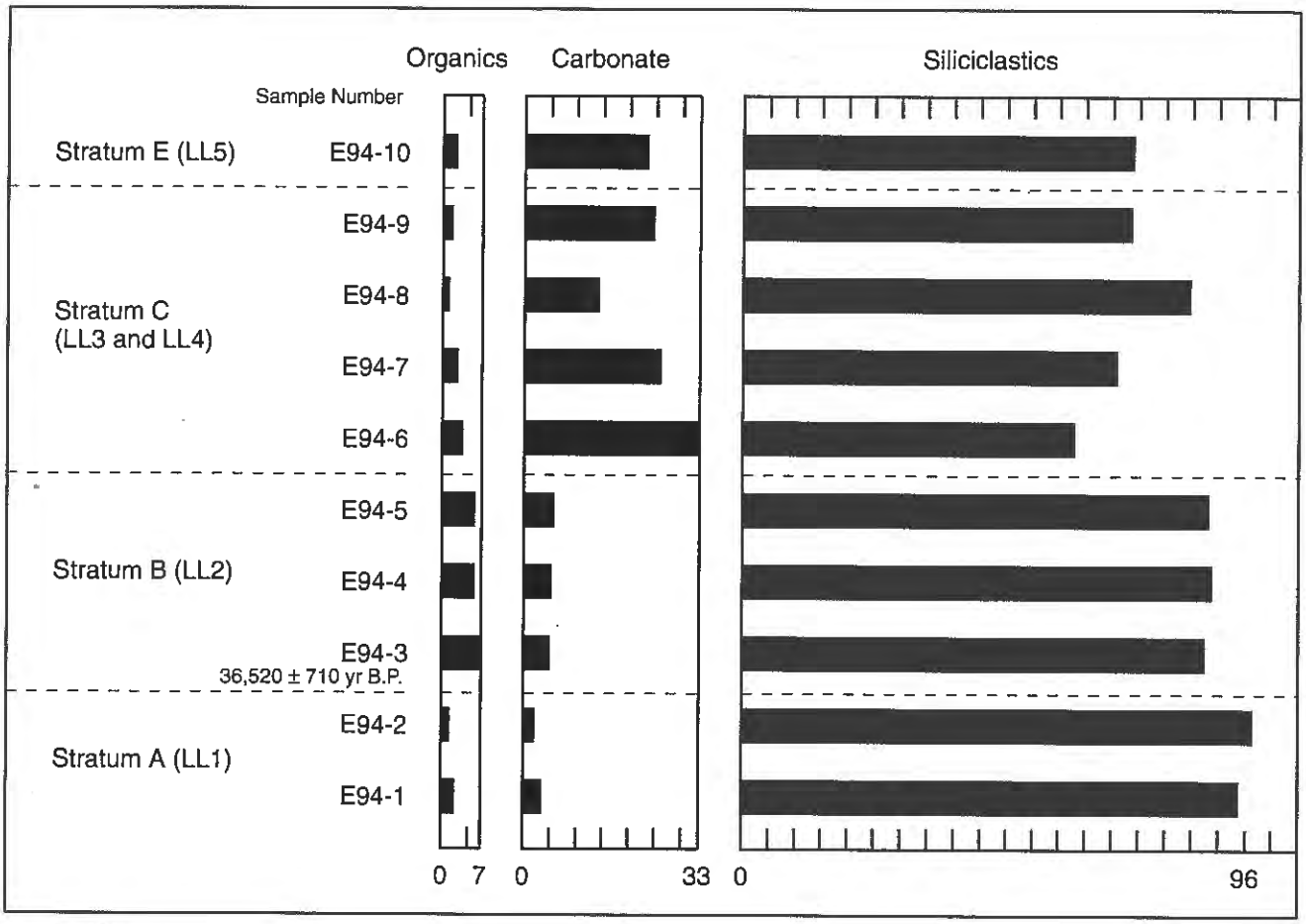

Figure 98. Results of Thermal Analysis (Loss-On-Ignition).

indicates that the taxon matches not only that taxon, but others also (Watts and Winter 1966). Indeterminable pollen grains were divided into five categories, as proposed by Cushing (1967): broken, concealed, corroded, crumpled, and degraded. Well-preserved pollen grains and macrofossils that were not identified are expressed simply as unknowns.

Loss-on-Ignition of Organic and Carbonate Carbon Methods

In order to obtain a more complete understanding of the depositional record, loss-on-ignition of organic carbon and carbonate was undertaken on 10 sediment samples from the Merrell Site. Organic carbon and carbonate content provide an independent means of interpreting the stratigraphic sequence which, in turn, can be correlated with the pollen assemblages. Changes in the carbonate and organic carbon content of sediment may also indicate environmental changes that occurred in the watershed and the catchment basin through time. This information can be used to reconstruct past paleoenvironmental conditions.

The Merrell Site samples were analyzed following Dean's (1974) loss-on-ignition technique. Samples were dried at 105°C to determine dry weight. Percent loss-on-ignition was determined by combustion at 550°C for 1 hr for organic carbon and at 1,000°C for 1 hr for carbonate content.

Results

Organic carbon content in all of the Merrell Site samples is low, 7.8 percent or less. Organic carbon varies from 1.8 percent to 6.4 percent in the samples analyzed for pollen (Figure 98). Carbonate content is low in the lower one-half of the sequence, with values ranging from 3.6 percent to 5.5 percent (Figure 98). In the upper one-half of the sequence, carbonate content ranges from 14.2 percent to 33 percent (Figure 98).

The low organic carbon content in the lower samples is probably the result of oxidation of organic materials. In the samples analyzed for pollen, most of the indeterminable degraded pollen grains appear to be oxidized, which is consistent with the low organic carbon content. Loss-on-ignition values of less than 5 percent for carbonate may indicate the removal of OH ions from clays between 550 and 1,000°C rather than the presence of carbonates (Dean 1974).

Palynomorphs

The pollen in the three samples is fairly well-preserved. In sample E94-6, pollen is moderately abundant. However, in samples E94-3 and E94-4, pollen is scarce. Therefore, the data from these two samples are less statistically valid than for sample E94-6. Pollen concentration is moderate for sample E94-6 (572,890 grains/grams of dry sediment) and low in samples E94-4 (163,683 grains/gram of dry sediment) and E94-3 (154,590 grains/gram of dry sediment).

The pollen sum varied from 85 to 315 grains/slide. Within the pollen sum, 18 taxa are represented and the number of taxa/sample ranged from eight to 16 (Figure 99). Aquatics are represented by four taxa. Indeterminable pollen consists of degraded, crumpled, and broken grains. Algae are divided into two categories. One category, designated as algae, is composed of all algae identified and counted except for Chrysophytes (eight taxa). The other category, Chrysophycophyta, is composed of only Chrysophytes. Chrysophytes are golden-brown algae (Lee 1980). Only one taxon of fungus was identified and counted. The total number of different taxa identified and counted is 36.

The Merrell Site pollen spectra from samples E94-3 and E94-4 are characterized by a dominance of *Picea*, *Pinus*, and Cupressaceae. The most abundant nonarboreal pollen (NAP) types in these two samples are Cyperaceae, Gramineae, Chenopodiaceae/Amaranthaceae, *Pteridium*-type, and *Dryopteris*-type (Figure 99). The pollen spectrum from sample E94-6 is dominated by NAP. The composites *Artemisia*, Tubuliflorae, and *Ambrosia*-type, and Cyperaceae, Gramineae, *Pteridium*-type, and *Dryopteris*-type are the dominant NAP types (Figure 99). In sample E94-6, *Picea*, *Pinus*, and Cupressaceae and the shrub, *Salix*, are the prominent arboreal pollen (AP) types (Figure 99).

Three aquatic taxa occur in sample E94-4 and one in E94-6. Indeterminable degraded grains are very common throughout the sequence. One fungal hypodia of *Gaeumannomyces* cf. *caricis* occurs in sample E94-4 (Figure 99).

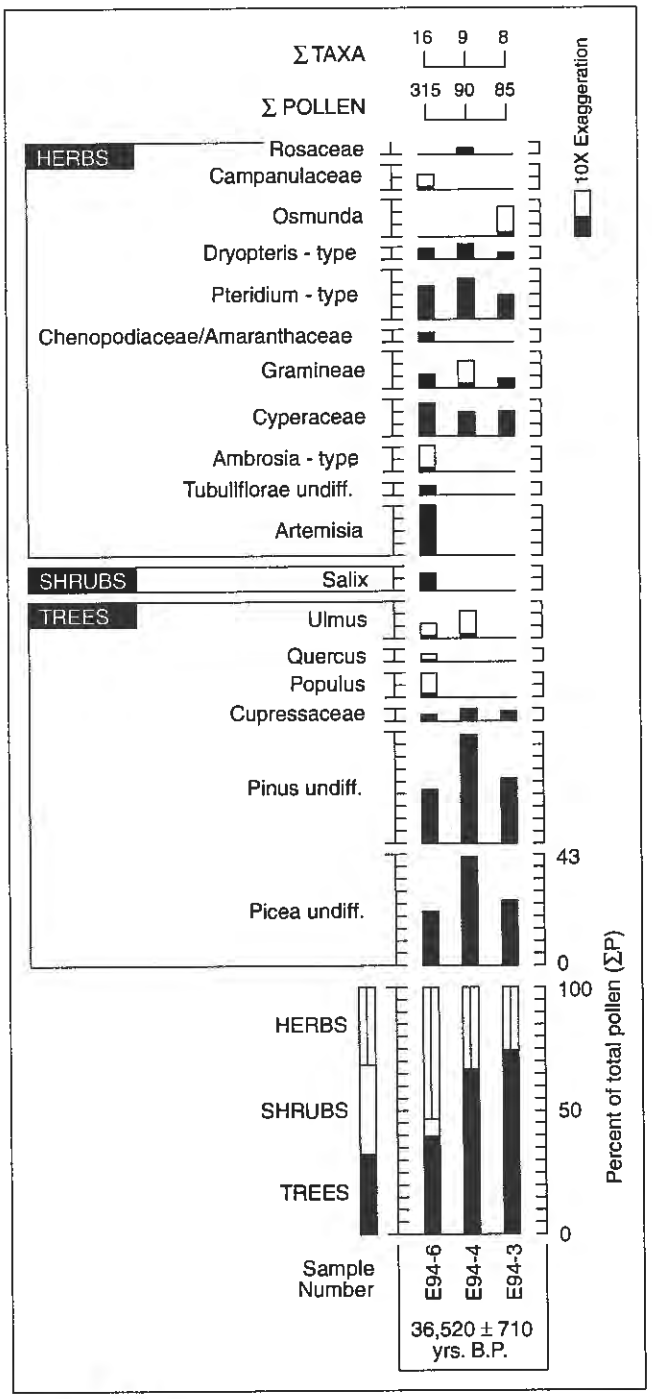

Figure 99. Diagram of pollen frequencies in strata A-C (1994 Test Pit E LL1-3a) (from Huber 1995).

Algae are consistently abundant in all of the samples. The most prominent are *Zygnema*-type resting spores and various species of *Pediastrum*, all green algae (Chlorophycophyta). Chrysophyte algae are extremely abundant in all samples (Figure 99).

Discussion

Based on the moderate pollen preservation and the low pollen concentration in the Merrell Site samples, interpretation of the pollen recovered is tenuous. However, some paleoecological inferences can be made. The abundance of conifer pollen (*Picea*, *Pinus*, and Cupressaceae) and open-ground plants (*Artemisia*, Tubuliflorae, and *Ambrosia*-type, and Cyperaceae, Gramineae, *Pteridium*-type, and *Dryopteris*-type) suggest the presence of an open conifer parkland.

The Merrell Site has a radiocarbon date of 36,520 ± 710 ^{14}C yr B.P. for the interval just above E94-3. At approximately 34,000 B.P., a similar environment, that of an open pine parkland, existed in the western Missouri Ozarks associated with mastodon (King 1973; King and Lindsay 1976).

The presence of the fungal hypodia of *Gaeumannomyces* cf. *caricis* indicates that the sedge is of local origin. Van Geel (1986) reports a correlation between the presence of this fungi and the local appearance of Cyperaceae in peat, indicating that the Cyperaceae pollen is probably from a local source.

Zygnema and *Mougeotia* are indicators of shallow and more or less mesotrophic habitats (Van Geel 1978). *Pediastrum boryanum* is an indicator of lake eutrophication (Cronberg 1982). The decline in *Zygnema* and *Mougeotia* and the increase in *Pediastrum boryanum* apparently suggests an increase in nutrient influx to the basin upward through the sequence. Most species of Chrysophytes occur in soft (calcium-poor), cool freshwaters (Lee 1980). Chrysophyte abundance is highest in samples E94-3 and E94-4, which have low carbonate content. A decrease in Chrysophytes in the E94-6 sample has a high carbonate content, also indicating change in the depositional environment.

Some indication of the ecologic setting associated with strata A (LL1), B (LL2), and the lower part of LL3 can be ascertained from pollen contained within these deposits (Figure 15). Distinct changes in biotic elements may reflect alternating interglacial (or interstadial) and glacial (stadial) conditions. Within the Centennial Valley deposits, there is a trend in declining proportions of tree (arboreal) pollen and increasing amounts of herbs and shrubs (Huber 1995). In the top part of stratum A, which is older than ca. 37,000 yr ^{14}C B.P., tree pollen is about 75 percent of the total pollen. About 45 percent of the pollen is *Pinus* (pine). About 25 percent is *Picea* (spruce), and about 5 percent is Cupressaceae (cypress family). About 25 percent of the pollen sprectra is composed of herbs. Both Cyperaceae (sedge family) and *Pterdium*-type comprise about 10 percent, while Gramineae (grass family), *Dryopteris*-type, and *Osmunda* are less than 5 percent. Pollen concentrations are low.

In stratum B, dated to ca. 37,000 ^{14}C yr B.P., changes occur in the relative abundance of pollen types, with a trend toward increasing amounts of herbs. Tree pollen still dominates at about 65 percent of total pollen. In contrast to stratum A, *Picea* is relatively more abundant than *Pinus*, and there is a slight increase in the proportion of Cupressaceae. *Ulmus* (elm) appears for the first time, in small amounts. In terms of herb pollen, there is relatively more Peridium-type (ca. 15%) and *Dryopteris*-type. Rosaceae is present only in this deposit. *Osmunda* is absent, and there is a decline in Gramineae. Pollen concentrations are low.

In the lower part of stratum C (LL3a), herbs are the dominant pollen type (>50%) and a form of shrub is also present. There is a large drop in the amount of *Picea* (from ca. 40% in stratum B to ca. 20% in stratum C). There is a small drop in the relative amount of *Pinus* and Cupressaceae, and *Ulmus* remains about constant. *Populus* and *Quercus* (oak) appear for the first time in frequencies of <3 percent. Shrubs are only present in stratum C; *Salix* (post oak) frequencies are >5 percent. The relative increase in herb pollen is partially a result of the introduction of *Artemisia* (ca. 20%), Tubuliforae, *Ambrosia*-type (ragweed), Chenopodiaceae/Amaranthaceae (goosefoot family), and Campanulanceae pollen. There is also a slight increase in the amount of Cyperaceae (>10%) and Gramineae (ca. 5%). Pollen concentration is moderate. It is feasible that this pollen spectra generally indicates a sparse Artemisia steppe or grassland with conifers growing in the foothills or other suitable habitats. Using the *Artemisia*/Graminae ratio as a guide, there is some indication that steppe-like conditions were more prevalent (Mandryk 1990). Climatically, it may have been wetter than today, but generally cold and dry.

Algae are present in sediments from strata A, B, and C (Huber 1995). *Zygnema*-type and *Pediastrum* are the most common.

Interpretation

The presence of conifer pollen in all three deposits (*Picea*, *Pinus*, and Cupressaceae) may imply a wooded setting in the vicinity. Trees were potentially more frequent within the watershed ca. 37,000 ^{14}C yr B.P. (strata A and B), indicating a more closed landscape setting. There may have initially been more pine and later more spruce. Higher amounts of spruce pollen have been interpreted elsewhere as an indication of cooler summer temperatures (Webb et

al. 1993). Cooler conditions reflected by the higher frequencies of *Picea* in stratum B may also be reflected by the presence of Rosaceae which is common in tundra settings. *Ulmus* is introduced in stratum B and *Populus* and *Quercus* are introduced in the basal part of stratum C. *Salix* appears only in stratum C.

Cyperaceae, Gramineae, *Pterdium*-type, and *Dryopteris*-type pollen are present throughout the sequence. *Osmunda* appears only in stratum A and Rosaceae appears only in stratum B. *Artemisia*, Tubuliflorae, *Ambrosia*-type, Chenopodiaceae/Amaranthaceae, and Campanulaceae appear only in the basal part of stratum C. A more open setting is indicated by the presence of more shrubs and herbs in srratum C.

Fluctuations from *Pinus*-dominated to *Artemisia*-dominated pollen spectra, as seen in the stratum A-C sequence, have been used elsewhere in the Rocky Mountains and to the south in the Great Basin to infer changing climatic conditions (Baker and Waln 1985; Mehringer 1985). The *Pinus*-dominated intervals may represent warmer conditions, while the *Artemisia*-dominated periods may be glacial-like conditions. High *Pinus* may be an indication of forested and warmer interstadial conditions. The presence of conifer pollen may suggest a more temperate climate, while more glacial-like conditions result in periglacial or tundra settings too cold for trees (Baker and Waln 1985; Baker 1986). In contrast, to the south of the region, pollen profiles associated with the intervals of deepest pluvial lakes (usually associated with late-glacial transitions) are dominated by conifer pollen, while the interstadial-age sediments contain relatively more non-arboreal pollen consisting mostly of *Artemisia* (Mehringer 1985). In these settings, *Picea* is an important constituent of full-glacial conditions.

East of the Centennial Valley is an Upper Pleistocene record which indicates that interglacial conditions warmer than present were associated with *Pseudotsuga* forests, warm interstadials characterized by *Pinus*, and periods of ice cover associated with tundra conditions (Baker and Waln 1985).

High amounts of pine, such as in stratum A, imply relatively warm conditions (Baker 1986). The presence of high amounts of pine and moderate amounts of spruce and the absence of *Artemisia* probably reflects a relatively closed forest. Some open spaces may be represented by herbs like Cyperaceae and Gramineae. Higher amounts of *Picea*, as seen in stratum B, are indicative of cooler climate. The rise in *Picea* in stratum B may be an indication of the occurrence of a slight cooling. *Artemisia*-dominated settings, as seemingly reflected in stratum C (LL3a), may be open, tundra-like landscapes such as those to the east (Baker and Waln 1985) or an interstadial if they follow the pattern to the south in Lake Bonneville (Mehringer 1985). The presence of *Artemisia*, Tubuliflorae, Graminae, and Cyperacea, with some *Picea*, *Pinus*, and *Salix*, as in stratum C, has been interpreted as a tundra-like cold climate (Baker 1986). As an example, relatively low percentages of *Pinus* pollen and relatively high amounts of *Picea*, *Artemisia*, Compositae (Tubuliflorae), Gramineae, and Cyperaceae are part of Late Pinedale pollen spectra to the east (Baker 1986). *Salix* might have also been associated with stream settings associated with stratum C. *Ambrosia* (found only in stratum C) is also indicative of colder climate. This may indicate an open parkland setting with scattered spruce and pine with the areas among the scattered trees covered by meadow or tundra species. The climate might have been cold, representing the onset of a stadial interval.

The decreasing abundance of the algae (spore) *Zygnema*-type may be an indicator of less shallow and mesotrophic aquatic habitats. The decline of *Zygnema*-type and *Mougeotia* and the increase in *Pediastrum boryanum* may reflect an increase in the nutrient influx into the depositional basin (cf. Huber 1995:10) occupied by the Merrell Site.

Phytoliths

Susan C. Mulholland

Introduction

Phytoliths, mineral deposits that form in and between plant cells, are botanical microfossils that can provide information not available from analysis of other types of fossil material (Rovner 1983). Although many other minerals may form deposits, this analysis has focused on opaline silica since it generally exhibits good preservation in sediments. Also, relatively well-known comparative collections of silica phytoliths are available. Known silica-rich families include the Gramineae (grasses), Cyperaceae (sedges), and Equisetaceae (horsetails). Other families vary in amount of silicification from rare (Labiatae-mint) to abundant (Ulmaceae-elm); even families with relatively abundant production often contain species with low to absent phytolith production (Piperno 1985, 1988). All plant parts may produce phytoliths: leaf, stem, and root as well as inflorescence. Most parts used by humans therefore have the potential to be recorded in sediments, although roots fluctuate greatly in amount of phytolith production.

Silica can be preserved under sediment conditions that destroy organic microfossils. Phytoliths tend to be deposited at the site of production (Dimbleby 1978:129; Rovner 1988:158). Deposition normally occurs through surface or near-surface decomposition of plants; thus, phytoliths are incorporated directly into sediments. Fire or strong wind erosion, however, can and do expose phytoliths to wind transport. Phytoliths have been recorded in atmospheric dust (Folger, Burckle, and Heezen 1967; Twiss, Suess, and Smith 1969), indicating transport over considerable distances. The question of water transport has not yet been addressed.

Phytolith studies have been applied to various archaeological and paleoecological problems (Piperno 1988). Identification of crops in sediments has been attempted for maize (Pearsall 1978; Piperno 1984), rice (Fujiwara 1982), and various Old World cereals (Helbaek 1961; Rosen 1987). Study of farming practices includes identification of field surfaces (Pearsall and Trimble 1984), canals (Turner and Harrison 1981), and use of irrigation (Rosen 1987). Food residues (charred organics on ceramics) also often contain phytoliths (Thompson 1986; Jones 1993; Thompson and Mulholland 1994).

Environmental reconstruction has also been attempted using phytoliths. Carbone (1977) interpreted past environments, mostly forests, by comparison to modern soil A-horizons; Lewis (1981, 1987) and MacDonald (1974) investigated changing types of prairie from Paleoindian to recent times. Studies comparing phytolith and pollen data indicate that phytolith data complement those obtained from pollen grains; in some cases (i.e., grasslands), more information is available from phytoliths (Kurmann 1985). Pollen grains are much more diverse for forests (Piperno 1985); however, even in such environments, phytoliths provide independent support for environmental interpretation (Schreve-Brinkman 1978).

Most phytolith research to date has been focused on identification of the original plant source by particle morphology. The ultimate goal is to identify plant taxa in order to reconstruct plant use and/or vegetation at sites (Piperno 1988; Rovner 1988). Recently, chemical and physical techniques have been applied to obtain other types of information from phytoliths. Dating of occluded carbon was first accomplished on sediments from a river terrace in Ohio (Wilding 1967). The process started with 45 kg of sediment and yielded .75 g of carbon; the age obtained was 13,300 ± 450 ^{14}C yr B.P. AMS dating has greatly reduced the amount of phytolith material needed (Mulholland and Prior 1993). Another application involves thermoluminescence dating of phytoliths from hearths in Ecuadorian sites (Rowlett and Pearsall 1993). Environmental reconstruction has made use of oxygen, hydrogen, and carbon stable isotope ratios for a direct indication of paleotemperature (Bombin and Muehlenbachs 1980; Kelly et al. 1991; Fredlund 1993).

Methods and Materials

Three sediment samples from the Merrell Site in southwestern Montana, Beaverhead County, were processed (Table 10). The objective of this study was to assess phytolith abundance and degree of preservation within the samples. Classification is to phytolith type rather than to plant taxa. At this stage of research, only some phytolith types can be confidently assigned to a plant taxon. However, differences between relative amounts of phytolith types can be interpreted in terms of patterns of plant or vegetation types.

Separation of phytoliths from the sediment matrix is based on both particle size and specific gravity. Sand (larger

Table 10. Provenience of Sediment Samples Analyzed for Phytoliths.

Sample	Description
#1	E 94-6 Stratum 3, light-colored silt
#2	E 94-4 Stratum 2, dark organic silt
#2	E 94-3 Stratum 1, light-colored silt

than 88μ) is removed by sieving; clay (smaller than 5 to 10μ) is removed by settling. Particles with a specific gravity from 2.3 to 1.5 are then extracted with a heavy liquid solution of zinc bromide and water. To increase phytolith recovery, the extraction step is repeated twice. Slides for light microscopic examination are prepared with Permount (index of refraction = 1.54) and examined with a Zeiss Universal petrographic microscope equipped with a Nomarski Differential Interference Contrast (DIC) condenser system. The Nomarski DIC increases contrast in transparent particles, including phytoliths, by introducing a shadow effect.

The objective of this study was to assess plant contributors to the samples. A basic scan of the extraction provides quantitative information on phytolith types present. Basic analysis consists of identification of approximately 200 phytoliths to shape type (see below). Reference material from regional species (northern Minnesota, North Dakota) provides the known samples of potential grass and non-grass plant contributors. However, no samples are present from Montana or the Northwestern Plains, limiting the identifications that can be inferred from the phytolith assemblages.

Few phytoliths in the Upper Midwest are unique to a plant taxon; interpretation of plant contributors usually relies on comparison of phytolith assemblages from the unknown samples to those from reference plant specimens. The relative amounts of various phytolith types is often the best indicator of plant contributor. In sediments, the likelihood of several (or numerous) plants mixing together complicates plant identification enormously. However, ceramic vessels provide a restricted context that may represent one or a few plants and provide a simpler problem.

The use of phytolith assemblages (as opposed to unique shapes) requires extensive comparative material. Although it is not proven that phytolith shape is genetically controlled and, therefore, absolutely consistent in a taxon across environments, shape morphology at least intuitively appears more stable than type frequency. In addition, all quantitative data are subject to statistical variation, requiring information regarding error factors or confidence intervals. Therefore, it is doubly important to obtain comparative phytolith data from the regional vegetation. This study does not have the requisite materials from the Northwestern Plains for comparison; the plant collection is mostly from northern Minnesota and central North Dakota. Differences in vegetation and climate, therefore, reduce the accuracy of the interpretation.

Phytolith Classification

Classification of individual phytoliths is initially to shape type. At this stage of research, only some phytolith types can be confidently assigned to a plant taxon. However, differences in phytolith assemblages between closely spaced samples can be interpreted in terms of patterns of plant groups or vegetation types. The classification scheme is based on the type of cell that becomes silicified (Mulholland and Rapp 1985; Mulholland 1987; Mulholland and Rapp 1992). Table 11 lists the most common types observed to date, most of which cannot be assigned to a specific plant taxon. Category 7, however, is definitely an indicator of grasses. Grasses contain specialized silica-cells that function to collect silica (Esau 1977:85), as well as other anatomical elements that may become silicified. Every grass species examined to date has phytoliths from grass silica cells; no other plant taxon produces phytoliths with these shapes. Distinctive silica-bodies have been the subject of much taxonomic research (Metcalfe 1960; Twiss, Suess, and Smith 1969; Brown 1984; Mulholland 1989). General morphological subdivisions of grass silica-body types used in this study are listed in Table 12.

Grass silica-bodies exhibit both multiplicity and redundancy (Rovner 1971). Multiplicity is the production of many types by a taxon; redundancy is the occurrence of one type in many taxa. These factors complicate identification of grasses by phytoliths. Most efforts to correlate grass silica-bodies to grass taxa either focus on identification of certain important species by unique morphological characteristics (Pearsall 1978; Piperno 1984) or correlate general shape types to subfamilies and tribes (Twiss, Suess, and Smith 1969; Brown 1984; Mulholland 1989). The unique species identifiers are as yet few in number; correlations of more general shapes to grass subfamilies are more widely applicable, although not without exceptions (Mulholland 1989). While extensive studies of local taxa are necessary to verify hypotheses of phytolith patterns developed in other regions, analysis of sediments can be based on some general correlations.

Based on North American reference material (Mulholland 1989), grass silica-bodies are identified to

Gramineae subfamilies as follows. Sinuates and rectangles indicate the tribes Poeae, Triticeae, Aveneae, and Phalarideae of the Pooideae. Rondels are found in most of the subfamilies, particularly from inflorescence material. Although most abundant in the Pooideae, rondels cannot be used as indicators of these taxa without consideration of other subfamilies. Saddles indicate Chloridoideae, although they also occur in some species of the Arundinoideae (Ollendorf, Mulholland, and Rapp 1988) and Pooideae (low amounts). Dumbbells are produced by the Panicoideae, Aristideae (Arundinoideae), Chloridoideae, and Stipeae (Pooideae). Some tentative distinctions may be made between dumbbells from these taxa. Stipeae tend to produce dumbbells with tops smaller than the base; dumbbells with saddle-like tops are characteristic of the Chloridoideae. The Aristideae produce large quantities of dumbbells with long shafts. In the absence of these special types, dumbbells may generally be taken to indicate the Panicoideae.

Other phytolith types are generally not as well identified to specific plant taxa. Silicified bulliform cells are considered indicative of the Gramineae. The other phytolith types (#1, 2, and 4-6 from Table 11) may be produced by both grasses and other plant taxa (forbs, shrubs, and trees). Subdivisions of these types need to be identified based on morphological differences between taxa. Trichomes in particular are silicified in numerous taxa, exhibiting considerable morphological variation. A study of some North Dakota species indicates differences in size and shape of trichomes and trichome bases (Mulholland 1987). Piperno (1988) identifies some shapes (trichomes and other types) that may be unique to particular species in tropical regions. Patterns of phytolith production in plant families (Piperno 1988:21-37) provide information regarding possible contributors that must be checked against local reference material.

Results

The silica phytolith abundance in all three samples was extremely low; less than five phytoliths total were observed. In addition, these particles were weathered and nondiagnostic in shape (rods). Phytolith abundance in sediments is a reflection of two major factors: the amount of original phytolith deposition from the vegetation and subsequent sedimentary processes that degrade phytoliths. The low amount of phytoliths observed in these samples indicates that one or both of these factors had heavily affected the materials. This situation is uncommon, particularly for sediments with a significant silt component.

Non-silica particles were also observed in low abundance, although not as low as phytoliths. Samples 1 (E 94-6) and 3 (E 94-3) contained a few pollen grains. Opaque

Table 11. Phytolith Categories (Mulholland and Rapp 1992).

1. **Trichomes** - Hairs and papillae. Spherical to ovoid with a conical top.
2. **Stomata** - Guard and/or subsidiary cells. The entire complex is ovoid in shape. Guard cells are shaped like a telephone receiver. Subsidiary cells are ovoid to trianguloid.
3. **Bulliform cells** - Enlarged thin-walled epidermal cells. Keystone shapes.
4. **Epidermal groundmass cells** - Unspecialized epidermal cells. Various thin rectangular box shapes with interlocking edges.
5. **Rods** - Fibers, sclereids, xylem cells, and other cylindrical shaped cells.
6. **Rectangles/Squares** - Large blocky cells. Cube to rectangular box. Thicker than groundmass cells or silica-cells.
7. **Silica-bodies** - Phytoliths from specialized silica-accumulating cells. Truncated to beveled pyramids, cones, rectangular boxes, and cylinders. At least one broad face (base) is present. Note that, although silica-bodies are equated with short cells in botanical texts, some very long bodies are included here with the shorter ones. The long bodies are consistently silicified and resemble the other silica-bodies in surface texture (unlike groundmass cells that become silicified). For these reasons, the longer cells are included here.

Table 12. Major Shape Types of Grass Silica-Bodies (Mulholland and Rapp 1992).

I. Body is a rectangular box to truncated or beveled pyramid; cross section of base approximately rectangular to square or other polygon (base may have lobes, but general outline is a polygon); top is a flat to slightly concave or convex face or elevated ridge(s).	
A. Nonlobate: sides of base lack definite lobes	
1. Base has 3 sides	TRIANGLE
2. Base has 4 sides	RECTANGLE
3. Base has 5 sides	PENTAGON
B. Lobate: sides of base have definite lobes	
1. Minimal base diameters approximately equal	CROSS
2. Minimal base diameters unequal	
a. Bilobate: Maximum of 2 lobes per side	
1. Shaft/lobe ratio > 2/3	SINUATE
2. Shaft/lobe ratio < 2/3	DUMBBELL
b. Polylobate: More than 2 lobes per side	
1. Shaft/lobe ratio > 2/3	SINUATE
2. Shaft/lobe ratio < 2/3	DUMBBELL
II. Body is a short cylinder to truncated or beveled cone; cross section of base approximately oval to circular or other curved shape (base may have concave or flat segments, but general outline is curved shape); top is a flat to slightly concave or convex face or elevated ridge(s).	
A. Entire: edges of base all convex	RONDEL
B. Flattened: some edges of base straight	RONDEL
C. Indented: some edges of base concave	RONDEL
III. Body is saddle-like; cross section of top (or both top and base) has two opposite convex edges that flare outward from the face surface and two opposite lower edges that are usually concave; top is concave.	
A. Tabular: top and base same size and shape	SADDLE
B. Plateau: top smaller than or different shape	SADDLE
C. Ridge: top is a ridge	SADDLE

particles were observed in all three samples, but a greater abundance was present in sample 2 (E 94-4). The opaque particles resemble charcoal flecks observed in archaeological sediment samples. They remain unidentified, but have a specific gravity between 1.5 and 2.3 (since they were recovered by the heavy liquid procedure).

Conclusions

The total amount of phytolith material is indicative of extremely intense weathering activity or a total lack of silica deposition or a combination of both. Since silica phytoliths are widespread in plant families (Piperno 1988), it seems of low probability that no phytoliths were deposited. In addition, the postulated tundra/meadow environment would probably contain Gramineae and Cyperaceae, families that both produce abundant phytoliths today. Phytoliths from grasses and shrubs have been recovered from sediments in the area (Natural Trap Cave, Wyoming), although total amounts are not given (Gilbert and Martin 1984).

Postdepositional processes that degrade silica include both mechanical abrasion and chemical dissolution. Mechanical abrasion is most prevalent in sandy sediments; however, these samples are largely silt and clay. Chemical dissolution in pH greater than 8.5 or 9 is commonly cited as a condition in which silica dissolves in sediments (Mason 1966:167). Given the sediment size range, chemical dissolution in high pH conditions is the most probable explanation. The extremely sparse amount of phytoliths probably relates directly to the postdepositional processes

that had acted on the sediment, although a low silica-content of the original vegetation could have contributed to the problem.

Although these three samples did not yield phytoliths, sediments do have micro-environmental variations sufficient to yield widely different phytolith abundances. Lewis (1987) recovered significant (>100) phytoliths from only three of 18 samples in the Horner bison kill site in Wyoming; only two others had more than 25 phytoliths. Total phytolith abundance was quite variable, ranging from none to more than 300. Phytolith abundance in the High Plains varies, but not always in inverse relationship to strong pH; sites with higher pH sometimes have the best phytolith preservation (Lewis 1981).

Microstratigraphic sampling at the Merrell Site may yield better phytolith results than developed here. Sediment pH at the site would also be helpful data. The presence of pollen grains in two samples holds additional promise for vegetational reconstruction. [Pollen was also recovered at Natural Trap Cave.] The opaque particles may be charcoal, dark mineral grains, or perhaps organically coated particles. Future research should include analysis of these types of remains.

Prehistoric Archaeology

Christopher L. Hill, Dale P. Herbort, Leslie B. Davis, and Matthew J. Root

The Merrell Site Artifact Inventory

Christopher L. Hill and Dale P. Herbort

Introduction

Besides the collection of artifacts recovered in 1994, 21 artifacts from the Locality were reported by Bump (1989, 1990), two of which are tools. One is a dacite biface fragment (Figure 100), while the other is an obsidian uniface flake tool (Bump 1989). The remaining materials are debitage (waste flakes).

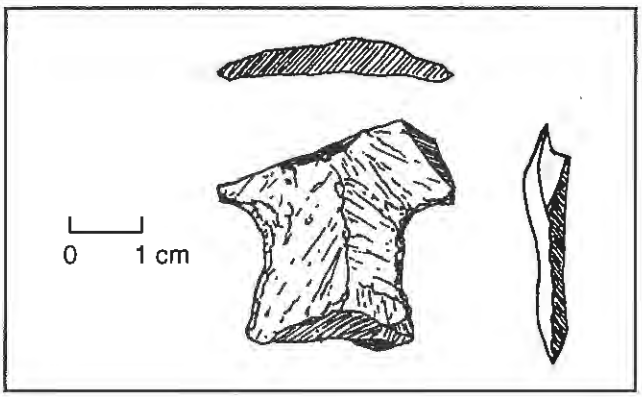

Figure 100. Proximal portion of dacite projectile from the beach at the Merrell Site.

The Merrell Site lithic assemblage was analyzed by Herbort (1994) (see Davis et al. 1995). It consists of 74 pieces of lithic debitage and four stone tools recovered from both excavated test units and surface collection (Herbort 1994).

Technological analysis addressed technological reduction systems and lithological utilization (Herbort 1994; Davis et al. 1995). Technological analysis relies heavily on the existence of striking platforms on the flake, indicating the mode of flake detachment and the directive strategy of tool manufacture. Lithological analysis examines the numerous varieties of lithic raw materials utilized for tool manufacture and the change in reduction strategies applied from one material to another.

Of the 74 pieces of lithic debitage, 38 retain identifiable striking platforms (Herbort 1994). These were divided into 28 primary reduction flakes, four secondary reduction flakes, and six tertiaty reduction flakes. Thirty-six flakes were indeterminate, that is, they lack identifiable striking platforms. The small number of flakes, coupled with their distribution across several lithological material types, renders technological analysis meaningless. Correlation of flake reduction types and lithology is presented in Table 13.

Table 13. Correlation of Technological Flake Stage with Lithology.

	Chert	Dacite	Obsidian	Vitrophyre	Total
Primary Reduction	10	13	4	1	28
Secondary Reduction	1	1	2		4
Tertiary Reduction			6		6
IND	15	7	14		36
Totals:	**26**	**21**	**26**	**1**	**74**

Four stone tools, consisting of one projectile point proximal fragment (Figure 100), one projectile point preform, one sidescraper, and one teshoa knife, are also present in the assemblage. None of the artifacts are particularly noteworthy. The projectile point is too fragmentary to permit type classification and, hence, to infer temporal-cultural affinity.

Nine lithologies are present in the collection. Most prominent is obsidian (37%), followed by dacite (27%), various local cherts (33%), vitrophyre (1%), and quartzite (1%). Obsidian (n=29) ranges in appearance from pitch black and vitreous to smokey brown crystal, representing at least three source areas. Dacite (n=21) consists of a fine "grained dull material that likely originated in local alluvial gravels." Local cherts consist of five variants: Ordovician-age gray nodular chert (n=16), Madison Formation brown agate (n=4), Madison Formation dendritic agate (n=2), Madison Formation tan chert (n=3), and Madison Formation brown chert (n=1). A single flake of Centennial Mountains vitrophyre is present. A single item of coarse-grained quartzite, the teshoa, is also present, which had clearly originated in local gravel deposits, as indicated by an incipient cone-shaped cortical surface on the teshoa. All of the materials present are procurable within 50 mi (79 km) of the site location, most within 20 mi (32 km).

Table 14. Merrell 1994 Lithic Debitage.

Date	Cat. #	Obj	Datum	Stratum	Quad	North	East	D B Dat	Scr	Class	Material	Comments
6/8/94	M.Area S-9	X	X	X	X	X	X	X	no	L	Flakes	O(4); C(3): B(2)
6/9/94	Sec. Col.-S-10	X	X	X	X	X	X	X	no	L	Flakes	K,D(?)
6/9/94	CN-12	X	X	C North	X	X	X	X	X	L	Flake	K
6/9/94	MA A1-2-1	X	X	MA A1 North	X	X	X	X	X	L	Flakes	lg, C
6/11/94	MA A1-2-2	X	X	MA A1 South	X	X	X	X	X	L	Flakes	K
6/9/94	MA A1-4-4	X	X	MA A1 North	X	X	X	X	X	L	Flakes	C,O
6/10/94	MA A1-5-3	X	X	MA A1 South	X	X	X	X	X	L	Flake	D
6/11/94	MA A1-6-4	X	X	MA A1 North	X	X	X	X	X	L	Flake	
6/12/94	MA A1-7-4	X	X	MA A1 South	X	X	X	X	X	L	Flake	C
6/11/94	MA A1-8-9	X	X	MA A1 South	X	X	X	X	X	L	Flakes	K, D, C
6/12/94	MA A-9-6	X	X	MA A1 South	X	X	X	X	X	L	Flake	C
6/9/94	MA B1-1-2	X	X	MA B1 North	X	X	X	X	X	L	Flake	O
6/11/94	MA B1-1-3	X	X	MA B1 South	X	X	X	X	X	L	Flakes	O(7)
6/11/94	MA B1-2-1	X	X	MA B1 South	X	X	X	X	X	L	Flakes	O(3)
6/11/94	MA B1-3-1	X	X	MA B1 South	X	X	X	X	X	L	Flake	O
6/9/94	MA B1-5-1	X	X	MA B1 North	X	X	X	X	X	L	Flakes	C(?) (6)
6/10/94	MA B1-6-4	X	X	MA B1 North	X	X	X	X	X	L	Flake	C(?)
6/10/94	MA B1-7-4	X	X	MA B1 North	X	X	X	X	X	L	Flake	C(?)
6/12/94	EN-1-1	X	X	E North	X	X	X	X	X	L	Flake	D
6/13/94	EN-5-1	X	X	E North	X	X	X	X	X	L	Flake	C, black
6/13/94	ES-12-1	X	X	E South	X	X	X	X	X	L	Flake	D

In sum, the Merrell Site lithic assemblage is of insufficient size and lithological variation to derive any specific technological reduction strategy. The artifact assemblage is small and fragmentary, preventing conclusions regarding site function, age, and cultural affinity.

Artifact Spatial Context

The small sample of artifactual obsidian recovered during test excavations appears to represent multiple occupations (see below). Given subsurface disturbance, however, it was not possible to isolate the respective events via 10-cm-level interval excavation. The chief agency of disturbance is bioturbation resulting from the burrowing of rodents, mostly in the upper meter of the landform. Most of the obsidian, as well as dacite and chert detritus (debitage), was collected from two designated beach fronts in redeposited surface contexts. The lithic material appears to have been eroded from the landform and deposited on the beach fronts. Small amounts of lithic debitage were likely originally widely spatially distributed in low density throughout the upper meter or so of the landform, but, even within the landform sediments (mostly stratum E), they lack primary context as a result of bioturbation.

Conclusions Regarding The Artifacts

Although the lithic artifact assemblage from the Merrell Site is small (Tables 14 and 15), some conclusions can be drawn. It was not possible to determine whether the assemblage represents a single component. More than one temporally discrete episode of obsidian use and, thereby, occupation was indicated by obsidian hydration measurements. These measurements suggest the former presence of multiple components (see below). No cores or complete points were recovered. The fragmentary nature of the single point did not allow the use of typological classification to assign an age range or cultural affiliation to the artifacts. Early-stage reduction flakes (decortication and primary debitage) comprise most of the identifiable debitage (n=29, 76%); these are predominantly chert, dacite, and obsidian. Almost all of the decortication debitage and most of the primary flakes are chert or dacite. Only four pieces are obsidian. If this is potentially representative of the reduction strategy of the assemblage, it would indicate that early-stage reduction of chert and dacite may have been more prevalent than obsidian.

There are far fewer pieces of secondary (n=4, ca. 10%) and tertiary (n=6, ca. 16%) identifiable debitage. There are single examples of secondary debitage on chert and dacite, while all of the other secondary and tertiary debitage consists of obsidian. That, too, if representative, would indicate that later-stage reduction activities, such as tool-finishing and maintenance, were associated with the working of obsidian.

The fragments of marginally retouched artifacts (tools) are composed of obsidian and dacite.

Artifact Crossdating

Leslie B. Davis

The proximal end of a stemmed dacite projectile point (Figure 100) was found on the beach near the shoreline at the Merrell Site by R. Bump during a visit accompanied by L. B. Davis and BLM personnel in 1992. This point, which was made on a flake rather than a bifacial preform, is not readily classified morphometrically or technologically for artifact crossdating purposes, by reference to the regional Northern Rockies projectile point chronology (Greiser 1984). Nor was a close counterpart point type found via a literature search; thus, this form appears not to be represented in other local and regional archaeological sources (Swanson 1972; Butler 1978). The presence of

Table 15. Merrell Site 1994 Lithic Artifacts.

6/8/94	M. Area S-4	X	X	X	X	X	X	X	no	L-a	Point frag	Midsection, O
6/8/94	M. Area S-5	X	X	X	X	X	X	X	no	L-a	Uniface scraper	C, tan
6/8/94	Sec. Col. S-6	X	X	X	X	X	X	X	no	L-a	Utilized flake	C, blk
6/94	S-7	X	X	X	X	X	X	X	no	L-a	Utilized flake	D
6/94	S-8	X	X	X	X	X	X	X	no	L-a	Core fragment	Quartzite
6/9/94	CN-2-1	X	X	C North	X	X	X	X	no	L-a	Tool frag?	O
6/9/94	MA A1-3-2	X	X	MA A1 North	X	X	X	X	no	L-a	Utilized flake	C, mottled drk red/blk
5/16/94												
8/15/94												
5/16/91												

stemming suggests a Middle Middle Prehistoric (syn. Middle to Late Archaic) period technocomplex affiliation. That places the timing of its loss or discard at some time between 5,000 and 4,000 B.P.

Hydration Age Determination of Merrell Site Obsidian Artifacts

Leslie B. Davis

Sources of Obsidian

Ten obsidian artifacts (lithic debitage) recovered from Excavations A and B were analyzed by x-ray fluorescence (Hughes 1995: Table 16). Analysis was undertaken to provide trace element concentrations from which a parent material match might be used to determine source affinity. Given the location of the Merrell Locality in the Centennial Valley, it was predicted that the obsidian specimens would be attributed to the Bear Gulch source (composed of lag deposits) defined in the Centennial Mountains located directly south of the Centennial Valley. This source is considered equivalent to the Camas/Dry Creek source of Michels (1983) and the Bear Gulch source of Hughes and Nelson (1987).

Three obsidian quarries are reported in the Centennial Valley; petrography indicated that they may be part of the same rhyolitic formation. Other trace element sourcing and obsidian hydration measurements of artifacts recovered from the Centennial Valley have been reported elsewhere (Foor and Donahue 1987).

Based on Hughes (1995), the trace element data indicate that seven of the flakes are likely composed of obsidian characteristic of the Bear Gulch chemical type. The other three specimens have a trace element "fingerprint" that conforms to the chemical profile of volcanic glass of the Obsidian Cliff Plateau, Wyoming variety (Hughes and Nelson 1987; Davis, Aaberg, and Schmitt 1995).

Hydration Thickness Measurements and Age Analysis

The 10 obsidian specimens analyzed by Hughes (1995) were also submitted for hydration measurement (reported in μ) as the basis for determining the number of hydration years elapsed since these specimens were used and lost/discarded during prehistoric times. Since hydration age calculation is controlled to some extent by geochemistry, source-specific rates of hydration have been established. Michels (1983) proposed a rate of 5.18μ squared per 1,000 years B.P. for Camas/Dry Creek obsidian and a rate of 4.65 for Obsidian Cliff (Michels 1981). Application of those rates, employing the diffusion equation of Friedman and Smith (1961) (which does not provide for effective hydration temperature), yielded the hydration age estimates shown in Table 17. Magnitudes indicate a time range from ca. 8,409 to 1,305 B.P., a time span of ca. 7,000 years. A single measurement yielded an age of 8,409 B.P. and two apparently more recent clusters are indicated. The older of these two sets yielded hydration ages between 4,551 and 2,936 B.P. (n=4) and the younger set ranges from 1,977 to 1,305 B.P. (n=5). A strict interpretation of these results would suggest an Early Prehistoric period and two Middle Middle to Late Middle Prehistoric period (= Middle to Late Archaic period) episodes of obsidian utilization. Previous applications of Michels' rates to obsidian from the Hell Gap component at the Indian Creek site in southwestern Montana met age predictions based on radiocarbon dates for Hell Gap (Davis 1986) at Indian Creek and elsewhere (cf. Frison 1974) at 10,000 B.P.

A more robust way of calculating hydration rates derives from the pairing of obsidian hydration values with associated radiocarbon ages (Davis, Foor, and Smith 1997; Davis 1981: Fig. 17) for southwestern Montana (irrespective of specific source) (Table 17). That approach met expectations set by radiocarbon dates when applied to early and late Late Prehistoric period obsidian artifacts at the Antonsen bison kills in the Gallatin Valley of Montana (Davis and Zeier 1978). On that basis, a second set of hydration ages is suggested in Table 17. Again, three episodes of obsidian use are indicated. Derived ages for these three intervals are: (1) ca. 7,000 B.P.; (2) 4,000 to 3,250 B.P.; and (3) ca. 2,450 to 1,800 B.P. In the absence of independent chronometric indicators of the age of these obsidian artifacts at Merrell, the meaning of measured differences between the derived hydration ages is not easily resolved.

Analyses of the hydration measurements from the two excavation strata, by the depth at which each artifact was recovered below the present surface of the Merrell Site landform, yielded the arrays shown in Table 18. The stratigraphic ordering (depth b.s.) of hydration values fits for Excavation A1, that is, the larger value (signifying an older age) is from the deepest level. Excavation B1 values do not fit the expected stratigraphic order. This would appear to suggest that postdepositional disturbance has occurred. This relocation of artifacts is likely an effect of rodent burrowing. The archaeological integrity of the obsidian artifact-bearing deposits appears to have been destroyed Thus, the sparse artifact accumulations at the Merrell Site had either been redeposited or mixed as a result of bioturbation and possibly erosion.

Table 16. Trace and Selected Minor Element Concentrations of Obsidian Artifacts from the Merrell Site (Hughes 1995).[1]

Cat. Number	Zn	Ga	Rb	Sr	Y	Zr	Nb	Source (Chemical Type)
3007	74+4	21+3	190+3	51+3	52+2	339+4	59+2	Bear Gulch
3008	68+4	21+3	189+3	47+3	52+2	314+4	57+2	Bear Gulch
3009	69+4	19+3	189+3	47+3	51+2	317+4	59+2	Bear Gulch
3110	63+5	15+4	186+4	45+3	51+/2	313+ 4	61+2	Bear Gulch
3011	77+5	22+4	232+4	3+3	75+2	160+4	40+2	Obsidian Cliff
3012	85+4	25+4	256+3	4+3	85+2	172+3	46+2	Obsidian Cliff
3013	72+4	18+3	182+4	47+33	49+2	310+4	61+2	Bear Gulch
3014	107+4	27+3	262+3	5+3	81+2	166+3	45+2	Obsidian Cliff
3015	74+4	25+3	183+3	50+3	51+2	317+4	58+2	Bear Gulch
3016	77+3	20+3	188+3	47+3	50+2	308+4	54+2	Bear Gulch

[1]Measurements based on x-ray tube current of 0.25 mA.

Table 17. Hydration Rind Thickness Measurements and Hydration Age Estimates B.P.

Specimen Number	Provenience	Mean of Stratum/Depth (cm b.s.)	Source Affinity Measurements in Microns (μ)	SMM Rate*	Michels' Rates
3007	MA-A1/30-40	6.6	Bear Gulch	7,000	8,409
3008	MA-B1/10-20	3.0	Bear Gulch	2,150	1,737
3009	MA-B1/10-20	2.9	Bear Gulch	2,050	1,623
3010	MA-B1/10-20	3.2	Bear Gulch	2,450	1,977
3011	MA-B1/0-10	4.2	Obsidian Cliff Plateau	3,650	3,793
3012	MA-B1/0-10	4.1	Obsidian Cliff Plateau	3,550	3,615
3013	MA-B1/0-10	3.9	Bear Gulch	3,250	2,936
3014	MA-A1/10-20	4.6	Obsidian Cliff Plateau	4,000	4,551
3015	MA-B1/20-30	2.6	Bear Gulch	1,800	1,305
3016	MA-B1/0-10	2.9	Bear Gulch	2,050	1,623

*Rate for the Southern Montana Montane (SMM) Subregion (Davis 1981).

Table 18. Hydration Rind Thickness Arrayed By Test Excavation Unit Level Provenience.

Level	Test Pit A1	Test Pit A2
1/0-10 cmbs	4.6	2.9, 3.9, 4.1, 4.2
2/10-20 cmbs	4.6	2.9, 3.0, 3.2
3/20-30 cmbs		2.6
4/30-40 cmbs	6.6	

Paleoindians in the Centennial Valley and Environs

Leslie B. Davis and Matthew J. Root

Multiregional Overview

The Merrell Locality and Site are located within the southern part of the Northern Rocky Mountains Physiographic Province (Fenneman and Johnson 1946), which is characterized by relatively short mountain ranges separated by broad basins. This area is similar to and continuous with the Basin and Range, which is separated from it only by the lava veneer of the Snake River Plain (Thornbury 1965). The research locality is thus situated inside a geological, physiographic, and environmental region wherein the eastern Columbia Plateau, northwestern Great Basin, and northern Rocky Mountain natural and cultural areas converge. More specifically, southern and southeastern Idaho and the Snake River Plain (e.g., Plew 2000) and southwestern Montana are included. At least three distinctive Paleoindian adaptations are thus expected to be represented. Archaeologists working in those cultural areas have demonstrated such different technological adaptations. Because movements of peoples and artifacts between and across these contiguous natural areas took place variably through time, the Paleoindian archaeology of the Centennial Valley and environs should be reflected in the presence of artifacts representing multiple Paleoindian traditions and complexes. As well, that this locality was easily reached and traversed by Great Plains Paleoindians is evidenced by diagnostic projectile points representing several Paleoindian complexes believed to originate on the plains.

Our use and implications drawn from the term Paleoindian here are consistent with that employed by Plateau and Basin archaeologists. In southwestern Idaho, usage is as follows: Early Birch Creek (11,000-8,200 B.P.) (Swanson 1972); Big Game Hunting Tradition (Butler 1978), which includes Clovis (12,000-11,000 B.P.), Folsom (11,000-10,600 B.P.), and Plano (10,600-7,800 B.P.); Early Prehistoric (15,000 7,500 B.P.) (Ringe et al. 1988); and Paleo-Indian, Big Game Hunting Period, or Paleo-Indian Tradition (15,000-7,800 B.P.) (Plew 2000). Elsewhere in the Intermountain West, dozens of fluted points closer to Clovis than Folsom, from surface contexts (Hester 1973), were grouped into the Fluted Point Tradition estimated to date from 11,000 to 8,000 B.P. A Great Basin origin has been suggested for the Fluted Point Tradition (Davis 1978). Unfortunately, the archaeological basis provides only sketchy support for these designations because of the paucity of early, radiocarbon-dated, artifact-bearing stratigraphic contexts.

Our approach in this section consists of typological classification of Paleoindian point surface finds and providing spatial and chronological parameters derived for the southwestern Montana region. Although archaeological excavations of sites or localities in the Centennial Valley and environs are few, they have yielded stone artifacts attributable to certain of the Paleoindian complexes recognized in the Northern Rocky Mountain Region. Surface collections made by private collectors, federal agency personnel, and archaeologists in this area routinely include Paleoindian projectile points, sometimes in numbers that outnumber other types of projectile points in those collections. An explanation for the relatively high proportion of Paleoindian points in these collections may lie in the lateral extent of erosional settings where artifacts were found, e.g., along deflated margins of inundated valleys (reservoirs) and in the bottoms and on the side slopes of deeply eroded gullies created by road-building. Additionally, erosion of stream terraces and deflation of forested areas have exposed shallowly buried Paleoindian points.

Figure 101 presents a chronological framework that provides for typed Paleoindian projectile points expected in the study area (adapted from Greiser 1984), not all of which have been documented in the study area.

Plains Paleoindians

Plains Paleoindian projectile points are rare in the Centennial Valley and environs. A **Clovis** component (Frison 1978, 1991a) at Indian Creek (24BW626) dates ca. 11,000 B.P. (Davis and Baumler 2000).

The proximal portion of an obsidian **Folsom** complex point made of Bear Gulch, Idaho obsidian was found on the surface of U.S.D.A. Forest Service property in the Beaverhead National Forest north of Lima Reservoir by R. Gibson (Jasmann 1963; L. B. Davis, pers. comm., R. Gibson) (Figure 102). Another **Folsom** point was found in a disturbed buried context near Norris, Montana (Jasmann 1963). Two **Folsom** points were collected by J. Feathers on the Argenta Flat west of Dillon. The **Folsom** complex is represented in situ at Indian Creek (Davis and Greiser 1992; Baumler and Davis 2000), where it dates ca. 10,400 B.P., and at MacHaffie (24JF4) (Forbis and Sperry 1952; Forbis 1955; Davis et al. 1991; Davis, Hill, and Fisher 2003), where it dates ca. 10,400-10,100 B.P. These sites are on the flanks of the Elkhorn Mountains. A major Folsom campsite is located on the west flank of the Bridger Mountains in the Gallatin Valley. The subsequent **Agate Basin** complex (Figure 103) (cf. Frison and Stanford 1982) component represented in situ at Indian Creek is not radiocarbon dated. **Hell Gap** complex (Agogino and Frankforter 1965; Frison 1974) projectiles are represented in situ

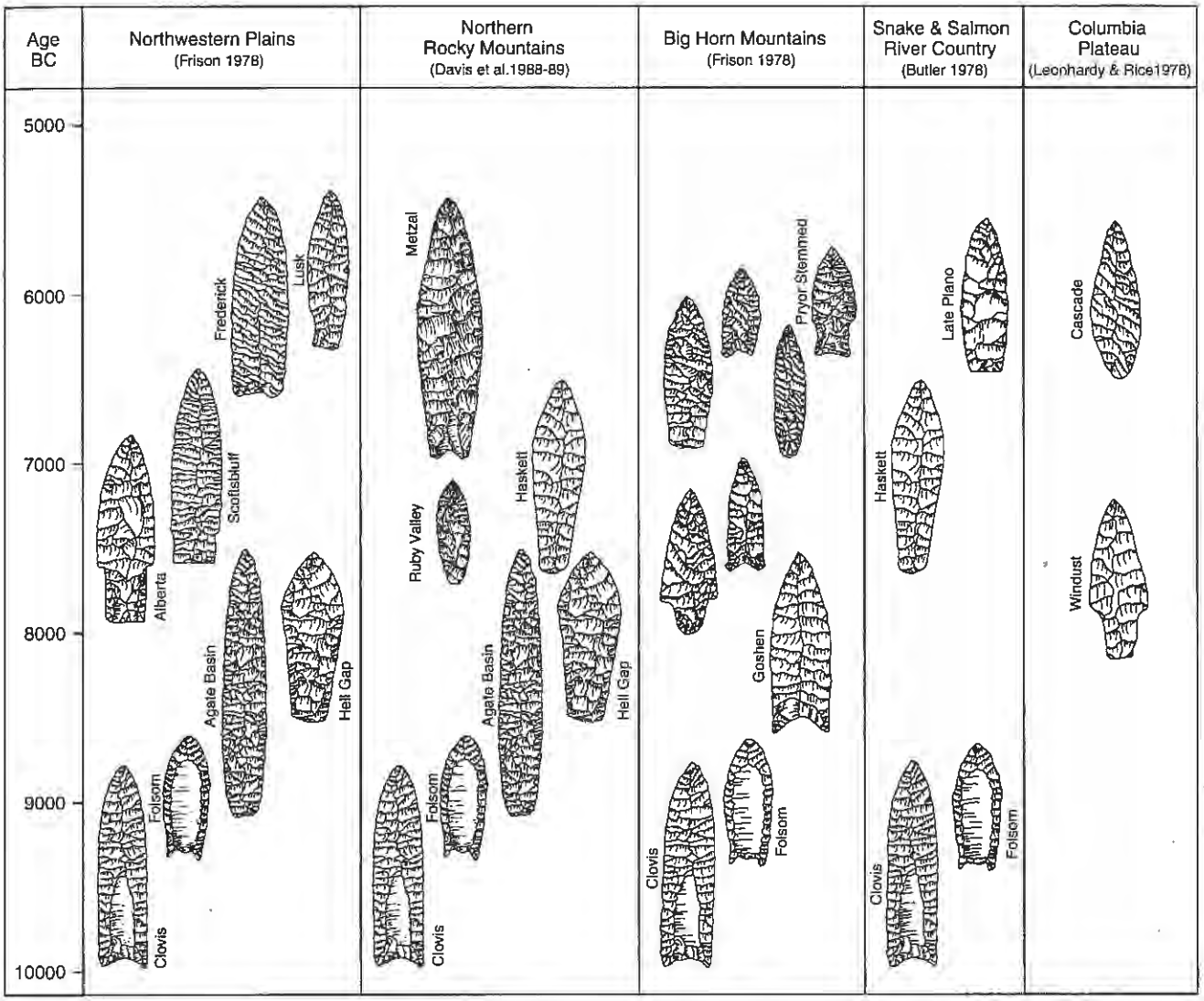

Figure 101. Multiregional summary of Early Projectile Point Sequences (adapted from Greiser 1984).

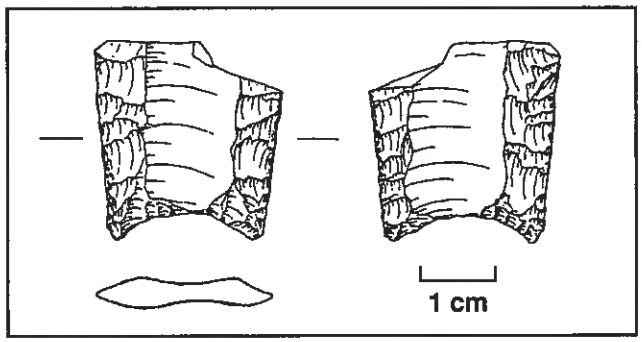

Figure 102. Proximal portion of an obsidian Folsom point found by R. Gibson in forested terrain north of Lima Reservoir.

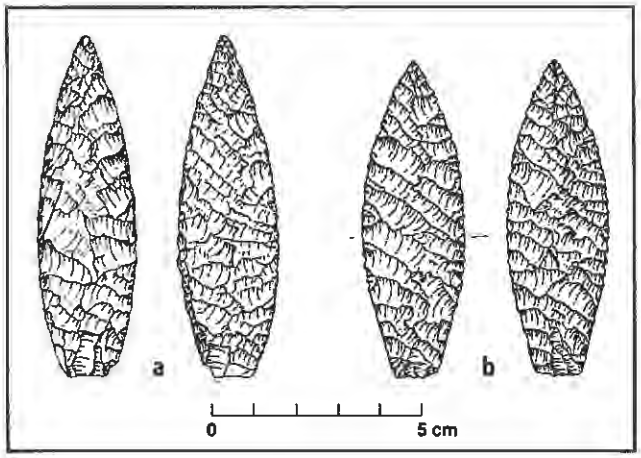

Figure 103. Agate Basin points from Centennial Valley collections.

at Indian Creek where the component is radiocarbon dated ca. 10,000 B.P. (Davis 1986; Davis and Greiser 1992), at the Hell Roaring Creek site (24GA1160) in Gallatin Canyon as a surface collection, and on the surface at Canyon Ferry Lake on the upper Missouri River (Greiser 1986; Davis and Helmick (1982).

Small to medium-sized lanceolate **Ruby Valley** points, associated with the Alder complex, defined and named at the Barton Gulch site (24MA171) (Davis et al. 1989) on the eastern margin of the Upper Ruby River valley southwest of Virginia City, are present in modest numbers (Figure 104). There, they date ca. 8,800-8,200 B.P. They are even more numerous in eroded context at Canyon Ferry Lake (Greiser 1984; Davis and Helmick 1982). Sites in the Centennial Valley have yielded a substantial number of the thick, heavy, indented base, basal marginally heavily ground, bibeveled points identified and typed as **Metzal** points at Barton Gulch (Davis, Aaberg, and Greiser 1988). These points are diagnostic for the Hardinger complex at the Barton Gulch type site (Figure 105), where they date ca. 7,500 B.P. Single **Metzal** points have been recovered along Hebgen Reservoir near West Yellowstone (V. McCoy and J. Jelinski) and in the Upper Yellowstone Valley.

An in situ **Scottsbluff** (Cody complex: cf. Frison and Todd 1987) assemblage excavated at the MacHaffie site (24JF4) (Forbis and Sperry 1952; Forbis 1955; Knudson 1983; and Davis et al. 1991) is dated ca. 9,700-9,200 B.P. (Davis, Hill, and Fisher 2002). Another in situ **Scottsbluff** (Cody complex) assemblage, excavated at the Mammoth Meadow locality at the South Everson Creek site (24BE559) near Lemhi Pass, is reported (Bonnichsen et al. 1992) (Figure 106). **Eden** (Cody complex) points were recovered along Lima Reservoir by D. Merrell and one made of obsidian by V. McCoy near West Yellowstone, as was another by J. Jelinski at Hebgen Lake. **Eden** and **Scottsbluff** points were recovered from an exposed Paleoindian locality at Canyon Ferry Lake near Townsend, Montana (Keyser and Bonnichsen 1982; Helmick 1984). The mid-portion of a mottled black-brown chert **Alberta** (Cody complex) point was found on the surface by A. Nash near Cherry Creek along the Madison River and another of dacite by R. Nichols along Mudd Creek at the north end of the Big Hole Basin.

The Dry Creek Headwaters site (24GA1000) on the west flank of the Bridger Mountains east of the Gallatin Valley yielded **Folsom**, **Goshen**, and **Agate Basin** points from cultivated fields (Davis et al. n.d.).

Columbia Plateau and Great Basin

"Plains Paleoindian" point types, specifically **Clovis** and **Folsom** points, occur at locations in Idaho(see below).

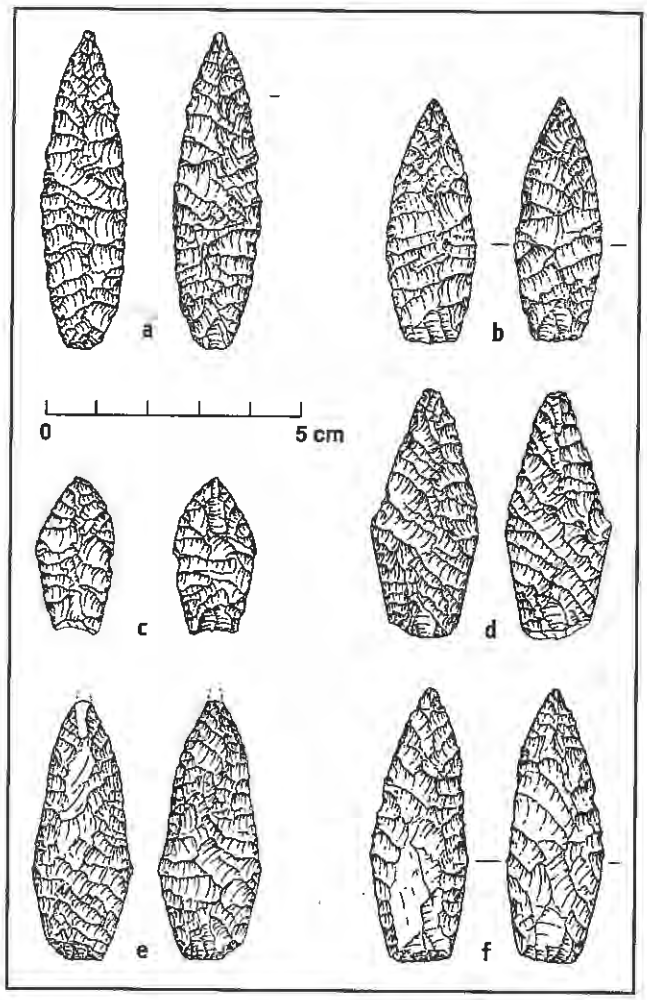

Figure 104. Ruby Valley points from Centennial Valley collections.

Paleoindian points of types geoculturally associated with the southern and southeastern Columbia Plateau and northern Great Basin areas of Idaho are prominent elements in Centennial Valley Paleoindian point collections. Lanceolate points that appear to qualify as **Cascade** (Figure 107) in type are numerous in collections. However, they appear to be heavily maintained or reworked broken points. Modifications obscure their production technology and introduce considerable variability. Most were made from obsidian and dacite. **Haskett** points (Butler 1961, 1965a-b, 1973), for example, one made from Obsidian Cliff Plateau, Wyoming obsidian found near Ennis, Montana by B. Morris (Davis, Aaberg, and Schmitt 1995: cover) and one made from Bear Gulch, Idaho obsidian, respectively, were found near West Yellowstone, Montana by V. and R. McCoy and south of Lima by D. Merrell. **Haskett** points have only recently been recognized at a few mountainous and foothill southwest Montana surface sites (Figure 108). The tendency among regional archaeologists to

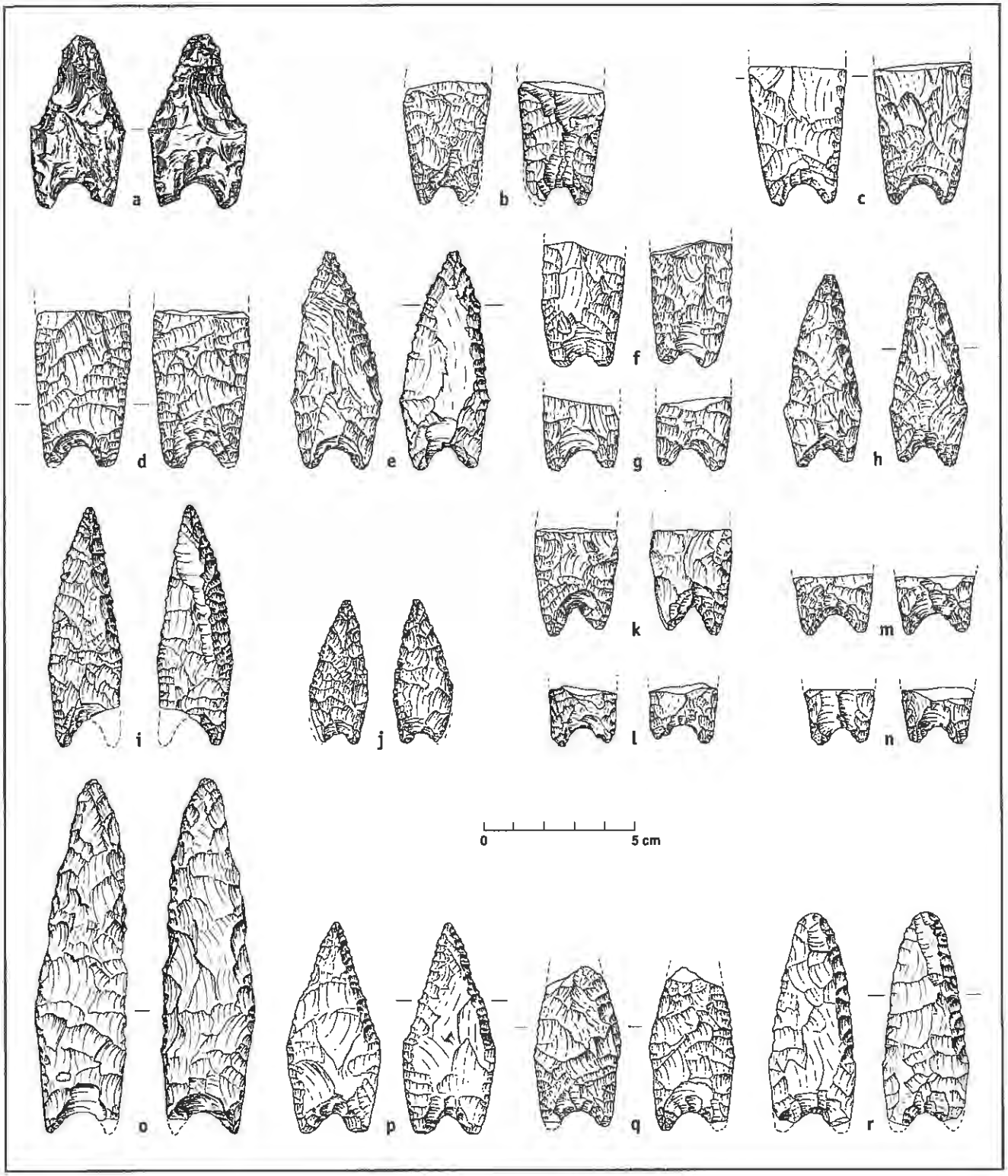

Figure 105. Metzal points from Centennial Valley and adjacent area collections.

uncritically classify proximal ends of lanceolate points as **Agate Basin** may have obscured the actual frequencies of **Haskett** points.

Snake River Plain

The best evidence indicates that the earliest human groups first ventured on to the Snake River Plain during

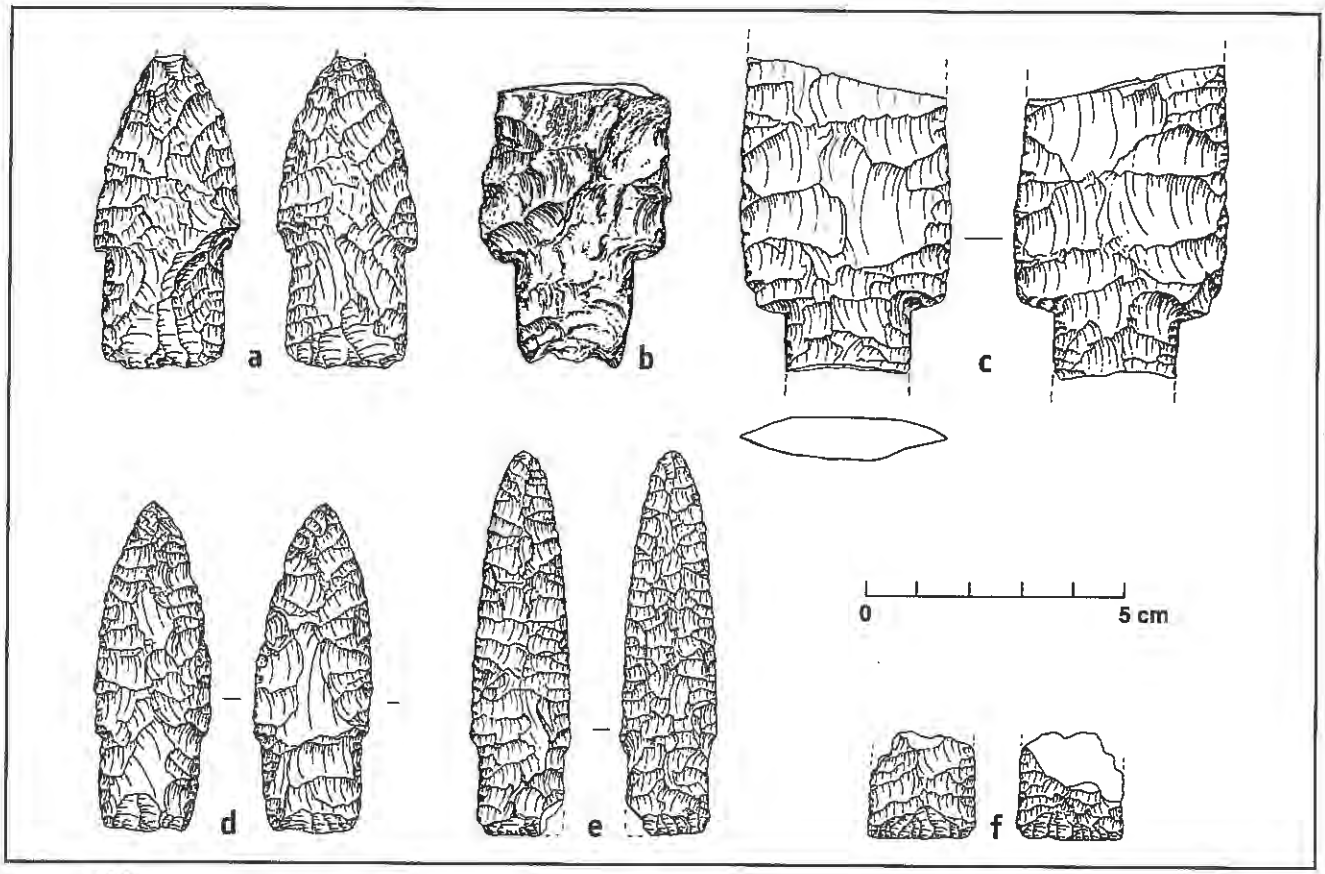

Figure 106. Alberta, Scottsbluff, and Eden points from Centennial Valley collections.

Clovis times, or about 13,500 calendar years ago (ca. 11,500 radiocarbon years). Excavations at Wilson Butte Cave in the early 1960s produced a radiocarbon age of 14,500 ± 500 B.P. on a piece of bone, which was originally used to argue for early human presence in North America (Gruhn 1961, 1965). Excavations in 1988–1989, however, indicated that the evidence for such an early occupation was unclear, though stemmed points were recovered (Gruhn 1995).

Kelvin's Cave is a small lava tube north of Twin Falls with 2 m of archaeological deposits that span the Late Pleistocene and Holocene. In stratigraphic Unit 3, Late Pleistocene faunal remains are *spatially* associated with stone artifacts that are not time-diagnostic. Remains include camel (*Camelops hesternus*), Musk ox (*Symbos* sp.), and Pleistocene horse (*Equus* sp.). None of the bone exhibits cut marks or other signs of cultural modification and the *cultural* association of the bone and artifacts remains uncertain (Plew 2000: 33–34; Yohe and Woods 2002:8).

Jaguar Cave is in the upper end of the Birch Creek Valley, and has been reported as a possible **Clovis**-age archaeological site. An antler tine with purported cut marks was spatially associated with a possible hearth that was radiocarbon dated to 11,580 ± 250. Charcoal from a depression was dated to 10,320 ± 350, and this deposit also contained the remains of many mountain sheep (*Ovis canadensis*) (Plew 2000:31–32; Wright and Miller 1976:302). It was reported that domestic dog bones were associated with these early dates, but direct dating of the dog bones yielded radiocarbon ages of 940 ± 80 B.P. and 3220 ± 80 B.P., demonstrating no such association. The earliest clear evidence of human occupation of the cave is a bighorn sheep metatarsal with definite cut marks that dates to 7,380 ± 100 B.P. The uncertain association of human activity with the early dates casts doubt on whether this is a Paleoindian site (Yohe and Woods 2002:10).

Clovis. Most **Clovis** components on the western Snake River Plain are marked only by surface finds, with the Simon site the single exception. That site is on the Camas Prairie (Butler 1963), and contained three large **Clovis** points that are more than 120 mm long, two smaller **Clovis** points, and 28 bifacial blanks or cores, including four made of quartz crystal. The Simon site is usually called a cache, which implies that the points and tools were stored for later retrieval and use. Such concentrations of large projectile points, which were purposely interred, may not be caches. They may be associated with burials (as with the

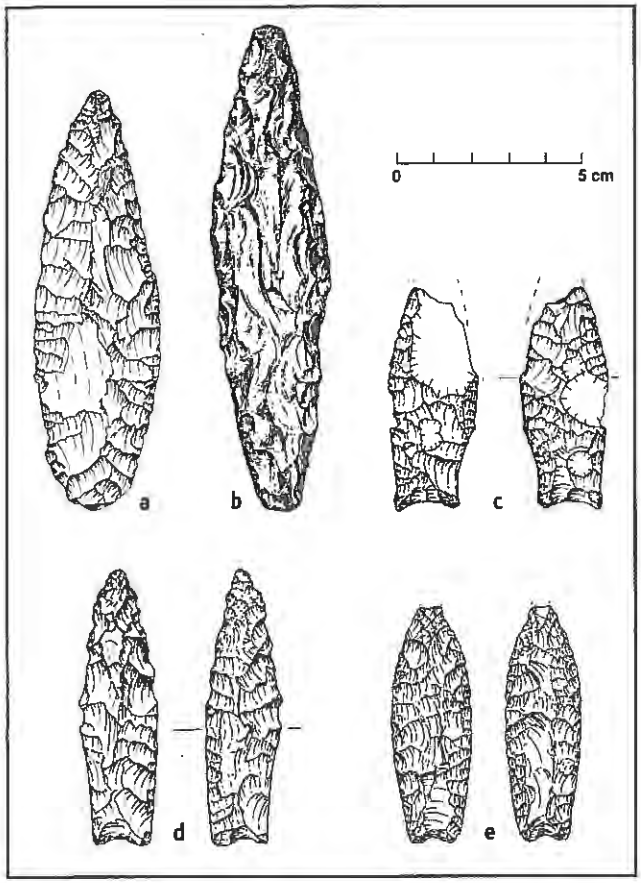

Figure 107. Cascade point variants from Centennial Valley collections.

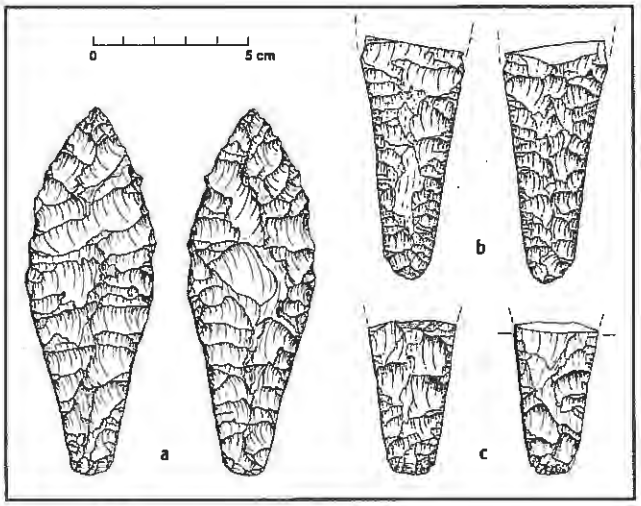

Figure 108. Haskett points from Centennial Valley and southwestern Montana collections.

Anzick site), or they might be offerings of other kinds (e.g., Woods and Titmus 1985). Thus, the status of the Simon site as a cache or offering (associated with a burial or otherwise) is unclear.

There are scattered surface finds of **Clovis** points across the Snake River Plain. These points include four collected in Owyhee County, southwest Idaho. A large chert **Clovis** point was found in the West Clover area in the Bruneau River drainage (Titmus and Woods 1990). A smaller chert point was collected from the Big Springs Creek drainage (Plew and Scott 2003). A small obsidian point was found along a small tributary of Jordan Creek (Huntley 1980). Finally, the base of a large, translucent green agate **Clovis** point was surface-collected from the Alkali Creek site. This tool-stone crops out in several localities in southwest Idaho (Huntley 1985). A local resident collected the base of a chert **Clovis** point from the Blue Lakes locality on the north side of Snake River, near Twin Falls. This locality also contains the remains of Imperial mammoth, horse, camel, and extinct bison (Titmus 1987). An unusual, complete point with concave, lateral basal margins was collected from Coyote Wells in eastern Oregon in the western Snake River Plain. This point was classified as **Clovis** (Yohe and Uren 1993), though it bears little resemblance to western **Clovis** points. The lateral margins are not ground, which is extremely unusual for **Clovis** points (Titmus and Woods 1991) The point has short flutes (more accurately basal thinning flakes) and the concave lateral margins near the base give a "fishtail" appearance in plan view. Typologically, this point is not **Clovis**, and it is possible that it was made by a modern flintknapper.

Folsom. The lone excavated **Folsom** context in the Snake River Plain is Owl Cave, part of the Wasden site west of Idaho Falls. Owl Cave is a collapsed lava tube that contains three Folsom points, the bones of mammoth (*Mammuthus* cf. *columbi*), extinct bison (*Bison bison antiquus*), camel (*Camelops* sp.), dire wolf (*Canis* cf. *dirus*), pronghorn (*Antilocapra americana*), and fox (*Vulpes fulva*). The mammoth bone is modified, which appears to be the result of human activity. Though the bones and **Folsom** points were recovered from the same stratigraphic level, there is no clear evidence of a cultural association between the mammoth bone and the **Folsom** points. **Folsom** groups may have visited the cave and left the **Folsom** points after earlier hunters butchered mammoth and left their modified bones in the cave (Miller 1989). As Miller indicates (1989:382), a late occurrence of mammoth and cultural association with **Folsom** points is but one of two possibilities based on extant evidence. The three radiocarbon dates on mammoth bone are within the **Clovis** time range, and only the youngest overlaps with the two earliest dates known for **Folsom** of ca. 10,900 radiocarbon years B.P. (Fiedel 1999). The obsidian hydration dates on **Folsom** artifacts from Owl Cave range from 12,293 ± 435 to 11,424 ± 206 years, most of which are younger than calibrated **Folsom**

radiocarbon ages. None of these overlap with the mammoth bone radiocarbon dates, of which the earliest is 12,850 ± 150 radiocarbon years (Miller 1989:Table 1). Given the absence of any **Folsom** mammoth association elsewhere in North America and disparate distributions of dates from mammoth bones and **Folsom** artifacts, their association at Owl Cave is uncertain, at best.

Preliminary results of the investigation of two Folsom sites on the Idaho National Engineering and Environmental Laboratory (INEEL) in Butte County (10BT116 and 10BT719) suggest that a **Folsom** camp is represented by bone, tools, and debitage (Yohe and Woods 2002). Titmus and Woods (1991) list 12 other isolated finds of **Folsom** points from the Snake River Plain and the upper Salmon River valley. Butler (1973) also reports a **Folsom** point from the Curlew Valley in the Snake River Plain of extreme northern Utah. There is a pattern of most **Clovis** points being found in the eastern Snake River Plain and most **Folsom** points being found in the western Snake River Plain. Whether this empirical pattern represents a sampling error, or a real difference in settlement patterns is not known (Yohe and Woods: 2002:27).

Other Paleoindians/Paleoarchaic. The Buhl burial, found near Kanaka Rapids on the Snake River in the eastern Snake River Plain, is that of a 17–21-year-old woman. AMS dating on bone collagen produced an age of 10,675 ±95 B.P., which is considered a minimum age for the burial. The woman was interred with a large stemmed biface, an eyed bone needle, and two incised bone ornament fragments that may be part of the same object. The stemmed biface has a tranchet tip, but otherwise is similar to **Windust** points from the Columbia Plateau and stemmed points from the Great Basin. Craniofacial features indicate an affiliation with American Indian and East Asian populations. Isotopic analysis of bone collagen indicated a diet composed principally of continental terrestrial or aquatic foods, but with a marine food contribution. The marine contribution is most likely from anadromous fish taken from the Snake River (Green et al. 1998).

Plano Period. This period is characterized by lanceolate points and a focus on bison hunting, including *Bison b. antiquus,* with a shift to modern bison late in the period. Mountain sheep remains are found in sites in the mountain valleys above the Snake River Plain (Butler 1986:129; Plew 2000:37).

The Haskett site, located south of American Falls, is the type site for the Haskett complex. **Haskett** points are characterized by long, contracting stems, and at the type site were associated with bison tooth fragments and flake knives. The only date on **Haskett** points in the Snake River Plain is from Redfish Overhang, where they are associated with radiocarbon dates of 10,100 ± 330 B.P. and 9,800 ± 300 B.P. (Sargeant 1973). **Haskett** points have also been recorded at sites at the INEEL, though litrle is known of those localities (Yohe and Woods 2002:21)

A **Haskett** point made from Obsidian Cliff Plateau obsidian was found near Ennis, Montana by B. Morris (Davis Aaberg, and Schmitt 1995:cover). A **Haskett** point of Bear Gulch (Idaho) obsidian was collected by V. and R. McCoy near West Yellowstone, and another from the same source was found by D. Merrell south of Lima.

The Bison Rockshelter and Veratic Rockshelter in the Birch Creek valley, eastern Idaho, contained lanceolate points similar to **Haskett** points. These points are within the Early Birch Creek phase (11,000–8200 B.P.), defined by Swanson (1972). The 1988–1989 excavations at Wilson Butte Cave recovered stemmed points resembling **Haskett** points, shouldered points resembling **Alberta** points, and concave-base points. The dates from this stratum vary widely, however, leaving the age of Stratum C uncertain, though the points suggest late Paleoindian occupation (Gruhn 1995). The upper levels of the Wasden site also contain lanceolate projectile points associated with *Bison b. antiquus* bones indicative of at least two coordinated mass kills at ca. 8,000 B.P. (Butler 1986:219).

Conclusions

The inspection of locally collected artifacts, in combination with a multiregional literature search, led to recognition of several named Paleoindian point types (a la Greiser 1984) (Figure 101). Certain collections contain unnamed, but obviously cognate forms, most of which have not been radiocarbon dated elsewhere in the region. Moreover, the predominant Holocene human occupation of the Centennial Valley appears to have been by peoples of the Alder complex (**Ruby Valley** points) and Hardinger complex (**Metzal** points). These late Paleoindian lifeways were operative in southwest Montana from ca. 8,800 to 7,500 years ago, that is, from late Anathermal to early Altithermal times.

It was expected from the outset of research that, while evidence for southwest Montana Paleoindians would establish the presence of peoples of the Fluted Point and Stemmed Traditions (cf. Bryan 1980: 83-92), still earlier points might have preceded them in time and space. However, predictions from other regional summaries, as well as Bryan's, provide for all point types discerned, e.g., Butler 1961; Holmer 1986a-b, 1995; Lohse 1994, 1995; Swanson 1972; Plew 2000; Leonhardy and Rice 1970. Later Stemmed Point (Middle Prehistoric period) manifestations are abundant, as are later Side-Notched Point manifestations much more abundant in the Centennial Valley.

Acknowledgements

Christopher L. Hill

This research was conducted as a project of the First Montanans Search Program supported by the Kokopelli Archaeological Research Fund and grants from the Bureau of Land Management. I am particularly grateful to Don Merrell (Lima, MT), Mark Sant (BLM-Dillon, MT), Terri Wolfgram (Bozeman, MT), David Batten (Emporia State University, KS), Robert Bump, and Troy Helmick (Townsend, MT) for contributing to productive field experiences. Seppo Valuppu, Richard Hughes, and Tom Origer conducted laboratory studies of materials from the Merrell Site which are encorporated in this report. Thanks to Thomas A. Foor (University of Montana-Missoula) and Gerald R. Clark (then with the BLM-Butte, MT) for making this investigation by the Museum of the Rockies possible.

The stratigraphic studies reported here were conducted under a cooperative agreement between the United States Bureau of Land Management (BLM) and the Museum of the Rockies at Montana State University-Bozeman (MOR) and an antiquities permit granted to L. B. Davis. L. B. Davis initiated and organized the 1994-1996 MOR excavations at the Merrell Locality. Funds for the 1994-1996 excavations were provided by the BLM and the Kokopelli Archaeological Research Fund (KARF, directed by L. B. Davis). The 1995 excavations, along with stratigraphic and paleoenvironmental analyses, were also partially funded by a MONTS EPSCoR grant from Montana State University to me. Stratigraphic studies conducted in 1996 used private funds, while observations made in 1997 were conducted with funds provided by the KARF Ice-Age Research Program (at the Museum of the Rockies, Montana State University-Bozeman). Topographic and elevation data used in this report include data compiled from measurements made by J. Albanese, D. Batten, and T. Helmick. D. Batten served as field director for the 1994-1996 excavations and critically reviewed my efforts at interpreting the spatial location of excavation levels and fossil specimens, especially from the South Block area. My observations of the 1996 stratigraphy were supplemented by profile sketches made by J. D. Norris, M. Reinholtz, and D. Batten (Unit W:132N/124E North Wall exposure, 6/20/96 field notes). The collaboration of J. Albanese, D. Batten, R. Bump, L. Davis, R. Dundas, J. Feathers, J. Huber, M. Sant, and members of the excavation teams in conducting the research is acknowledged with many thanks and considerable appreciation.

We express our appreciation to the archaeological field crews which consisted of Chris Crofutt, Jackie Gillette, Jennifer Husted, Kyle McGuire, Roy Reynolds, Cheryl Robson, Jenny Younger, Seth Wolfgram, and Terry Wolfgram. Thanks go to Jenny Younger and Rebecca Gilluly for cataloging and laboratory assistance.

Robert G. Dundas

Thanks to Chris Bell (herps/rodents), Doug Long (fish), Steve Emslie (birds), David Polly, and Elaine Anderson for assisting in the identification of specimens from the Merrell Site. Discussions with Christopher Hill clarified many aspects of the stratigraphic position of recovered faunal remains.

Leslie B. Davis

I am grateful to Dr. Joseph Feathers, then at Western Montana College, Dillon, for having introduced me to southwest Montana Paleoindian archaeology during the mid-1960s by showing me a recently disturbed upland pediment location near Argenta, Montana, where he had collected two Folsom point distal fragments. Later, a small-scale, short-term test excavation program at the South Everson Creek quarry/workshop and occupation site (24BE559), funded by the Bureau of Land Management, heightened my interest in investigating Paleoindian research possibilities in southwest Montana. Archaeologist B. J. Earle, then with the Bureau of Land Management in the Dillon Resource Area Office, further acquainted me with the overall archaeological promise of that area by sharing and illustrating interesting early artifacts (Figures 105, a; 106, b; and 107, b) recovered from that locality. She introduced me to Burl Stephens (Dillon) who later bequeathed his artifact collection to the Museum of the Rockies (Davis, Earle, and Davis 2000). Archaeologist John Taylor, then with the BLM Curation Facility in Billings, kindly showed me the Paleoindian points from Montana sites under his care and loaned specimens to the Museum for study.

Artifacts shown me from collections held by private individuals are presently the best empirical basis for estimating the Paleoindian adaptation and research potential of the Centennial Valley: Bob Gibson (Bozeman), Don Merrell and Lewis and Demaris Hoadley (Lima), Bud Morris (Ennis), and Alice Nash (Bozeman). Valerie McCoy (Belgrade) kindly loaned the West Yellowstone Scottsbluff point for study. Troy Helmick (Townsend) assisted in the field during the ground-truthing phase of that collections research project by locating findspots on maps. He also prepared most of the artifact line drawings for this report.

Stephen A. Aaberg (Aaberg Resource Consulting [Billings]) produced the computer-drafted figures from draft versions provided him by C. L. Hill. Frankie Jackson (MSU-Bozeman) prepared line drawings of selected fossil specimens.

Diane Fuhrman (Generic Technical Services, Bozeman) wordprocessed this report. Publication design and layout were by Bruce Eng of ENGDESIGN.

References Cited

Agenbroad, L. D., and B. R. Barton
1991 *North American Mammoths: An Annotated Bibliography 1940-1990.* The Mammoth Site of Hot Springs, South Dakota, Inc., Scientific Papers, Volume 2. Hot Springs, South Dakota.

Agogino, G. A., and E. Galloway
1965 *The Sister's Hill Site: A Hell Gap Site in North-Central Wyoming.* Plains Anthropologist 10(29):190-195.

Aitken, M. J.
1985 *Thermoluminescence Dating.* Academic Press, New York.

Albanese, J. P.
1995 Reconnaissance Geologic Study of the Merrell Locality, Beaverhead County, Montana. Report to the Museum of the Rockies, Montana State University-Bozeman, Bozeman, Montana.
1997 A Reconnaissance Geologic Study of the Merrell Locality, Beaverhead County Montana. Report to the Museum of the Rockies, Montana State University-Bozeman, Bozeman, Montana.

Albanese, J. P., L. B. Davis, and C. L. Hill
1995 Upper Pleistocene Geology of the Merrell Site (24BE1659), Centennial Valley, Montana. *Current Research in the Pleistocene* 12:107-109.

Alden, W. C.
1953 *Physiography and Glacial Geology of Western Montana and Adjacent Areas.* United States Geological Survey, Professional Paper 231.

Baker, R. G.
1986 Sangamonian(?) and Wisconsinan Paleoenvironments in Yellowstone National Park. *Geological Society of America, Bulletin* 97:717-736.

Baker, R. G., and K. A. Waln
1985 Quaternary Pollen Records from the Great Plains and the Central United States. In *Pollen Records of Late-Quaternary North American Sediments*, edited by V. M. Bryant, Jr. and R. G. Holloway, pp. 191-203. American Association of Stratigraphic Palynologists Foundation

Banerjee, D., L. Bøtter-Jensen, and A. S. Murphy
2000 Estimation of the Quartz Equivalent Dose in Retrospective Dosimeter Using a Single-Aliquot Regenerative-Dose Protocol. *Applied Radiation and Isotopes* 52:831-844.

Bard, E., B. Hamelin, R. G. Fairbanks, and A. Zindler
1990 Calibration of the 14C Timescale Over the Past 30,000 Years Using Mass Spectrometric UTh Ages from Barbados Corals. *Nature* 345:405-409.

Bartholomew, M. J., S. E. Lewis, G. S. Russell, M. C. Stickney,
E. M. Wilde, and S. A. Kish
1999 *Late Quaternary History of the Beaverhead Canyon, Southwestern Montana. In* Guidebook to the Geology of Eastern Idaho, edited by S. S. Hughes and G. D. Thakray, pp. 237-250. Idaho Museum of Natural History, Pocatello.

Bartlein, P. J., M. E. Edwards, S. L. Shafer and E. D. Barker, Jr.
1995 Calibration of Radiocarbon Ages and the Inrerpretation of Paleoenvironmental Records. *Quaternary Research* 44:417-424.

Batten, D. C.
1994 Merrell 1994 Methods. Ms.
1995 Merrell Stratigraphy (Summary of 1994 Field Studies). Ms.
1996 Merrell Site (24BE1659) Methods and Procedures (Summary of Field Studies in 1994 and 1995). Ms.

Batren, D. C., and L. B. Davis
1996 The Merrell Locality 1996 Investigations. Report by the Museum of the Rockies to the Dillon Resource Area, Bureau of Land Management.

Bekoff, M.
1977 *Canis latrans. Mammalian Species* 79:1-9.

Benson, L., and R. S. Thompson
1987 The Physical Record of Lakes in the Great Basin. In *North America and Adjacent Oceans During the Last Deglaciation*, edited by W. F. Ruddiman and H. E. Wright, Jr., pp. 241-260. Boulder, Colorado, Geological Society of America, The Geology of North America, v. K-3, pp. 241-260.

Benson L. V., D. R. Currey, R. I. Dorn, K. R. Lajoie, C. G. Oviatt, S. W. Robinson, G. I. Smith, and S. Stine
1990 Chronology of Expansion and Contraction of Four Great Basin Lake Systems During the Past 35,000 Years. *Palaeogeography, Paleoclimatology, Palaeoecology* 78:241-278.

Bombin, M., and K. Muehlenbachs
1980 Potential of $^{18}O/^{16}O$ Ratios in Opaline Plant Silica as a Continental Paleoclimatic Tool. Paper, American Quaternary Association, 6th Biennial Meeting. *Abstracts and Program*, pp. 43-44.

Bonnichsen, R., M. Beatty, M. D. Turner, J. C. Turner,
and D. Douglas
1992 Paleoindian Lithic Procurement at the South Fork of Everson Creek, Southwestern Montana: A Preliminary Statement. In *Ice Age Hunters of the Rockies*, edited by D. J. Stanford and J. S. Day, pp. 285-321. Denver Museum of Natural History and University Press of Colorado.

Brodkorb, P.
1964 Catalogue of Fossil Birds: Part 2 (Anseriformes Through Galliformes). *Bulletin of the Florida State Museum, Biological Sciences* 8(3):195-335.

Brown, D. A.
1984 Prospects and Limits of a Phytolith Key for Grasses in the Central Plains. *Journal of Archaeological Science* 11:345-368.

Bump, R.
1990 Soil Formation and Paleoenvironmental Interpretation at the Merrell Pleistocene Fauna Site; Centennial Valley, Beaverhead County Montana. Draft ms., Bureau of Land Management, Dillon, Montana.
1991 May 17, 1995 Letter to District Archaeologist, BDO, Regarding the Merrell Paleontological Site with Accompanying Map.

Bryan, A. L.
1980 The Stemmed Point Tradition: An Early Technological Tradition in Western North America. In *Anthropological Papers in Memory of Earl H. Swanson, Jr.*, edited by L. B. Harten, C. N. Warren, and D. C. Tuohy, pp. 77-107. Special Publication of the Idaho Museum of Natural History. Pocatello.

Butler, B. R.
1961 The Old Cordilleran Culture in the Pacific Northwest. *Occasional Papers of the Idaho State University Museum* No. 5. Pocatello.
1962 Contribution to the Prehistory of the Columbia Plateau: A Report on Excavations in the Palouse and Craig Mountain Sections. *Occasional Papers of the Idaho State University Museum* No. 9. Pocatello.
1963 An Early Man Site at Big Camas Prairie, South-Central Idaho. *Tebiwa* 6:22–33.
1965a The Structure and Function of the Old Cordilleran Culture Concept. *American Anthropologist* 6:1120-1131.
1965b A Report on Investigations of an Early Man Site Near Lake Channel, Southern Idaho. *Tebiwa* 8(2):1-20.
1965c Contributions to the Archaeology of Southwestern Idaho. *Tebiwa* 8(1):41-48.
1973 Folsom and Plano Points from the Peripheries of the Upper Snake Country. *Tebiwa* 16(1):69-71.
1978 *A Guide to Understanding Idaho Archaeology* (Third Edition): The Upper Snake and Salmon River Country. A Special Publication of the Idaho Museum of Natural History. Pocatello.
1986 Prehistory of the Snake and Salmon River Area. In *Handbook of North American Indians, Volume 11, Great Basin*, edited by W. L. D'Azevedo, pp. 127–134, general editor W. C. Sturtevant. Smithsonian Institution, Washington, D.C.

Butler, D. R., C. J. Sorenson, and W. Dort
1983 Differentiation of Morainic Deposits Based on Geomorphic, Stratigraphic, Palynologic, and Pedologic Evidence, Lemhi Mountains, Idaho. In *Tills and Related Deposits*, edited by E. B. Evenson, C. Schlkuchter, and J. Rabassa, pp. 373-380. Rotterdam, Balkema.

Campbell, J. M.
1965 A Folsom Site in Idaho. *Plains Anthropologist* 3(6):1-12.

Carbone, V. A.
1977 Phytoliths as Paleoecological Indicators. In *Amerinds and Their Paleoenvironments in Northeastern North America*, edited by W. Newman and B. Salwin, pp. 194-205. Annals of the New York Academy of Sciences No. 288.

Chadwick, O. A., R. D. Hall, and F. M. Phillips
1997 Chronology of Pleistocene Glacial Advances in the Central Rocky Mountains. *Geological Society of America, Bulletin* 109(11):1443-1452.

Christiansen, R. C., and R. H. Blank
1972 *Volcanic Stratigraphy of the Rhyolite Plateau in the Yellowstone National Park*. United States Geological Survey, Professional Paper 729-B.

Christiansen, R. L., and G. F. Embree
1987 *Island Park, Idaho: Transition from Rhyolites of the Yellowstone Plateau to Basalts of the Snake River Plain*. Centennial Field Guide No. 6. Geological Society of America, Boulder, Colorado, pp. 103-108.

Clark, P. U., and P. J. Bartlein
1994 Correlation of Late-Pleistocene Mountain Glaciation in Western North America with North Atlantic Heinrich Events. American Quaternary Association Program with *Abstracts* of the 13th Biennial Meeting The Limnological Research Center, University of Minnesota, Minneapolis, Minnesota.

Condit, D., E. H. Finch, and J. T. Pardee
1982 Phosphate Rock in the Three Forks-Yellowstone Park Region, Montana, *U. S. Geological Survey, Bulletin* No. 795-G:147-211.

Cronberg, G.
1982 Pediastrum and Scenedesmus (Chlorococcales) in Sediments from Lake Vaxjosjon, Sweden. *Archiv für Hydrobiologie Supplement* 60(4):500-507. *Algological Studies* No. 29.
1986 Blue-green Algae, Green Algae and Chrysophyceae in Sediments. In *Handbook of Holocene Palaeoecology and Palaeohydrology*, edited by B. E. Berglund, pp. 507-526. John Wiley & Sons, Ltd., Chichester.

Currey, D. R., and C. G. Oviatt
1985 Durations, Average Rates, and Probable Causes of Lake Bonneville Expansions, Stillstands, and Contractions During the Last Deep-Lake Cycle, 32,000-10,000 Years ago. In *Problems and Prospects for Predicting Great Salt Lake Levels*, edited by P. A. Kay and H. F. Diaz, pp. 9-24. Center for Public Affairs and Administration, University of Utah, Salt Lake City.

Cushing, E. J.
1967 Evidence for Differential Pollen Preservation in Late Quaternary Sediments in Minnesota. *Review of Paleobotany and Palynology* 4:87-101, pp. 87-101.

Cwynar, L. C., E. Burden, and J. H. McAndrews
1979 An Inexpensive Sieving Method for Concentrating Pollen and Spores from Fine-grained Sediments. *Canadian Journal of Earth Science* 16:1116-1120.

Daugherty, R. D.
1962 The Intermontane Western Tradition. *American Antiquity* 28:144-150.

Davis, L. B.
1982 Montana Archaeology and Radiocarbon Chronology: 1962-1981. *Archaeology in Montana, Special Issue* No. 3.
1984 Late Pleistocene to Mid-Holocene Adaptations at Indian Creek, West-Central Montana Rockies. *Current Research in the Pleistocene* 1:9-10.
1986 Age and Source Analysis for Obsidian Hell Gap Complex Artifacts in the Montana Rockies. *Current Research in the Pleistocene* 3:27-28.
1997 Extinct Faunas in Northern Rockies and Plains Archaeological Contexts. In *Partners in Paleontology: Proceedings of the Fourth Conference on Fossil Resources*, edited by J. Johnston and J. McChristal, pp. 53-55. Natural Resources Report NPS/NRFLFO/NRR-97/01. U. S. Department of the Interior, National Park Service, Florissant Fossil Beds National Monument.

Davis, L. B., S. A. Aaberg, W. P. Eckerle, J. W. Fisher, Jr., and S. T. Greiser
1989 Montane Paleoindian Occupation of the Barton Gulch Site, Ruby Valley, Southwestern Montana. *Current Research in the Pleistocene* 6:7-9.

Davis, L. B., S. A. Aaberg, G. G. Fredlund, L. S. Cummings, and K. Puseman
1996 Barton Gulch Site Geochronology and Paleoecology. *Current Research in the Pleistocene* 13:85-87.

Davis, L. B., S. A. Aaberg, and S. T. Greiser
1988 Paleoindians in Transmontane Southwestern Montana: The Barton Gulch Occupations, Ruby River Drainage. *Current Research in the Pleistocene* 5:9-11.

Davis, L. B., S. A. Aaberg, and J. G. Schmitt
1995 The Obsidian Cliff Plateau Prehistoric Lithic Source, Yellowstone Park Wyoming. *Selections from the Division of Cultural Resources* No. 6. National Park Service, Rocky Mountain Region, Denver.

Davis, L. B., J. P. Albanese, L. S. Cummings, and J. W. Fisher, Jr.
1991 Reappraisal of the MacHaffie Site Paleoindian Occupational Sequence. *Current Research in the Pleistocene* 8:17-20.

Davis, L. B., T. A. Foor, and D. L. Smith
1997 Cattleguard No. 3: Mitigation Excavations at the South Everson Creek Chert Quarry/Workshop Site (24BE559) in Southwestern Montana. *Archaeology in Montana* 38(1):1-60.

Davis, L. B., and S. T. Greiser
1992 Indian Creek Paleoindians: Early Occupation of the Elkhorn Mountains' Southeast Flank, West-Central Montana. In *Ice Age Hunters of the Rockies*, edited by D. J. Stanford and J. S. Day, pp. 225-283. Denver Museum of Natural History and the University Press of Colorado.

Davis, L. B., and T. Helmick
1982 Inundated Prehistoric Occupation Sites Along Canyon Ferry Lake. *Archaeology in Montana* 23(3):41-84.

Davis, L. B., and C. L. Hill,
1995 Locating Paleoamerican Occupations in S. W. Montana Placered Valleys, *Current Research in the Pleistocene* 12:111-113.

Davis, L. B., C. L. Hill, J. P. Albanese, and K. W. Karsmizki
1995 The 1994 Geoarchaeological Assessment of the Merrell Locality (24BE1659), Centennial Valley, Southwest Montana. Technical Report to the Dillon Resource Office, Burte District, Bureau of Land Management by the Museum of the Rockies, Montana Srate University-Bozeman.

Davis, L. B., C. L. Hill, and J. W. Fisher, Jr.
2003 Radiocarbon Dates for Paleoindian Components (Folsom, Scottsbluff) at the MacHaffie Site, West-Centtal Montana Rockies. *Current Research in the Pleistocene* 19:18-20

Davis, L. B., and M. C. Wilson
1994 Late Quaternary Stratigraphy, Paleontology, and Archaeology of the Sheep Rock Spring Site (24JF292), Jefferson County, Montana. *Current Research in the Pleistocene* 11:100-102.

Davis, L. B., and C. D. Zeier
1978 Multi-Phase Late Period Bison Procurement at the Antonsen Site, Southwestern Montana. In: Bison Procurement and Utilization: A Symposium, edited by L. B. Davis and M. Wilson, pp. 222-235. *Plains Anthropologist, Memoir* No. 14.

Dean, W. E., Jr.
1974 Determination of Carbonate and Organic Matter in Calcareous Sediments and Sedimentary Rocks by Loss on Ignition: Comparison with Other Methods. *Journal of Sedimentary Petrology* 44:242-248.

Dimbleby, G.
1978 *Plants and Archaeology*. Humanities Press, Inc., Atlantic Highlands, New Jersey.

Dundas, R. G.
1990 The Merrell Locality: A Late Pleistocene Fauna from Southwestern Montana. *Geological Society of America, Abstracts with Programs* 22(6):8-9.
1991 A Late Pleistocene Occurrence of *Equus* and *Camelops hesternus* from the Flint Creek Area, Western Montana. *PaleoBios* 13(51):7-11.
1992 A Scimitar Cat (*Homotherium serum*) from the Late Pleistocene Merrell Locality, Southwestern Montana. *Paleobios* 14(1): 9-12.
1994 *The Demise of the Late Pleistocene Dire Wolf (Canis dirus): A Model for Assessing Carnivore Extinctions*. Ph.D. Dissertation, University of California-Berkeley.
1996 I. Fossil Fauna from the Merrell Locality 1994 and 1995 MOR Excavation II. Fossil Specimens Listed by Taxon. Ms.
1997 Fossil Inventory 1996 MOR Excavations. Ms.

Dundas, R. G., C. L. Hill, and D. C. Batten
1996 Lare Pleistocene Fauna from the Merrell Locality, Centennial Valley, Montana: Summary of the Vertebrate Remains from the 1994 and 1995 Excavations. *Current Research in the Pleistocene* 13:103-105.

Eardley, A. J.
1960 Phases of Orogeny in the Deformed Belt of Southwesrern Montana and Adjacent Areas of Idaho and Wyoming. In *West Yellowstone; Earthquake Area*. Billings Geological Society 11th Annual Field Conference, September 1960, pp. 86-91.

Esau, K.
1977 *Anatomy of Seed Plants*. Second Edition. John Wiley and Sons, New York.

Evans, G. L.
1961 The Friesenhahn Cave. *Bulletin of the Texas Memorial Museum* 2(1):3-22.

Faegri, K., and J. Iverson
1975 *Textbook of Pollen Analysis* (third edirion). Hafner Press, New York.

FAUNMAP Working Group
1994 FAUNMAP: A Database Documenting Late Quaternary Distributions of Mammal Species in the United States. *Illinois State Museum, Scientific Papers* 25(1&2).

Feathers, J. K., and C. L. Hill
2001 Dating Middle and Late Wisconsin Episode Stratigraphic Sequences in the Rockies and Missouri Plateau: Luminescence and Radiocarbon Chronologies. *Geological Society of America, Abstracts with Programs* 33(6):A287.

Fenneman, N. M., and D. W. Johnson
2001 A Physical Division of the United States. *Map Sheet* 1:7,000,000. U.S. Geological Survey Physiographic Committee.

Feth, J. H.
1961 A New Map of Western Conterminous United States Showing the Maximum Known or Inferred Extent of Pleisrocene Lakes. *Geological Survey Research* 1961, pp. B-110-B-113.

Fiedel, S. J.
1999 Older Than We Thought: Implications of Corrected Dates for Paleoindians. *American Antiquity* 64:95–115.

Flenniken, J. J., and P. J. Wilke
1989 Typology, Technology, and Chronology of Great Basin Dart Points. *American Anthropologist* 91:149-158.

Folger, D. W., L. H. Burckle, and B. C. Heezen
1967 Opal Phytoliths in a North Atlantic Dust Fall. *Science* 155:1243-1244.

Forbis, R. G.
1995 *The MacHaffie Site*. Ph.D. Dissertation, Columbia University, New York.

Forbis, R. G., and J. D. Sperry
1952 An Early Man Site in Montana. *American Antiquity* 18:127-133.

Foor, T., and J. Donahue
1987 The University of Montana Archaeological Investigations in the Centennial Valley 1986. University of Montana, Missoula, Montana.

Foreman, S. L., R. P. Smith, W. R. Hackett, J. A. Tullis,
and P. A. McDaniel
1993 Timing of Late Quaternary Glaciations in the Western United States Based on Loess on the Eastern Snake River Plain, Idaho. *Quaternary Research* 40:30-37.

Foth, H. D., L. V Withee, H. S. Jacobs, and S. J. Thien
1982 *Laboratory Manual for Introductory Soil Science*, Sixth Edition. Wm. C. Brown Company, Dubuque.

Fredlund, G.
1993 Paleoenvironmental Interpretations of Stable Carbon, Hydrogen, and Oxygen Isotopes from Opal Phytoliths, Eustis Ash Pit, Nebraska. In *Current Research in Phytolith Analysis: Applications in Archaeology and Paleoecology*, edited by D. M. Pearsall and D. R. Piperno, pp. 37-46. MASCA Research Papers in Science and Archaeology No. 10.

Frison, G. C.
1978 *Prehistoric Hunters of the High Plains*. Academic Press, Inc., New York.
1988 *Paleoindian Subsistence and Settlement During Post-Clovis Times on the Northwestern Plains: The Adjacent Mountain Ranges and Intermontane Basins*. In: Americans Before Columbus: Ice-Age Origins, edited by R. C. Carlisle, pp. 83-106. Ethnology Monographs No. 12. University of Pittsburgh.
1991 *Prehistoric Hunters of the High Plains*. Second Edition. Academic Press, Inc., New York.

Frison, G. C. (ed.)
1974 *The Casper Site: A Hell Gap Bison Kill on the High Plains*. Academic Press, Inc., New York.

Frison, G. C., and R. Bonnichsen
1966 The Pleistocene-Holocene Transition on the Plains and Rocky Mountains of North America. In *Humans at the End of the Ice Age: The Archaeology of the Pleistocene-Holocene Transition*, edited by L. G. Straus, B. V. Eriksen, J. M. Erlandson, and D. R. Yesner, pp. 303-318. Plenum Press, New York.

Frison, G. C., and D. J. Stanford
1982 *The Agate Basin Site: A Record of Paleoindian Occupation of the Northwestern High Plains*. Academic Press, Inc., New York.

Fujiwara, H.
1982 Detection of Plant Opals Contained in Pottery Walls of the Jomon Period in Kumamotu Prefecture. *Archaeology and Natural Science* 4:55-66.

Gilbert, B. M., and L. D. Martin
1984 Late Pleistocene Fossils of Natural Trap Cave, Wyoming, and the Climatic Model of Extinction. In *Quaternary Extinctions: A Prehistoric Revolution*, edited by P. S. Martin and R. G. Klein, pp. 138-147. University of Arizona Press.

Good, J. M., and K. L. Pierce
1996 *Interpreting the Landscape: Recent and Ongoing Geology of Grand Teton and Yellowstone National Parks*. Grand Teton Natural History Association, Moose, Wyoming.

Gould, W. R.
1992 *Key to the Fishes of Montana*. Montana Cooperative Fishery Research Unit, Montana Stare University, Bozeman, Montana.

Graham, R.
1986 Appendix 2, Part 1, Taxonomy of North American Mammoths. In *The Colby Mammoth Site, Taphonomy and Archaeology of a Clovis Kill in Northern Wyoming*, edited by G. C. Frison and L. C. Todd, pp. 165-190. University of New Mexico Press, Albuquerque.
Graham, R. W., H. A. Semken, Jr., and M. A. Graham
1987 *Late Quaternary Mammalian Biogeography and Environments of the Great Plains and Prairies*. Illinois State Museum, Scientific Papers No. 22.
Green, T. J., B. Cochran, T. W. Fenton, J. C. Woods, G. L. Titmus, L. Tieszen, M. A. Davis, and S. Miller
1998 The Buhl Burial: A Paleoindian Woman from Southern Idaho. *American Antiquity* 63:437–456.
Greiser, S. T.
1984 Projectile Point Chronologies for Southwestern Montana. *Archaeology in Montana* 25(1):35-52.
1986 Artifact Collections from Ten Sites at Canyon Ferry Reservoir. *Archaeology in Montana* 27(1&2):1-190.
Gruhn, R.
1961 *The Archaeology of Wilson Butte Cave, South-central Idaho*. Occasional Papers of the Idaho State College Museum No. 6. Pocatello
1965 Two Early Radiocarbon Dates from the Lower Levels of Wilson Butte Cave, South-central Idaho. *Tebiwa* 8:57.
1995 Results of New Excavations at Wilson Butte Cave, Idaho. *Current Research in the Pleistocene* 12:16-17.
Guthrie, R. D.
1990 Late Pleistocene Faunal Revolution--A New Perspective on the Extinction Debate. In *Megafauna and Man, Discovery of America's Heartland*, edited by L. D. Agenbroad, J. I. Mead, and L. W. Nelson, pp. 42-53. Scientific Papers No. 1. The Mammoth Site at South Dakota, Inc. Hot Springs, South Dakota.
Hamilton, W.
1965 *Geology and Petrogenesis of the Island Park Caldera of Rhyolite and Basalt, Eastern Idaho*. United Srates Geological Survey, Professional Paper 504-C.
Harris, A. H.
1985 *Late Pleistocene Vertebrate Paleoecology of the West*. University of Texas Press, Austin.
Haynes, G.
1991 *Mammoths, Mastodonts, and Elephants: Biology, Behavior, and the Fossil Record*. Cambridge University Press.
Helbaek, H.
1961 Studying the Diet of Ancient man. *Archaeology* 14:95-101.
Helmick, T. C.
1984 Cody Complex Artifacts in the Townsend Basin. *Archaeology in Montana* 25(1):35-51.
Herbort, D. P.
1994 Analysis of the Merrell Site (24BE1659) Lithic Assemblage. Report to the Museum of the Rockies, Montana State University-Bozeman.
Hester, J. J.
1972 *Blackwater Draw Locality No. 1. A Stratified Early Man Site in Eastern New Mexico*. Fort Burgwin Research Center, Southern Methodist University, Ranchos se Taos, New Mexico.
Hill, C. L.
1993 Sedimentology of Pleistocene Deposits Associated with Middle Paleolithic Sites in Bir Tarfawi and Bir Sahara East. In *Egypt During the Last Interglacial*, by F. Wendorf and Associates, pp. 66-105. Plenum Press, New York.
1995 A Geoarchaeological Assessment of the Merrell Site (24BE1659), Centennial Valley, Southwest Montana: An Interim Technical Report on the 1994 Field Season for the Bureau of Land Management. Unpublished ms. provided to J. P. Albanese.
1999 Radiocarbon Geochronology of Strata Containing *Mammuthus* (Mammoth), Red Rock River, Montana. *Current Research in the Pleistocene* 16:118-120.
2001a Late Pliocene and Pleistocene Geology and Paleontology in the Three Forks Basin Montana. In *Mesozoic and Cenozoic Paleontology in the Western Plains and Rocky Mountains: Guidebook for the Field Trips*, edited by C. L. Hill, pp. 113-125. Society of Vertebrate Paleontology 61st Annual Meeting, Bozeman, Montana. *Museum of the Rockies, Occasional Paper* No. 3.
2001b Pleistocene Mammals of Montana and Their Geological Context. In *Mesozoic and Cenozoic Paleontology in the Western Plains and Rocky Mountains: Guidebook for the Field Trips*, edited by C. L. Hill, pp. 113-125. Society of Vertebrate Paleontology 61st Annual Meeting, Bozeman, Montana. *Museum of the Rockies, Occasional Paper* No. 3.
Hill, C. L., and J. P. Albanese
1996 Lithostratigraphy and Geochronology of Deposits Containing Pleistocene Fossils, Centennial Valley, Montana. American Quaternary Association Program and *Abstracts* of the 14th Biennial Meetings, p. 167. Northern Arizona University, Flagstaff.
Hill, C. L., and D. Batten
1997 Spatial Distribution of Pleistocene and Holocene Faunal Remains from the MOR South Block Excavations, Merrell Locality, Centennial Valley. Ms.
Hill, C. L., and L. B. Davis
1998 Stratigraphy, AMS Radiocarbon Age and Stable Isotope Geochemistry of the Lindsay Mammoth, Eastern Montana. *Current Research in the Pleistocene* 15:109-112.
Hill, C. L., L. B. Davis, and J. P. Albanese
1995 Stratigraphic and Climatic Context of Upper Pleistocene Faunas from the Centennial Valley, Southwest Montana. Geological Society of America *Abstracts* with Program. Rocky Mountain Section, Volume 27(4):14. Forty-Seventh Annual Meeting at Montana State University-Bozeman.
Holman, J. A.
1995 Pleistocene Amphibians and Reptiles in North America. *Oxford Monographs on Geology and Geophysics* No. 32. Oxford University Press, New York.
Holmer, R. N.
1986 Common Projectile Points of the Intermountain West. In *Anthropology of the Desert West: Essays in Honor of J. D. Jennings*, edited by C. Condie and D. D. Fowler, pp. 89-115. University of Utah Anthropological Papers No. 110.
Honkala, F. S.
1949 *Geology of the Centennial Region, Beaverhead County, Montana*. Ph.D. Dissertation, University of Montana (copy in the U.S. National Archives, Washington D.C.)
1954 Geology of the Centennial Region of Southwestern Montana (*Abstract*), *Geological Society of America Bulletin* 65(12), pt. 2:1377-1378.
1960 Structure of the Cenrennial Mountains and Vicinity, Beaverhead Couny, Montana. Billings Geological Society 11th Annual Field Conference, pp. 107-115.
Hostetler, S. W., F. Giorgi, G. T. Bates, and P. J. Bartlein
1994a Lake-Atmosphere Feedbacks Associated with Paleolakes Bonneville and Lahontan. *Science* 263:665-668.
1994b Simulation of the Climate of the Western U. S. at the Last Glacial Maximum Using a Regional Climate Model. American Quaternary Association Program and *Abstracts* of the 13th Biennial Meeting. The Limnological Research Center, University of Minnesota, Minneapolis, Minnesota.
Huber, J. K.
1995 Results of a Palynological Study of Three Sediment Samples from the Merrell Mammoth Site, Beaverhead County, Montana. *Archaeometry Laboratory Report* No. 95-13 to the Museum of the Rockies.
Huber, J. K., and C. L. Hill
1997 Paleoecological Inferences from Pollen, Algae, and

Chrysophycophata in Pleistocene Sediments from Centennial Valley, Montana. *Current Research in the Pleistocene* 14:125-127.

Hughes, R. E.
1995 Geochemical Research Laboratory, *Letter Report* 95-30 to L. B. Davis, Museum of the Rockies.

Hughes, R. E., and F. W. Nelson
1987 New Findings on Obsidian Source Utilization in Iowa. *Plains Anthropologist* 32(117):313-316.

Huntley, J. L.
1980 A Fluted Point from the Jordan Creek Drainage in Northwestern Owyhee County. *Idaho Archaeologist* 3(3):7–9.
1985 A Clovis Fluted Projectile Point from Southwest Idaho. *Idaho Archaeologist* 8(1):13–14

Hurlow, H. A.
1995 Structural Style of Pliocene-Quaternary Extension Between the Red Rock and Blacktail Faults, Southwestern Montana. *Northwest Geology* 24:221-228.

Jasmann, A. D.
1963 Folsom and Clovis Projectile Points Found in Southwestern Montana. *Archaeology in Montana* 5(3):10-18.

Jefferson, G. T., and A. E. Tejada-Flores
1993 The Late Pleistocene Record of *Homotherium* (Felidae: Machairodontinae) in the Southwestern United States. In: New Additions to the Pleistocene Vertebrate Record of California, edited by R. G. Dundas and D. J. Long, pp. 37-46. *PaleoBios* 15(3).

Jones, J. G.
1993 Analysis of Pollen and Phytoliths in Residue from a Colonial Period Ceramic Vessel. In *Current Research in Phytolith Analysis: Applications in Archaeology and Paleoecology*, edited by D. M. Pearsall and D. R. Piperno, pp. 31-35. MASCA Research Papers in Science and Archaeology No. 10.

Jones, J. K., and E. C. Birney
1988 *Handbook of Mammals of the North-Central States.* University of Minnesota Press, Minneapolis, Minnesota.

Kapp, R. O.
1969 *How to Know Pollen and Spores.* W. C. Brown Company, Dobuque, Iowa.

Karrow, P. F., A. Dreimonis, and P. J. Barnett
2000 A Proposed Diachronic Revision of Late Quaternary Time-Stratigraphic Classification in the Eastern and Northern Great Lakes Area. *Quaternary Research* 54:1-12.

Kelly, E. F., R. G. Amundson, B. D. Marino, and M. J. DeNiro
1991 Stable Isotope Ratios of Carbon in Phytoliths as a Quantitative Method of Monitoring Vegetation and Climate Change. *Quaternary Research* 35:222-233.

Kennedy, C. C.
1948 (1947-1948) Geology of a Portion of the Lyon Quadrangle in Southwestern Montana, unpublished U.S. Geological Survey document. (Quoted in Honkala 1949).

King, J. E.
1973 Late Pleistocene Palynology and Biogeography of the Western Missouri Ozarks. *Ecological Monographs* 43(4):539-565.
1985 Palynological Applications to Archaeology: An Overview, edited by G. Rapp, Jr., and J. A. Gifford, pp. 135-154. *Archaeological Geology*, Yale University Press, New Haven.

King, J. E., and E. H. Lindsay
1976 Late Quaternary Biotic Records from Spring Deposits in Western Missouri. In *Prehistoric Man and His Environments: A Case Study in the Ozark Highland*, edited by W. R. Wood and R. B. McMillan, pp. 63-78. Academic Press, New York.

Kisko, L. M.
1967 *A Consideration of the Dire Wolves from the New World Pleistocene with a Statistical Study of Their Metapodials.* Master's Thesis, University of Toronto.

Knudson, R.
1983 *Organizational Variability in Late Paleo-Indian Assemblages.* Washington State University, Laboratory of Anthropology, Reports of Investigations No. 60. Pullman.

Kurman, M. H.
1985 An Opal Phytolith and Palynomorph Study of Extant and Fossil Soils in Kansas (U.S.A.). *Palaeogeography, Palaeoclimatology and Palaeoecology* 49:217-235.

Kurtén, B.
1984 Geographic Variation in the Rancholabrean Dire Wolf (*Canis dirus* Leidy) in North America. In *Contributions in Quaternary Vertebrate Paleontology: A Volume in Memorial to John E. Guilday*, edited by H. H. Genoways and M. R. Dawson, pp. 218-227. Carnegie Museum of Natural History, Special Publication No. 8.

Kurtén, B., and E. Anderson
1980 *Pleistocene Mammals of North America.* Columbia University Press, New York.

Kutzbach, J. E.
1994 Simulation of the Influence of Mountain Uplift on Global Climate. American Quaternary Association Program and *Abstracts* of the 13th Biennial Meeting. The Limnological Research Center, University of Minnesota, Minneapolis, Minnesota.

Kutzbach, J. E., and H. E. Wright, Jr.
1985 Simulation of the Climate of 18,000 yr B.P.: Results for the North American/North Atlantic/European Sector. *Quaternary Science Reviews* 4:147-187.

Lee, R. E.
1980 *Phycology.* Cambridge University Press, New York.

Leonhardy, F. C., and D. G. Rice
1970 A Proposed Cultural Typology for the Lower Snake River Region, Southeastern Washington. *Northwest Anthropological Research Notes* 4:1-29.

Lewis, R. O.
1981 Use of Opal Phytoliths in Paleoenvironmental Reconstruction. *Journal of Ethnobiology* 1:175-181.
1987 Opal Phytolith Studies from the Horner Site, Wyoming. In *The Horner Site*, edited by G. C. Frison and L. C. Todd, pp. 451-459. Academic Press, Inc.. New York.

Lohse, E. S.
1994 The Southeastern Idaho Prehistoric Sequence. *Northwest Anthropological Research Notes* 28:3-66.
1995 Northern Intermountain West Projectile Point Chronology. *Tebiwa* 25(1):3-51.

Lundelius, E. L., R. W. Graham, E. Anderson, J. Guilday, J. A. Holman, D. W. Steadman, and S. David Webb
1983 Terrestrial Vertebrate Faunas. In *Late Quaternary Environments of the United States*, Volume 1, The Late Pleistocene, edited by S. C. Porter, pp. 311-353. University of Minnesota Press.

MacDonald, L. L.
1974 *Opal Phytoliths As Indicators of Plant Succession in North-Central Wyoming.* Master's Thesis, University of Wyoming, Laramie.

Machette, M. N.
1985 Calcic Soils of the Southwestern Unites States. In: Soils and Quaternary Geology of the Southwestern United States, edited by D. L. Weide, pp. 1-23. *Geological Society of America, Special Paper* No. 203.

Maglio, V. J.
1973 Origin and Evolution of the Elephantidae. *Transactions of the American Philosophical Society*, 63(3):149.

Maher, L. J., Jr.
1972 Absolute Pollen Diagram of Redrock Lake, Boulder County, Colorado. *Quaternary Research* 2:531-553.

Maloney, N. A.
1961 *Comparative Morphology of Spores of the Ferns and Fern Allies of Minnesota* [Ph.D Thesis]. University of Minnesota, Minneapolis.

Mandryk, C. A.
1990 Could Humans Survive the Ice-Free Corridor?: Late-Glacial Vegetation and Climate in West Central Alberta. In *Megafauna and Man*, edited by L. D. Agenbroad, J. I. Mead, and L. W. Nelson, pp. 67-79. The Mammoth Site of Hot Springs, South Dakota, Inc., Scientific Papers, Vol. 1. Hot Springs, South Dakota.

Mannick, M. L.
1980 *The Geology of the Northern Flank of the Upper Centennial Valley, Beaverhead and Madison Counties, Montana*, Master of Science Thesis, Montana State University, Bozeman, Montana.

Mansfield, G. R.
1911 The Origin of Cliff Lake, Montana. *Geographic Society of Philadelphia, Bulletin* 9:10-19.
1920 Coal in Eastern Idaho. *U.S. Geological Survey, Bulletin* No. 716F:123-154.

Mason, B.
1966 *Principles of Geochemistry*. Third Edition. Wiley and Sons, New York.

McAndrews, J. H., A. A. Berti, and G. Norris
1973 *Key to Quaternary Pollen and Spores of the Great Lakes Region.* Royal Ontario Museum Life Sciences, Miscellaneous Publication.

McMannis, W. J., and F. Honkala
1960 Geological Road Log, Madison Canyon Slide to Southern Gravelly Range via Centennial Valley. Billings Geological Society 11th Annual Field Conference, pp. 284-288.

Mehringer, P. J., Jr.
1985 Late-Quaternary Pollen Records from the Interior Pacific and Northern Great Basin of the United States. In *Pollen Records of Late-Quaternary North American Sediments*, edited by V. M. Bryant, Jr. and R. G. Holloway, pp. 167-190. American Association of Stratigraphic Palynologists Foundation, Dallas, Texas.

Metcalfe, C. R.
1960 *Anatomy of the Monocotyledons*. I. Gramineae. Clarendon Press, Oxford.

Michels, J. W.
1981 The Hydration Rate for Obsidian Cliff Obsidian at Archaeological Sites in Yellowstone National Park, Wyoming. *MOHLAB Technical Reports* No. 2 State College, Pennsylvania.
1983 Hydration Rate Constants for Camas-Dry Creek Obsidian, Clark County, Idaho. *MOHLAB Technical Reports* No. 26. State College, Pennsylvania.

Miller, S. J.
1989 Characteristics of Mammoth Bone Reduction at Owl Cave, The Wasden Site, Idaho. In *Bone Modification*, edited by R. Bonnichsen and M. H. Sorg, pp. 381–393. Peopling of the Americas Publications. Center for the Study of the First Americans, Oregon State University, Corvallis.

Montagne, J. M.
1972 Quaternary System, Wisconsin Glaciation. In *Geologic Atlas of the Rocky Mountain Region*. Rocky Mountain Association of Geologists.

Moore, P. D., and J. A. Webb
1978 *An Illustrated Guide to Pollen Analysis*. Hodder and Stoughton, London.

Mulholland, S. C.
1987 *Phytolith Analysis at Big Hidatsa, North Dakota*. Ph.D. Dissertation, University of Minnesota.
1989 Phytolith Shape Frequencies in North Dakota Grasses: A Comparison to General Patterns. *Journal of Archaeological Science* 16:489-511.
1994 Phytolith Analysis of Sediment Samples from the Merrell Mammoth Site, Beaver Head County, Montana. *Archaeometry Laboratory Report* No. 94-15. University of Minnesota, Duluth.

Mulholland, S. C., and C. Prior
1993 AMS Radiocarbon Dating of Phytoliths. In *Current Research in Phytolith Analysis: Applications in Archaeology and Paleoecology*, edited by D. M. Pearsall and D. R. Piperno, pp. 21-23. MASCA Research Papers in Science and Archaeology No. 10.

Mulholland, S. C., and G. Rapp, Jr.
1985 Grass Silica Phytoliths. *Society for Archaeological Sciences Newsletter, Research Report* 5, 8(2):5-6.
1992 A Morphological Classification of Grass Silica-Bodies. In *Phytolith Systematics: Emerging Issues*, edited by G. Rapp, Jr. and S. C. Mulholland, pp. 65-89. Plenum Press, New York.

Murray, A. S., and A. G. Wintle
2000 Dating Quartz Using an Improved Single-Aliquot Regenerative-Dose (SAR) Protocol. *Radiation Measurements* 32:57-73.

Myers, W. B., and W. Hamilton
1964 Deformation Accompanying the Hebgen Lake Earthquake of August 17, 1959. *United States Geological Survey, Professional Paper* 435-I.

Nichols, D., W. J. Perry, and H. C. Haley
1985 Reinterpretation of the Palynology and Age of Laramide Syntectonic Deposits, Southwestern Montana, and Revision of the Beaverhead Group. *Geology* 13:149-153.

Nowak, R. M.
1979 *North American Quaternary Canis*. Monograph of the Museum of Natural History, University of Kansas No. 6.
1991 *Walker's Mammals of the World*. Fifth Edition, Two Volumes. The Johns Hopkins University Press, Baltimore.

Ollendorf, A. L., S. C. Mulholland, and G. Rapp, Jr.
1988 Phytolith Analysis As a Means of Plant Identification: *Arundo donax* and *Phragmites communis*. *Annals of Botany* 61:209-214.

O'Neill, J. M., T. H. Leroy, M. C. Stickney, and P. E. Carrara
1995 Neotectonic Evolution and Historic Seismicity of the Upper Madison Valley and Adjacent Gravelly Ranges in the Cliff Lake 15' Quadrangle, Southwest Montana. *Geological Society of America, Abstracts with Programs* 27:A50.

Origer, T.
1998 Letter Report of Obsidian Hydration Measurements of Paleoindian Projectile Points from Lima Reservoir, Montana. Obsidian Hydration Laboratory, Anthropological Studies Center, Sonoma State University, Rohnert Park, California, 14 May.

Pardee, J. T.
1950 Late Cenozoic Block Faulting in Western Montana, *Bulletin of the Geological Society of America* 61:359-406.

Pearsall, D. M.
1978 Phytolith Analysis of Archaeological Soils: Evidence for Maize Cultivation in Formative Ecuador. *Science* 199:177-178.

Pearsall, D. M., and M. K. Trimble
1984 Identifying Past Agricultural Activity Through Soil Phytolith Analysis: A Case Study from the Hawaiian Islands. *Journal of Archaeological Science* 11:119-133.

Phillips, F. M., M. G. Zreda, J. C. Gosse, J. Klein, E. B. Evenson, R. D. Hall, O. A. Chadwick, and P. Sharma
1997 Cosmogenic ^{36}Cl and ^{10}Bl Ages of Quaternary Glacial and Fluvial Deposits of the Wind River Range, Wyoming. *Geological Society of America, Bulletin* 109(11):1453-1463.

Pierce, K. L.
1979 History and Dynamics of Glaciation in the Northern Yellowstone Park Area. *U. S. Geological Survey, Professional Paper* 729-F.

Pierce, K. L., J. D. Obradovich, and I. Friedman
1976 Obsidian Hydration Dating and Correlation of Bull Lake and Pinedale Glaciations near West Yellowstone, Montana. *Geological Society of America, Bulletin* 87: 703-710.

Pierce, K. L., and L. A. Morgan
1992 The Track of the Yellowstone Hotspot: Volcanisim, Faulting, and Uplift, edited by P. K. Link, M. A. Kantz, and L. B. Platt, pp. 1-

53. *Regional Geology of Eastern Idaho and Western Wyoming.* Geological Society of America, Memoir No. 179.

Piperno, D. R.
1984 A Comparison and Differentiation of Phytoliths from Maize and Wild Grasses: Use of Morphological Criteria. *American Antiquity* 49:361-383.
1985 *Phytolith Analysis and Tropical Paleoecology: Production and Taxonomic Significance of Siliceous Forms in New World Plant Domesticates and Wild Species.* Review of Palaeobotany and Palynology 45:185-228.
1988 *Phytolith Analysis: An Archaeological and Geological Perspective.* Academic Press, Inc., New York.

Plew, M. G.
2000 *The Archaeology of the Snake River Plain.* Boise State University, Idaho.

Plew, M. G., and G. R. Scott
2003 A Clovis Point from the Big Springs Creek Area, Owyee County, Idaho. *Idaho Archaeologist* 26(1):7–9.

Pohl, R. W.
1978 *How to Know the Grasses.* Third Edition. Wm. Brown Pub. Co., Dubuque Iowa.

Porter, S. C., K. L. Pierce, and T. D. Hamilton
1983 Late Wisconsin Glaciation in the Western United States. In *Late Quaternary Environments of the United States,* Volume I, edited by H. E. Wright, Jr., pp. 71-111. University of Minnesota Press, Minneapolis.

Pough, R. H.
1953 *Audubon Guides, All the Birds of Eastern and Central North America.* Doubleday & Company, New York.

Prescott, G. W.
1982 *Algae of the Western Great Lakes Area.* Otro Koeltz Science Publishers, Koenigstein.

Prescott, J. R., D. J. Huntley, and J. T. Hutton
1993 Estimation of Equivalent Dose in Thermoluminescence Dating - the Australian Slide Method. *Ancient TL* 11:1-5.

Prescott, J. R., and J. T. Hutton
1988 Cosmic Ray and Gama Ray Dose Dosimetry for TL and ESR. *Nuclear Tracks and Radiation Measurements* 14:223-235.

Rasmussen, D. L.
1974 New Quaternaty Mammal Localities in the Upper Clark Fork River Valley, Western Montana. *Northwest Geology* 3:62-70.

Rawn-Schatzinger, V. M.
1992 The Scimitar Cat (*Homotherium serum* Cope), Osteology, Functional Morphology, and Predatory Behavior. *Illinois State Museum, Reports of Investigations* No. 47.

Rawn-Schatzinger, V. M., and R. L. Collins
1981 Scimitar Cats, *Homotherium serum* Cope from Gassaway Fissure, Cannon County, Tennessee and the North American Distribution of Homotherium. *Journal of the Tennessee Academy of Science* 56(1):15-19.

Reeves, B. O. K.
1969 The Southern Alberta Paleo-Cultural Paleo-Environmental Sequence. In *Post-Pleistocene Man and His Environment on the Northern Plains,* edited by R. G. Forbis, L. B. Davis, O. A. Christensen, and G. Fedirchuk, pp. 6-47. The University of Calgary Archaeological Association Proceedings.

Rice, H. S.
1965 *The Culture Sequence at Windust Cave.* Master's Thesis, Department of Anthropology, Washington State University, Pullman.

Richmond, G. M.
1986a Stratigraphy and Chronology of Glaciations in Yellowstone National Park. In *Quaternary Glaciations in the Northern Hemisphere,* edited by V. Sibrava, D. Q. Bowen, and G. M. Richmond, pp. 83-98. *Quaternary Science Reviews* 5.
1986b Stratigraphy and Correlation of Glacial Deposits of the Rocky Mountains, the Colorado Plateau, and the Ranges of the Great Basin. In: Quaternary Glaciations in the Northern Hemisphere, edited by V. Sabra, D.Q. Bowen, and G.M. Richmond, pp. 99-127. *Quaternary Science Reviews* 5: 99-127.

Richmond, G. M., and D. S. Fullerton
1986 Summation of Quaternary Glaciations in the United States of America. In: Quaternary Glaciations in the Northern Hemisphere, edited by V. Sabra, D. Q. Bowen, and G. M. Richmond, pp. 183-196. *Quaternary Science Reviews* 5.

Ringe, B. L., R. N. Holmer, S. J. Miller, J. Hearst, and W. Akersten
1988 Super Conducting Super Collider. *Idaho Museum of Natural History, Reports of Investigations* No. 5. Pocatello.

Robbins, C. S., B. Bruun, and H. S. Zim
1966 *A Guide to Field Identification, Birds of North America.* Golden Press, New York.

Rosen, A. M.
1987 Phytolith Studies at Shiqmim. In *Shiqmim I,* edited by T. E. Levy, pp. 243-249. *BAR International Series* No. 356.

Ross, C. P., D. A. Andrews, and I. J. Witkind
1955 *Geologic Map of Montana.* U. S. Geological Survey, prepared in cooperation with the Montana Bureau of Mines and Geology, Butte.

Rovner, I.
1971 Potential of Opal Phytoliths for Use in Paleoecological Reconstruction. *Quaternary Research* 1:343-359.
1983 Plant Opal Phytolith Analysis: Major Advances in Archaeobotanical Research. In *Advances in Archaeological Method and Theory,* edited by M. Schiffer, Volume 6, pp. 225-266. Academic Press, Inc., New York.
1988 Macro- and Micro-Ecological Reconstruction Using Plant Opal Phytolith Data from Archaeological Sediments. *Geoarchaeology* 3:155-163.

Rowlett, R. M., and D. M. Pearsall
1993 Archaeological Age Determination Derived from Opal Phytoliths by Thermoluminescence. In *Current Research in Phytolith Analysis: Applications in Archaeology and Paleoecology,* edited by D. M. Pearsall and D. R. Piperno, pp. 25-29. MASCA Research Papers in Science and Archaeology. Pennsylvania State University, State College.

Roy, W. R., and R. D. Hall
1981 *Glacial Geology of the South Boulder Valley Tobacco Root Range, Montana.* Montana Geological Society 1981 Field Conference, Southwest Montana, pp. 125-132.

Ruddiman, W. F.
1994 Evidence of Uplift, Climate Change, and Ice-Sheet Development. American Quaternary Association Programs and *Abstracts* of the 13th Biennial Meeting. The Limnological Research Center, University of Minnesota, Minneapolis.

Ruppel, E. T.
1982 Cenozoic Block Uplifts in East-Central Idaho and Southwest Montana. *Geological Survey, Professional Paper* No. 1224. U. S. Government Printing Office, Washington D.C.

Sappington, L.
1979 Letter from Sappington at Laboratory of Anthropology, University of Idaho, to Sara Scott ar the Helena National Forest.

Sargeant, K. E.
1973 *The Haskett Tradition: A View from Redfish Overhang.* Master's Thesis, Department of Anthropology, Idaho State University, Pocatello, Idaho.

Schmitt, J. G., J. C. Haley, D. R. Lageson, B. K. Horton, and P. A. Azevedo
1995 Sedimentology and Tectonics of the Babback-McKnight Canyon-Red Butte Area, Southwest Montana: New Perspectives on the Beaverhead Group and the Sevier Orogenic Belt. *Northwest Geology* 24:245-313.

Schneider, N. P.
1990 Terrace Geomorphology of the Central Madison Valley. In *Quaternary Geology of the Western Madison, Tobacco Root Range*

and the Jefferson Valley, edited by R. D. Hall, pp. 24-50. Rocky Mountain Friends of the Pleistocene Guidebook.

Schreve-Brinkman, E. J.
1978 A Palynological Study of the Upper Quaternary Sequence in the El Abra Corridor and Rock Shelters (Colombia). *Palaeogeography, Palaeoclimatology and Palaeoecology* 25:1-109.

Schofield, J. D.
1981 *Structure of the Centennial and Madison Valleys Based on Gravitational Interpretation.* Montana Geological Society 1981 Field Conference, Southwest Montana, pp. 275-283.

Scholten, R., K. Keenmon, and W. O. Kupsch
1965 Geology of the Lima Region, Southwestern Montana and Adjacent Idaho. *Bulletin of the Geological Society of America* 66:345-404.

Sonderegger, J. L.
1981 *Geology and Geothermal Resources of the Eastern Centennial Valley.* Montana Geological Society 1981 Field Conference, Southwest Montana, pp. 357-363.

Sonderegger, J. L., J. D. Schofield, R. B. Berg, and M. L. Mannick
1982 The Upper Centennial Valley, Beaverhead and Madison Counties, Montana. *Montana Bureau of Mines and Geology, Memoir* No. 50.

Sowers, T. A., and M. Bender
1995 Climate Records During the Last Deglaciation. *Science* 269:210-214.

Spaulding, W. G.
1991 Pluvial Climatic Episodes in North America and North Africa: Types and Correlation with Global Climate. *Palaeogeography, Palaeoclimatology and Palaeoecology* 84:217-227.

Stickney, M. C.
1995 Oral communication ro C. L. Hill.

Stickney, M. C., and J. J. Bartholomew
1987 Seismicity and Late Quaternary Faulting of the Northern Basin and Range Province, Montana and Idaho. *Bulletin of the Seismology Society of America* No. 77:1602-1625.

Stickney, M. C., M. J. Bartholomew, and E. Wilde
1987 Trench Logs Across the Red Rock, Blacktail, Lima Reservoir, Georgia Gulch, Vendome, and Divide Faults, Montana, *Geological Society of America, Abstracts with Programs* 19(5):337-338.

Srokes, D., and L. Stokes
1996 *Stokes Field Guide to Birds,* Western Region. Little, Brown and Company, New York.

Sturchio, N. C., K. L. Pierce, M. T. Murrell, and M. L. Sorey
1994 Uranium-Series Ages of Travertines and Timing of the Last Glaciation in the Northern Yellowstone Area, Wyoming-Montana. *Quaternary Research* 41:265-277.

Swanson, E. H., Jr.
1961 Folsom Man in Idaho. *American Antiquity* 28:151-158.
1972 *Birch Creek: Ecology in the Cool Desert of the Northern Rockies 9,000 B.C. - A.D. 1850.* The Idaho State University Press.

Thompson, R. G.
1986 The Recovery of Opal Phytoliths from Ceramics and Plains Anthropological Studies. Paper presented at the 44th Annual Plains Conference. *Program and Abstracts*, p. 58. Lincoln, Nebraska.

Thompson, R. G., and S. C. Mulholland
1994 Identification of Corn in Food Residues on Utilized Ceramics at the Shea Site (32CS101). *Phytolitharien Newsletter* 8(2):7-11.

Thornbury, W. D.
1965 *Regional Geomorphology of the United States.* John Wiley and Sons, New York.

Titmus, G. L.
1987 The Blue Lakes Clovis. *Idaho Archaeologist* 10(2):39–40.

Titmus, G. L., and J. C. Woods
1990 West Clover Clovis. *Idaho Archaeologist* 13(1):15–17.
1991 Fluted Points from the Snake River Plain. In *Clovis Origins and Adaptations*, edited by R. Bonnichsen and K. L. Turnmire, pp.119–131. Peopling of the Americas Publications. Center for the Study of the First Americans, Oregon State University, Corvallis.

Turner, B. L., III, and P. D. Harrison
1981 Prehistoric Raised-Field Agriculture in the Maya Lowlands. *Science* 213:299-405.

Turner, M. D., M. T. Beatty, M. Klages, P. McDaniel, J. C. Turner, and R. Bonnichsen
1991 Late Pleistocene-Early Holocene Paleoclimates and Environments of Southwestern Montana. *Current Research in the Pleistocene* 8:119-122.

Turner, M. D., J. C. Turner, and R. Bonnichsen
1988 A Long Pleistocene Glacial Sequence in Southwestern Montana. *Current Research in the Pleistocene* 5:96-97.

Tushingham, A. M., and W. R. Peltier
1993 Implications of the Radiocarbon Timescale for Ice-Sheet Chronology and Sea-Level Change. *Quaternary Research* 39:125-129.

Twiss, P. C., E. Suess, and R. M. Smith
1969 Morphological Classification of Grass Phytoliths. *Soil Science Society of America, Proceedings* 33:109-115.

Udvardy, M. D. F.
1977 *The Audubon Society Field Guide to North American Birds, Western Region.* Alfred A. Knopf, New York.

Van Andel, T. H.
1997 Middle and Upper Paleolithic Environments and the Calibration of ^{14}C Dates Beyond 10,000 B.P. *Antiquity* 72:26-31.

Van Geel, B.
1978 A Palaeoecological Study of Holocene Peat Bog Sections in Germany and the Netherlands, Based on the Analysis of Pollen, Spores and Micro and Macroscopic Remains of Fungi, Algae, Cormophytes and Animals. *Review of Palaeobotany and Palynology* 25:1-120.
1986 Application of Fungal and Algae Remains and Other Microfossils in Palynological Analyses. In *Handbook of Holocene Palaeoecology and Palaeohydrology*, edited by B. E. Berglund, pp. 497-505. John Wiley & Sons, Ltd., Chichester.

Van Zant, K. L.
1976 *Late and Postglacial Vegetational History of Northern Iowa.* Ph.D Thesis, University of Iowa, Iowa City.
1979 Late Glacial and Postglacial Pollen and Plant Macrofossils from Lake West Okoboji, Northeastern Iowa. *Quaternary Research* 12:353-380.

Watts, W. A., and R. C. Bright
1968 Pollen, Seed, and Mollusk Analysis of a Sediment Core from Pickerel Lake, Northeastern South Dakota. *Geological Society of America, Bulletin* 79:855-876.

Watts, W. A., and T. C. Winter
1966 Plant Macrofossils from Kirchner Marsh, Minnesota – A Palaeoecological Study. *Geological Society of America, Bulletin* 77:1339-1360.

Webb, T., III, P. J. Bartlein, S. P. Harrison, and K. H. Anderson
1993 Vegetation, Lake Levels, and Climate in Eastern North America for the Past 18,000 Years. In *Global Climates Since the Last Glacial Maximum*, edited by H. E. Wright, Jr., J. E. Kutzbach, T. Webb III, W. F. Ruddiman, F. A. Street-Perrott, and P. J. Bartlein, pp. 415-467. University of Minnesota Press, Minneapolis.

Wilding, L. P.
1967 Radiocarbon Dating of Biogenetic Opal. *Science* 156:66-67.

Williams, N. E.
1981 Aquatic Organisms and Palaeoeoecology: Recent and Future Trends. In *Perspectives in Running Water Ecology*, edited by M. A. Lock and D. D. Williams, pp. 289-303. Plenum Press, New York.

Witkind, I. J.
1972 Geologic Map of the Henrys Lake Quadrangle, Idaho and

Montana. *United States Geological Survey, Map* I-781-A.
1975 Geology of a Strip Along the Centennial Fault, Southwestern Montana and Adjacent Idaho. *United States Geological Survey Map* I-890
1975 Preliminary Map Showing Known and Suspected Active Faults in Western Montana. Open-file Report 75-285. U. S. Geological Survey, Denver.
1976 Geologic Map of the Southern Part of the Red Rock Lake Quadrangle, Southwestern Montana and Adjacent Idaho. *United States Geological Survey, Map* I-943.

Witkind, I. J., and H. J. Prostka
1980 Geologic Map of the Southern Part of the Lower Red Rock Lake Quadrangle, Beaverhead and Madison Counties. *United States Geological Survey, Map* I-1216.

Woods, J. C., and G. L. Titmus
1985 A Review of the Simon Clovis Collection. *Idaho Archaeologist* 8(1):3–8.

Wright, G. A., and S. J. Miller.
1976 Prehistoric Hunting of New World Wild Sheep: Implications for the Study of Sheep Domestication. In *Cultural Change and Continuity: Essays in Honor of James Bennett Griffin*, edited by C. E. Cleland, pp. 293–312. Academic Press, New York.

Yohe, R. M., II, and J. Uren
1993 A Clovis Point from Coyote Wells, Malheur County, Eastern Oregon. *Idaho Archaeologist* 16(2):15–17.

Yohe, R. M., II, and J. C. Woods
2002 *The First Idahoans: A Paleoindian Context for Idaho.* State Historic Preservation Office, Idaho State Historical Society, Boise.

Zeveloff, S. I.
1988 *Mammals of the Intermountain West.* University of Utah Press, Salt Lake City, Utah.

Appendix A. Merrell Site Datum Controls.

David C. Batten

Table 1. Locations of Corners in South Block (Excavation Area I) with Respect to General Site Grid. The following two corners were shot in with a transit and tape:

SW corner of	Northing	Easting
If	163.20N	121.23E
Ic	164.06N	121.13E

The locations of the following corners could then be calculated:

Ia	160.48N	124.02E
Ib	162.27N	124.02E
Id	159.62N	123.12E
Ie	161.41N	123.12E

Table 2. Elevation Points, Their Locations and Elevations.

Elevation Point	Northing	Easting	Elevation (masl)
El	127.52	120.55	2011.51
E2	159.00	124.69	2010.97
E3	119.49	126.36	2009.29
E4	154.72	126.64	2009.40
E5	155.81	126.48	2009.35
E6	159.34	125.93	2009. 10
E7	165.55	123.21	2009.85
E8	169. 17	121.95	2009.38
E9	111.88	125.08	2009. 10
E10	140.17	126.11	2009.05
Ell	122.27	91.29	2012.73
E12	150.28	126.17	21011.28 (blue flag)
E13	147.34	125.72	2011.52 (D. Austin's orange flag)

Table 3. Locations of Excavation Areas in South Block and Their Status at Closing of the Excavation Season.

XU	Location of SW corner of XU Northing/Easting		
J	121	125	excavated through Strat Unit B (into A:')
K	123	125	excavated through Strat Unit B
L	125	125	15 cm x 31 cm portion excavated thru B
M	127	125	not excavated
N	129	125	excavated through Strat Unit B
O	131	125	excavated through Strat Unit B
P	133	125	excavated through Strat Unit B
Q	135	125	not excavated
R	121	123	east half to top of Strat Unit B
S	123	123	east half to top of Strat Unit B
T	125	123	east half to top of Strat Unit B
U	127	123	east half to top of Strat Unit B
V	129	123	20-30 cm above B
W	131	123	20-30 cm above B
X	133	123	NW 1/4 excavated through Strat Unit B
Y	135	123	not excavated
Z	121	121	Tier 1
AA	123	121	Tier 1
BE	125	121	Tier 1
CC	127	121	Tier 1
DD	129	121	Tier 1
EE	131	121	Tier 1
FF	133	121	Tier 1
GG	135	121	Tier 1

Table 4. Excavated Excavation Areas in South Block, and Tbeir Starting Elevations.

XU	Tier	Quadrants Excavated	Start elev (20xx.xx) SW	NW	NESE
N	2	SW, NW	09.60	09.58	
O	2	SW, NW	09.58	09.54	
P	3	SW, NW			
J	3	SW, NW			
K	3	SW, NW			
X	3	SE, NE			

Table 5. Datum Points.

Datum	Elevation @ground	@string
I	2010.23	2010.37
J	2009.79	2009.91
M	2009.64	2009.73
New M	2009.64	2009.63
O	2009.56	2009.63
S	2010.10	2010.07
U	2009.76	2009.83
V	2009.62	2009.66
X	2009.60	2009.70

Appendix B. Descriptions of Sediments and Soils at Various Stations.

John P. Albanese

Stations are located in Figure 2. Abbreviations used in descriptions are:

vfg	very fine-grained	ps	poorly sorted
fg	fine-grained	ws	well-sorted
mg	medium-grained	vws	very well-sorted
cg	coarse-grained	brn	brown
ls	limestone	wh	white
qtz	quartzite	wr	well-rounded

STATION 1 (18)

Stratum	Thickness (cm)	Description
E	92+	Colluvium, massive; composed of sand, vfg-fg, silty, clayey; contains randomly distributed ls pebbles, .5 - 6 cm long. A soil with Ak-Bk soil horizons is superimposed on the colluvium. The A-horizon is dark brn in color and ±41 cm thick; the Bk-horizon is 51+ cm thick.
		* The section is situated at the bottom of a draw drained by a southeast-trending, first-order ephemeral stream. All succeeding measured sections, unless otherwise stated, were measured along the ±3-4-m-high scarp that borders Lima Reservoir on the west.

STATION 1 A

E	210	Colluvium, massive; composed of fg sand with 5-10%, randomly distributed, wr, 1-8-cm-long pebbles, principally composed of ls. Two soil horizons are superimposed on the massive colluvium: (a) Ak, 91 cm thick, pale grayish brn color. (b) Bk, 119+ cm thick, prominent wh $CaCO_3$ cement, Stage 2 - 3.
		* In most of Ak soil horizon, pebbles have film of $CaCO_3$ on basal surface; at base of Ak-horizon and within all of Bk-horizon, pebbles are completely coated by film of wh $CaCO_3$.

STATION 2

E	152	Colluvium as at Stations 1 and 1A; massive sand with intermixed pebbles. Displays two soil horizons: an upper, 15-cm-thick, weak A horizon and a lower 137-cm-thick Bk-horizon with Stage 1 $CaCO_3$ development (carbonate-coated pebbles) in the upper 61 cm and Stage 2 development (filaments) in the lower 91 cm.
A	158	Upper 71 cm displays pronounced limonitic mottling and staining; Unit can be divided into two main lithologic units: (a) upper 48 cm consists of sand, massive vfg - fg, silty, clayey, basal 20 cm contains "vague," thin (±1-cm) "lenses" of dispersed .5-1-cm long, wr pebbles; and (b) lower 110 cm consists of massive lt green, clayey silt. The upper 64 cm of unit is highly fractured; displays rectangular fracture pattern with fractures spaced .5-1 cm apart; the intensity of fracturing decreases with depth; fractures may be result of frost action.

STATION 3

B - C	67	Limonite-stained zone lies 48-67 cm below ground surface; "vague" exposure since much of interval is covered.
Covered Interval	333	
A	160	

STATION 4

E	37	Colluvium.
B - C	55	Limonitic stain in basal ±30 cm.
A	460	Upper ±350 cm; sand, massive, vfg moderately with HC1, few isolated pebbles, coated with $CaCO_3$; basal 110 cm composed of lt gray siltstone.

STATION 5

E	60	Colluvium.
B - C	115	Limonitic, highly fractured (rectangular).
A	175	Basal 1.4 m is covered.

STATION 5A

E	46	Colluvium.
B - C	76	Limonitic stain prominent.
A	298	Sand, massive, lt gray, vfg, silty; jointed, limonitic stain along joint planes. No pebbles observed.

STATION 6		
E	49	Colluvium.
B - C	125	Basal 30 cm of interval displays limonitic stain.
A	320	Basal 150 cm of interval is covered.
STATION 7		
E	50	Colluvium.
C	91	
B	30	Fades out into limonitic gley zone ca. 3.7 m south of Station 7.
A	277	Sand, massive vfg, silty, clayey; some mg fraction, limonitic stain; "jointed," rectangular, 2 x 4 cm.
		* 6.1 m north of Station 7; isolated pebbles (±1 cm long) in basal portion of stratum A; two lenses occur 1.16 m and 1.4 m above base of exposure; consist of cg sand and intermixed pebbles (±1 cm long); lenses are ±4 cm thick and ±2 m long.
STATION 9		
E	43	Colluvium.
C	165	Thin interbeds of sand; same type sediments as in excavated stratum E.
B	51	Dark brown, organic-rich bed; displays individual "stacked" lenses of different hue; three long bone fragments, 6-8 cm long, lie immediately below unit at point 1.2 m south of Station 9.
A	245	
STATION 10		
E	40	Colluvium.
C	155	Interbedded sand lenses; consist of laminated, cg, ws, loose, clean sand and lt green vfg, vws, silty sand. Lenses are 1-4 cm thick and ±1 m long. Some sand lenses also contain pebbles that are .5-5 cm long.
B	55	Dark brown, organic-rich bed; not solid color, contains some 1-2-cm-thick laminae. Bed undulates 30 cm/7 m. At point located 7.3 m north of station, stratum B has relief of 46 cm in 122 cm horizontal distance.
A	280	Sand, massive, vfg, silty; "salt and pepper" texture; grades to sandy silt; some limonitic staining.
STATION 11		
E	61	Colluvium.
C	100	Interbedded sands.
B	52	Organic-rich horizon.
A	233	
STATION 12		
E	60	Colluvium.
C	76	Interbeds of sand.
B	30	Organic-rich horizon.
A	334	Sand, massive lt gray, vfg, silty, clayey, some limonitic stain, lt limonitic stain along planes, rectangular structure (2 x 5 cm); sand contains some scattered pebbles, .5-2 cm long; also, local concentrations of pebbles occur in basal portion of Unit where they constitute up to 25% of sediment; few 10-15-cm-long cobbles are randomly oriented; stratum A displays some soft sediment deformation, e.g., flame structures with 46 cm of relief.

STATION 12A (located 4.6 m north of Station 12)

E	73	Colluvium (sand and pebbles).
C	110	
C(4)	13	Sand and pebbles, massive; "fades out" to south.
B	14	Color change from gray (south) to dark brown (north).
A	361	

STATION 12B (located at intersection of top of scarp and grid line 160 N)

E	44	
C(6)	116	
C (4)	20	
C	24	
B	0	Unit is absent due to truncation at a point (E6) located 10 cm to south of Station 12B.
A	280	Sand, massive, vfg, silty; "salt and pepper" texture; grades to sandy silt; some limonitic staining.

STATION 30

E	43	Colluvium.
A	121	Sand, vfg - fg, silty, clayey; contains random pebbles .5-2-cm-long plus local ±25-cm-long concentration (3%-4%) of pebbles; contains spotty limonitic staining. A 1-cm-thick layer of yellow iron stain at very top of unit.
	64	Covered.

STATION 31A

E	46	Colluvium, sandy.
C(6)	91	Sand, massive, vfg - mg, ps, silty, very clayey with randomly scattered pebbles (ls and qtz), 1-6 cm long. Unit has Stages 1 and 2 $CaCO_3$ development (white $CaCO_3$ cement); displays limonitic stain, blocky, highly weathered.
C(5)	38	Sand, massive, lt brown (limonitic stain), vfg - cg, ps, clayey, silty; contains scattered pebbles and cobbles 4-10 cm long, principally composed of ls and qtz; few 1-2-cm-long pebbles. Lithology changes ±40 cm to south of Station 31A, where bed (C4) consists of wh, sandy (vfg), clayey silt impregnated with $CaCO_3$.
D	21-61 cm	Mammoth bone-bearing horizon; composed of silty, clayey sand and intermixed cobbles and pebbles. Cobbles range to 25 cm in length and are randomly distributed. They are composed of limestone and quartzite. Stratum D is only ±7 m wide. The basal contact slopes ±25° to the east and unconformably overlies stratum A. The mammoth bone is concentrated in the central portion of the unit within a ±2-m-wide area. Stratum D is the "remnant" of a debris-flow deposit that had accumulated at the bottom of an "paleoarroyo" that was incised into both strata C and A (see Plate 3). Stratum D extends 4 m south of Station 31A. Here, it displays dark "limonitic" staining in its upper portion.
A(1)	20+	Sand, thinly bedded; layers 2-4 cm thick and composed of very clean vfg-fg, ws sand, which alternates and interfingers with more consolidated sand lenses that are fg and vws. Sand lenses are 30-60 cm long.

* Stratum C(5) fades out and interfingers with stratum C(4) at a point located--cm south of Station 13A. C(4) is a clayey silt that contains a few mg-sized sand grains; color is white due to $CaCO_3$ cement. C(4) varies in thickness from 20 cm at its north edge to a maximum of 60 cm. It is approximately 7 m long and fades out to the south in the vicinity of Station 12A (see Plate 3).

STATION 33

E	280	All exposed sediment is colluvium. In descending order, sub-units are: (a) 23 cm, Ak soil horizon; sand, fg-mg, fs, contains dispersed pebbles, 1-2-cm-long, some covered with $CaCO_3$;

pebbles increase in size to south (8-10 cm long); are covered with $CaCO_3$.
(b) 17 cm, transition between Ak and Ck soil horizons.
(c) 46 cm, Bk soil horizon, lt green, sandy (vfg), clayey silt; Stage 2 - 3 $CaCO_3$ development at top, $CaCO_3$ cement content diminishes downward.
(d) 97 cm, Ck soil horizon, lt brown sediment A/A, contains +20% randomly distributed pebbles (.5-2 cm) long) in upper 25 cm; marked decrease in $CaCO_3$ content; interval displays pronounced rectangular (blocky) structure (rectangles .5-1 cm long).
(e) 46 cm; cobble deposit, modern beach deposits.

TEST PIT/EXCAVATION AREA C (2 x 2 m)

E	56	Sand and intermixed pebbles; pebbles are coated with $CaCO_3$.
----------erosional surface----------		
C	43	Sand, laminated, vfg - fg, silty, clayey; contains horizontal lenses (±.5 cm thick and 30-76 cm long) of fg - mg sand with included wr pebbles (.5-1 cm long); laminae are ±.3-cm thick and discontinuous and display faint limonitic staining; Unit is superimposed by Bk soil horizon with Stage 2 development; displays wh $CaCO_3$ concretions, .5-1 cm wide. Unit also contains root casts that attain lengths of 76 cm and are filled with white $CaCO_3$.
----------erosional surface----------		
	183+	Sand, lt gray, general massive appearance, hint of laminae, vfg, silty, clayey grades to sandy silt; contains ±1% pebbles and bone scraps (1-2 cm long) disseminated throughout interval; Unit displays three erosional surfaces that slope 10°.

* Stratum C probably formed in an ephemeral or braided-stream environment. Erosional surfaces separate strata E and C and also occur within C. Pit walls display indications of soft sediment deformation.

TEST PIT/EXCAVATION AREA E - South Wall (2 x 2 m)

E(LD5)	46	Colluvium, sandy.
C(LD3 & 4)	170	Fluvial section composed of interdigitated lenses comprised of lt gray, vfg silty sand. Lenses are 2-4 cm thick and 2-3 m long; Unit displays prominent limonitic staining.
B(LD1 & 2)	51	Organic-rich horizon; consists of 2.5-10-cm-thick individual lenses that vary from light to dark brown in color. The lenses are composed of vfg, silty, clayey sand. A mammoth tooth lies in the center of Unit. Prominent examples of soft sediment deformation are displayed on the wall of stratum E, e.g., flame structures, folds, intrusive masses, and small normal faults. Krotovina are prominent in walls. The sediments on the walls of strata C and E were documented in detail by CLH.
A	280	Sand, massive, vfg, silty; "salt and pepper" texture; grades to sandy silt; some limonitic staining.

LAKE SHORE RECONNAISSANCE – 1994

LOCALITY 1: Shoreline exposure, ± 4 m high.

At the north side of the locale, exposures display strata composed of vfg, silty sands equivalent to stratum A at the Merrell site. These fine-grained sediments interfinger with sediments to the south that consist of 30-60-cm-thick red and gray lenses mainly composed of pebbles and cobbles of limestone.

LOCALITY 2: Shoreline exposures, ±4.6 m high.

Northern Exposure

Exposed sediment consists of massive debris-flow deposits composed of .5-10-cm-long, limestone cobbles and pebbles encased in a matrix of red, vfg- granule size, ps sand; no fining upward. Surface soil consists of Ak-C-Bk-horizons. Ak-horizon better developed than at Merrell site.

Southern Exposure

Section consists mainly of debris-flow sediment as above; however, most of the steep face of the line escarpment is covered by a 60-80-cm-thick veneer of recent colluvium composed of pebbles and sand. At the base of the bank, a vfg, silty sand that grades to sandy silt is exposed. It displays 10-15-cm-thick horizontal bedding. A similar lithology is exposed at the top of the bank. A coarse debris-flow sediment (mostly covered) lies between the two fine-grained sediment exposures.

LOCALITY 3: Shoreline exposure, ±5 m high.

Exposed sediment section is similar to that at Locality 2. A red diamectite is present in the upper one-third of the scarp. The lower two-thirds is thin-bedded (10-15 cm) and mainly consists of lenses of either vfg or cg sand; basal 25 cm of exposure consists of massive, silty clay that grades to clayey silt.

Locality 3A: Shoreline exposure, southern end; bank is ±6 m high.

Exposed sediments, in descending order:

Est. Thickness (cm)	Description
100	Stratum 4; reddish-colored beds (8-60 cm thick) composed of silty sand; few pebbles at top.
350	Stratum 3; lt brn, thin-bedded, clayey silt.
33	Stratum 2; lacustrine sediment, dark brn, laminated (laminae are .5-8 cm thick); interval contains abundant gastropods.
150	Stratum 1; alluvium, grayish brn, sandy, thin-bedded (1.25-18 cm thick); overbank deposits.

LOCALITY 3B: Shoreline exposure, located ±60 m south of Locality 3A.

Sediment is similar to that at Locality 3A. Stratum 2 is 43 cm thick and contains abundant gastropods. Stratum 3 is ±110 cm thick, thin-bedded (2.5-6.5 cm thick), and composed of sli sandy (vfg) silt.

LOCALITY 3C: Shoreline exposure, ±4 m high.

Exposed sediments, in descending order:

Est. Thickness (cm)	Description.
120	Covered.
60	Stratum 3; thin-bedded, sandy silt.
55	Stratum 2; lacustrine; contains abundant gastropods.
15	Stratum 1; thin-bedded alluvium; gastropods at base.
150	Alluvium; consists of lenses, 10-20 cm thick, composed of cg sand and cobbles.

Appendix C. Merrell Locality Identified Fossil Specimens Listed By Taxon.

Robert G. Dundas

The following lists the specimens in the Museum of the Rockies collection. Under each taxon is a general specimen identification, along with associated information in brackets. Within the brackets are excavation year/museum box number/catalog number or, in the absence of a catalog number, whatever is written on the bag in which the specimen is stored.

Osteichthyes
- Parietal fragment [1994/MS-686/LI94.5.246]. CN-25-3
- Skull bone fragment, ?suborbital [1994/MS-686/LI94.5.248]. CN-17-2
- Skull bone fragment [1994/MS-686/LI94.5.249]. CN-18-5
- 2 bones: ?opercular fragment and a parietal fragment [1994/MS-686/LI94.5.247]. CN-25-2
- Trunk vertebra [1995/MS-751/LI95.2.536]. (95.2.36)
- Skull bone fragment [1995/MS-751/LI95.2.21].

Anatidae
- thoracic vertebra [1994/MS-686/LI94.5.245]. CS-18-4
- extreme distal end of left humerus [1994/MS-685/L194.5.455/EN-20-2].

Olar buccinator
- proximal end of a left humerus [1996/MS-974/LI96.4.190] Beach

cf. Rana
- left distal humerus [1995/MS-759/L195.2.535/: O SW 1/4, L-3, waterscreen, 6/25/95 DA, SW].

Lemmiscus curtatus
- right dentary with i1, m1 and m2 [1995/MS-751/LI95.2.36].

Ondatra zibethicus
- left dentary fragment with m2 and m3 [1994/MS-688/LI94.5.454]. 7MAAI-71 (1994)
- left lower m1 [1994/MS-685/LI94.5.97]. No context
- right calcaneum [1994/MS-743/LI94.5.28]. ES-7-2

Spermophilus sp.
- edentulous right dentary fragment, with aveoli for m2 and m3 [1994/MS-686/LI94.5.256]. CS-5-1
- ?Fossil left dentary fragment with p4 and m1 [1994/MS-743/ES-8-1].
- ?Fossil partial edentulous right dentary [1994/MS-743/EN-8-3].

Canis latrans
- lower right p4 [1995/MS-756/LI95.2.309].

Canis lupus
- proximal half of right metatarsal 3 [1994/MS-740/LI94.5.130].

cf. Antilocapra americana
- proximal end of proximal phalange [1994/MS-741/LI94.5.456]. CS-14-4
- proximal phalange [1995/MS-759/LI95.2.537].

cf. Odocoileus sp.
- proximal phalange [1994/MS-685/L194.5.454/MAA1-7-1].

Cervidae, large species
- left i1 or i2 [1994/MS-741/LI94.5.455]. CN-23-2
- deciduous lower left molariform tooth [1994/MS-604/LI94.5.457]. Beach S-1

Bison sp.
- tooth fragment [1994/MS-604/LI94.5.458]. Beach S-1
- tooth fragment [1994/MS-604/Main Beach-S-2].
- left 2nd phalange [1994/MS-746/LI94.5.460]. Beach Second Collection Areas S-4
- proximal end of a right ulna [1994/MS-745/LI94.5.462]. Beach Surface #4
- 2 upper molar fragments [1994/MS-740/Beach Surface #29].
- tooth fragment [1994/MS-740/Beach Surface #19].
- (cf.) proximal phalange [1995/MS-764/LI95.2.535]. Ib #3
- (cf.) tooth fragment [1996/MS-986/LI96.4.181]. Surface
- naviculocuboid [1991/MS-562/LI91.1.3]. Beach BLM #20
- partial proximal end of a metacarpal 3/4 [1991/MS-562/LI91.1.5]. Beach BLM #23
- right scaphoid [?/MS-562/L191.1.3/BLM #27].
- left innominate fragment [1993/MS-744/LI93.2.1]. Beach Surface #35

Camelops sp.
- (cf.) tooth fragment [1994/MS-741/CS-20-2].
- buccal enamel fragment from upper M2 or M3 [1994/MS-685/LI94.5.86].
- distal end of proximal phalange [1994/MS-746/LI94.5.459]. Beach, second Collection Area S-4
- proximal epiphysis of phalange [1994/MS-740/LI94.5.134].FS 123.

Equus sp.
- proximal sesamoid of foot [1994/MS-688/LI94.5.185]. MAA1-4-1
- (cf.) tooth fragment [1994/MS-686/CN-6-2].
- (cf.) very worn incisor [1994/MS-741/CN-11-2].
- tooth fragment [1994/MS-741/CS-24-1].
- upper molar fragment [1994/MS-741/CS-13-1].
- upper molar fragment [1994/MS-741/CS-18-2].
- 4 tooth fragments [1994/MS-604/Secondary Collection Area-S-1].
- 5 tooth fragments [1994/MS-604/Main Beach-S-2]
- upper molar fragment [1994/MS-740/Beach Surface #29].
- left cuneiform [1994/MS-740/LI94.5.126].
- 10 tooth fragments [1994/MS-740/Beach Surface #24].
- (cf.) tooth fragment [1995/MS-752/Ib NW 1/4].
- medial phalange [1995/MS-753/LI95.2.134].
- unerupted partial left molar [1995/MS-764/LI95.2.155].
- portion of mandibular symphysis with broken right i2 [1995/MS-764/LI95.2.162].
- (cf.) carpal/tarsal fragment [1995/MS-749/Surface (Trench I)].
- distal end of proximal phalange [1995/MS-751/LI95.2.23].
- partial medial phalange [1995/MS-759/LI95.2.106].
- upper molar fragment [1995/MS-759/Overburden from around tusk 6/27/95 BG].
- right upper molariform tooth [1996/MS-972/LI96.4.96]. FS161 Beach
- lower molar fragment [1996/MS-974/LI96.4.94]. FS 161 Beach
- tooth fragment [1996/MS-975/LI96.4.61]. FS2 No context36 = FS162
- distal half of a radius [1996/MS-986/LI96.4.191]. Old L196/4/180
- tooth fragments [1996/MS-986/LI96.4.181]. FS161 Surface
- tooth fragment [?/MS-747/BLM#4].
- upper molar fragment [?/MS-747/BLM#9].
- tooth fragment [?/MS-560/BLM #16].
- tarsal fragment [?/MS-560/BLM#16].
- partial right navicular [1991/MS-562/LI91.1.4]. Beach BLM #22
- partial medial phalange [1991/MS-562/LI91.1.6]. Beach BLM #24
- proximal end of a proximal phalange [?/MS-562/BLM Beach recovery].
- tooth fragments [?/MS-744/Beach collection].
- left innominate fragment [1993/MS-744/LI93.2.2]. Beach Surface #35

Mammuthus sp.
- interior skull fragment [1994/MS-686/CN-21-3].
- enamel fragments [1994/MS-686/CN-23-5].
- tooth fragment [1994/MS-686/CN-12-3].
- (cf.) limb bone fragment [1994/MS-686/CN-7-2].
- tooth fragment [1994/MS-686/CN-4-2].
- 2 tooth fragments [1994/MS-686/CN-5-1].
- 3 tooth fragments [1994/MS 686/CN-16-4].
- enamel fragment [1994/MS-686/CS-14-5].
- 7 tooth fragments [1994/MS-686/CS-12-1].
- tusk fragments [1994/MS-686/CS-24-4].
- (cf.) 9 molar fragments [1994/MS-686/CS-21-1].
- (cf.) tooth fragment [1994/MS-686/CS-18-4].
- tooth fragment [1994/MS-686/CS-13-4].
- (cf.) 3 tooth fragments [1994/MS-686/CS-20-3].
- (cf). tooth fragment [1994/MS-741/CN-20-1].
- enamel fragment [1994/MS-741/CN-25-1].
- enamel fragment [1994/MS-741/CN-26-1].
- tooth fragment [1994/MS-741/CN-11-2].
- enamel fragment [1994/MS-741/CN-8-1].
- seven tooth fragments [1994/MS-741/CN-14-1].
- tooth [1994/MS-741/LI94.5.451].
- (cf.) tooth fragment [1994/MS-741/CN-18-4].
- proximal phalange [1994/MS-741/LI94.5.363]. CN-14-3
- (cf.) dentary fragment [1994/MS-741/CN-23-4].
- partial phalange [1994/MS-741/CS-11-2].
- (cf.) partial epiphysis of vertebra [1994/MS-741/CS-26-1].
- enamel fragment [1994/MS-741/CS-28-1].
- enamel fragment [1994/MS-741/CS-14-1].
- 2 enamel fragments [1994/MS-741/CS-9-1].
- (cf.) cranial fragment [1994/MS-741/CS-17-1].
- tooth fragment [1994/MS-741/CS-13-1].
- (cf.) two cranial fragments [1994/MS-741/CS-18-3].
- 2 tooth fragments [1994/MS-741/CS-11-1].
- tooth fragment [1994/MS-741/CS-15-1].
- (cf.) rib fragment [1994/MS-685/ES-25-3].

- (cf.) head of rib [1994/MS-685/EN-26-3].
- (cf.) limb bone fragment [1994/MS-685/EN-8-2].
- tooth fragment [1994/MS-685/EN-12-2].
- (cf.) tusk fragment [1994/MS-685/EN-26-1].
- dozens of tooth fragments [1994/MS-685/XU:E mammoth tooth frag/bone from wall 8/16/94 KM].
- phalange [1994/MS-685/LI94.5.98]. ES-26-2
- tooth [1994/MS-685/LI94.5.100]. ES-26-1
- 6 tooth fragments [1994/MS-685/ES-27-1].
- 3 tooth fragments [1994/MS-685/ES-26-7].
- tooth fragment [1994/MS-685/ES-25-1].
- (cf.) rib shaft fragment [1994/MS-685/ES-26-5].
- (cf.) 2 rib fragments [1994/MS-685/ES-26-4].
- small tusk fragment [1994/MS-604/Second Collection Area Beach].
- tooth fragment [1994/MS-604/Beach unit 1-S-1].
- 4 tooth fragments [1994/MS-604/Secondary Collection Area-S-1].
- 2 molar fragments [1994/MS-604/Main Beach-S-1].
- (cf.) unidentified limb fragment [1994/MS-604/LBD C14-1].
- (cf.) scapula or ilium fragment [1994/MS-604/Beach S-2].
- tusk fragments [1994/MS-604/Main Beach-S-5].
- (cf.) unidentified bone fragment [1994/MS-746/Main Beach-S-4].
- basicranial fragment with one occipital condyle [1994/MS-746/LI94.5.134]. Main Beach S-3
- (cf.) partial carpal/tarsal [1994/MS-740/Far Beach Surface #27].
- (cf.) partial carpal/tarsal [1994/MS-740/Far Beach Surface #26].
- ?left metacarpal V [1994/MS-740/LI94.5.115].
- (cf.) unidentified bone fragment [1994/MS-740/Far Beach Surface #20].
- left trapezium [1994/MS-740/LI94.5.119].
- ?proximal phalange [1994 /MS-740/LI94.5.120].
- (cf.) partial rib [1994/MS-745/Beach Surface Bone 10/26/94 BG, RR].
- 3 tooth fragments [1994/MS-745/Beach Bone 8/15/94 KM, LBD, RR].
- metapodial missing proximal end [1994/MS-745/LI94.5.114].
- tooth fragment [1994/MS-743/ES-26-8].
- (cf.) a few small tusk fragments [1994/MS-743/EN-26-4].
- 2 tusk fragments [1994/MS-743/EN-25-4].
- 3 tusk fragments [1994/MS-743/EN-27-1].
- enamel fragment [1994/MS-743/EN-14-2].
- (cf.) two small tusk fragments [1994/MS-743/EN-17-2].
- 4 tusk fragments [1995/MS-752/IbNW1/4].
- 22 tusk and molar fragments [1995/MS-752/IaNW1/4].
- 9 tooth fragments [1995/MS-752/Ia SE 1/4].
- (cf.) rib shaft fragment [1995/MS-753/Ia Bone #5].
- (cf.) rib shaft fragment [1995/MS-753/Ia Bone #6].
- (cf.) rib shaft fragment [1995/MS-753/Ia Bone #8].
- tusk fragments [1995/MS-753/Ia Bone #12].
- ilium or scapula fragment [1995/MS-753/Ia Bone #14].
- (cf.) rib shaft fragment [1995/MS-753/Ia Bone #17].
- limb bone fragment [1995/MS-753/Ia Bone #19].
- 7 tusk fragments [1995/MS-753/Ia Bone #22].
- 10 tusk fragments [1995/MS-753/Ia Bone #23].
- (cf.) rib shaft fragment [1995/MS-753/Ia Bone #24].
- (cf.) limb bone ftagment [1995/MS-753/Ia Bone #25].
- tooth fragment [1995/MS-754/Ia Bone #26].
- rib fragment [1995/MS-754/Ia Bone #27].
- partial innominate [1995/MS-754/Ia Bone #28].
- partial pelvis (mostly ilium) [1995/MS-754/LI95.2.140].
- partial ilium (continued) [1995/MS-748/Ia Bone #30].
- (cf.) diaphysis of large limb bone [1995/MS-765/Ia Bone #31].
- left proximal ulna [1995/MS-757/LI95.2.118].
- tusk fragments (dozens) [1995/MS-758/Ib Bone #21].
- (cf.) neural spine and upper neural arch of vertebra [1995/MS-764/Ib Bone #6].
- distal phalange [1995/MS-764/LI95.2.156].
- (cf.) unidentified bone fragment [1995/MS-764/Ib Bone #21].
- (cf.) limb bone diaphysis fragment [1995/MS-750/Ib Debris Flow Shoveled-Up Bone].
- (cf.) partial neural spine of thoracic vertebra [1995/MS-750/Ib Debris Flow Shoveled-Up Bone].
- (cf.) partial shaft of rib [1995/MS-750/Ib Bone above tusks in rocks].
- (cf.) limb bone fragment [1995/MS-766/J Bone #4].
- (cf.) limb bone fragment [1995/MS-766/J Bone #8].
- (cf.) rib shaft fragment [1995/MS-766/J Bone #12].
- (cf.) limb bone fragment [1995/MS-766/J Bone #13].
- (cf.) head of rib [1995/MS-767/K Bone #2].
- (cf.) rib shaft fragment [1995/MS-767/K Bone #3].
- (cf.) limb bone fragment [1995/MS-767/K SW 1/4 Bone #9].
- (cf.) limb bone fragment [1995/MS-767/K Bone #19].
- (cf). rib shaft and vertebra fragment [1995/MS-767/K Bone #22].
- (cf.) rib fragments [1995/MS-767/K SW 1/4 Bone #23].
- (cf.) 18 rib fragments [1995/MS-767/K Bone #23Y].
- (cf.) bone fragment [1995/MS-767/K Bone #27].
- 19 tusk fragments [1995/MS-767/K Bone #29].
- tusk fragment [1995/MS-760/N Bone #1].
- 26 tusk fragments [1995/MS-760/L Bone #2].
- 2 tusk fragments [1995/MS-760/L 30E, 15N, 86 BD].
- (cf.) 20 tusk fragments [1995/MS-749/K NW 1/4 L-1 Waterscreen].
- (cf.) 100+ tusk fragments [1995/MS-749/K NW 1/4 L-2 Waterscreen].
- (cf.) several tusk fragments [1995/MS-749/X Waterscreen matrix bone].
- (cf.) tusk fragments [1995/MS-749/X NW 1/4 Waterscreen Bone].
- (cf.) proximal end of phalange; rib fragments, several rusk fragments, partial centrum of a vertebra [1995/MS-749/Surface (3 bags)].
- 100+ rusk fragments [1995/MS-751/L Waterscreen].
- enamel fragments [1995/MS-751/N SW 1/4 L-2 Waterscreen].
- (cf.) tusk fragment [1995/MS-751/P NW 1/4 L-2 Waterscreen].
- (cf.) 4 tusk fragments [1995/MS-751/P NW 1/4 L-3 Waterscreen].
- (cf.) tusk fragment [1995/MS-751/P SW 1/4 L-4 Waterscreen].
- 5 tusk fragments [1995 MS-759/Area next to trench (South 95) black layer area 6/24/95].
- 2 tusk fragments [1995/MS-759/I collected from slump over tusks 6/20/95 TW, KM, DB].
- partial proximal phalange [1995/MS-759/I overburden over tusk 6/27/95 TW, DA, MC, KM].
- 3 tusk fragments [1995/MS-759/I overburden 6/25/95 TW, MC, BG].
- 8 tusk fragments [1995/MS-759/XU:IB SW SE level: Bone removed from area of tusk 6/26/95 TW, DE, RR, CH, BG].
- merapodial [1996/MS-970/LI96.4.91]. FS 161 Beach
- (cf.) rib fragment [1996/MS-970/LI96.4.98]. FS161 Beach
- left astragalus [1996/MS-970/LI96.4.99]. FS161 Beach
- left calcaneum [1996/MS-971/LI96.4.193].
- phalange [1996/MS-971/LI96.4.95].FS161 Beach
- proximal end of a left scapula [1996/MS-971/LI96.4.90]. FS161 Beach
- (cf.) cranial fragment [1996/MS-972/LI96.4.92]. BS 161 Beach
- right navicular [1996/MS-972/LI96.4.63]. FS63 L-3
- (cf.) unidentified [1996/MS-972/LI96.4.93]. FS161 Beach
- (cf.) several hundred tusk fragments [1996/MS-973/LI96.4.175]. FS125 4-1
- (cf.) rusk fragments [1996/MS-973/LI96.4.174]. FS129 T-2
- (cf.) tusk fragments [1996/MS-973/LI96.4.173]. FS138 T-3
- (cf.) tusk fragments [1996/MS-973/LI96.4.171]. FS130 L-4
- (cf.) tusk fragments [1996/MS-973/LI96.4.130]. FS5 4-4
- (cf.) tusk fragments [1996/MS-973/LI96.4.176]. FS129 T0-2
- (cf.) tusk fragments [1996/MS-973/LI96.4.172]. FS143 K-1
- (cf.) tusk fragments [1996/MS-973/LI96.4.118]. FS146 4-2

- (cf.) tusk fragments [1996/MS-973/LI96.4.122]. FS113 S-2
- (cf.) tusk fragment [1996/MS-974/LI96.4.80]. FS81 T-2
- (cf.) tusk fragment [1996/MS-974/LI96.4.45]. FS37 L-3
- (cf.) tusk fragments [1996/MS-974/LI96.4.47]. FS30 L-1
- (cf.) tusk fragments [1996/MS-974/LI96.4.42]. FS33 L-2
- (cf.) tusk fragments [1996/MS-974/LI96.4.44]. FS36 L-3
- (cf.) tusk fragments [1996/MS-974/LI96.4.125]. FS109 T-4
- (cf.) large bone fragment [1996/MS-974/LI96.4.123]. FS120 T-2
- (cf.) tusk fragments [1996/MS-974/LI96.4.124]. FS91 T-1
- (cf.) tusk fragments [1996/MS-974/LI96.4.94]. FS161 Beach
- (cf.) tusk fragments [1996/MS-974/LI96.4.178]. FS122 T-2
- (cf.) tusk fragments [1996/MS-975/LI96.4.89]. FS63 T-2
- (cf.) tusk fragments [1996/MS-975/LI96.4.88]. FS83 4-2
- (cf.) tusk fragments [1996/MS-975/LI96.4.69]. FS57 4-3
- (cf.) tusk fragments [1996/MS-975/LI96.4.23]. FS61
- (cf.) tusk fragments [1996/MS-975/LI96.4.26]. FS23
- (cf.) tusk fragments [1996/MS-975/LI96.4.60]. FS51
- (cf.) tusk fragments [1996/MS-975/LI96.4.23]. FS61 T-2
- (cf.) tusk fragments [1996/MS-975/LI96.4.26]. FS51 W-3
- (cf.) tusk fragments [1996/MS-975/LI96.4.60]. FS62 T-2
- (cf.) bone fragments [1996/MS-975/LI96.4.7]. FS63 T-2
- (cf.) tusk fragments [1996/MS-975/LI96.4.37]. FS63 T-2
- tooth fragment [1996/MS-975/LI96.4.61]. FS 2 No Context
- (cf.) tusk fragments [1996/MS-976/LI96.4.168]. FS133 4-3
- (cf.) tusk fragments [1996/MS-976/LI96.4.162]. FS142 K-1
- (cf.) tusk fragments [1996/MS-976/LI96.4.159]. FS141 5-6
- (cf.) tusk fragments [1996/MS-976/LI96.4.158]. FS136 T-3
- (cf.) tusk fragments [1996/MS-976/LI96.4.163]. FS129 T-2
- (cf.) tusk fragments [1996/MS-976/LI96.4.164]. FS132 4-2
- (cf.) tusk fragments [1996/MS-976/LI96.4.170]. FS129 T-2
- (cf.) tusk fragments [1996/MS-976/LI96.4.167].FS124 S-3
- (cf.) tusk fragments [1996/MS-976/LI96.4.166]. FS 140 S-5
- (cf.) tusk fragments [1996/MS-976/LI96.4.165]. FS129 T-2
- (cf.) tusk fragments [1996/MS-976/LI96.4.142]. FS102 L-3
- (cf.) tusk fragments [1996/MS-978/LI96.4.111]. FS156 T-3
- (cf.) tusk fragments [1996/MS-978/LI96.4.102]. FS160 4-3
- (cf.) tusk fragments [1996/MS-978/LI96.4.104]. FS158 4-3
- (cf.) tusk fragments [1996/MS-978/LI96.4.139]. FS139 S-4
- (cf.) tusk fragments [1996/MS-978/LI96.4.101]. FS160 4-3
- (cf.) tusk fragments [1996/MS-978/LI96.4.105].
- right calcaneum [1996/MS-985/LI96.4.182].old 96.4.180 FS162 Surface
- right astragalus [1996/MS-985/LI96.4.183]. Old 76.4.180 FS162 Surface
- distal phalange [1996/MS-985/LI96.4.189]. old 96.4.180 #4 FS162 Beach
- left metatarsal 4 [1996/MS-985/LI96.4.186]. old 96.4.180 #3 FS162 Beach
- left metatarsal 5 [1996/MS-985/LI96.4.184]. old 96.4.180 #2 FS162 Beach
- right metatarsal 3 [1996/MS-985/LI96.4.185]. old 96.4.180 #1 FS162 Beach
- sesamoid [1996/MS-985/LI96.4.187]. old 96.4.180 #5 FS162 Beach
- right metatarsal 1 [1996/MS-985/LI96.4.188]. old 96.4.180 #5 FS162 Beach
- (cf.) limb bone fragment [1996/MS-986/LI96.4.180 #10]. FS162 Beach
- (cf.) pelvic fragment [1996/MS-986/LI96.4.180 #9]. FS162 Beach
- (cf.) cranial fragment [1996/MS-986/LI96.4.180 #11]. FS162 Beach
- (cf.) cranial fragment [1996/MS-986/LI96.4.180 #14]. S162 Beach F
- (cf.) rib fragment [1996/MS-986/LI96.4.180 #15]. S162 Beach F
- (cf.) scapula fragment [1996/MS-986/LI96.4.180 #8]. S162 Beach F
- tooth fragment [1996/MS-986/LI96.4.181]. FS163 No Context
- (cf.) tusk fragments [1996/MS-986/LI96.4.181]. FS163 No Context
- (cf.) scapula fragment [1996/MS-986/LI96.4.181]. FS163 No Context
- right metatarsal 4 [1996/MS-986/LI96.4.192]. Old 99.4.181 FS163 No context
- (cf.) head of a rib [?/MS-747/BLM#1].
- (cf.) tusk fragments [?/MS-747/BLM #3].
- tooth fragments [?/MS-747/BLM #4].
- (cf.) limb bone fragment [?/MS-747/BLM#6].
- (cf.) limb bone fragment [?/MS-747/BLM#7].
- tooth fragments [?/MS-747/BLM#9].
- tusk fragments [?/MS-747/BLM#9].
- tooth fragments [?/MS-560/BLM #12].
- (cf.) partial rib [?/MS-560/BLM #13].
- (cf.) bone fragment [?/MS-560/BLM #14].
- (cf.) cranial fragment [?/MS-562/BLM #19].
- (cf.) partial vertebra [?/MS-562/BLM #21].
- (cf.) tarsal or carpal fragment [?/MS-562/BLM #26].
- (cf.) bone fragment [?/MS-562/BLM #29].
- (cf.) rib fragment [?/MS-562/BLM beach recovery].
- tooth fragments [?/MS-744/Beach collection].
- (cf.) tusk fragments [?/MS-744/Beach collection].

III. Surface Marks

A. Specimens with surface marks that warrant further examination.

1994 Excavations

MS-685

EN-2: cf. *Odocoileus* sp., proximal phalange possesses what may be ?tooth marks on the surface.
Is one of the marks a tooth puncture mark?
Also, the specimen surface looks somewhat etched. ?Had it gone through a large carnivore's digestive tract?

EN-26-1: *Mammuthus* sp., tusk fragment with 2 grooves on the surface. The grooves have ridges along their surfaces.

ES-26-5: cf. *Mammuthus* sp., partial rib fragment has some surface marks worthy of further examination.

ES-26-4: cf. *Mammuthus* sp., 2 rib fragments. Marks on the smaller fragment should be examined further.

MS-604

Beach S-2: cf. *Mammuthus* sp., scapula or ilium fragment. A deep striation (groove) on one side.

1995 Excavations

MS-767

K Bone #20: Unidentified bone fragment from large mammal. Check the bone surface. There are ?puncture marks on the surface of ?tooth marks.

K Bone #21: ?*Mammuthus* sp., vertebra fragment, zygopophysis with articular facet. A groove occurs on the bone surface. The groove has ridges running along the bottom.

K SW 1/4 Bone #23: cf. *Mammuthus* sp., rib fragments. Check bone surface. Are these tooth marks or tool marks?

K Bone #23 Y: cf. *Mammuthus* sp., rib fragments. Check marks on bone surface.

MS-760

N Bone #2: Unidentified bone fragment from "medium-sized" mammal. Examine marks on surface. Tooth marks?

MS-756

X Bone #2: 4 unidentifiable bone fragments. One fragment has a deep groove on the surface with ridges along the surface within the groove.

B. Specimens with surface marks, but which do not necessarily require examination.

1994 Excavations

MS-686

CS-26-2: The largest of the unidentifiable fragments has parallel striae on the bone surface.

MS-741

CN-11-4: A few parallel striations are present on this limb bone fragment.

MS-604

Channel Bone for Dating: Of the 20+ rib fragments from unidentified large mammals, a few of the largest specimens have parallel striations on the surface.

1995 Excavations

MS-753

Ia Bone #8: cf. *Mammuthus* sp., rib fragment, one side with numerous striations, some are parallel sets, suggestive of trampling. Also, a couple of deeper grooves are present.

Ia Bone #12: *Mammuthus* sp., tusk fragments. On the largest fragment are multiple sets of parallel srriations. Also, striations occur on at least one of the smaller fragments.

Ia Bone #14: *Mammuthus* sp., scapula or ilium fragment. Striations present on one side.

MS-758

Ib Bone #21: *Mammuthus* sp., tusk fragments. Many surface striations on various pieces of the tusk. Note more detailed description in the inventory.

MS-764

Ib Bone #14: Large mammal scapula or ilium fragment in two pieces. Sets of parallel striations occur on the surface.

MS-766

J Bone #12: cf. Mammuthus sp., medial section of rib. A few surface striations are present.

J Bone #16: unidentifiable limb bone fragment from large mammal. Striations on bone surface.

J Bone #18: unidentifiable limb bone fragment. Deep striation (groove) on bone surface.

MS-767

K Bone #28: unidentifiable bone fragment. Parallel striations on the bone surface.

MS-756

P SW L-1 Bone #1: unidentified limb bone fragment from large ungulate. Many parallel sets of striations on bone surface.

X Bone #6: parallel sets of striae on bone surface.

IV. Invertebrate Specimens That Require Identification

1994 Excavations

MS-686

CN-25-3	bivalve shell
CN-12-3	gastropod shell
CS-14-5	gastropod shell
CS-15-4	bivalve shell
CS-26-2	bivalve shell
CS-18-4	gastropod shell

MS-743

EN-25-4	bivalve shell

1995 Excavations

MS-760

O Bone #3 gastropod shell

MS-749

O SW 1/4 L-2 Waterscreen:	bivalve shell
O SW 1/4 L-5 Waterscreen:	bivalve shell
O NW 1/4 L-3 Waterscreen:	bivalve shell, 3 gastropod shells (2 different species)

MS-751

N SW 1/4, L-2, Waterscreen: fragment of an arthropod carapace (?Recent)

MS-759

X Overburden 7/5/95 DA: gastropod shell

Faunal materials are listed by box number (e.g., MS-970), then by specimen number (e.g., LI96.4.91) or, in the absence of a specimen number, by data noted on the outside of bags contain the specimens.

Appendix D. Inventory of Faunal Remains Recovered from the Late Pleistocene Merrell Locality.

1996 Museum of the Rockies Excavations

MS-970

Beach FS 161	*Mammuthus* sp., metapodial. LI 96.4.91
Beach FS161	cf. *Mammuthus* sp., rib fragment, 21x 6 x 4 cm. Striations present on bone surface. LI 96.4.98
Beach FS161	*Mammuthus* sp., left astragalus. LI 96.4.99

MS-971

Beach LI 96.4.193	*Mammuthus* sp., left calcaneum.
Beach LI 96.4.95	*Mammuthus* sp., phalange. Also, 10 unidentifiable bone fragments; largest is 5 x 1 x cm.
Probably Beach LI 96.4.90	*Mammuthus* sp., proximal end of a left scapula. Striations present on the surface.

MS-972

Beach FS16 1 LI 96.4.96	*Equus* sp., right upper molariform tooth (not the P2 or M3).
Beach FS161 LI 96.4.92	cf. *Mammuthus* sp., cranial fragment, ca. 20 x 17 x 13 cm.
Beach FS161 LI 96.4:63	*Mammuthus* sp., right navicular.
Beach FS 161 LI 96.4.93	cf. *Mammuthus* sp., unidentified. Multiple striae on bone surface.

MS-973

U1 FS4 LI 96.4.52	2 unidentifiable bone fragments; 3 x 1.5 x 1 cm and 2 x 1 x .5 cm.
T2 FS129 LI 96.4.175	cf. *Mammuthus* sp., several hundred tusk fragments, largest is ~3 x 2 cm. Also, several hundred unidentifiable bone fragments.
LI 96.4.29	Unknown location 4 unidentifiable bone fragments; largest is 2 x .5 x .5 cm.
T2 FS129 LI 96.4.174	cf. *Mammuthus* sp., 100+ tusk fragments; largest is 7.5 x 3 x 1 cm.
T3 FS138 LI 96.4.173	cf. *Mammuthus* sp., 100+ tusk fragments; largest is 4 x 1.5 cm. Also, 24 unidentifiable bone fragments; largest is 4 x 4 x 2.5 cm.
L4 FS130 LI 96.4.171	cf. *Mammuthus* sp., a couple of tusk fragments. Two dozen plus unidentifiable bone fragments; largest is 2.5 x .5 cm.
U4 FS5 LI 96.4.130	cf. *Mammuthus* sp., 50+ tusk fragments; largest 5.5 x 2 x 1.5 cm.
T2 FS129 LI 96.4.176	cf. *Mammuthus* sp., several hundred tusk fragments; largest 3 x 1.5 cm. Also several dozen unidentifiable bone fragments.
K1 FS143 LI 96.4.172	cf. *Mammuthus* sp., 50+ tusk fragments. Largest 2 x 1.5 cm.
U2 FS146 LI 96.4.118	cf. *Mammuthus* sp., 16 tusk fragments; largest is 3 x 1.5 cm. Also, three unidentifiable bone fragments.
S2 FS113 LI 96.4.122	cf. *Mammuthus* sp., 30+ tusk fragments; largest is 3 x 1.5 cm. Also, several unidentifiable bone fragments.
V2 FS112 LI 96.4.121	Sediment (no fossil material).
T1 FS145 LI 96.4.117	4 unidentifiable bone fragments; largest is 3.5 x 2 x 1 cm.
V2 FS147 LI 96.4.115	Bag of sediment containing a couple of small bone fragments.

MS-974

W3 FS47 LI 96.4.72	5 unidentifiable bone fragments; largest is 6 x 2 x 1 cm.
M1 FS53 LI 96.4.70	3 unidentifiable bone fragments; largest is 2 x 1.5 x .75 cm.
V2 FS58 LI 96.4.71	6 unidentifiable bone fragments; largest is 3.5 x 2 x 1 cm.
W2 FS45 LI 96.4.82	~35 unidentifiable bone fragments; largest is 4 x 1.5 x 1 cm.
L4 FS85 LI 96.4.81	~50 unidentifiable bone fragments; largest is 4 x 1.5 x 1 cm.
T2 FS81 LI 96.4.80	cf. *Mammuthus* sp., tusk fragment, 4 x 2.5 x 1.5 cm.
XL FS84 LI 96.4.78	10 unidentifiable bone fragments; largest is 2 x 1 x 1.5 cm.
L3 FS37 LI 96.4.45	cf. *Mammuthus* sp., 10 x 3 cm piece of tusk broken into many fragments.
S3 FS28 LI 96.4.48	Unidentifiable bone fragment, 4 x 3 x 1 cm.
S3 FS26 LI 96.4.46	Rock.
L1 FS31 LI 96.4.49	2 unidentifiable bone fragments; 5 x 3 x 1 cm and 18 x 6 x 1 cm (diaphysis fragment of large mammal limb bone).

S2 FS25 LI 96.4.50	~15 unidentifiable bone fragments; largest is 3 x 2 x .25 cm.
T1 FS24 LI 96.4.51	7 unidentifiable bone fragments; largest is 3.5 x 2 x 1 cm.
M1 FS3 LI 96.4.54	10 unidentifiable bone fragments; largest is 2.5 x 1 x .5 cm.
L1 FS30 LI 96.4.47	cf. *Mammuthus* sp., 10 tusk fragments; largest is 2.5 x 1.5 cm. Also, one unidentifiable bone fragment, 3 x 3 x 1 cm.
Unprovenance FS1 LI 96.4.53	Modern piece of wood.
T1 FS14 LI 96.4.28	Unidentifiable bone fragment, 3.5 x 1.5 x 1 cm.
L3 FS73 LI 96.4.33	Unidentifiable bone fragment, 4 x 3 x 1 cm.
T3 FS88 LI 96.4.79	Unidentifiable bone fragment, 3 x 2.5 x 1 cm.
T2 FS79 LI 96.4.75	Unidentifiable bone fragment, 2 x 1.5 x 1 cm.
S3 FS54 LI 96.38	15 Unidentifiable bone fragments; largest is 1.5 x 1 x 1 cm.
L2 FS33 LI 96.4.42	cf. *Mammuthus* sp., 20 tusk fragments; largest is 7.5 x 2 x 1 cm. Also, 10 unidentifiable bone fragments.
L2 FS34 LI 96.4.43	Unidentifiable bone fragment, 3.5 x 2 x 2 cm.
L4 FS86 LI 96.4.76	Unidentifiable bone fragment, 5 x 3 x 1.5 cm.
L3 FS36 LI 96.4.44	cf. *Mammuthus* sp., ~60 tusk fragments; largest is 4 x 1 x .5 cm. Also, 2 unidentifiable bone fragments.
T2 FS90 LI 96.4.77	Unidentifiable bone fragment, 3.5 x 3 x 2 cm.
V3 FS114 LI 96.4.126	11 unidentifiable bone fragments; largest is 5 x 2 x 1 cm.
U2 FS148 LI 96.4.114	25 unidentifiable bone fragments; largest is 11 x 2 x 2 cm.
T4 FS109 LI 96.4.125	cf. *Mammuthus* sp., 18 tusk fragments; largest is 3.5 x 2 x .5 cm. Also, 5 unidentifiable bone fragments.
U3 FS149 LI 96.4.113	Mid-shaft of rib fragment from large mammal, 8.5 x 3.5 x 1 cm.
V2 FS111 LI 96.4.119	Unidentifiable bone fragment, 7.5 x 2.5 x 1.5 cm.
U1 FS144 LI 96.4.116	11 unidentifiable bone fragments; largest is 3 x 2.5 x 1 cm.
T2 FS120 LI 96.4.123	cf. *Mammuthus* sp., (ID based on robustness) fragment from a larger, undetermined element, insufficient detail for further ID. Size 8.5 x 4.5 x 3 cm.
T1 fs91 LI 96.4.124	Vial with 3 bivalve shells. Vial with mollusk shell fragment. cf. *Mammuthus* sp., ~40 tusk fragments; largest is 3.5 x 1.5 x 1 cm. Also, 4 unidentifiable small bone fragments.
Beach FS161 LI 96.4.94	cf. *Mammuthus* sp., 2 tusk fragments, 5.5 x 1.5 x .25 cm. *Equus* sp., lower molar fragment. 11 unidentifiable bone fragments; largest is 9 x 2 x 1 cm.
Beach FS161 LI 96.4.190	*Olar buccinator*, proximal end of a left humerus.
W2 FS20 LI 96.4.74	Unidentifiable bone fragment, 13 x 6 x 3.5 cm. Probably a mammoth limb fragment based on robustness.
T2 FS122 LI 96.4.178	cf. *Mammuthus* sp., 42 tusk fragments; largest is 5 x 2.5 x .5 cm. ~40 unidentifiable bone fragments; largest is 7 x 3 x 3 cm.
T2 FS117 LI 96.4.177	11 unidentifiable bone fragments; largest is 8 x 4 x 3 cm.

MS-975

T2 FS62 LI 96.4.89	Bag of 100+ bone fragments, most under 4 x 2 cm. Many are cf. *Mammuthus* sp., tusk fragments. Other fragments are unidentifiable.
U2 fs83 LI 96.4.88	~35 unidentifiable bone fragments; largest is 7 x 2.5 x 1 cm. 2 of the fragments are cf. *Mammuthus* sp. tusk fragments.
W1 FS9 LI 96.4.27	Unidentifiable bone fragment, 3 x 1 x .5 cm.
W2 FS111 LI 96.4.66	Unidentifiable bone fragment, 8 x 3 x 1 cm.
W FS 46 Ground Level LI 96.4.73	52 unidentifiable bone fragments; largest is 5 x 1 x 1 cm.
W3 fs49 LI 96.4.67	2 unidentifiable bone fragments; largest is 8.5 x 4.5 x 2 cm.
U3 FS57 LI 96.4.69	cf. *Mammuthus* sp., 100+ tusk fragments; largest is 5 x 2 x 1cm.
W3 FS59 LI 96.4.68	8 unidentifiable bone fragments; largest is 3.5 x 3 x 1.5 cm.
T2 FS55 LI 96.4.65	Unidentifiable bone fragment, 5.5 x 5.5 x 3.5 cm.
T2 FS61 LI 96.4.23	cf. *Mammuthus* sp., 2 tusk fragments; largest is 3.5 x 2 x 1.5 cm.
T1 FS12 LI 96.4.24	Unidentifiable bone fragment, 3.5 x 1.5 x 1.5 cm.

V2 FS16 LI 96.4.25	Unidentifiable bone fragment, probably mammoth limb bone based on robustness and size, 14 x 5.5 x 2.5 cm. Surface marks (made by excavators?).
L3 FS71 LI 96.4.32	Unidentifiable bone fragment, 3 x 2 x 2 cm.
L3 FS69 LI 96.4.30	Unidentifiable bone fragment, 4 x 2 x 1.5 cm.
M4 FS23 LI 96.4.26	cf. *Mammuthus* sp., tusk fragment, 1.5 x 1 x .25 cm.
L3 FS75 LI 96.4.31	Unidentifiable bone fragment, 5.5 cm, 1.5 x 1.5 cm.
W2 FS18 LI 96.4.22	Unidentifiable bone fragment, 7.5 x 3 x 2 cm.
M2 FS77 LI 96.4.62	30+ unidentifiable bone fragments; largest is 2.5 x 1 x .5 cm.
M3 FS22 LI 96.4.40	7 unidentifiable bone fragments; largest is 4 x 1.5 x .5 cm.
W3 FS51 LI 96.4.60	cf. *Mammuthus* sp., ~30 tusk fragments; largest is 3 x 1 x .75 cm.
T2 FS61 LI 96.4.23	cf. *Mammuthus* sp., 2 tusk fragments; largest is 3.5 x 2 x 1.5 cm.
T1 FS12 LI 96.4.24	Unidentifiable bone fragment, 3.5 x 1.5 x 1.5 cm.
V2 FS16 LI 96.4.25	Unidentifiable bone fragment, probably from mammoth limb bone based on robustness and size, 14 x 5.5 x 2.5 cm. Surface marks on bone (made by excavators?).
L3 FS71 LI 96.4.32	Unidentifiable bone fragment, 3 x 2 x 2 cm.
L3 FS69 LI 96.4.30	Unidentifiable bone fragment, 4 x 2 x 1.5 cm.
M4 FS23 LI 96.4.26	cf. *Mammuthus* sp., tusk fragment, 1.5 x 1 x .25 cm.
L3 FS75 LI 96.4.31	Unidentifiable bone fragment, 5.5 x 1.5 x 1.5 cm.
W2 FS18 LI 96.4.22	Unidentifiable bone fragment, 7.5 x 3 x 2 cm.
M2 FS77 LI 96.4.62	30+ unidentifiable bone fragments; largest is 2.5 x 1 x .5 cm.
M3 FS22 LI 96.5.40	7 unidentifiable bone fragments, 4 x 1.5 x .5 cm.
W2 FS6 LI 96.4.64	Unidentifiable bone fragment, 8.5 x 3 x 2.5 cm.
T2 FS62 LI 96.4.7	Bag of ~100 bone fragments, most about 4 x 2 x 1 cm. Some fragments are cf. *Mammuthus* sp., but most are unidentifiable.
L3 FS42 LI 96.4.39	Unidentifiable bone fragment, 3.5 x 3.5 x 2 cm.
L3 FS40 LI 96.4.41	Unidentifiable bone fragment, 5 x 2.5 x 2 cm.
L3 FS67 LI 96.4.36	Unidentifiable bone fragment, 5 x 3 x 1 cm.
L3 FS65 LI 96.4.35	Unidentifiable bone fragment, 4.5 x 1.5 x 1.5 cm.
L3 FS64 LI 96.4.34	Unidentifiable bone fragment, 1.5 x .1 x .1 cm.
L3 FS63 LI 96.4.37	cf. *Mammuthus* sp., ~40 tusk fragments; largest is 3 x 1.5 x .25 cm. Also, 100+ unidentifiable bone fragments; largest is 6 x 2 x 1.5 cm.
No Context FS2 LI 96.4.61	*Mammuthus* sp., tooth fragment, 6 x 3.5 x 1.5 cm. *Equus* sp., tooth fragment, 3.5 x 1.5 x .1 cm. 1 Recent small lumbar vertebra. 9 unidentifiable bone fragments; largest is 8 x 4 x 2 cm.

MS-976

U1 FS125 LI 96.4.169	4 unidentifiable bone fragments; largest is 3.5 x 1 x .25 cm.
U3 FS133 LI 96.4.168	cf. *Mammuthus* sp., 22 tusk fragments; largest is 2.5 x 1.5 x .25 cm. 60+ unidentifiable bone fragments; largest is 4 x 2.5 x 1 cm.
K1 FS142 LI 96.4.162	cf. *Mammuthus* sp., 18 tusk fragments, 2 x 2.5 x .25 cm. 9 unidentifiable bone fragments, 4 x 2 x 1.5 cm.
V2 FS134 LI 96.4.160	78 unidentifiable bone fragments; largest is 2.5 x 1 x .25 cm.
S6 FS141 LI 96.4.159	cf. *Mammuthus* sp., 47 tusk fragments; largest is 3 x 1.5 x .25 cm. Also, 20+ misc. unidentifiable bone fragments; largest is 1 x 1 cm.
T3 FS 136 LI 96.4.158	cf. *Mammuthus* sp., 70+ tusk fragments; largest is 4.5 x 1.5 x 1.5 cm.
T2 FS129 LI 96.4.163	cf. *Mammuthus* sp., bag of 200+ tusk fragments; largest is 7 x 2 x 1 cm.
U2 FS132 LI 96.4.164	cf. *Mammuthus* sp., 6 tusk fragments; largest is 2.5 x 2 cm. Also, ~50 unidentifiable bone fragments; largest is 5 x 3 x 1.5 cm.
T2 FS129 LI 96.4.170	cf. *Mammuthus* sp., 86 tusk fragments; largest is 3.5 x 2 x .25 cm. Also, 56 unidentifiable bone fragments; largest is 4.5 x 5 x 3 cm.
S3 FS124 LI 96.4.167	cf. *Mammuthus* sp., ~50 tusk fragments; largest 2.5 x 1.5 x .25 cm. Also 100+ unidentifiable bone fragments; largest is 5.5 x 4.5 x 3.5 cm.

V2 FS110 LI 96.4.143	22 unidentifiable bone fragments; largest is 5 x 3 x 1 cm.
S5 FS140 LI 96.4.166	cf. *Mammuthus* sp., 23 tusk fragments; largest is 7 x 3 x .75 cm. Also, 8 unidentifiable bone fragments; largest is 3.5 x 3 x 1 cm.
T2 FS129 LI 96.4.165	Bag of dirt and cf. *Mammuthus* sp., tusk fragments under 4 x 2 cm.
M3 FS93 LI 96.4.147	Vial with ?rugose coral fragment, Paleozoic age fossil. Septa are visible. Reworked from limestone in the area. Also one small bone fragment, 1 x .25 cm.
M4 GS94 LI 96.4.148	1 unidentifiable bone fragment, 1 x .1 cm. 10 pieces of calcite.
No Context FS108 LI 96.4.149	10 unidentifiable bone fragments; largest is 4.5 x 1 x .2 cm. Thin-walled bone from limb, could be large bird.
S1 FS107 LI 96.4.150	5 unidentifiable bone fragments; largest is 1.5 x .25 cm.
U3 FS97 LI 96.4.151	10 unidentifiable bone fragments; largest is 1.75 x 1 cm.
S4 FS92 LI 96.4.152	~20 unidentifiable bone fragments; largest is 2.5 x 2 cm.
L1 FS100 LI 96.4.153	1 unidentifiable bone fragment, .5 x .5 cm.
S5 FS98 LI 96.4.154	~15 unidentifiable bone fragments; largest 3 x 1.5 cm.
U1 FS128 LI 96.4.156	3 unidentifiable bone fragments; largest is 5 x 1.5 cm.
L5 FS95 LI 96.4.146	~20 unidentifiable bone fragments; largest is 3.5 x 1.5 x .5 cm.
U2 FS96 LI 96.4.145	6 unidentifiable bone fragments; largest is 1 x .5 cm.
V2 FS106 LI 96.4.141	Sediment (no bone).
U4 FS99 LI 96.4.144	6 unidentifiable bone fragments; largest is 7 x 5 x 1 cm.
L3 FS102 LI 96.4.142	cf. *Mammuthus* sp., 9 tusk fragments; largest is 2.5 x 1.5 cm. Also 50+ unidentifiable bone fragments; largest is 3.5 x 1 cm.

MS-978

T2 FS155 LI 96.4.106	7 unidentifiable bone fragments; largest is 4.5 x 2.5 cm.
T4 FS103 LI 96.4.128	Unidentified bone fragment, 7.5 x 2.5 cm.
T3 FS156 LI 96.4.111	cf. *Mammuthus* sp., 18 tusk fragments; largest is 4 x 2 cm.
	50+ unidentifiable bone fragments; largest is about 3 x 2 cm.
U3 FS160 LI 96.4.102	cf. *Mammuthus* sp., 30 tusk fragments; largest is 3 x 2 cm. About 30 unidentifiable bone fragments.
V3 FS115 LI 96.4.133	Unidentifiable bone fragment, limb fragment from a large mammal, 9 x 2 x 3 cm.
L2 FS11 LI 96.4.132	4 unidentifiable bone fragments; largest is 2 x 1 cm.
V2 FS105 LI 96.4.135	unidentifiable bone fragment, 5.5 x 4 x 1 cm.
T2 FS118 LI 96.4.129	unidentifiable bone fragment, 2.5 x 1 x 1 cm.
T1 FS151 LI 96.4.109	unidentifiable bone fragment.
T3 FS154 LI 96.4.110	unidentifiable bone fragment, 4 x 2.5 x 2 cm.
U3 FS158 LI 96.4.104	cf. *Mammuthus* sp., 32 tusk fragments, 3 x 2 x 1 cm. ~20 unidentifiable bone fragments, 4 x 2 x 1.5 cm.
V3 FS131 LI 96.4.140	~13 unidentifiable bone fragments; largest is 2 x 2 cm.
U1 FS126 LI 96.4.138	unidentifiable bone fragment, ?rib fragment from a large mammal. 5.5 x 3 x 1.5 cm.
V2 FS137 LI 96.4.137	~50+ unidentifiable bone fragments; largest is 5.5 x 1.5 x 2 cm.
S4 FS139 LI 96.4.139	cf. *Mammuthus* sp., 60+ tusk fragments; largest is 5 x 2 x 1 cm. ~20 unidentifiable bone fragments; largest is 3.5 x 3.5 x 2.5 cm.
U3 FS160 LI 96.4.101	cf. *Mammuthus* sp., 50+ tusk fragments; largest is 5.5 x 2.5 x 2 cm. ~10 unidentifiable bone fragments; largest is 6.5 x 2.5 x 1 cm.
T2 FS121 LI 96.4.127	unidentifiable bone fragment, 10 x 8.5 x 5 cm.
Context Unknown LI 96.4.105	cf. *Mammuthus* sp., 100+ tusk fragments; largest is 6 x 3 x 1 cm. numerous small unidentifiable bone fragments, under 3 x 1.5 cm.

MS-985

Surface FS162 LI 96.4.182	*Mammuthus* sp., right calcaneum.

Surface FS162 LI 96.4.183	*Mammuthus* sp., right astragalus.
Surface FS162 LI 96.4.189	*Mammuthus* sp., distal phalange.
Surface FS162 LI 96.4.180 #4	2 unidentifiable bone fragments; largest is 6 x 3 cm.
Surface FS162 LI 96.4.186	*Mammuthus* sp., left metatarsal 4.
Surface FS162 LI 96.4.184	*Mammuthus* sp., left metatarsal 5.
Surface FS162 LI 96.4.185	*Mammuthus* sp., right metatarsal 3.
Surface FS162 LI 96.4.187	*Mammuthus* sp., sesamoid.
Surface FS162 LI 96.4.188	*Mammuthus* sp., right metatarsal 1.

MS-986

Surface FS162 LI 96.4.180 #10	cf. *Mammuthus* sp., limb bone fragment, 27 x 9 x 2.5 cm.
Surface FS162 LI 96.4.180 #18	unidentifiable bone fragment, 4.5 x 1 x 1 cm.
Surface FS162 LI 96.4.180 #9	cf. *Mammuthus* sp., pelvic fragment 18 x 10 x 5 cm.
Surface FS162 LI 96.4.180 #11	probably *Mammuthus* sp., cranial fragment, 8 x 9 cm.
Surface FS162 LI 96.4.191	*Equus* sp., distal half of a radius.
Surface FS162 LI 96.4.180 #14	possibly *Mammuthus* sp., cranial fragment from a large mammal, 7 x 8.5 cm.
Surface FS162 LI 96.4.180 #15	cf. *Mammuthus* sp., rib fragment, 20 x 4 cm.
Surface FS162 LI 96.4.180 #17	limb bone fragment, probably mammoth, 8.5 x 5 x 2.5 cm.
Surface FS162 LI 96.4.180 #13	unidentifiable bone fragment, 10 x 2 x .75 cm.
Surface FS162 LI 96.4.180 #6	unidentified proximal end (head) of rib from a large mammal.
Surface FS162 LI 96.4.180 #7	unidentifiable bone fragment, 10 x 4 x 1 cm. - 1 rock.
Surface FS162 LI 96.4.180 #8	cf. *Mammuthus* sp., scapula fragment.

MS-987

Possibly Surface FS163 LI 96.4.181	11unidentifiable bone fragments; largest 18.5 x 9.5 x 4 cm. One exhibits weathering cracks on surface. Most look like fragments of mammoth limb bone. One appears to be a fragment of a rib shaft. Fracture edges on the bones are sharp.
Possibly Surface FS163 LI 96.4.181	36 unidentifiable bone fragments. 2 fragments have small articular surfaces, but they are from much larger elements; largest is 8 x 7 x 4 cm. 3 rib fragments from medium-sized mammal.
Possibly Surface FS163 LI 96.4.181	55 unidentifiable bone fragments; largest is 10 x 5 x 1.5 cm. *Mammuthus* sp., tooth fragment, 8 x 4.5 x .25 cm. cf. *Mammuthus* sp., tusk fragment, 17 x 4.5 x .5 cm.
Possibly Surface FS163 LI 96.4.181	17 unidentifiable bone fragments; largest is 8 x 4.5 x .5 cm. cf. *Mammuthus* sp., tusk fragment, 9 x 4 x .5 cm. cf. *Odocoileus* sp., (Recent) metacarpal missing distal epiphysis.
Possibly Surface FS163 LI 96.4.181	6 unidentifiable tooth fragments; largest is 7 x 1.5 x .25 cm. *Mammuthus* sp., 4 tooth fragments; largest is 5 x 5 x .25 cm. *Equus* sp., 7 tooth fragments; largest is 6.5 x 2 x 1.5 cm. cf. *Bison* sp., tooth fragment, 5 x 1.5 x 1.25 cm. *Spermophilus* sp., partial cranium, with only incisors present. (?Fossil?, dark in color, but uncertain whether Fossil or Recent).
Possibly Surface FS163 LI 96.4.181	cf. *Mammuthus* sp., scapula fragment, 19 x 9 x 5.5 cm. cf. *Mammuthus* sp., unidentifiable bone fragment, 26 x 9 x 8 cm. ID based on size and robustness of bone.
Possibly Surface FS163 LI 96.4.192	*Mammuthus* sp., right metatarsal 4.

1995 Museum of the Rockies Excavations

North Block

MS-752

Ib NW 1/4
cf. *Equus*, tooth fragment.

Mammuthus sp., 4 tusk fragments

Approximately 100 unidentifiable bone fragments 1 to 6 cm long. Most appear to be limb bone fragments. A couple are skull fragments. All appear to be from large mammals. The fracture edges are mostly angular. Very few show evidence of edge rounding. A couple of the fragments are probably pieces of mammoth podial elements. There are also two small enamel fragments from a large mammalian herbivore.

3 rocks.

Ia NW 1/4

Mammuthus sp., 13 tusk and molar fragments, all under 4 cm in length.

Mammuthus sp., 9 tusk and molar fragments, 1 to 3 cm in length.

Large mammalian herbivore, 15 small tooth fragments, insufficient for identification.

Approximately 60 unidentifiable bone fragments, 1-8 cm in length. Many additional fragments smaller than 1 cm in length. Most of the fragments are cancellous bone and appear to be from a large mammalian limb bone(s). One 8-cm-long fragment is definitely from a mammoth limb bone.

50+ unidentifiable bone fragments, 1-7 cm in length. Many additional fragments under 1 cm in length. Mostly limb bone fragments although a couple are skull fragments.

1 rock.

Sesamoid bone of a large ungulate.

Ia SE 1/4

Mammuthus sp., 9 tooth fragments, all 1-2 cm in length.

9 unidentifiable bone fragments.

Ia SW 1/4

Approximately 50 unidentifiable bone fragments 1-6 cm in length. Many additional fragments under 1 cm in size. One fragment is a piece of a diaphysis of a limb bone from a relatively small mammal. The bone fragment is 6 cm long x 1 cm in diameter. Also a couple of enamel fragments.

28 unidentifiable bone fragments under 1cm in length; includes 1 enamel fragment

25 unidentifiable bone fragments 1-6 cm long. Three are rib fragments; the largest two are 6 cm long x 1 cm in diameter. The rib fragments are from a relatively small mammal.

14 unidentifiable bone fragments, 1-4 cm in length.

Recent cf. *Mustela*, upper P4, and dentary fragment with p2-p4.

Recent 10 miscellaneous bone fragments of small mammal, including skull fragments, partial radius missing distal end, complete ulna, and a calcaneum.

Ib SW/NW 1/4

3 unidentifiable bone fragments, each about 1 cm in size.

Ib SW 1/4

35 unidentifiable bone fragments 1 to 7 cm in length.

Approximately 100 unidentifiable bone fragments from 1 to 7 cm in length. Includes both limb bone and skull fragments. One enamel fragment present, 2 cm long, but with insufficient detail for identification.

MS-753

Ia Bone #1	unidentifiable cancellous bone, 2 fragments under 3 cm in size.
Ia Bone #3	large mammal, partial articular head of humerus in three fragments, 4 x 3 cm in size. Insufficient detail for ID.
Ia Bone #4	*Equus* sp., medial phalange in several pieces.
Ia Bone #5	cf. *Mammuthus* sp., fragment of rib shaft, 14.5 x 3.5 cm in size.
Ia Bone #6	cf. *Mammuthus* sp., fragment of rib shaft (in three pieces), 19 cm long x 4 cm wide. Also, 2 smaller rib fragments each 9 cm long.
Ia Bone #8	cf. *Mammuthus* sp., section of rib shaft, 37 cm long x 4 cm wide. One side of rib: some surface exfoliation of bone. Other side of rib: numerous striations, some parallel sets; indicative of trampling. Also, a couple of deeper grooves present.
Ia Bone #9	Large mammal, partial carpal/tarsal. May be identifiable with good comparative collection and considerable time.
Ia Bone #10	large mammal, skull fragment, 5 x 2.5 cm.
Ia Bone #11	Large mammal, rib fragment, 14 x 2 cm wide, no diagnostic features.
Ia Bone #12	*Mammuthus* sp., tusk fragments. Tusk fragment 18 cm long x 5 cm wide. The outer surface preserves multiple sets of parallel striations indicarive of trampling by large ammalian herbivores. Tusk fragment 11 x 3.5 cm. Sets of parallel striae on outer surface. Tusk fragments: 7.5 x 1.5 cm; 6.5 x 2 cm; 5 x 2.5 cm; and 7.5 x 2.5 cm; 5.5 x 3 cm; 7.5 x 3 cm. 7 tusk fragments under 7 x 2.5 cm in size.
Ia Bone #14	*Mammuthus* sp., ilium or scapula fragment, 13 x 10 cm. Could be either because both elements have the features found in this specimen. Striations present on one side.
Ia Bone #15	Unidentifiable bone fragment, 5.5 x 1 cm.
Ia Bone #16	Unidentifiable bone fragment, large mammal, 8 x 2 cm.

Ia Bone #17 cf. *Mammuthus* sp., section of rib shaft, 16.5 cm long x 4 cm wide. Also, 2 smaller fragments, each less than 5 cm long.

Ia Bone #18 Unidentifiable bone fragment, 6 x 2.5 cm. Could be a piece of scapula from a large mammal.

Ia Bone #19 *Mammuthus* sp., limb bone fragment, 13 x 7.5 x 7.5 cm. Also, a smaller bone fragment 7 x 8 cm in size.

Ia Bone #20 Unidentified limb bone fragment, 4 x 2 cm in size.

Ia Bone #21 Partial epiphysis of articular head of humerus, 7.5 x 6 cm, from unidentified large mammal. Articular surface damaged, making ID difficult.

Ia Bone #22 *Mammuthus* sp., 7 tusk fragments. Sizes: 7 x 2.5 cm; 7 x 3 cm; 8.5 x 2.5 cm; 6.5 x 1.5 cm, other 3 fragments are small.

Ia Bone #23 *Mammuthus* sp., 10 tusk fragments. Sizes: 6 x 1.5 cm; 7 x 1.5 cm; 8 x 3 cm; and 5.5 x 3 cm; other 5 fragments are less than 4 cm in length.

Ia Bone #24 cf. *Mammuthus* sp., section of rib shaft, 17.5 cm long x 4 cm wide.

Ia Bone #25 cf. *Mammuthus* sp., 7.5 cm, x 5 cm fragment of a large limb bone.

MS-754

Ia Bone #26 *Mammuthus* sp., tooth fragment, includes 5 plates; total length 6 cm. Occlusal surface preserved, but sides and bottom of the tooth broken.
Width: 6.75 cm (incomplete tooth).
Height: 8 cm (incomplete tooth).
Measurements could not be used to determine to which tooth this fragment belongs because it is too incomplete. One bag of about 15 tooth fragments, each 2-6 cm.

Ia Bone #27 cf. *Mammuthus* sp., rib fragment, 11.5 x 3.5 cm.

Ia Bone #28 *Mammuthus* sp., partial innominate (pelvic fragment) in 2 pieces; part of the pubis or ischium around the obturator foramen. Overall length of both pieces together is 34 cm. Individual sizes: 17 x 8 x 6 cm and 22 x 11.5 x 13 cm.

Ia Bone #29 Unidentifiable bone fragments. 8 fragments 5.5-7.5 cm in length and 1.5-4 cm in width. Some could be mammoth rib fragments. Also in bag are 8+ smaller fragments, each under 4 cm in length.

Ia Bone #30
LI 95.2.140 *Mammuthus* sp., partial pelvis, in many fragments. Most or all are fragments of the ilium. One piece is an epiphyseal fragment, probably from the dorsal border of the ilium. The size of the epiphysis fragment is 8.5 cm x 7.5 x 2 cm thick. Note: The highest (dorsal) borders of each ilium appear to be actively growing bone tissue in living male elephants into their fifties and so the lack of epiphyseal fusion in this case should not be used as an indication of age of the individual. (See Gary Haynes, 1991, *Mammoths, Mastodonts and Elephants...*, p. 351).

Other fragment sizes: 2.5 x 9 cm; 16 x 13.5 x 7.5 cm; 15 x 8 x 2.5 cm; 15 x 6.5 cm; 24 x 4.5 x 2.5 cm; 17 x 8 cm.

Ia Bone #31 Bag 2 of 2. 2 unidentifiable bone fragments. Fragment sizes: 16.5 x 3.5 cm x 2.5 cm and 15 x 4 x 2 cm.

MS-748

Ia Bone #30 *Mammuthus* sp., continuation of bone #30 ID. Partial ilium (pelvic fragment). Size of ilium fragment: 56 cm long x 22 cm wide.

MS-765

Ia Bone #31 cf. *Mammuthus* sp., fragmented diaphysis of large limb bone in several bags.

Note: The limb bone fragments may be pieced together if the fragments are cleaned and can be glued together at some point in the future. At present, not enough is intact to determine what bone is represented because all of the pieces are too small. Unfortunately, the femur, tibia, humerus, and ulna all have shapes to diaphyseal fragments like the small pieces here.

One bag with a fragment from a large limb bone. No diagnostic characters present. Fragment size: 31 cm long x 7 cm wide x 3 cm thick. Bone is a diaphysis fragment.

Bag 1 of 4. Over 40 bone fragments from a large limb bone. Most fragments are 4 to 9 cm in length.

Bag 2 of 4. 3 bone fragments from a diaphysis of a large limb bone. Fragment sizes: 24.5 cm long x 3.5 cm wide x 3 cm thick; 11 cm long x 2 cm wide x 1.5 cm thick; and 9 cm long x 6 cm long.

Bag 3 of 4. 2 bone fragments from a diaphysis of a large limb bone. Fragment sizes: 27 cm long x 2.5 cm wide x 2.5 cm thick and 27.5 cm long x 4.5 cm wide x 3.5 cm thick.

Bag 4 of 4. 6 bone fragments from the diaphysis of a large limb bone. Fragment sizes: 18.5 cm long x 4.5 cm wide x 3 cm thick; 17.5 cm long x 4 cm wide x 1.5 cm thick; 23 cm long x 6.5 cm wide x 2 cm thick; 24 cm long x 6.5 cm wide x 2 cm thick; 16 cm long x 7 cm wide x 2.5 cm thick; and 15.5 cm long x 6.5 cm wide x 3 cm thick.

MS-757

Excavation Area I
LI 95.2.118 *Mammuthus* sp., proximal end of a left ulna. Only the proximal end is represented. The bone had been broken at midpoint through the semilunar notch. A portion of the olecranon process is also missing. No useful measurements were possible.

Note: The proximal epiphysis had fused. Fusion of the proximal epiphysis of the ulna in modern elephants occurs at about age 19 years for females and under 32 years (probably in the 20s) for males. There are variations of a few years either way on the ages of epiphyseal fusion, however. Also, with the same bone is a bag with four bone fragments. Part of the ulna? Fragment sizes: 9 cm long x 5.5 cm wide x 6 cm thick; 8.5 cm long x 8 cm wide x 4 cm thick; 7.5 cm long x 2.5 cm wide x 1 cm thick; and 12 cm long x 5.5 cm wide x 2 cm thick.

MS-758

Ib Bone #21 — *Mammuthus* sp., tusk fragments.

Fragment sizes: 8.5 x 4.5 cm; 8.5 x 5 cm; 11.5 x 3.5 cm; 7 x 3 cm; and 12 x 4 cm (with many surface striations); 11 x 5 cm (deep groove across the surface perpendicular to the length of the tusk, and parallel striations to this groove). One bag of 63+ tusk fragments that range in size from 3 to 9 cm length x 1 to 3 cm in width. Some striations on surfaces.

53 tusk fragments ranging in size from 2 to 10 cm in length x 1 to 2.5 cm width. Some have striations on the surfaces. Also, two fragments from a large limb bone present, 4 x 1.5 cm in size.

3 bags with several hundred tusk fragments, all under 11 cm in length by less than 4 cm in width; most much smaller (about 1-3 cm in length x 1-2 cm width). All tusk fragments about .5 cm in thickness.

Note: Care should be exercised in identifying striations on tusk surfaces as the result of trampling by large mammalian herbivores. Many scratches are produced on tusk surfaces during the life of elephants by everyday use.

MS-764

Ib Bone #1 — 2 bags

(1) skull fragment, from unidentified large mammal, 6 x 4 cm.

(2) 3 limb bone diaphysis fragments from a large mammal. No diagnostic characters present. Two fragments fit together; combined size is 10.5 cm long x 4 cm wide x 1 cm thick. Third fragment size; 8.5 cm long 1.5 cm wide.

Ib Bone #2 — Unidentified bone fragment from a large ungulate, 13 x 1.5 cm.

Ib Bone #3 LI 95.2.535 — *Bison* sp., proximal phalange.

Ib Bone #4 — Unidentifiable fragment from large mammal limb bone, 5.5 x 5 cm in size.

Ib Bone #5 — Unidentifiable bone fragment from large mammal, 5 x 3 cm.

Ib Bone #6 — cf. *Mammuthus* sp., neural spine and upper neural arch of a thoracic vertebra.

Ib Bone #7 — Rib fragment, 14.5 cm long x 1.5 cm wide, from deer-sized mammal. No diagnostic features present.

Ib Bone #8 — Shaft of rib in 3 pieces. From large unidentified mammal. Size: 31.5 cm long x (2.5-3.5) cm wide x 1.25 cm thick.

Ib Bone #9 — Partial rib including part of articular end and shaft, from deer-sized mammal. Rib in two pieces; together, size is 12 cm long x 10.5 cm wide.

Ib Bone #10 — Shaft of rib in 2 pieces. From large mammal. Overall size together 25 cm long x (3 to 4) cm wide.

Ib Bone #11 — Shaft of rib, 20.5 cm long x 4.5 cm wide. From large mammal.

Ib Bone #12 LI 95.2.155 — *Equus* sp., unerupted partial upper left molar. Based on tooth eruption patterns in living domestic Equus, this specimen is probably from an individual ca. 1 to 3 years of age depending on which tooth this is. It could be the P3, P4, M1 or M2. It is not the P2 or M3.

Ib Bone #13 LI 95.2.156 — *Mammuthus* sp., distal phalange.

Ib Bone #14 — Large mammal scapula fragment or ilium fragment in 2 pieces. No diagnostic features are present since it is only a small fragment. Together, size is 8 cm long x 3 cm wide x .5 cm thick. Sets of parallel striae on one surface suggestive of trampling by large mammals.

Ib Bone #15 — Unidentifiable fragment of compact bone, 3 cm long x 3.5 cm wide x 1 cm thick.

Ib Bone #16 — Unidentifiable skull fragment of a large mammal in two pieces. Together, the size is 5 x 3.5 x .25 cm thick.

Ib Bone #17 — Unidentifiable bone fragment with small partial articular surface. Unfortunately, no diagnostic features are present. Appears to come from a much larger bone. Size; 3.5 x 2 x 1.5 cm.

Ib Bone #18 — Scapula or ilium fragment. Looks like part of the same bone as Ib Bone #14. Size: 5.5 x 3 x 1.5 cm thick.

Ib Bone #19 LI 95.2.162 — *Equus* sp., portion of dentaries at the mandibular symphysis. Alveolus for right i1 present, i2 broken, with partial wall of i3 alveolus. On the left side of the symphysis, the wall for the left i1 alveolus is present.

Ib Bone #20 — Large mammal, fragmented limb bone. Perhaps one partial limb bone, perhaps more, are present. In its current state, it is too fragmented for further ID. The fragments are from the diaphysis. No articular surfaces are present. There are also a couple of fragments from a ?rib of a large mammal. Altogether, there are 32 fragments that range in size

from (3 to 13) cm in length x (1 to 4) cm wide. Also, a couple of pieces look like they may be from a neural spine of a thoracic vertebra.

Ib Bone #21 — cf. *Mammuthus* sp., unidentified bone fragment, 11.5 x 6.5 x 4 cm. Potentially, it could be a piece from a number of different elements. The robustness of the bone and rough surface texture suggests proboscidean.

MS-750

Ib Isolated bone (locations of bones not mapped). 9 bags of material.

Ib Debris flow, shoveled-up bone.
cf. *Mammuthus*, fragment from diaphysis of a large limb bone. No diagnostic features present. Size: 15.5 cm long x 5 cm wide x 1.5 cm thick.

Ib Debris flow, shoveled-up bone.
5 unidentifiable limb bone fragments. All less than 6 x 2.5 cm in size.

Ib Debris flow, shoveled up bone. cf. *Mammuthus* sp., partial neural spine of thoracic vertebra; tip and base are broken.

Ib Bone above tusk in rocks. Partial atlas of a large ungulate. Needs to be glued together; ID may be possible with good comparative collection.

Ib Debris flow, shoveled-up bone. Unidentified bone fragment from a large mammal, 11.5 x 7 x 2 cm thick.

Ib Bone above tusks in rocks. 2 small bone fragments, 2.5 x 2 cm (skull fragment), 2.5 cm x .5 cm fragment. Both fragments are unidentifiable.

Ib Bone above tusks in rocks. 2 unidentifiable fragments from a large mammal limb bone.
Sizes: 6 x 4 x 2 cm thick and 6 x 3 x 1 cm thick.

Ib Bone above tusk in rocks. 2 unidentifiable bone fragments from a large mammal. Sizes: 6 x 3.5 x 1 cm thick and 9 x 2 x 1 cm thick.

Ib Bone above tusks in rocks. cf. Mammuthus sp., partial shaft of rib. Size: 21 cm long x 4 cm wide x 1.5 cm thick.

South Block

MS-766

J Bone #2 — 2 unidentifiable bone fragments from a large mammal. Sizes: 4.5 x 1 x 1 cm thick and 4 x 2 x 1.5 cm thick.

J Bone #3 — 2 unidentifiable bone fragments from a large mammal. Sizes: 3.5 x 2.5 x 2.5 cm thick; 2.5 x 1.5 x 2 cm thick.

J Bone #4 — cf. *Mammuthus* sp., fragment of compact bone from a limb. Referred to mammoth on basis of bone thickness and surface texture. Size: 11 x 4.5 x 2 cm.

J Bone #5 — Unidentifiable bone fragment, 4.5 x 2.5 x .75 cm thick.

J Bone #6 — 2 bags

(1) Unidentifiable fragment from diaphysis of large mammal limb bone; Size: 11 cm long x 4 cm wide x 1.5 cm thick.

(2) Two small unidentifiable bone fragments, Sizes: 4.5 x 1.5 x 1 cm; 4 x 1.5 x 1 cm.

J Bone #7 — Unidentifiable bone fragment, 4.5 x 2.5 x 2 cm in size.

J Bone #8 — cf. *Mammuthus* sp., compact bone fragment from unidentified limb bone. Size: 10.5 cm long x 4 cm wide x 4 cm thick. Identified on the basis of thickness of the compact bone and surface texture.

J Bone #9 — Unidentifiable cancellous bone fragment, 6 x 3 x 2cm.

J Bone #10 — Unidentifiable bone fragment, 8.5 x 1.5 x 1.25 cm.

J Bone #11 — 22 unidentifiable bone fragments. Size ranges from (1 to 5) cm long x (1 to 3) cm wide.

J Bone #12 — cf. *Mammuthus* sp. Section of rib shaft; 13.5 cm long x 6 cm wide x 1.75 cm thick. A few surface striations present.

J Bone #13 — cf. *Mammuthus* sp. Unidentified limb bone fragment in 3 pieces. Partial articular surface is present, but insufficient for further ID. Size: 9 cm long x 5.5 cm wide x 4 cm thick.

J Bone #14 — Unidentifiable bone fragment. Size: 5.5 x 2.5 x 1.25 cm.

J Bone #15 — Large mammal, fragment of rib shaft. Size: 10 x 4.5 x 2.5 cm thick.

J Bone #16 — Unidentifiable limb bone fragment from a large mammal. Size: 11 x 4 x 2.5 cm thick. Striations present on bone surface.

J Bone #17 — 2 unidentifiable bone fragments. Sizes: 6.5 x 3.5 x 1.25 cm thick; 3.5 x 1.5 x 1 cm thick.

J Bone #18 — Unidentifiable limb bone fragment. Size: 9.5 x 4 x 2 cm thick. Groove (deep striation) present on surface of bone.

J Bone #19 — cf. *Mammuthus* sp., fragment of rib shaft in two pieces. Size: 12 cm long x 5 cm wide x 2.25 cm thick.

J SW 1/4 Bone #1 — unidentifiable bone fragment from a large mammal. Size: 5.5 cm long x 3.5 cm wide x 1.5 cm thick.

J SW 1/4 Bone #2 — unidentifiable bone fragment from a large mammal. Size: 6 cm long x 3.5 cm wide x 1.5 cm thick.

J SW 1/4 Bone #3	section of rib shaft from unidentified large mammal. Size: 11.5 cm long x 4 cm wide x 2 cm thick. Many other small fragments of the rib are also in the bag.
J SW 1/4 22 Bone #4	unidentifiable bone fragments. All under 4.5 x 2 cm in size.

MS-767

K Bone #1	2 unidentifiable bone fragments. Sizes: 4 x 1.5 x .75 cm; 3 x 1.5 x .75 cm.
K Bone #2	cf. *Mammuthus* sp., head of rib in 3 pieces. A large portion of the articular surface is broken. Overall size; 13 cm long x 6 cm wide x 3.25 cm thick.
K Bone #3	cf. *Mammuthus* sp., section of a rib shaft; 10 cm long x 5 cm wide x 2.5 cm thick.
K Bone #4	Unidentifiable limb bone fragment from a large mammal; probably mammoth. Size: 7.5 cm long x 3 cm wide x 1.75 cm thick.
K Bone #5	Unidentifiable bone fragment, 4.5 cm long x 2.5 cm wide x .75 cm thick.
K Bone #6	Unidentifiable fragment of compact bone; thickness suggests mammoth. Size 5 cm long x 2 cm wide x 1.75 cm thick.
K Bone #7	Unidentifiable bone fragment, 4.5 cm long x 2 cm wide x 1.5 cm thick.
K Bone #8	Unidentifiable bone fragment, 5.5 cm long x 3.25 cm wide x 1 cm thick. Bone surface exhibits moderate weathering in the form of surface cracks.
K SW 1/4 Bone #9	cf. *Mammuthus* sp., fragment from unidentified limb bone. Size: 12.75 cm long x 5.5 cm wide x 2.75 cm thick.
K SW 1/4 Bone #10	Unidentifiable bone fragment. Size: 4.5 cm long x 3.25 cm wide x 1.75 cm thick.
K SW 1/4 Bone #11	Unidentifiable limb bone fragment, probably mammoth, based on thickness. Size: 7.5 cm long x 3 cm wide x 2 cm thick.
K Bone #12	Unidentifiable bone fragment in 3 pieces from large mammal. Size: 7 cm long x 2 cm wide x .75 cm thick.
K Bone #13	Unidentifiable limb bone fragment, probably mammoth, based on thickness. Size: 8 cm long x 2.25 cm wide x 2.25 cm thick.
K SW 1/4 Bone #14	3 unidentifiable bone fragments. Sizes: 5 x 2 x 1 cm; 3.5 x 2.5 x 1.25 cm; 4 x 2.5 x .75 cm.
K Bone #15	Unidentifiable bone fragment from a large mammal. Size: 6.5 cm long x 3.25 cm wide x 1.5 cm thick.
K Bone #16	Unidentifiable bone fragment from a large mammal. Size: 8 cm long x 3.5 cm wide x 1.75 cm thick.
K SW 1/4 Bone #17	Unidentifiable bone fragment, probably mammoth. Outer bone surface plus mostly cancellous bone. Size: 5.5 cm long x 5 cm wide x 2.5 cm thick.
K SW 1/4 Bone #18	2 unidentifiable bone fragments. Sizes: 4.5 x 2 x 1.5 cm; 5.5 x 2.5 x 2.5 cm.
K Bone #19	cf. *Mammuthus* sp., limb bone fragment, insufficient detail for ID. May be possible to ID with better comparative collection because there is a small portion of an articular surface. Size: 5.5 x 5.5 x 3 cm thick.
K Bone #20	Unidentified bone fragment from a large mammal. Could be from several skeletal elements. It may be identified with a good comparative collection and time. Note: check the bone surface. Puncture marks on bone surface. Tooth marks?
K Bone #21	?mammoth vertebra fragment, zygopophysis with articular facet intact. Note: mark on bone surface (groove with ridges along surface; tooth marks?)
K Bone #22	2 bags of material. Bag 1. cf. *Mammuthus* sp., medial section of rib fragment in 5 pieces; largest fragment is 7.5 cm long x 5 cm wide x 1.5 cm thick. Bag 2. cf. *Mammuthus* sp., vertebra fragment in 2 pieces. Sizes: 5 x 4.5 x 4 cm; 3.5 x 2.5 x 2.5 cm.
K SW 1/4 Bone #23	cf. *Mammuthus* sp., rib fragments (2 pieces). Sizes: 6 cm long x 2.5 cm wide x 2 cm thick; 4.5 cm long x 1.75 cm wide x .75 cm thick. Note: check bone surface. Tooth marks or tool marks on surface of larger fragment.
K Bone #23 Y	cf. *Mammuthus* sp., 18 rib fragments. Largest fragment: 4.5 cm long x 4 cm wide x 1.75 cm thick. All other fragments are much smaller. Note: check surface marks on bone.
K Bone #24	2 unidentifiable bone fragments from a large mammal. Sizes: 5 x 2.5 x 2 cm and 2.5 x 1.5 x .5 cm.
K Bone #25	Unidentifiable bone fragment, 4.5 x 2.5 x 1.5 cm.
K Bone #26	6 rib fragments from a large mammal, all under 4 x 1.5 cm in size.
K Bone #27	cf. *Mammuthus* sp. Unidentified bone fragment with partial articular surface. Bone surface texture and the articular facet are characteristic of proboscidean. Fragment is 8 x 5 cm in size.
K Bone #28	Unidentifiable bone fragment, 4 x 3.5 x .75 cm. Note: parallel striations on bone surface.
K Bone #29	*Mammuthus* sp., 19 tusk fragments, all under 5 cm long x 2.5 cm wide.

MS-760

N Bone #1	*Mammuthus* sp., tusk fragment, 4 cm long x 2 cm wide.

N Bone #2	Unidentified bone fragment from "medium-sized" mammal. Tooth marks present. Evidence of having been chewed.
N NW 1/4 Bone #3	Unidentifiable bone fragment from a large mammal, 11 x 5 x 3.5 cm in size. Also, 2 smaller fragments of cancellous bone.
N Bone #4	Unidentifiable bone fragment from a large mammal, 7 x 6 x 2 cm thick.
N Bone #5	Unidentifiable bone fragment from a large mammal, 6 x 3 x 1.5 cm.
N SW 1/4 Bone #6	10+ unidentifiable bone fragments, all under 4 x 2 cm in size.
N SW 1/4 Bone #7	7 tooth fragments from ?one tooth? Unable to ID further in present condition. Perhaps further ID could be made if the fragments are be pieced together and glued.
N Bone #8	Unidentifiable bone fragment from a large mammal, 4.5 x 2.5 x 1.5 cm.
L Bone #1	3 unidentified bone fragments from a large mammal, largest is 6 cm long x 2.5 cm wide x 3 cm thick.
L Bone #2	*Mammuthus* sp., 26 tusk fragments; largest is 7 cm long x 4.5 cm wide x 4 cm thick. Either innermost portion of tusk or near the tusk tip.
L 30E, 15N, 86 BD	*Mammuthus* sp., 2 tusk fragments; largest is 2 x 1.5 x 1.25 cm.
O SW 1/4 Bone #1	Unidentifiable bone fragment, 1.5 x 1 x .25 cm.
O Bone #2	Unidentifiable bone fragment, 5.5 x 2.25 x 1 cm.
O Bone #3	Gastropod shell. (Needs ID by invertebrate paleontologist)
O Bone #4	Unidentifiable bone fragment, 2.5 x 1.25 x .5 cm.
O Bone #5	Unidentifiable bone fragment, 3 x 1.25 x .25 cm.

MS-749

O SW 1/4	Surface sweepings, waterscreen: 3 unidentifiable bone fragments less than 2 x 1 cm in size.
O SW 1/4 L-2	Waterscreen: 7 unidentifiable bone fragments less than 2 x 1 cm in size. Vial with diaphysis fragment of ? rodent limb bone and bivalve shell (needs ID by invertebrate paleontologist).
O SW 1/4 L-3	Waterscreen: 6 unidentifiable bone fragments less than 1 x 1cm in size.
O SW 1/4 L-4	Waterscreen: 20+ unidentifiable bone fragments, all under 2 x 1cm in size. Vial containing: (1) Rodentia, partial upper right incisor. (Larger than *Spermophilus columbianus*). (2) Small mammal, distal end of metapodial. (3) Enamel fragment from large mammalian herbivore, 1 cm long x .5 cm wide.
O SW 1/4 L:5	Waterscreen: 20+ unidentifiable bone fragments; largest is 3 x 1 cm. Two vials: (1) (a) Distal fused tibia-fibula, possibly muskrat; b) Rodentia, partial scapula. (2) Interesting specimen. Rock fragment, 1 x 1.5 cm. The rock fragment is a piece of chert with a fossil on each side. On the rock fragment is a Pleistocene/Recent bivalve shell.
O SW 1/4 L-7	7 unidentifiable tooth fragments; largest is .7 x .3 cm.
O SW 1/4 L-8	Bag of unidentified bone fragments, the largest of which is 3.5 x 2.5 x 1.5 cm.
O NW 1/4	Surface sweeping: Unidentified ??
O NW 1/4 L-3	Waterscreen: About 20 unidentifiable bone fragments, the largest is 1.5 x 3 cm. 4 Vials: (1) labelled possible Cretaceous crinoid. It is an invertebrate fossil, but looks more like a Paleozoic coral fragment, not a crinoid. (2) bivalve shell and two specimens of two different species of gastropod. (Need ID by an invertebrate paleontologist) (3) gastropod shell. (Needs ID by invertebrate paleontologist). (4) unidentified fragment of bone.
O NW 1/4 L-4	Waterscreen: About, 20 unidentifiable bone fragments under 1 x 1 cm in size.
O NW 1/4 L:6	Waterscreen: Unidentified bone fragment from a large mammal, 4 x 2 x .5 cm in size.
O NW 1/4 L:8	Waterscreen: Bag of about 30 unidentifiable bone fragments, most under 1 x 1 cm in size.
K NW 1/4 L-1	Waterscreen bone: Bag with unidentifiable bone fragments under 1 x 1cm in size. cf. *Mammuthus* sp., about 20 tusk fragments; largest fragment 2.5 x 1 cm.
K NW 1/4 L-2	Waterscreen: cf. *Mammuthus* sp., 100+ tusk fragments; largest is 6.5 x 3.5 x 1.5 cm thick.
K SW 1/4 L-2	Waterscreen bone: Five unidentifiable bone fragments; largest is 2.5 x 1 cm.
K SW 1/4 L-4	Bag of unidentifiable bone fragments; largest is 6 x 2.5 x 1 cm; most are much smaller than this.
K SW 1/4 L-5	40+ unidentifiable bone fragments, all under 6 x 3 cm; most are under 1.5 x 1 cm.
K SW 1/4 L-5	About 50 unidentifiable bone fragments; largest is 5.5 x 2.5 x 2.5 cm; most are much smaller than this. The largest fragment is likely a mammoth phalange fragment, but is too incomplete for unquestionable ID.

X	Waterscreen matrix bone: cf. *Mammuthus* sp., several small tusk fragments, all under 2.5 x 2.5 cm.
	20+ unidentifiable bone fragments.
X NW 1/4	Waterscreen bone: cf. *Mammuthus* sp., several tusk fragments, all under 5.5 x 2 cm.
	20+ unidentifiable bone fragments, most under 1 x 1cm.
	Surface (3 bags)
	Bag 1: Trench I cf. *Mammuthus* sp. a) proximal end (articular surface) of a phalange. b) 2 fragments of the mid section of a rib; largest 10 x 5 x 2.5 cm. c) several tusk fragments; largest 10 x 3 x 1.5 cm. - a couple of unidentifiable bone fragments.
	Bag 2: (largest plastic bag) Backhoe Trench I cf. *Mammuthus* sp. a) 3 rib fragments; largest is 11.5 x 4 x 2 cm. b) 3 tusk fragments, about 2.5 x 2.5 cm in size.
	Bag 3: (large plastic bag) Trench I cf. *Mammuthus* sp., partial centrum of a vertebra. cf. *Equus* sp., carpal/tarsal fragment.

MS-756

P SW L-1 Bone #1	Unidentified large ungulate limb bone fragment, 16 x 6 x 4 cm. Many parallel sets of striations present on bone surface, indicative of trampling by large mammalian herbivores.
P SW 1/4 L-3 Bone #2	Unidentifiable bone fragment, 3.5 x 2 cm.
P SW 1/4 L-3 Bone #3	11 small fragments from the skull of a large mammal; largest is 2 x 1.25 cm.
S Bone #1	Unidentifiable bone fragment in 2 pieces, 9 x 2.5 cm. Surface cracking of the bone indicates some weathering.
S Bone #2	Unidentifiable bone fragment, 6.5 x 3 x 1 cm. Some surface cracking of the bone indicating minor weathering.
S Bone #3	Diaphysis fragment from a large mammal limb bone, possibly a metapodial fragment from a large artiodactyl. Size: 11 x 4 x 2.25 cm.
S Bone #4, #5, #6	3 unidentified bone fragments, each about 3.5 x 2 cm.
T Bone #1	Medial section of rib fragment from unidentified large mammal. Size: 6 x 3.5 x 1.5 cm thick. T Bones #1 and #4 fit together. Are T bones #1-#6 from the same rib?
T Bone #2	Medial section of rib fragment from unidentified large mammal. Size: 7 x 3.5 x 1.5 cm. Some surface exfoliation of bone.
T Bone #3	Medial section of rib fragment from unidentified large mammal. Size: 5.25 x 3.5 x 1.5 cm.
T Bone #4	Medial section of rib fragment from unidentified large mammal. Size: 5.5 x 3.5 x 1.5 cm.
T Bone #5	Medial section of rib fragment from unidentified large mammal. Size: 6 x 3.5 x 1.5 cm. Some surface exfoliation of bone.
T Bone #6	Medial section of rib fragment from unidentified large mammal. Size: 5.5 x 2.75 x 1 cm.
U Bone #1	2 unidentifiable bone fragments; largest is 3.5 x 2 cm.
U Bone #2	Unidentifiable bone fragment, 5 x 2 cm.
U Bone #3, #4, #5	Medial section of rib from unidentified large mammal. Rib is in 4 pieces and all pieces fit together. Size: 11 x 3.5 x 1.25 cm.
X Bone #2	4 unidentifiable bone fragments. (? fragment of large mammal rib?) Note: 1 fragment has a deep groove on the surface with ridges along the surface of the groove. Tooth mark? Largest fragment size: 4 x 3 x 1 cm.
X Bone #3	6 unidentifiable bone fragments; largest is 4.5 x 1.5 cm.
X Bone #4	5 unidentifiable bone fragments; largest is 5 x 3.5 x 2.5 cm.
X Bone #5	13 unidentifiable bone fragments, all under 4 x 2.5 cm in size.
X Bone #6	?Metapodial fragment from a large artiodactyl. Size: 17 x 4 x 2 cm. Surface cracking is present indicating that the bone has been weathered. Also many sets of parallel striae suggest that the bone was trampled by large mammalian herbivores.
LI 95.2.309	*Canis latrans*, lower right p4.
X Bone #8	7 unidentifiable limb bone fragments from a large mammal; largest fragment is 6 x 2.5 cm.
X Bone #9	3 unidentifiable bone fragments; largest is 5.75 x 3 x 1.5 cm. Surface cracking of the bone suggests weathering prior to burial.
X Bone #10	5 unidentifiable bone fragments, largest is 3.5 x 2.5 x 2.5 cm.
X Bone #11	15 unidentifiable bone fragments; largest is 5.5 x 2.25 x 2 cm.
X Bone #11	Unidentifiable bone fragment, 2.75 x 2.5 x 1.5 cm.
X Bone #12	4 unidentifiable bone fragments, all about 2.5 x 2 x 1 cm.
X Bone #13	4 unidentifiable bone fragments; largest is 2.5 x 1.25 cm.

X Bone #14	Unidentifiable bone fragment in two pieces. Overall size: 6 x 2.75 x 1.5 cm.
X Bone #15	4 unidentifiable bone fragments; largest is 5 x 2 x 1.5 cm.
X Bone #16	Unidentified. Potentially identifiable, partial podial of a large mammal. Size: 3 x 2.5 x 2.5 cm.
X Bone #17	5 unidentifiable bone fragments from a large herbivore limb bone; largest is 8 x 2.5 x 1.5 cm.

MS-751

J SW 1/4	Shavings: 13 unidentifiable bone fragments; largest is 6.5 x 1.5 cm, most under 1 x 1 cm.
J SW 1/4 L-1	Waterscreen bone: 3 unidentifiable bone fragments under 3 x 1cm in size.
J SW 1/4 L-2	Waterscreen bone: 20+ unidentifiable bone fragments, most under 1 x 1 cm in size; largest is 5.5 x 1 cm.
J SW 1/4 L-4:	20+ unidentifiable bone fragments, most under 1 x 1cm in size; largest is 4.5 x 2 cm.
J NW 1/4 L-1	Waterscreen bone: 5 unidentifiable bone fragments; largest is 3 x 1 x 1.5 cm.
J NW 1/4 L-2	Waterscreen: 100+ unidentifiable bone fragments, most under 1 x 1 cm in size; largest is 5 x 3.5 x 1 cm. There is one rodent incisor fragment.
J NW 1/4 L-3	Waterscreen bone: 50+ unidentifiable bone fragments; largest is 6 x 3 cm. Most fragments are much smaller.
J NW 1/4 L-4	Waterscreen bone: 23 unidentifiable bone fragments; largest is 5 x 3 x 2 cm.
L	Waterscreen screen: *Mammuthus* sp., 100+ tusk fragments; largest is 5.5 x 3 cm. Most are under 1 x 1 cm in size. Also present are several unidentifiable bone fragments.
N SW 1/4 L-1	Waterscreen: 6 unidentifiable bone fragments under 1 x 1 cm. Also, enamel fragment from a large herbivore tooth, 1.5 x 1 cm in size.
N SW 1/4 L-2	Waterscreen: Vial:
N SW 1/4 L-2 LI 95.2.36	*Lemmiscus curtatus*, right dentary with i1, m1, and m2. ID based on being microtine with 5 triangles; no lingual wing development on lingual side of anterocap.
N SW 1/4 L-2 LI 95.2.536	Osteichthyes, fish trunk vertebra. Fragment of an arthropod carapace. (Needs ID by entomologist). *Mammuthus* sp., enamel fragment, 1.5 x .75 cm.
N SW 1/4 L-3	10+ unidentifiable bone fragments; largest is 5 x 3 x 1cm.
N SW 1/4 L-3	Waterscreen: 4 unidentifiable bone fragments under 2.5 x 1.5 cm. One fragment of enamel from a large artiodactyl tooth, 1.5 x 1 cm in size.
N SW 1/4 L-4	Waterscreen: 8 unidentifiable bone fragments, most under 1 x 1 cm.
N SW 1/4 L-5	Waterscreen: About 10 unidentifiable bone fragments under 1 x 1 cm. Also a vial with 1 .5-cm-long fragment of a rodent incisor.
N SW 1/4 L-6	Waterscreen: 20+ unidentifiable bone fragments under 1 x 1 cm. One fragment is about 3.5 x 3 cm in size.
N SW 1/4 L-7	Waterscreen: 2 unidentifiable bone fragments under 1 x 1 cm in size.
N SW 1/4 L-8	Bag of unidentifiable bone fragments; largest 4.5 x 2 cm in size, but most are under 1 x 1 cm. Also, a vial with artiodactyl tooth fragments. About 10 fragments, the largest of which is 1 x 2 cm, most are much smaller.
N SW 1/4 L-9	14 unidentifiable bone fragments; largest is 2.5 x 1 cm.
N NW 1/4 L-1	Waterscreen:
N NW 1/4 L-1 LI 95.2.21	Vial: Osteichthyes, skull bone fragment. *Spermophilus* sp., right femur from a young individual. Distal epiphysis is missing. (This specimen is Recent). 3 small unidentifiable bone fragments, each about 1 x .5 cm. One of the 3 is a skull fragment.
N NW 1/4 L-2	Waterscreen: Rodentia, small fragment of an incisor. From rodent about the size of a small ground squirrel. Small diaphysis fragment from a ?rodent limb bone, 1 x .4 cm. 3 small enamel fragments from a large herbivore tooth; largest fragment is 2 x .5 cm. 7 unidentifiable bone fragments under 3 x 1.5 cm in size.
N NW 1/4 L-4	Waterscreen: 10+ unidentifiable bone fragments under 2.5 x 1 cm in size. Vial: a) large carnivore (canid or felid) tooth fragment; b) rodent incisor.
N NW 1/4 L-4 LI 95.2.23	*Equus* sp., distal end of proximal phalange. 20+ unidentifiable bone fragments all under 3 x 1 cm in size. A couple are small enamel fragments from large herbivores.

N NW 1/4 L-5	Waterscreen: 12 unidentifiable bone fragments; the largest is 4.5 x 3 x 2.5 cm.
	2 of diaphysis fragments from the limb of a small mammal. No diagnostic features are present.
N NW 1/4 L-5	Waterscreen: 2 unidentifiable bone fragments about 1.5 x 1.5 cm in size.
N NW 1/4 L-6	Waterscreen: 10 unidentifiable bone fragments under 2 x 1 cm.
N NW 1/4 L-8	Waterscreen: About 100 unidentifiable bone fragments; largest is 7.5 x 2.5 cm, but most are smaller, about 1 x 1 cm.
N NW 1/4 L-9	3 unidentifiable bone fragments under 2 x 1 cm in size.
P NW 1/4 L-1	Waterscreen bone: 4 unidentifiable bone fragments under 2 x 1 cm.
P NW 1/4 L-2	Waterscreen bone: Vial with enamel fragment from tooth of a large herbivore, size 1.5 x .5 cm. Also in vial, cf. *Mammuthus* sp., tusk fragment, 2 x .5 cm.
	10+ unidentifiable bone fragments under 2 x 1 cm.
P NW 1/4 L-3	Waterscreen bone: cf. *Mammuthus* sp., 4 tusk fragments; largest is 2.5 x 1 cm.
	unidentifiable bone fragment, 2 x .75 cm.
P NW 1/4 L-5	Waterscreen bone: 4 unidentifiable bone fragments under 2 x 1.5 cm.
P SW 1/4 L-3	Waterscreen bone: small enamel fragment, 1.5 x .75 cm in size.
	10+ unidentifiable bone fragments under 2.5 x 1.5 cm in size.
P SW 1/4 L-4	Waterscreen bone: cf. *Mammuthus* sp., small fragment of tusk, 1.5 x 1 cm in size.
	10 unidentifiable bone fragments under 2 x 1.5 cm in size.

MS-759

Bags are listed by what is written on the label on the outside of each bag and the tag inside.

Overburden 6/23/95 RR
12 undentifiable bone fragments from a large mammal; largest 7 x 2.5 x 1 cm.

Enamel fragment from a large herbivore, 2.5 x 1 cm in size.

59 cm SW of Datum U, 297 cm NW of Datum S, CH 7/11/95
Unidentifiable bone fragment, 4.5 x 5.5 cm.

Unit S, overburden, 6/29/95 SW
3 unidentifiable bone fragments; largest is 8.5 x 4.5 cm.

X NE 1/4 Strat. Unit B Bone from screen 7/7/95 DA, DB
20+ unidentifiable bone fragments under 1 x 1 cm; one fragment 3.5 x 1.5 cm.

X Overburden 7/5/95 DA
Vial with gastropod shell (Needs ID by invertebrate paleontologist). Also a diaphysis fragment of a rodent limb bone, 1.75 cm long.

50+ unidentifiable bone fragments under 4 x 2 cm in size.

Area next to trench (South 95) overburden 6/23/95
2 unidentifiable bone fragments; largest is 3.5 x 2 cm.

xu: B natural west exposure south of backhoe trench CLH cleaning 6/95
Mid section of a rib fragment from a large herbivore, 8.5 x 4.5 x 2.25 cm.

South - 95 site overburden 7/8/95 KRM
Unidentifiable large mammal limb fragment, 8.5 x 4.5 x 1 cm.

Overburden RR 6/23/95
Mid section of a large mammal rib fragment, 19 x 3.5 x 1.5 cm. May be identifiable with a better comparative collection, but the specimen is not particularly significant. Some surface cracking indicates weathering.

Recent, mid section of a rib fragment from a medium-sized mammal; fragment size 5 x 2 x 1 cm.

South 95 overburden bone, eastern unit 6/28/95 DB, DA, SW, KM
14 unidentifiable bone fragments; largest is 5.5 x 3.5 cm.

Recent, cf. *Mephitis* sp., canine and metapodial.

Area next to trench (South 95) overburden bone 6/23/95 RR, SW
Recent, material includes both *Lepus* and *Spermophilus* noted below. Lepus sp.: right and left tibia; proximal left femur; distal half ?left femur; sacrum; vertebra; 2 metapodials; 3 phalanges. *Spermophilus* sp.: left innominate; right dentary; several cranial fragments including edentulous maxillae; upper incisors. Also, several miscellaneous unidentifiable bone fragments are present.

Area next to trench (South 95), Black layer area 6/24/95
Mammuthus sp., 5 tusk fragments; largest is 3.5 x 1.5 cm.

4 unidentifiable bone fragments; largest is 5.5 x 5 cm.

Area next to trench (South 95) 6/23/95 SW
5 unidentifiable bone fragments; largest is 10.5 x 3 cm.

Found on Beach 7/11/95 CH
Scapula fragment from a large mammal.

Overburden from I rodent bones 6/29
Recent, *Spermophilus* sp., 1 vial containing:
- left dentary with teeth
- cranial fragment
- partial right innominate
- partial right tibia
- 3 metapodials
- 1 partial incisor
- partial right femur

Recent, cf. *Catostomus*, (fish) right operculum in two pieces, in vial.

Surface 6/20/95 LBD rodent jaw
Recent, *Spermophilus* sp., right dentary with teeth.

XU: O SW 1/4 L-3 Waterscreen 6/25/95 DA, SW
cf. *Rana*, left distal humerus. Definitely not *Scaphiopus* because the condylar morphology is wrong. Too robust for a hylid. Of Ranidae and Bufonidae, it compares best with *Rana*.

XU: ? SW 1/4 L-3 (may be wall scrape) 7/9/95 DA, MC
fragment of enamel and dentine from tooth of an unidentified large herbivore, 1 x .5 cm in size.

I collected from slump over tusks 6/20/95 TW, KM, DB
Mammuthus sp., 2 tusk fragments, 3 x 1.5 cm is the largest.

12 unidentifiable bone fragments; largest is 4.5 x 3 cm.

I overburden over tusk 6/23/95 TW, DA, MC, KM
Bag of about 50 unidentifiable bone fragments; largest is 15 x 4 cm. Most are under 6 cm long. Most are from large mammal limb bones.

Mammuthus sp., partial proximal phalange. The distal articular surface is 7 cm wide. The proximal end is broken on each side. Greatest height is 9 cm.

Unit I Removal of overburden, random screening 6/20/95
LI 95.2.106
Equus sp., left half of a medial phalange.

Unidentifiable limb fragment from a large mammal, 10.5 x 3.5 x 2.5 cm.

Unidentifiable skull fragment, 5.5 x 3.5 x 1.5 cm.

I overburden 6/25/95 TW, MC, BG
Mammuthus sp., 3 tusk fragments; largest is 6.5 x 3.5 cm.

Recent, *Spermophilus* sp., 2 right dentaries with teeth.

Shaft fragment of rib from a deer-sized mammal; size 12 x 1.5 x 1 cm.

? cranial fragment of a large herbivore (encased in dirt so hard to see); about 9 x 6 cm.

10 unidentifiable bone fragments.

I Bone overburden from tusk area 6/24/95 (everyone:)
About 30 unidentifiable bone fragments under 6 x 4 cm in size.

Enamel fragment from a large mammalian herbivore tooth, 3 x 1 cm.

Recent, *Spermophilus* sp., left femur.

Limb bone diaphysis fragment from unidentified medium-sized mammal; fragment size 3 x 1.5 cm.

Overburden from Excavation Area I
LI 95.2.537
cf. *Antilocapra americana*, proximal phalange. Specimen is slightly larger than comparative specimen UMZM 4027.

distal metapodial fragment, ? camelid. Need better comparative material.

Overburden from around tusk 6/27/95 BG:
10 unidentifiable bone fragments; largest is 6 x 3 cm.

Equus sp., upper molar fragment.

XU: IB SW SE level: Bone removed from area of tusk 6/26/95 TW, DE, RR, CH, BG:
5 unidentifiable limb bone fragments; largest is 12 x 3.5 cm.

Mammuthus sp., 8 tusk fragments; largest is 3 x 2 cm.

1994 Museum of the Rockies Excavation

MS-688

MAB 1-10-7	30+ unidentifiable bone fragments. Most are less than 2 cm in size.
MAB 1-9-5	20+ unidentifiable bone fragments. Most are less than 2 cm in size.
MAB 1-6-3	10+ unidentifiable bone fragments.
MAB 1-7-3	30+ unidentifiable bone fragments.
MAB 1-8-4	30+ unidentifiable bone fragments.
MAB 1-10-6	30 unidentifiable bone fragments.
MAB 1-9-4	20+ unidentifiable bone fragments.
MAB 1-8-3	25 unidentifiable bone fragments.
MAB 1-7-2	8 unidentifiable bone fragments.
MAB 1-6-2	4 unidentifiable bone fragments.
MAB 1-5-2	8 unidentifiable bone fragments.
MAA 1-4-2	8 unidentifiable bone fragments.
MAA 1-5-1	7 unidentifiable bone fragments.
MAA 1-6-2	3 unidentifiable bone fragments.
MAA 1-7-2	5 unidentifiable bone fragments. One fragment shows signs of weathering.
MAA 1-8-7	8 unidentifiable bone fragments.
MAA 1-9-5	20+ unidentifiable bone fragments. One artiodactyl tooth fragment.
MAA 1-10-3	8+ unidentifiable bone fragments. One skull fragment.
MAA 1-10-4	8+ unidentifiable bone fragments.
MAA 1-9-4	8+ unidentifiable bone fragments.
MAA 1-8-8	15+ unidentifiable bone fragments, Including an enamel fragment.

MAA 1-7-3 20+ unidentifiable bone fragments.

MAA 1-6-3 10 unidentifiable bone fragments. One fragment with a partial articular facet, but without other diagnostic features.

MAA 1-5-2 2 unidentifiable bone fragments.

MAA 1-4-3 1 unidentifiable bone fragment.

MAA 1-3-1 5 unidentifiable bone fragments.

MAA 1-1-2 2 unidentifiable bone fragments.

MAB 1-9-2 Recent, unidentified small mammal, right ulna.

MAB 1-10-4 Recent, *Spermophilus* sp., right dentary fragment. cf. *Spermophilus* sp., radius.

MAB 1-8-1 Recent, *Spermophilus* sp.
- right tibia.
- right femur missing distal epiphysis.
- partial right innominate.

MAB 1-10-3 Recent, *Spermophilus* sp., right femur missing distal epiphysis.

MAA 1-6-1 Recent, *Spermophilus* sp.
- sacrum
- partial right innominate.
- cranial fragment.
- right dentary with p4 and m1.

MAA 1-10-2 Recent, *Spermophilus* sp.
- left tibia missing proximal end.
- right tibia.
- partial incisor.
- 2 skull fragments.
- proximal epiphysis of the tibia.
- ?distal tibia fragment.

MAA 1-10-1 Recent, *Spermophilus* sp., left dentary with teeth, 2 cranial ftagments, edentulous left dentary, left maxillary fragment, partial right femur with both ends damaged, proximal scapula fragment.

MAA 1-9-3 Recent, *Spermophilus* sp., two cranial fragments, scapula fragment, left tibia. (?Fossil), cranial fragment from unidentified small mammal and podial element.

MAA 1-9-2 Recent, *Spermophilus* sp., left maxillary fragment, left dentary with teeth.

MAA 1-7-1 Recent, *Spermophilus* sp., partial cranium, right dentary with teeth, partial left innominate, partial scapula. (1994)

MAA 1-7-1 LI 94.5.454 (fossil), *Ondatra zibethicus*, partial left dentary fragment with m2 and m3.

MAA 1-8-2 Recent, *Spermophilus* sp., scapula fragment, cranial fragment, left maxillary fragment, right ulna.

MAA 1-8-3 Recent, *Spermophilus* sp., three auditory bullae, maxillary fragment, five vertebrae, head of femur, cranial fragment.

MAA 1-8-2 Recent, *Spermophilus* sp., right ulna, scapula fragment, limb bone diaphysis fragment, cranial fragment, left maxillary fragment.

MAB 1-9-1 unidentifiable enamel fragment from tooth of large mammal; 1.5 x .5 cm in size.

MAB 1-10-2 unidentifiable enamel fragment from tooth of large mammal; 3 x 1.5 cm in size.

MAB 1-9-3 *Camelops*? sesamoid bone. Also present is an unidentifiable bone fragment.

MAB 1-7-1 Recent, Proximal epiphysis of tibia of a small mammal.

MAB 1-10-5 4 unidentifiable bone fragments, all under 2 x 2 cm in size.

MAB 1-10-1 Unidentifiable enamel fragment from tooth of large mammal, 1 x 1cm in size.

MAB 1-6-1 Unidentifiable enamel fragment from tooth of large mammal, 1 x 1cm in size.

MAB 1-8-2 2 unidentifiable bone fragments; largest is 6 x 2.5 cm.

MAA 1-8-5 Distal epiphysis of a femur, small mammal. May be able to ID further with considerable investment of time. Also unidentifiable bone fragment 1 x 1 cm in size.

MAA 1-8-6 2 unidentifiable bone fragments from a large mammal, each about 4 x 4 cm.

MAA 1-8-1 2 unidentifiable bone fragments from a small mammal, each about 1 x .4 cm. They are not enamel fragments as is labelled on the bag.

MAA 1-4-1 LI 94.5.185 *Equus* sp., proximal sesamoid of foot.

MAA 1-8-4 Potentially indentifiable with good comparative collection. Partial carpal or tarsal from a large mammal, 2.5 x 2 cm in size.

MS-686

CS-20-1 Recent, *Spermophilus* sp., 2 right dentaries, the ascending ramus missing on each.

CS-11-3 Recent, cf. *Spermophilus* sp., lumbar vertebra.

CS-7-1 Recent, *Spermophilus* sp., right dentary missing m2 and m3, right humerus missing proximal epiphysis.

CS-22-1 Recent, *Spermophilus* sp., partial cranium including left maxilla with no teeth, three incisors, partial lefr innominate.

CS-8-1	Recent, *Spermophilus* sp., partial cranium including basicranial region and portions of both maxillaries and zygomata, right humerus missing proximal epiphysis.
CS-15-3	Recent, *Spermophilus* sp., proximal end of left tibia, partial left innominate.
CS-9-2	Recent, *Spermophilus* sp., left tibia missing proximal end.
CS-14-3	Recent, *Spermophilus* sp., left dentary and left ulna.
CS-16-2	Recent, *Spermophilus* sp., left femur with proximal and distal ends damaged.
	Phalange missing distal end. May be small carnivore.
CS-18-1	Recent, *Spermophilus* sp., left edentulous dentary.
CN-25-2	(Recent or fossil ?), Tooth and bone are rather dark in color, looks fossil. Specimen consists of a cranial fragment with incisor from an unidentified rodent.
CN-19-1	Recent, *Spermophilus* sp., partial left dentary.
CN-10-2	Recent, *Spermophilus* sp., left tibia, and atlas.
CN-4-1	Recent, small mammal metapodial.
CN-7-1	Recent, *Spermophilus* sp., distal end of left humerus.
CN-20-4	Recent, *Spermophilus* sp., partial right innominate.
CN-15-1	Recent, phalange of ?large rodent.
CN-14-2	Recent, edentulous right dentary, cf. *Thomomys*.
CN-12-2	Recent, unidentifiable bone fragment from a small mammal.
CN-16-3	Recent, *Spermophilus* sp., two metapodials and partial right innominate.
CN-6-1	Recent, *Spermophilus* sp., right humerus, left humerus, partial right humerus, partial right innominate.
CN-21-2	Recent, *Spermophilus* sp., partial left dentary and an axis.
CN-27-1	3 unidentifiable bone fragments under 2.5 x 1.5 cm in size.
CN-26-2	4 unidentifiable bone fragments under 2.5 x 1.5 cm in size.
CN-21-3	?*Mammuthus* sp., interior skull fragment, 11.5 x 5.5 x 3.5 cm.
	About 20 unidentifiable bone fragments under 2.5 x 3 cm.
	Recent, *Spermophilus* sp., few fragments of broken skeletal elements.
CN-22-4	30+ unidentifiable bone fragments; largest is 5.5 x 2 cm in size.
CN-25-3	bivalve shell (needs ID by invertebrate paleontologist).
	25+ unidentifiable bone fragments all under 3 x 2 cm in size.
	unidentifiable tooth fragment from large herbivore, 1.75 x 1 cm in size.
CN-25-3 LI 94.5.246	Osteichthyes, parietal fragment.
CN-23-5	*Mammuthus* sp., 3 enamel fragments; largest is 1.75 x 1 cm.
	40+ unidentifiable bone fragments; largest is 6.5 x 1.5 cm.
	3 unidentifiable tooth fragments from a large ungulate, all under 1.5 x 1.5 cm.
CN-19-2	18 unidentifiable bone fragments; largest is 4 x 2 cm. Several are skull fragments from large mammals.
CN-14-7	About 40 unidentifiable bone fragments; largest is 3.5 x 1.5 cm.
CN-24-3	26 unidentifiable bone fragments, the largest is 4 x 2.5 cm. Includes a couple of skull fragments from large mammals.
CN-24-3 LI 94.5.245	Anatidae, thoracic vertebra.
CN-20-8	50+ unidentifiable bone fragments, most under 1 x 1 cm, largest is 5 x 1.5 cm. Some are skull fragments from large mammals. Some material is clearly weathered.
CN-17-2	11 unidentifiable bone fragments; largest is 3 x 1.5 cm. A couple are skull fragments from a large mammal.
CN -17-2 LI 94.5.248	Osteichthyes, skull bone fragment, ?suborbital.
CN-9-3	3 unidentifiable bone fragments, all under 3 x 1.5 cm. One is a skull fragment from a large mammal.
CN-15-2	6 unidentifiable bone fragments; largest is 3.5 x 1 cm.
CN-13-3	8 unidentifiable bone fragments; largest is 3 x .75 cm.
CN-18-5	20+ unidentifiable bone fragments, most are under 2 x 2 cm, largest is 15.5 x 4.5 x 1.5 cm. Some smaller pieces are skull fragments from a large mammal. Some fragments exhibit weathering.
CN-18-5 LI 94.5.249	Osteichthyes, skull bone fragment.

CN-12-3	*Mammuthus* sp., tooth fragment, 2 x 1.5 cm.
	About 40 unidentifiable bone fragments; largest is 6 x 2 cm.
	1 gastropod shell. (Needs ID by invertebrate paleontologist).
CN-11-5	13 unidentifiable bone fragments; largest is 3 x 2.5 cm.
CN-1-1	5 unidentifiable bone fragments; largest is 3.5 x .75 cm.
CN-7-2	6 unidentifiable bone fragments; largest is 3 x 1.5 cm.
	cf. *Mammuthus* sp., limb bone fragment, 6.5 x 5 cm. ID based on size and texture of the bone surface.
CN-8-2	9 unidentifiable bone fragments; largest is 3.5 x 1 cm.
CN-6-2	15 unidentifiable bone fragments; largest is 4 x 2 cm.
	cf. *Equus* sp., tooth fragment, 3.5 x 1.25 cm. Material insufficient to confirm ID.
CN-4-2	*Mammuthus* sp., tooth fragment, 2 x .75 cm.
	8 unidentifiable bone fragments; largest is 3.5 x 1.5 cm.
CN-3-1	Four unidentifiable bone fragments; largest is 3.5 x 1.5 cm.
CN-5-1	*Mammuthus* sp., two tooth fragments; largest is 1.5 x 1 cm.
	Ten unidentifiable bone fragments; largest is 4 x 2 cm.
CN-16-4	About 30 unidentifiable bone fragments, most are under 2 x 2 cm, largest is 4.25 x 2.5 cm.
	Mammuthus sp., three tooth fragments; largest is 3 x 2 cm.
CN-10-4	About 40 unidentifiable bone fragments, most are under 2 x 2 cm, the largest is 5 x 4.5 cm. The largest fragment could be a mammoth scapula fragment.
CS-27-2	30+ unidentifiable bone fragments; largest is 3 x 2.5 cm. Several have articular surfaces but none have diagnostic features. They are small fragments of larger bones.
CS-10-1	About 40 unidentifiable bone fragments, most are smaller than 2 x 2 cm. The largesr is 5.5 x 4 cm.
CS-1-1	1 unidentifiable bone fragment, about 1.5 x 1 cm in size.
CS-4-1	12 unidentifiable bone fragments; largest is 2 x 1.5 cm.
CS-2-1	6 unidentifiable bone fragments; largest is 2.5 x 1 cm.
CS-5-1	32 unidentifiable bone fragments, all under 2.5 x 1.5 cm.
CS-S-1 LI 94.5.256	*Spermophilus* sp., edentulous right dentary fragment. Alveoli for m2 and m3 present.
CS-6-1	23 unidentifiable bone fragments; largest is 2.5 x 1.5 cm.
CS-14-5	*Mammuthus* sp., enamel fragment, 2 x 1cm.
	Gastropod shell, (needs id of invertebrate paleontologist).
	60+ unidentifiable bone fragments; largest is 6.5 x 2 cm, most are under 2 x 2 cm.
CS-15-4	Bivalve shell, (needs id of invertebrate paleontologist).
	60+ unidentifiable bone fragments; largest is 4.5 x 3 cm, most are under 2 x 2 cm.
CS-8-2	About 30 unidentifiable bone fragments; largest is 4 x 3 cm, most are under 2 x 2 cm.
CS-3-1	8 unidentifiable bone fragments; largest is 2.5 x 1.5 cm.
CS-7-2	About 30 unidentifiable bone fragments; largest is 5 x 2 cm.
CS-9-3	About 30 unidentifiable bone fragments; largest is 3.5 x 3 cm.
CS-11-4	About 60 unidentifiable bone fragments, most are under 3 x 3 cm, largest is 4.5 x 3.5 cm.
CS-12-1	*Mammuthus* sp., 7 tooth fragments, mostly enamel.
	40+ unidentifiable bone fragments; largest is 4 x 3.5 cm, most are under 2 x 2 cm.
CS-19-2	10+ unidentifiable bone fragments; largest is 4.5 x 2 cm.
CS-26-2	Bivalve shell (needs ID by invertebrate paleontologist).
	3 enamel fragments from large mammal, about 2.5 x .5 cm.
	20+ unidentifiable bone fragments, most are under 2 x 2 cm; largest is 12 x 2 cm. The largest fragment is a limb bone fragment with parallel striae on surface.
CS-28-2	10 unidenrifiable bone fragments all under 2 x 2 cm excepr one which is 6 x 1.5 cm.

CS-25-2	4 tooth fragments from unidentified large mammal. All are under 2.5 x 1 cm in size.
	About 30 unidentifiable bone fragments, most are under 1 x 2 cm, largest is 6 x 3.5 cm.
CS-25-2 LI 94.5.247	Osteichthyes, two bones. One is ?opercular fragment and the other a parietal fragment.
CS-24-4	*Mammuthus* sp., tusk fragment, 3 x 1 cm.
	20+ unidentifiable bone fragments; largest is 5 x 2 cm.. Weathering and abrasion are noted for some of the fragments.
CS-23-2	10 unidentifiable bone fragments; largest 7 x 2 cm. Also two enamel fragments from large ungulate.
CS-22-2	20+ unidentifiable bone fragments; largest is 5 x 1.5 cm, most are under 2 x 1 cm.
CS-21-1	cf. *Mammuthus* sp., 9 molar fragments; largest is 3.5 x 1.5 cm.
	(looks Recent) *Spermophilus* sp., partial lefr dentary with p4 and m1.
	About 10 unidentifiable bone fragments; largest is 4 x 1 cm.
CS-16-3	About 40 unidentifiable bone fragments, most under 2 x 1 cm, largest is 6 x 3.5 cm. Includes 1 tooth fragment from large ungulate, but insufficient material for ID. No diagnostic features (2.5 x .5 cm).
CS-17-2	About 30 unidentifiable bone fragments, some are skull fragments; largest fragment is 4.5 x 3 cm.
CS-18-4	Gastropod shell (needs id of invertebrate paleontologist).
	cf. *Mammuthus* sp., tooth fragment, 1.5 x 1.5 cm.
	30+ unidentifiable bone fragments, most under 2 x 1 cm, largest is 5 x 2.5 cm.
CS-13-4	*Mammuthus* sp., tooth fragment, 1.5 x 1 cm.
	50+ unidentifiable bone fragments; largest is 4 x 2.5 cm, most are under 2 x 1 cm.
CS-20-3	cf. *Mammuthus* sp., three tooth fragments; largest is 1.5 x 1.5 cm.
	20+ unidentifiable bone fragments; largest is 3 x 2 cm, most under 1 x 2 cm.

MS-741

CN-18-1	Tooth fragment from unidentified artiodactyl. No diagnostic characters present. Size 3 x .75 cm.
CN-20-1	cf. *Mammuthus* sp., tooth fragment, 1.5 x 1.5 cm.
CN-20-3	Unidentified large ungulate incisor fragment. Too incomplete for further ID.
CN-23-3	2 tooth fragments from unidentified large artiodactyl. No diagnostic characters present. Each fragment is about 1.5 x .75 cm.
CN-24-2	Tooth fragments from large ungulate(s). Fragments under 3 x 2 cm.
CN-25-1	*Mammuthus* sp., enamel fragment, 1 x 1 cm.
	Enamel fragment from unidentified large artiodactyl, 2.5 x .5 cm.
CN-26-1	*Mammuthus* sp., enamel fragment, 2 x .5 cm.
CN-12-1	1 enamel fragment from unidentified artiodactyl. No diagnostic characters present; 1.5 x 1.5 cm.
CN-11-2	*Mammuthus* sp., tooth fragment, 2.5 x 2 cm.
	Unidentifiable bone fragment, 3 x 2 cm.
	cf. *Equus* sp., very worn incisor fragment.
CN-10-1	2 unidentifiable enamel fragments each about 2 x 1 cm.
CN-8-1	*Mammuthus* sp., enamel fragment, 1.5 x 1 cm.
	Unidentifiable bone fragment, 4 x 1.5 cm.
CN-14-1	*Mammuthus* sp., 7 tooth fragments; largest is 4 x 2.5 cm.
CN-17-1	2 unidentifiable tooth fragments from large ungulate, each ~ 3 x .75 cm.
CN-21-1	Unidentifiable tooth fragment, 3.5 x 2.5 cm.
CN-22-1	Unidentifiable tooth fragment from large ungulate, 2 x .5 cm.
CN-23-1	Unidentifiable incisor fragment from large ungulate, 2.75 x .75 cm.
CN-23-2 LI 94.5.455	Cervidae, left i1or i2, compares well with *Cervus elaphus*, but is rather small for elk. It compares somewhar favorably to a few specimens of *Odocoileus* but is too large.
CN-11-1	Recent, *Antilocapra americana*, right maxillary fragment with P3 and P4.
CN-16-2 LI 94.5.451	*Mammuthus* sp., partial tooth.
CN-20-2	Artiodactyl enamel fragment, 2.5 x 1 cm.
C Slump 1	Recent, *Spermophilus* sp., cranium.
CN-14-5	Recent, - Goose/duck, proximal humerus. - unidentified bone fragment. - rib
CN-13-2	Recent, *Spermophilus* sp., cranium.
CN-11-3	Unidentified skull fragment, probably mammoth, but lacks diagnostic features. Size: 9.5 x 6 cm.

CN-18-4	cf. *Mammuthus* sp., tooth fragment, 2.25 x 1.75 cm.
	one unidentifiable bone fragment, 2 x 1.5 cm.
	rib shaft fragment from a large mammal, ?mammoth, 6.75 cm long x 4 cm wide.
CN-20-6	Unidentifiable skull fragment from a large mammal, 8 x 4.5 cm in size. Exhibits weathering cracks on surface.
CN-22-3	Unidentified bone fragment, 2.5 x 1.5 cm. Partial rounded articular surface, however, it appears to be only a small fragment. Insufficient detail for further ID.
CN-24-1	2 tooth fragments, possibly mammoth. Texture on outer surface looks like mammoth tooth; largest fragment is 1.25 x .75 cm. It is not tusk, as is recorded on the tag inside the specimen bag.
CN-16-1	Enamel fragment from unidentified large mammal. No diagnostic characters present. Size: 2 x .5 cm. It is not tusk, as is recorded on the tag inside the specimen bag.
CN-11-4	Unidentifiable diaphysis fragment from limb bone of a medium-sized mammal. No diagnostic characters present. Size 6 x 1.5 cm. A few parallel striations present on the surface.
CN-9-2	Unidentifiable bone fragment, 2.75 x 2 cm.
CN-14-6	Unidentifiable bone fragment, 3 x 2 cm.
CN-18-2	Unidentifiable skull fragment from large mammal, 2.5 x 2 cm.
CN-20-5	Unidentifiable skull fragment from large mammal, 5.5 x 5 cm.. Some surface cracking of bone suggestive of weathering.
CN-22-2	?rib fragment from large mammal, 13.5 x 2.5 cm.. Some cracking and exfoliation on bone surface suggests weathering.
CN-13-1	Recent, *Lepus* sp., right tibia in two pieces.
CN-10-3	Potentially identifiable partial carpal/tarsal from large ungulate.
CN-9-1	Recent, *Lepus* sp, right calcaneum. Is this part of an associated leg along with specimens CN-13-1 and CN-14-4?
CN-14-4	Recent, *Lepus* sp., right femur.
CN-20-7	4 unidentifiable skull fragments from large mammal; largest fragment is 5.5 x 3.5 cm.
CS-23-1	Rib, proximal end with articular surfaces, from large mammal.
CN-14-3 LI 94.5.363	*Mammuthus* sp., proximal phalange in 4 pieces. Proximal end broken. Distal transverse width is 8.25 cm. Greatest height (i.e. length) is 10.5 cm. Distal anteroposterior width (i.e., thickness) is 5 cm.
CN-23-4	cf. *Mammuthus* sp., ?dentary fragment. Deep surface cracking on bone surface suggests weathering. Fragment size is 15.5 x 8.5 x 3 cm thick.
CS-11-2:	*Mammuthus* sp., partial phalange, 5.5 x 7.5 x 5 cm thick.
CS-26-1:	cf. *Mammuthus* sp., partial epiphysis of vertebra centrum in 3 pieces. Total size: 5.5 x 5 cm.
CS-24-1:	*Equus* sp., tooth fragment, 3 x 1.5 cm.
	Tooth fragment from unidentified large ungulate, 3 x 1 cm. No diagnostic features present. Neither fragment is mammoth as is recorded on the tag in the specimen bag.
CS-25-1:	2 unidentifiable bone fragments, each about 4 x .75 cm.
	4 tooth fragments from large ungulate. No diagnostic characters present; largest fragment is 2.5 x 1 cm.
CS-24-3	2 unidentified bone fragments from a large mammal.
CS-28-1	*Mammuthus* sp., enamel fragment, 1.5 x 1 cm.
	Tooth fragment from unidentified artiodactyl. Not enough detail for ID.
CS-27-1	3 unidentifiable tooth fragments; largest is 1.5 x 1 cm.
CS-16-1	Unidentifiable skull fragment from large mammal, 4 x 2.5 cm.
CS-14-1	*Mammuthus* sp., enamel fragment, 1.5 x .75 cm.
	Unidentifiable tooth fragment from large artiodactyl, 1.75 cm x .75 cm.
CS-9-1	*Mammuthus* sp., two enamel fragments; largest is 3 x 1.5 cm. Neither is tusk as is recorded on tag in specimen bag.
CS-13-3	Unidentifiable bone fragment, 4 x 2.5 cm.
CS-14-4 LI 94.5.456	cf. *Antilocapra americana*, proximal end of proximal phalange.
CS-15-2	Recent, Aves. Distal end of limb fragment.
CS-17-1	cf. Mammuthus sp., cranial fragment. ID based on size and texture of bone. Fragment size: 10.5 x 8 x 4 cm. Bone surface had cracked indicating weathering.
CS-13-1	*Mammuthus* sp., tooth fragment, 3 x 1.5 cm.

Equus sp., upper molar fragment in 2 pieces. Together, the tooth fragment is 5.5 x 2 x .75 cm.

CS-24-2 Unidentified bone fragment from a large mammal.

CS-19-1 Recent, Rodent tibia and cf. *Lepus* sp., metapodial. Metapodial surface is etched.

CS-18-3 cf. *Mammuthus* sp., two cranial fragmenrs. ID based on size and texture of the bone. Largest is 12.5 x 7.5 x 2 cm thick.

Unidentifiable bone fragment from a medium-sized mammal, 3 x 1 cm.

CS-14-2 Unidentifiable skull fragment, 3 x 2 cm.

CS-11-1 *Mammuthus* sp., two tooth fragments. Largest is 2.5 x 2.5 cm.

CS-20-2 2 tooth fragments, including: One fragment is unidentifiable, .75 x .5 cm. Other fragment cf. *Camelops*, 1.5 x 1.5 cm.

CS-18-2 *Equus* sp., upper molar fragment, 2.75 x .75 cm.

CS-15-1 *Mammuthus* sp., tooth fragment, 1.5 x 1.5 cm.

Unidentifiable tooth fragment (not mammoth, however).

CS-13-2 Unidentified, hollow diaphysis fragment from a limb bone, 2.5 cm long x .5 cm wide. The ID of possible bird or rabbit as recorded on tag in specimen bag is as accurate as possible.

MS-685

ES-25-3 cf. *Mammuthus* sp., rib fragment in three pieces. Together it is 12 cm long x 6 cm wide x 3 cm thick.

ES-26-6 15 unidentifiable bone fragments. Largest is 10 x 6 x 1.5 cm. They are probably mammoth limb bone fragments taking into account the general size and thickness.

EN-2 cf. *Odocoileus* sp., proximal phalange. Compares well with *O. hemionus* UMZM 4945. It is too robust for *Antilocapra*. There are tooth marks? on the surface and it looks like it's gone through a large carnivore's digestive tract; surface etched. These features should be examined further.

EN-26-3 cf. *Mammuthus* sp., head of rib, 6 x 4 cm.

EN-8-2 cf. *Mammuthus* sp., unidentified limb bone fragment with partial articular surface. 6.5 x 2.5 cm.

EN-21-3 tooth fragment from unidentified large ungulate, 3.5 x 1 cm.

EN-21-1 tooth fragment from unidentified large ungulate, 3.5 x 1 cm.

EN-21-2 tooth fragment from unidentified large ungulate, 2.5 x .5 cm.

EN-14-2 *Camelops* sp., buccal side, outer enamel fragment, probably from the upper M2 or M3, 5.5 x 2 cm.
LI 94.5.86

EN-26-2 5 unidentifiable bone fragments. They include: a mid section of a rib, 6 x 3.5 cm (largest fragment of the five); a vertebra fragment, two small skull fragments; one unidentifiable bone fragment.

EN-12-2 *Mammuthus* sp., fragment from the root of a tooth, 3 x 1 cm.

EN-18-1 tooth fragment from unidentified large ungulate, 2.5 x 1 cm.

EN-15-3 enamel fragment from unidentified large mammal, 1.5 x 1 cm.

EN-26-1 cf. *Mammuthus* sp., tusk fragment, 3 x 2.5 cm. There are two grooves on the bone surface. The grooves have ridges along their bottoms. The surface marks should be examined further.

EN-14-1 unidentifiable bone fragment from a large mammal, 8 x 2.5 cm.

Caudal vertebra from a small mammal. Could be from any of several mammals.

EN-25-1: unidentifiable bone fragment, 1 x 1 cm. It is not a small inner ear bone as labelled on the tag in the specimen bag.

EN-25-2 unidentifiable bone fragment, 4 x 1.25 cm.

EN-20-2 Anseriformes, extreme distal end of left humerus. Compares well with *Anas*.

EN-25-3 unidentifiable bone fragment, 5.5 x 2.5 cm.

Potentially identifiable bone fragment, but requires excellent comparative collection and considerable time.

Text Pit/Excavation Area E
Mammoth tooth frag/bones from wall 8/16/94 KM

Mammuthus sp., Bag of several dozen fragments of mammoth tooth and a few bone fragments.

ES-26-2 *Mammuthus* sp., phalange.
LI 94.5.98 Minor damage to the distal end.
Proximal end, transverse diameter: 6.3 cm.
Proximal end, anteroposterior diameter: 5.0 cm.
Maximum height: 6.5 cm.
Distal end, transverse diameter: 5.4 cm.

ES-26-1 *Mammuthus* sp., tooth.
LI 94.5.100

ES-27-1 *Mammuthus* sp., six tooth fragments. Largest is 5 x 4 cm.

ES-26-7 *Mammuthus* sp., three tooth fragments. Largest is 3.5 x 3.5 cm.

ES-25-1 *Mammuthus* sp., tooth fragment, 1.5 x 1.5 cm.

Probably Trext Pit/Excavation Area E

LI 94.5.97 *Ondatra zibethicus*, left lower m1.

ES-26-3 2 unidentifiable bone fragments from large mammal. These are probably mammoth rib fragments. Largest: 8.5 x 3 cm.

ES-25-4 Unidentifiable skull fragment from a large mammal, 4.5 x 2.5 cm.

ES-26-5 cf. *Mammuthus* sp., partial mid section of a rib, 13 cm long x 3.5 x 2 cm. There are surface marks present. These should be examined further.

?rib fragment, 8 x 3 cm.

ES-26-4 cf. *Mammuthus* sp., two ?rib fragments; largest 11 x 3 cm. There are marks on the surface of the smaller fragment. These should be examined further.

ES-15-1 unidentified bone fragment from large mammal, 13 x 5 x 3 cm.

MS-604

LBD C14-2 ~20 bone fragments, mostly pieces of rib, from a large mammal(s). The rib fragments are midsections which are not easily identifiable. Largest fragment: 9 x 2 cm.

Near C-1 Recent, cf. *Antilocapra americana*, left calcaneum, heavily weathered.

Second Collection Area Beach

~90 unidentifiable bone fragments; largest is 7.5 x 4 cm.

Mammuthus sp., one small tusk fragment.

Beach U1-S-3 30 unidentifiable bone fragments; largest is 13.5 x 4.5 cm.

Beach Unir 1-S-1 *Mammuthus* sp., tooth fragment, 2.5 x 1.5 cm.

Two unidentifiable tooth fragments from large ungulate, ~2.5 x 1 cm.

Main Area S-3 Recent, two unidentified bone fragments.

Beach S-1 LI 94.5.457 Cervidae, deciduous lower left molariform tooth. Characters are between *Cervus elaphus* and *Alces alces*.

Beach S-1 LI 94.5.458 *Bison* sp., tooth fragment.

Main Area S-2 Recent, large cervidae, well worn premolar.

Secondary Collection Area S-3

Rib shaft from deer-sized mammal.

Recent, cf. *Marmota* sp., right humerus missing proximal end.

Secondary Collection Area S-1

Mammuthus sp., four tooth fragments; largest is 3.5 x 3 cm.

Equus sp., four tooth fragments; largest is 5.5 x 1.5 cm.

Four unidentifiable tooth fragments from large ungulate.

Main Beach S - 2 *Equus* sp., five tooth fragments, upper and lower dentition, largest is 7 x 3 cm.

Bison sp., tooth fragment, 3 x 2 cm.

15 unidentifiable tooth fragments from large ungulate(s), largest is 6 x 2 cm.

One unidentifiable bone fragment.

Main Beach S- 1 *Mammuthus* sp., two molar fragments, 3 x 2.5 cm, and two tusk fragments, 3 x 1.5 cm.

Artiodactyl tooth fragment, 3 x 1.5 cm.

LBD C14 - 1 cf. *Mammuthus* sp., unidentified limb bone fragment. No diagnostic features are present but size and surface texture suggest proboscidean. Size 18.5 x 9.5 x 2.5 cm thick.

Channel Bone for Dating

20 rib fragments from unidentified large mammal(s). No articular surfaces present. These are mid rib frags. Largest is 12.5 x 4.5 cm. Note: There are some parallel srriae present on a couple of the largest fragments.

Beach S-2 cf. *Mammuthus* sp., fragment from blade of scapula or fragment of ilium. Size 18.5 x 11.5 cm. ID based on shape and size of fragment. No other diagnostic characters are present. There is a deep striation (groove) on one side.

Recent, cf. *Antilocapra americana*, distal half of left radius, missing epiphysis.

Two rib fragments from unidentified large mammal.

Main Beach S-5 *Mammuthus* sp., three tusk fragments; largest is 8.5 x 3 cm. Also 2 molar fragments; largest is 4.5 x 3.5 cm.

8 unidentifiable limb bone fragments, probably mammoth, based on size, largest is 16.5 x 5.5 cm.

~100 unidentifiable bone fragments, all under 8 x 2 cm, most much smaller.

Main Beach S-4 neural spine of thoracic vertebra of medium-sized mammal. No diagnostic features, so could be from any of several animals.

a couple of skull fragments.

two rib shaft fragments from medium-sized to small mammal.

ulna/radius (fused) fragment from large artiodactyl. Possibly *Camelops*.

MS-746

Second Collection Area - S-2 .
Left ischium fragment from a large artiodactyl.

Secondary Collection Area - S-4
LI 94.5.460 - *Bison* sp., left medial phalange.
LI 94.5.459 - *Camelops* sp., distal end of proximal phalange.

Beach - S-2 Acetabulum fragment from a large ungulate, with a few surface striations present on the bone surface.

Beach U1-S-2 Recent, *Taxidea taxus*, atlas.

Beach - S-2 Vertebra, ?camel.

Main Beach S-4 cf. *Mammuthus* sp., unidentified bone fragment.

Math Beach S-3 LI94.5.134 *Mammuthus* sp., basicranial fragment with one occipital condyle.

MS-740

Beach Surface #8
LI 94.5.461 *Camelops*, proximal epiphysis of phalange.

Beach Surface #7
Recent, *Bos*, left astragalus.

Far Beach Surface #27
cf. *Mammuthus* sp., partial carpal or tarsal. Three articular surfaces present but most of the element is missing. May be identifiable with good comparative collection.

Beach Surface #29
Bison sp., 2 upper molar fragments.

Equus sp., upper molar fragment.

3 tooth fragments from unidentified large ungulate; largest is 4 x 1 cm.

Far Beach Surface #26
cf. *Mammuthus* sp., partial carpal or tarsal. Two partial articular facets are present, but most of element is missing. Probably identifiable with a good comparative collection.

LI 94.5.115 *Mammuthus* sp., ?left metacarpal V.

Beach Surface #21
Unidentified bone fragment from a large mammal. The bone is weathered. It may be identified with a good comparative collection.

Far Beach Surface #28
Ilium fragment from a large artiodactyl. Material too incomplete for further ID.

LI 94.5.126 *Equus* sp., left cuneiform.

Far Beach Surface #20
cf. *Mammuthus* sp., unidentified bone fragment. Possibly identifiable using a good comparative collection.

Beach Surface #10
Fragment of the pubis, including acetabular facet, from an unidentified large artiodactyl. Probably camel or bison.

No Context LI 94.5.119 *Mammuthus* sp., left trapezium.
Maximum height: 9.21 cm
Maximum transverse diameter: 9.55 cm
Maximum anteroposterior diameter: 5.70 cm
(Measurements taken with calipers).

No Context LI 94.5.130 *Canis lupus*, proximal half of right metatarsal 3.

No Context LI 94.5.120 *Mammuthus* sp., proximal phalange.
There is some surface exfoliation of bone due to weathering.
Maximum height: 7.46 cm.
Maximum anteroposterior diameter (proximal end): 6.18 cm.
Damage to sides of proximal and distal ends prevented measurements of transverse diameter.

Beach Surface #24
Equus sp., 10 tooth fragments, all under 7 x 2.5 cm. These include upper and lower dentition. None is more than half complete.

One unidentifiable tooth fragment from a large ungulate.

Beach Surface #23
Distal condylar fragment of large artiodactyl metapodial. Too incomplete for further ID.

Beach Surface #19
Bison sp., tooth fragment, 5 x 1.5 cm.

7 unidentifiable tooth fragments from large ungulates. A couple are probably horse, but diagnostic features are lacking; Largest: 7x 1.5 cm.

MS-745

Beach Surface Bone 10/26/94 BG, RR
cf. *Mammuthus* sp., partial rib (proximal end). 53 cm long x 5 cm wide x 2 cm thick.

Bone from exposed tusk area 8/16/94
6 unidentifiable bone fragments from large ungulate(s), all under 12 x 5 cm.

Beach Surface Bone 10/26/94 BG, RR
5 unidentifiable bone fragments from large ungulate(s); largest: 19.5 x 4 cm (rib fragment).

Far Beach Surface 8/16/94 RR
-10 unidentifiable bone fragments from large ungulate(s); largest 10.5 x 3 cm (limb bone fragment).

Beach Bone 8/15/94 KM, LBD, RR
Mammuthus sp., 3 tooth fragments; largest 4.5 x 1.5 cm.

~80 unidentifiable bone fragments; largest 14 x 5.5 cm.

4 unidentifiable tooth fragments from a large ungulate(s).

Mid section of a rib from a medium-sized mammal. No diagnostic features. 24.5 cm long x 2.25 cm wide x less than 1 cm thick.

Beach Bone 8/15/94 KM, LBD, RR
50+ unidentifiable bone fragments; largest is 12.5 x 2.5 cm. Also a few rocks.

Far Beach Surface Bone Fragments 8/15/94 LBD, KM, RR
~50 unidentifiable bone fragments; largest is 11.5 x 6 cm.

No Context
LI 94.5.114 *Mammuthus* sp., metapodial with proximal end missing. Damage too extensive to ID element further. Element also heavily weathered. Maximum height greater than 16.5 cm (proximal end missing). Remainder of element too damaged for useful measurement.

Beach Surface #4
LI 94.5.462 *Bison* sp., proximal end of a right ulna.

MS-743

EN-20-1 Recent, *Spermophilus* sp., left maxillary fragment, no teeth.

EN-8-1 Recent, *Spermophilus* sp., left dentary with i, p4, m1.

partial cranium of a microtine rodent, only incisors present.

EN-11-1 Recent, *Spermophilus* sp., cranial fragment, left humerus missing distal end, right scapula, proximal end of left scapula.

EN-13-1 Recent, *Spermophilus* sp., right innominate, sacrum, partial left innominate, right humerus, left ulna.

EN-18-2 Recent, *Spermophilus* sp., partial cranium (basicranial region).

EN-9-1 Recent, *Spermophilus* sp., 2 partial crania including right and left maxillaries with some teeth, right femur missing distal epiphysis, left humerus missing proximal and distal epiphyses.

EN-7-1 Recent, tibia with broken fused fibula, missing the proximal and distal epiphyses, from an unidentified small mammal, possibly juvenile cottontail rabbit.

Spermophilus sp., distal end of left tibia, lumbar vertebra, partial left innominate, left humerus missing proximal and distal epiphyses.

EN-10-1 Recent, distal end of left tibia from unidentified small mammal.

right calcaneum from unidentified small mammal.

EN-12-1 Recent, *Spermophilus* sp., two lumbar vertebrae, partial right dentary with teeth, right femur, proximal right femur missing epiphysis.

EN-19-1 Recent, *Spermophilus* sp., distal half of left humerus.

EN-3-1 Recent, *Spermophilus* sp., partial cranium including both maxillaries with no teeth, partial left dentary with no teeth, partial right dentary with i and m1, left femur missing distal epiphysis, partial right femur missing proximal and distal ends.

EN-15-1 Recent, cf. *Spermophilus* sp., partial left humerus missing proximal end.

EN-1 Recent, cf. *Spermophilus* sp., partial left tibia missing proximal end.

ES-12-2 (?Recent or ?Fossil), specimen is dark in color. Spermophilus sp., partial right dentary with only partial incisor present.

ES-8-1 Recent, *Spermophilus* sp., left dentary with no teeth, right and left maxillaries, right dentary w i and p4, auditory bulla, left humerus, partial left innominate, lumbar vertebra, left humerus missing proximal epiphysis, juvenile right ulna, juvenile right femur missing epiphyses, juvenile left humerus missing epiphyses.

(?Recent or ?Fossil), specimen is dark in color,

Spermophilus sp., left dentary fragment with p4 and m1.

ES-16-1 Recent, *Spermophilus* sp., right innominate.

Thomomys sp., partial cranium with upper left P4.

ES-11-1 (?Recent or ?Fossil), specimen is dark in color. cf. *Thomomys* sp., left humerus missing proximal end.

EN-17-1 Recent, *Spermophilus* sp., partial cranium including right maxilla with teeth, proximal left scapula, left humerus missing part of proximal end.

ES-7-1 Rodentia, partial incisor.

ES-9-1 Recent, *Spermophilus* sp., right femur missing distal epiphysis.

limb bone fragment from unidentified rodent.

ES-14-1 Recent, *Spermophilus* sp., 2 partial crania with no teeth, 4 upper incisors, 1 molar.

?rodent diaphysis fragment from limb bone.

ES-18-1 rodent basicranial fragment, from ?ground squirrel.

ES-25-5	~200+ unidentifiable bone fragments, most under 1.5 x 1 cm. Largest is 6.5 x 4 cm. There are several small tooth fragments, cf. mammoth, but no enamel present.
ES-26-8	100+ unidentifiable bone fragments; largest is 6.5 x 3 cm. Most are under 2.5 x 2.5 cm.
	Spermophilus sp., tooth fragment, 3 x 2.5 cm.
ES-3-1	4 unidentifiable bone fragments; largest is 2 x .5 cm.
ES-2-1	Unidentifiable bone fragment, 2.5 x 2 cm.
ES-8-2	20 unidentifiable bone fragments, most under 2 x 1 cm, largest is 5 x 2 cm.
ES-11-2	20+ unidentifiable bone fragments, most under 2.5 x 1 cm.
ES-4-1	4 unidentifiable bone fragments; largest is 3.5 x 2 cm.
ES-7-2	9 unidentifiable bone fragments; largest is 5 x 2.5 cm.
ES-7-2 LI 94.5.28	*Ondatra zibethicus*, right calcaneum.
ES-5-1	5 unidentifiable bone fragments; largest is 2.75 x 1.25 cm.
ES-9-2	~20 unidentifiable bone fragments; largest is 3.5 x 2 cm.
ES-12-?	~30 unidentifiable bone fragments; largest is 4 x 1.5 cm.
ES-6-1	~10 unidentifiable bone fragments, all under 3 x 2 cm. A few rocks present.
ES-10-1	~20 unidentifiable bone fragments; largest is 4.5 x 1 cm. Also a few rocks.
ES-14-2	~20 unidentifiable bone fragments, 4 x 3 cm is the largest.
ES-13-1	~15 unidentifiable bone fragments, all under 4 x 2 cm.
ES-27-2	50+ unidentifiable bone fragments, most under 3 x 1.5 cm, largest is 8 x 4.5 cm.
ES-16-2	~20 unidentifiable bone fragments, most under 2.5 x 2 cm, largest is 5.5 x 2.5 cm.
ES-18-2	~15 unidentifiable bone fragments and a couple of rocks. Largest bone fragment is 5 x 2 cm, but most under 2 x 1 cm.
ES-17-1	11 unidentifiable bone fragments; largest is 3.5 x 4 cm.
ES-23-1	7 unidentifiable bone fragments; largest is 4.5 x 3 cm.
ES-19-1	10 unidentifiable bone fragments; largest is 3 x 2 cm.
ES-20-1	11 unidentifiable bone fragments; largest is 3 x 2 cm.
ES-21-1	~20 unidentifiable bone fragments; largest is 4 x 1.75 cm.
ES-22-1	~20 unidentifiable bone fragments; largest is 4.5 x 2 cm.
ES-15-2	~30 unidentifiable bone fragments; largest is 3.5 x 1.5 cm.
EN-26-4	cf. *Mammuthus* sp., a few small tusk fragments.
	100+ unidentifiable bone fragments, most under 2 x 2 cm; largest is 7 x 4 cm.
EN-13-2	20+ unidentifiable bone fragments; largest is 7 x 2.5 cm.
EN-25-4	Bivalve shell (needs ID by invertebrate paleontologist).
	Mammuthus sp., 2 tusk fragments, ~2.5 x 2 cm.
	50+ unidentifiable bone fragments; largest is 4.5 x 2.5 cm.
EN-7-2	6 unidentifiable bone fragments, all under 1.5 x 1 cm.
EN-27-1	*Mammuthus* sp., 3 tusk fragments; largest is 2 x 1.5 cm.
	30+ unidentifiable bone fragments, most under 1 x 1 cm, largest is 4 x 2.25 cm.
EN-23-1	11 unidentifiable bone fragments; largest is 2 x 1 cm.
EN-11-2	14 unidentifiable bone fragments; largest is 3.5 x .75 cm.
EN-19-2	8 unidentifiable bone fragments; largest is 2.5 x 1.25 cm.
EN-18-3	8 unidentifiable bone fragments; largest is 3 x 1.25 cm.
EN-21-4	3 unidentifiable bone fragments, 1 is a rooth fragment from a large ungulate, largest is 2.75 x 2 cm.
EN-22-1	2 unidentifiable bone fragments less than 1.5 x 1.5 cm.
EN-16-1	17 unidentifiable bone fragments; largest is 3.5 x 2.5 cm.
EN-15-4	20+ unidentifiable bone fragments; largest is 4.5 x 3.5 cm.
EN-14-2	~20 unidentifiable bone fragments; largest is 4.5 x 3.25 cm.

	Mammuthus sp., enamel fragment, 2.5 x 1.5 cm.
E-24-1 (E-North)	~20 unidentifiable bone fragments; largest is 4.5 x 2.5 cm.
EN-8-3	11 unidentifiable bone fragments; largest 3.5 x 1.5 cm.
	Spermophilus sp., (one is clearly Recent, the other is dark in color (?Fossil). 2 partial right dentaries. Both lack teeth and are missing the anterior portion of each dentary, and also the ascending ramus is broken on each.
EN-1-2	unidentifiable bone fragment, 1 x .5 cm.
EN-12-3	14 unidentifiable bone fragments; largest is 5.5 x 3 cm.
EN-5-2	9 unidentifiable bone fragments; largest is 4 x 1.5 cm.
EN-6-1	7 unidentifiable bone fragments, 1 is a tooth fragment from a large ungulate, largest fragment is 1.75 x 1 cm.
EN-9-2	6 unidentifiable bone fragments, 1 is a tooth fragment from a large ungulate, largest fragment is 2.5 x 1.5 cm.
EN-10-2	6 unidentifiable bone fragments; largest is 2 x 2.25 cm.
EN-20-3	7 unidentifiable bone fragments; largest is 3 x 1.5 cm.
EN-17-2	23 unidentifiable bone fragments; largest is 5.5 x 2.75 cm.
	cf. *Mammuthus* sp., 2 small tusk fragments under 2 x 1 cm.

Merrell Locality (Beach Collection)

MS-747

BLM #1	cf. *Mammuthus* sp., head of rib.
BLM #2	5 unidentified bone fragments from a large element. All are likely mammoth. Three pieces are cranial fragments. No other diagnostic characteristics present.
BLM #3	cf. *Mammuthus* sp., 30+ tusk fragments; largest is 6 x 2.5 cm.
	50+ unidentifiable bone fragments; largest is 6.5 x 4 cm.
BLM #4	*Mammuthus* sp., 2 enamel fragments, each about 2.5 x 1 cm.
	Equus sp., tooth fragment, 6 x 1.5 cm.
	unidentified enamel fragment from a large mammal, 2.5 x 1 cm.
BLM #5	unidentifiable bone fragment from a large mammal, 12 x 4 x 2 cm.
BLM #6	cf. *Mammuthus* sp., unidentifiable limb bone fragment, 30 x 6.5 x 1.5 cm thick. Large size and robustness suggests mammoth.
BLM #7	cf. *Mammuthus* sp., unidentifiable limb bone fragment, 21 x 9.5 x 2 cm. Size and robustness suggest mammoth. The specimen is weathered.
BLM #8	Unidentified bone fragment from a large mammal, in several pieces; largest fragment is 6 x 4 x 3 cm. Possibly acetabular fragment.
BLM #9	*Equus* sp., tooth fragment from an upper molar.
	Mammuthus sp., 4 enamel fragments; largest is 7.5 x 3.5 cm.
	cf. *Mammuthus* sp., 2 bone fragments. One fragment is from the proximal end of a metapodial.
	cf. *Mammuthus* sp., 6 tusk fragments; largest is 5 x 2 cm.
	about 40 unidentifiable bone fragments most under 7.5 x 1.5 cm.
	enamel fragment from a large ungulate, 4.5 x 1 cm.
	60 unidentifiable bone fragments, most under 5 x 3 cm.
	6 unidentifiable bone fragments; largest is a cranial fragment, most likely mammoth, 7 x 5 cm.
	9 unidentifiable bone fragments.

BLM #10 and #11 not present. 1 listed as ash and shell.

MS-560

BLM #12	*Mammuthus* sp., enamel fragment, 6.5 x 3.5 x 2.5 cm.
	cf. *Mammuthus* sp., tusk fragment, 10 x 2.5 x .25 cm.
	2 unidentifiable bone fragments.
	limb bone fragment, 17 x 5 x 1 cm, suggestive of proboscidean.
	6 unidentifiable bone fragments.
	2 unidentifiable bone fragments.
	2 unidentifiable bone fragments.
	13 unidentifiable bone fragments.
BLM #13	cf. *Mammuthus* sp., partial rib in several pieces; largest fragment is 24 x 5 x 2.5 cm.

BLM #14 cf. *Mammuthus* sp., unidentifiable bone fragment, 12 x 12 x 10 cm, and several small bone fragments with it. No diagnostic features present. Size suggests proboscidean.

BLM #15 2 unidentifiable bone fragments; largest is 10.5 x 4.5 x 1.5 cm.

BLM #16 *Equus* sp., tooth fragment, 5.5 x 1 x .5 cm.

Equus sp., unidentified tarsal fragment (navicular or cuneiform fragment).

Recent, *Spermophilus* sp., partial cranium.

70+ unidentifiable bone fragments; largest is 9 x 2.5 x .5 cm.

BLM #17 unidentifiable bone fragment, no diagnostic features, but is probably mammoth based on size, 30 x 12 x 12 cm. May be a pelvic fragment.

MS-562

BLM #18 unidentified bone fragment in sediment (fine-grained matrix).

BLM #19 cf. *Mammuthus* sp., cranial fragment, 14 x 11 x 3.5 cm.

Beach BLM #20
LI91.1.3 *Bison* sp., naviculocuboid.

BLM #21 cf. *Mammuthus* sp., partial neural arch and partial neural spine of a vertebra.

Beach BLM #22
LI91.1.4 *Equus* sp., partial right navicular.

Beach BLM #23
LI91.1.5 *Bison* sp., partial proximal end of metacarpal III/IV.

Beach BLM #24
LI91.1.6 *Equus* sp., partial medial phalange.

BLM #25 Recent (not fossil) *Bos* metatarsal III/IV.

BLM #26 cf. *Mammuthus* sp., tarsal or carpal fragment. Too incomplete for further ID. 7 x 4 x 4 cm.

BLM #27 *Bison* sp., right scaphoid.

BLM #28 unidentified bone fragment of a large mammal, 9 x 6 x 2.5 cm. Material too incomplete for further ID.

BLM #29 cf. *Mammuthus* sp., bone fragment with a partial articular surface, too incomplete for further ID. Based on size, it is probably mammoth.

BLM (Beach recovery during 1995 backfill)
cf. *Mammuthus* sp., rib fragment, 19 x 3.5 x 3.5 cm. There are a couple of small fragments with it.

Equus sp., proximal end of a proximal phalange.

MS-744

Bag containing *Equus* sp., 2 tooth fragments (upper molar); largest is 7 x 3 x 1 cm. *Mammuthus* sp., 4 tooth fragments; largest is 4.5 x 5 x 1 cm.

cf. *Mammuthus* sp., 3 tusk fragments; largest is 12 x 4 x 1 cm.

2 unidentifiable bone fragments. Largest is 12 x 5 x 2 cm.

36 unidentifiable bone fragments; largest is 15 x 3.5 x 1cm. Also *Mammuthus* sp., enamel fragment, 4 x 1.5 x .25 cm.

Bag with 15 unidentifiable bone fragments; largest is 12.5 x 4.5 x 2 cm.

also zygopophysis of a vertebra (probably mammoth).

rib fragment.

Recent, *Bos*, left metatarsal III/IV.

Recent, *Bos*, partial scapula.

CN-18-3 *Mammuthus* sp., tooth fragment in several pieces, largest fragment is 8 x 2 x 1 cm.

15 unidentifiable bone fragments; largest is 12 x 4.5 x 3 cm.

cf. *Mammuthus* sp., about 18 tusk fragments; largest is
7.5 x 3.5 x .5 cm.

52 unidentifiable bone fragments; largest is 20.5 x 3.5 x 1 cm. *Equus* sp., 2 tooth fragments; largest is 7.5 x 2 x 1 cm (an upper molar fragment)

1993 Beach Surface #17
LI93.2.2 *Equus* sp., left innominate fragment.

1993 Beach Surface #35
LI93.2.1 *Bison* sp., left innominate fragment.

Bag containing the following:

cf. *Mammuthus* sp., 5 tusk fragments.

Recent humerus and carpometacarpus of Anatidae? (Didn't check ID further since the specimen is not fossil.)

14 unidentifiable bone fragments.

Mammuthus sp., tooth fragment, 7.5 x 6.5 x 3.5 cm.

Beach surface #3
Equus sp., 10 tooth fragments.

Mammuthus sp., 4 tooth fragments.

7 miscellaneous unidentified fragments.

Beach Surface #16 (1993)
unidentifiable bone fragment, 14.5 x 6 x 2 cm.

Beach Surface #1
unidentified diaphysis fragment. It is hollow. It may be bird or possibly rabbit. No diagnostic features. No further ID made since it is of little scientific value.

Beach Surface #2
Unidentified bone fragment. May be distal end of a metapodial.

Recent, *Spermophilus* sp., r. and l. dentaries, l. innominate, l. femur, partial humerus.
Small carnivore, l. edentulous dentary of a juvenile.

Appendix E. Technical Detail for Luminescence Dating.

Sample	UW352 Merrell Sample 1				
Type	sediment				
Context	sandy silt lens – Top of Unit A				
Burial Deep	2.7		**Fading**	No Test	
Grain Size	90-125 µm				
Method	osi				
TL		**OSL**			
technique		**technique**	single aliquot 60-120 grains, SAR		
plateau °C		**shine**	5s		
				dose rate (Gy/ka)	
Value	**error**	**fit**		**value**	**error**
De (GY)	186	17.5 sat exp	**alpha**	0.033029	0.016374
scale	1		**beta**	1.495449	0.082845
b-value (Gy µm2)	1.86	0.98	**gamma**	0.945853	0.050523
			cosmic	0.202376	0.04172
			total	2.676707	0.106886
moisture sediment	0.15	0.05			
Age (ka)	69.48837	7.102356			
calender	67488.37	7102.356 BC			
% error	10.22093				

Sample	UW352 Merrell Sample 1				
Type	sediment				
Context	sandy silt lens – Top of Unit A				
Burial Deep	2.7		Fading	No Test	
Grain Size	90-125 µm				
Method	osi				
TL		OSL			
technique		technique	multi-aliquot slide		
plateau °C		shine	5s		
				dose rate (Gy/ka)	
Value	error	fit		value	error
De (GY)	143.4	14.3 sat exp	alpha	0.033029	0.016374
scale	1		beta	1.495449	0.082845
b-value (Gy µm2)	1.86	0.98	gamma	0.945853	0.050523
			cosmic	0.202376	0.04172
			total	2.676707	0.106886
moisture sediment	0.15	0.05			
Age (ka)	53.57329	5.75479			
calender	51573.29	5754.79 BC			
% error	10.7419				

Sample	UW352 Merrell Sample 1				
Type	sediment				
Context	sandy silt lens – Top of Unit A				
Burial Deep	2.7		Fading	No Test	
Grain Size	90-125 µm				
Method	osi				
TL		OSL			
technique		technique	single aliquot 60-120 grains, SAR		
plateau °C		shine	5s		
				dose rate (Gy/ka)	
Value	error	fit		value	error
De (GY)	79.9	10.5 sat exp	alpha	0.033029	0.016374
scale	1		beta	1.495449	0.082845
b-value (Gy µm2)	1.86	0.98	gamma	0.945853	0.050523
			cosmic	0.202376	0.04172
			total	2.676707	0.106886
moisture sediment	0.15	0.05			
Age (ka)	29.85011	4.099831			
calender	27850.11	4099.831 BC			
% error	13.73472				

Sample	UW352				
Type	sediment				
Context	sandy silt lens – Unit C				
Burial Deep	1.1		Fading	No Test	
Grain Size	90-125 µm				
Method	osi				
TL		OSL			
technique		technique	single multi-aliquot slide		
plateau °C		shine	5s		
				dose rate (Gy/ka)	
Value	error	fit		value	error
De (GY)	83	8.3 sat exp	alpha	0.011577	0.00937
scale	1		beta	1.217129	0.072893
b-value (Gy µm2)	1.86	0.98	gamma	0.687216	0.039175
			cosmic	0.250275	0.051758
			total	2.166197	0.098055
moisture sediment	0.1	0.05			
Age (ka)	38.50066	4.209323			
calender	36500.66	4209.323 BC			
% error	10.93312				

Sample	UW353				
Type	sediment				
Context	sandy silt lens – Unit C				
Burial Deep	1.1		Fading	No Test	
Grain Size	90-125 µm				
Method	osi				
TL		OSL			
technique		technique	single aliquot, 60-120, SAR		
plateau °C		shine	5s		
				dose rate (Gy/ka)	
Value	error	fit		value	error
De (GY)	76.5	30.2 sat exp	alpha	0.011577	0.00937
scale	1		beta	1.217129	0.072893
b-value (Gy µm2)	1.86	0.98	gamma	0.687216	0.039175
			cosmic	0.250275	0.051758
			total	2.166197	0.098055
moisture sediment	0.1	0.05			
Age (ka)	35.31535	14.03284			
calender	33315.35	14032.84 BC			
% error	39.73579				

Sample	UW354 Merrell Sample 3				
Type	sediment				
Context	sand strata below rock-mud debris in NorthBblock				
Burial Deep	2.7		Fading	No Test	
Grain Size	90-125 µm				
Method	osi				
TL		OSL			
technique		technique	single aliquot 60-120 grains, SAR		
plateau °C		shine	5s		
				dose rate (Gy/ka)	
Value	error	fit		value	error
De (GY)	136.9	28.4 sat exp	alpha	0.016537	0.01471
scale	1		beta	1.644163	0.047823
b-value (Gy µm2)	1.86	0.98	gamma	0.885367	0.027009
			cosmic	0.236078	0.0475
			total	2.782145	0.074089
moisture sediment	0.06	0.02			
Age (ka)	49.20664	10.29171			
calender	47206.64	1029.71 BC			
% error	20.91529				

Sample	UW354 Merrell Sample 3				
Type	sediment				
Context	sandy strata below rock-mud debris in North Block				
Burial Deep	2.1		Fading	No Test	
Grain Size	90-125 µm				
Method	osi				
TL		OSL			
technique		technique	single aliquot 60-120 grains, SAR		
plateau °C		shine	5s		
				dose rate (Gy/ka)	
Value	error	fit		value	error
De (GY)	99.2	15.5 sat exp	alpha	0.016537	0.01471
scale	1		beta	1.644163	0.047823
b-value (Gy µm2)	1.86	0.98	gamma	0.885367	0.027009
			cosmic	0.236078	0.0475
			total	2.782145	0.074089
moisture sediment	0.06	0.02			
Age (ka)	35.65595	5.651577			
calender	33655.95	5651.577 BC			
% error	15.85031				

THE MERRELL LOCALITY

(24BE1659)

& Centennial Valley, Southwest Montana

Pleistocene Geology, Paleontology & Prehistoric Archaeology

Two field seasons of intensive excavations at the Merrell Locality and site – named after Donald G. Merrell, discoverer – investigated two Late Pleistocene bonebeds overlaid by Mid-Holocene (Middle Prehistoric Period) archaeological deposits contained in a eroding landform along Lima Reservoir. In this volume, contributors present the results of natural history and cultural studies of fossils, paleoecology, and early human adaptations, respectively to this unique setting in the Centennial Valley of southwest Montana.

With Bureau of Land Management support and assistance, excavations at Merrell were conducted by a team fielded by the Museum of the Rockies at Montana State University-Bozeman. Cooperative funding enabled accomplishment of this work as a project of the Kokopelli Archaeological Research Fund, an endowment administered by the Museum over a 10-year period.

Christopher L. Hill, Associate Curator of Geology and Biology and Director, Ice-Age Research Program at the Museum of the Rockies, holds an M.A. (1989) and a Ph.D. (1992) from the Institute for the Study of Earth and Man at Southern Methodist University in Dallas, Texas.

Leslie B. Davis, Curator of Prehistoric Archaeology & Ethnology and Director, Paleoindian Research Program at the Museum of the Rockies, holds an M.A. in Cultural Anthropology (1965) from the Department of Sociology and Anthropology at the University of Montana-Missoula and a Ph.D. (1972) in North American Archaeology from the Department of Archaeology at the University of Calgary in Alberta, Canada.

Edited by

Christopher L. Hill and Leslie B. Davis